

ABSTRACT

Title of Dissertation: TOTAL SYNTHESIS OF AN OXIDATION PRODUCT OF γ -CAROTENE – A PROVITAMIN A FOOD CAROTENOID

Kristine Crawford, Ph.D. 2011

Dissertation directed by: Professor Philip DeShong
Department of Chemistry and Biochemistry

Human serum carotenoids and their metabolites are known to function as antioxidants and inflammation mediators. In 1992, two oxidative metabolites of lycopene were isolated from human serum and tomato-based food products. These substances were subsequently prepared by partial synthesis from lycopene and characterized as a diastereomeric mixture of 2,6-cyclolycopene-1,5-diols I and II. Results of *in vitro* studies have demonstrated that the diols were more effective at inhibiting the growth of solid human tumor cells than lycopene. While the metabolisms of prominent hydrocarbon carotenoids such as lycopene and β -carotene have been extensively studied, the functional role of γ -carotene remains unexplored. Because the chemical structure of γ -carotene is a hybrid of lycopene and β -carotene, the total synthesis of the analogous metabolite of γ -carotene 2,6-cyclo- γ -carotene-1,5-diol was undertaken.

The total synthesis 2,6-cyclo- γ -carotene-1,5-diol was accomplished using a $C_{15}+C_{10}+C_{15}$ Wittig coupling strategy. The C_{15} -dihydroxyaldehyde key synthon with a defined stereochemistry, a protected C_{10} -Wittig salt, and the β -ionylidene-ethyltriphenylphosphonium chloride C_{15} -Wittig salt provided the three building blocks in this synthesis. To arrive at the C_{15} -dihydroxyaldehyde, citral epoxide was elongated to a

C₁₅-epoxynitrile which underwent acid-catalyzed cyclization to afford a C₁₅-dihydroxynitrile. After reduction with DIBAL-H, the key C₁₅-dihydroxyaldehyde was produced in 16% yield in three steps from citral epoxide. The major drawback of this synthesis was the cyclization step. According to this approach, 2,6-cyclo- γ -carotene-1,5-diol was prepared in high purity in 5 steps in 2.4% overall yield.

In a semi-synthetic approach, 12'-apo- β -carotene-12'-al was transformed into a C₂₅-Wittig salt and coupled to the C₁₅-dihydroxyaldehyde synthon to afford 2,6-cyclo- γ -carotene-1,5-diol in 16.8% overall yield in 3 steps. A third strategy involved the epoxidation of 12'-apo- Ψ -carotene-12'-al followed by cyclization to a C₂₅-dihydroxyaldehyde upon silica gel chromatography. Final coupling of C₂₅-dihydroxyaldehyde with the β -ionylideneethyltriphenylphosphonium chloride C₁₅-Wittig salt produced 2,6-cyclo- γ -carotene-1,5-diol in 6.0% overall yield in 2 steps. This strategy does not require access to large amounts of pure C₁₅-dihydroxyaldehyde and takes advantage of the commercial availability of 12'-apo- Ψ -carotene-12'-al, and is by far the most practical route to 2,6-cyclo- γ -carotene-1,5-diol. The present methodologies provide novel access to an oxidation product of γ -carotene that could be potentially formed in humans or biological systems.

**Total Synthesis of an Oxidation Product of γ -Carotene –
a Provitamin A Food Carotenoid**

by

Kristine Crawford

Dissertation submitted to the Faculty of the Graduate School of the
University of Maryland, College Park in partial fulfillment
of the requirements for the degree of
Doctor of Philosophy
2011

Advisory Committee:

Professor Philip DeShong, Chair

Professor Neil Blough

Associate Professor Jason Kahn

Senior Research Scientist Frederick Khachik

Associate Professor Andrei Vedernikov

Professor Liangli Yu

ACKNOWLEDGEMENTS

I wish to extend heartfelt thanks to my advisor, mentor and friend Fred Khachik. I met Fred at the USDA 15 years ago, where he generously spent several weekends teaching me how to extract zeaxanthin dipalmitate from Chinese gogi fruit. His passion for carotenoid research and enthusiastic teaching style are as vital today as they were back then, and I am again blessed to be his graduate student at the University of Maryland. Beyond helping me develop a deeper knowledge of carotenoid synthesis, I have great respect for Fred's innovative spirit, and am grateful to him for sharing his expertise as a clear, convincing writer and a determined experimentalist. As always, Fred has been a dependable, intelligent and honorable advisor. While it will not be possible to quantitate the immense and varied learning I received under Fred's tutelage, surely it will all be reflected in my future professional activities.

I extend many thanks to professor Michael Doyle, chairman of the chemistry department at the University of Maryland for accepting my enrollment into the doctoral program as a full-time employee of Martek Biosciences Corporation. In addition to Dr. Doyle, I am grateful to Drs. Fred Khachik, Janice Reutt-Robey, Lyle Isaacs and Philip DeShong for working with me to define an acceptable path forward to graduation and for their willingness to accept me as a graduate student under this unconventional circumstance. I thank my committee for their involvement, co-advisor Dr. Jason Kahn for the direction, vision, and wisdom he has provided over the years and Dr. Eugene Mazzola for the professional camaraderie and extensive help provided in interpreting and understanding the complex NMR spectra of stereochemically varied products.

My mentors and supervisors at Martek Biosciences Corporation have taken great care to train and develop me over the last ten years. I am blessed to work for a company that values and supports continuous education and collaboration with academia. I will be forever grateful to Drs. Dutt Vinjamoori, Norman Salem Jr. and Jim Flatt for their confidence and trust in me and for the opportunity they gave me to earn this doctoral degree in the midst of contributing to corporate objectives.

I am thankful to my parents Kathy, Butch and Mary, my sister Marsha and brother George for their encouragement over the years. My precious husband Jonathan and children Eliza and Ted have given me essential support and encouragement through it all. After every cumulative exam I arrived home to flowers and balloons. Throughout the program I kept their sweet gifts close by: Carpe Ph.D. Diem tee shirt, "Mommy - Best kid in school" badge, and "It's your time" flower. Some of the most heartwarming memories I have are doing homework with my children at the dining room table. Ted helped me rehearse my second year seminar while Eliza helped me format the presentation. Jonathan took on a variety of additional responsibilities over the years and the children have been willing to sacrifice some snuggle time. My family has made it possible for me to pursue my dream of earning a Ph.D. in chemistry. I love them more than anything!

TABLE OF CONTENTS

LIST OF TABLES	vi
LIST OF FIGURES	vii
LIST OF SCHEMES.....	ix
LIST OF ABBREVIATIONS.....	xiii
INTRODUCTION	1
DISCUSSION	42
Retrosynthetic Analysis of γ -Carotene Oxidation Product 40A	50
Synthesis of C ₁₅ -dihydroxyaldehyde 42 via C ₁₅ -epoxynitrile 47	55
Synthesis of citral epoxide (48)	58
Preparation of 4-(diethylphosphono)-3-methyl-2-butenenitrile (49).....	58
Synthesis of C ₁₅ -epoxynitrile 47	59
Cyclization of C ₁₅ -epoxynitrile 47 in dilute H ₂ SO ₄	61
Cyclization of C ₁₅ -epoxynitrile 47 with FeCl ₃ and ZrCl ₄	75
DIBAL-H reduction of C ₁₅ -dihydroxynitrile 46	79
Alternate route to the synthesis of C ₁₅ -dihydroxyaldehyde 42	79
Cyclization of C ₁₇ -epoxyethylester 56 with dilute H ₂ SO ₄	81
Reduction of C ₁₇ -dihydroxyethylesters 55 to C ₁₅ -triol 54 by LAH reduction.....	84
Synthesis of C ₂₅ -dihydroxyaldehyde 29	91
Structural characterization of C ₂₅ -dihydroxyaldehyde 29	92
Synthesis of 40A by Wittig coupling reaction between C ₂₅ -dihydroxyaldehyde 29 and Wittig salt 44	94
Partial Synthesis of C ₁₅ -dihydroxyaldehyde 42	102
Synthesis of C ₁₅ -nitrile 58	104
DIBAL-H reduction of C ₁₅ -nitrile 58	105
Synthesis of target Carotenoid 40A via alternative route to C ₂₅ -dihydroxyaldehyde 29	106
Synthesis of C ₁₅ -Wittig salt 28	108
Synthesis of C ₂₅ -dihydroxyaldehyde 29 via C ₂₅ -aldehyde 70	108

Epoxidation of 70	109
A simplified procedure for the synthesis of target carotenoid 40A from dihydroxy aldehyde 42	110
Reduction of (<i>all-E</i>)-12'apo- β -caroten-12'-al (74) with NaBH ₄	112
Synthesis of C ₂₅ -Wittig salt 72	112
Synthesis of 40A from Wittig salt 72 and C ₁₅ -dihydroxyaldehyde 42	112
Direct synthesis of target carotenoid 40A from γ -carotene (6).....	113
Investigation of the possible presence of γ -carotene oxidation product 40A in extracts of human plasma, tomato paste and algal biomass.....	115
CONCLUSION.....	117
EXPERIMENTAL SECTION.....	123
APPENDIX I.....	150
REFERENCES.....	151

LIST OF TABLES

Table 1.	Major dietary carotenoids and their concentration in human plasma. ^{5,6,8-11}	6
Table 2.	Concentration of carotenoids measured in human tissues. ^{6,13}	8
Table 3.	Proton chemical shifts of C ₁₅ -dihydroxynitriles 46 .	65
Table 4.	Carbon-proton connectivities determined for 46a1 by HMBC NMR.	66
Table 5.	Chemical shifts for H2 and H6 of 1,5-dihydroxy-2,6-cyclolycopene (21). ^{85,86,90}	69
Table 6.	Cyclization of C ₁₅ -epoxynitrile 47 with dilute sulfuric acid.	71
Table 7.	Lewis acid-catalyzed reactions of C ₁₅ -epoxynitrile 47 .	77
Table 8.	Chemical shifts for the bicyclic oxide (50) ⁸⁴ , cyanoepoxide 47 and C ₁₅ -dihydroxynitrile 46a1 .	78
Table 9.	The cyclization of C ₁₇ -epoxyethylesters 56 with dilute sulfuric acid.	81
Table 10.	Chemical shifts of key protons for C ₁₇ -dihydroxyethylesters 55a1 , 55a2 , and 55b .	84
Table 11.	Chemical shifts of key protons of C ₁₅ -dihydroxyaldehydes 42a1 , 42a2 , 42b1 , and 42b2 .	89
Table 12.	Carbon-proton connectivities determined for C ₂₅ -dihydroxyaldehyde 29 by HMBC NMR.	94
Table 13.	Carbon-proton connectivities determined for the target carotenoid 40A by HMBC NMR.	102

LIST OF FIGURES

Figure 1.	Structures of phytoene (1), phytofluene (2), ζ -carotene (3), neurosporene (4) and lycopene (5) with conventional numbering system and definition of ψ -end-group adopted for carotenoids.	3
Figure 2.	Structures of γ -carotene (6), α -carotene (7), and β -carotene (8) with conventional numbering system and definition of α -, β - and ϵ -end groups adopted for carotenoids.	4
Figure 3.	Structures of canthaxanthin (9), astaxanthin (10), α -cryptoxanthin (11), β -cryptoxanthin (12), lutein (13), and zeaxanthin (14).	5
Figure 4.	Products derived from chemical quenching of β -carotene (8) with singlet oxygen generated by illuminating a mixture of 8 /Rose Bengal/oxygen in organic solvent. ⁴¹	22
Figure 5.	Schematic representation of β -carotene (8) and zeaxanthin (14) oriented across a lipid membrane. ²⁶	26
Figure 6.	Lycopene-1,2-epoxide (19).	30
Figure 7.	1,5-Epoxyiridanyl-lycopene (20). ⁸⁴	31
Figure 8.	1,5-Dihydroxyiridanyl-lycopene (21). ⁸⁵	31
Figure 9.	Structure of 2,6-Cyclolycopene-1,5-diol (22) identified by Khachik. ⁴	32
Figure 10.	Lycopene-5,6-epoxide (23).	32
Figure 11.	Structure of 2,6-cyclolycopene-1,5-epoxide (24) isolated by Khachik <i>et al.</i> ⁸⁶	33
Figure 12.	<i>(all-E)</i> - β -carotene (8) and two of its sterically hindered stereoisomers... ..	49
Figure 13.	C ₁₅ -epoxynitriles 47a and 47b	60
Figure 14.	C ₁₅ -Dihydroxynitriles 46a1 , 46a2 , 46b1 and 46b2	62
Figure 15.	Normal phase HPLC profile of C ₁₅ -dihydroxynitriles 46a1 , 46a2 , 46b1 , and 46b2 . (HPLC condition K, Appendix I).	62
Figure 16.	¹³ C-NMR spectrum of C ₁₅ -dihydroxynitrile 46a1	63
Figure 17.	¹ H-NMR spectrum of C ₁₅ -dihydroxynitrile 46a1	64
Figure 18.	HMBC spectrum of C ₁₅ -dihydroxynitrile 46a1	66

Figure 19.	NOESY spectrum of C ₁₅ -dihydroxynitrile 46a1	67
Figure 20.	NOESY and HMBC crosspeaks and relative stereochemistry for 46a1	68
Figure 21.	NOESY crosspeaks and relative stereochemistries for 46a2 , 46b1 and 46b2	69
Figure 22.	Structures of C ₁₇ -epoxyethylesters.	80
Figure 23.	C ₁₇ -dihydroxyethylesters 55a , 55a2 , and 55b	83
Figure 24.	HPLC chromatogram of C ₁₅ -dihydroxyaldehydes 42a1 , 42a2 , 42b1 , and 42b2 . (Condition B, Appendix I).....	88
Figure 25.	¹ H-NMR spectrum of C ₁₅ -dihydroxyaldehyde 42a1	88
Figure 26.	¹³ C-NMR spectrum of C ₁₅ -dihydroxyaldehyde 42a1	90
Figure 27.	NOESY crosspeaks observed in key synthon 42a1	90
Figure 28.	NOESY crosspeaks observed for C ₂₅ -dihydroxyaldehyde 29	93
Figure 29.	HPLC chromatogram and spectra of target carotenoid 40A following purification by flash column chromatography and semi-preparative HPLC. (HPLC condition B, Appendix I).....	96
Figure 30.	¹ H-NMR spectrum of γ -carotene oxidation product 40A	98
Figure 31.	NOESY spectrum of γ -carotene oxidation product 40A	99
Figure 32.	Structure of 1,2,5,6-tetrahydro-2,6-cyclo- γ -carotene-1,5-diol 40A and observed NOESY crosspeaks.	99
Figure 33.	¹³ C-NMR spectrum of γ -carotene oxidation product 40A	100
Figure 34.	HMBC spectrum of γ -carotene oxidation product 40A	101

LIST OF SCHEMES

Scheme 1.	Enzymes in the carotenoid biosynthesis pathway in plants and algae. ²	2
Scheme 2.	Metabolic conversion of β -carotene (8) to vitamin A. ²⁰	9
Scheme 3.	Reaction of hydroxyl radical with guanine to form 8-OHdG.	13
Scheme 4.	Oxidation of linoleic acid by hydroxyl radical. ³²	16
Scheme 5.	Proposed pathway for formation of by-products obtained from the reaction of β -carotene (8) with alkylperoxyl radical (ROO•). ³⁶	19
Scheme 6.	Reaction products of singlet oxygen with olefins. ³²	21
Scheme 7.	Proposed metabolic pathway of lycopene in humans and tomato-based food products. ²⁹	34
Scheme 8.	C ₁₅ +C ₁₀ +C ₁₅ Wittig olefination strategy used by Traber and Pfander. ⁹⁰	36
Scheme 9.	Double Wittig coupling of C ₁₀ -dialdehyde 27 with Wittig salts 25 and 28 . ⁹⁰	37
Scheme 10.	Synthesis of Wittig salt 25 according to Traber and Pfander. ⁹⁰	38
Scheme 11.	Proposed metabolic oxidation of γ -carotene (6).	40
Scheme 12.	Synthesis of (<i>all-E</i>)- β -carotene (8) via enol ether condensation.	43
Scheme 13.	Synthesis of (<i>rac</i>)-zeaxanthin (14) via organometallic and Wittig coupling reactions. ¹⁰¹	44
Scheme 14.	Synthesis of retinal (16) via an alkenyl lithium reagent. ¹⁰²	44
Scheme 15.	Reductive coupling of carbonyl compounds in the presence of low valent titanium.	45
Scheme 16.	Role of titanium metal in reductive coupling of carbonyl compounds. ¹⁰³ ...	45
Scheme 17.	Synthesis of β -carotene (8) via Julia's sulphone coupling reaction.	46
Scheme 18.	Synthesis of Z-olefins by sulphone coupling with carbonyl compounds and reduction by sodium dithionite. ¹⁰⁵	47
Scheme 19.	Conventional Wittig Reaction. ¹⁰⁸	47
Scheme 20.	Proposed oxaphosphetane and betaine intermediates in a typical Wittig reaction. ¹⁰⁸	48

Scheme 21. General Wittig coupling strategy for the synthesis of astaxanthin (10) ¹¹⁰ and other symmetrical carotenoids.	48
Scheme 22. Structures of C ₁₅ -aldehyde and C ₁₀ -phosphonium salt building blocks.	49
Scheme 23. Building blocks used for the synthesis of targeted diol 40A . *Stereochemistries at C2, C5 and C6 will be determined.	50
Scheme 24. Retrosynthetic analysis of γ -carotene oxidation product 40A via C ₁₅ -dihydroxynitrile 46 ; *carotenoid numbering system has been used for compounds 40A-46 , 29 and 50	52
Scheme 25. Alternative route to the synthesis of C ₁₅ -dihydroxyaldehyde 42 via C ₁₇ -dihydroxyethylester 55 . *Carotenoid numbering system has been used for compounds 42 , 54 and 55	54
Scheme 26. Epoxidation of alkenes by peroxide under neutral conditions.	55
Scheme 27. Epoxidation of olefins with peroxide under basic conditions. ⁷¹	56
Scheme 28. Nucleophilic epoxidation of citral (53).	57
Scheme 29. Epoxidation of citral (53) via a peroxyoximidic acid intermediate.	57
Scheme 30. Synthesis of citral epoxide (48).	58
Scheme 31. Synthesis of 4-(diethylphosphono)-3-methyl-2-butenenitrile (49).	58
Scheme 32. Synthesis of C ₁₅ -epoxynitrile 47	59
Scheme 33. Synthesis of 58 by Knoevenagel condensation reaction.	61
Scheme 34. Acid-catalyzed cyclization of C ₁₅ -epoxynitrile 47	61
Scheme 35. Synthesis of C ₁₅ -dihydroxynitrile 46 by Amberlite IR-120 vs. silica gel.	72
Scheme 36. Rearrangement of 5 <i>E</i> - and 5 <i>Z</i> -lycopene-5,6-epoxides (23) by an S _N 2 mechanism. ⁸⁷	73
Scheme 37. C ₁₅ -dihydroxynitrile 46b formed from <i>cis</i> -epoxide 47b via an S _N 2-type reaction.	74
Scheme 38. Rearrangement of <i>cis</i> and <i>trans</i> -epoxides 47a and 47b by an S _N 1-type mechanism. ⁸⁷	75
Scheme 39. Formation of bicyclic oxide 50	76
Scheme 40. DIBAL-H reduction of C ₁₅ -dihydroxynitrile 46a1	79

Scheme 41. Synthesis of C ₁₇ -epoxyethylester 56	80
Scheme 42. Acid catalyzed intramolecular cyclization of C ₁₇ -epoxyethylesters 56	81
Scheme 43. Reduction of C ₁₇ -dihydroxyethylester 55 to C ₁₅ -triol 54	85
Scheme 44. TEMPO oxidation of C ₁₅ -triol 54 to C ₁₅ -dihydroxyaldehyde 42	86
Scheme 45. Sequence proposed for the organocatalytic oxidation of alcohols to aldehydes with TEMPO and oxygen.	87
Scheme 46. Mechanism proposed for the catalytic conversion of primary alcohols to aldehydes with TEMPO. ^{140,141}	87
Scheme 47. Synthesis of C ₂₅ -dihydroxyaldehyde 29	91
Scheme 48. Synthesis of protected Wittig salt 43	92
Scheme 49. Final step of the synthesis of γ -carotene oxidation product (40A).	95
Scheme 50. Mechanism proposed for epoxyalkane mediated Wittig coupling reactions. ¹⁴³	96
Scheme 51. Synthesis of Wittig salt 44 . ^{111,112}	97
Scheme 52. Partial synthesis of C ₁₅ -dihydroxyaldehyde 42 . Carotenoid numbering system has been used for compound 42	103
Scheme 53. HWE synthesis of C ₁₅ -nitrile 58	104
Scheme 54. Reduction of C ₁₅ -nitrile 58	105
Scheme 55. Epoxidation of C ₁₅ -aldehyde 68 with <i>m</i> -CPBA.....	105
Scheme 56. Synthesis of target carotenoid 40A via C ₂₅ -aldehyde 70	107
Scheme 57. Synthesis of C ₁₅ -Wittig salt 28 . ⁹²	108
Scheme 58. Synthesis of C ₂₅ -aldehyde 70	109
Scheme 59. Epoxidation of C- ₂₅ aldehyde 70 followed by cyclization to 29	109
Scheme 60. Simplified procedure for the synthesis of 40A	111
Scheme 61. Reduction of (<i>all-E</i>)-12'-apo- β -caroten-12'-al (74).	112
Scheme 62. Synthesis of C ₂₅ -Wittig salt 72	112
Scheme 63. Synthesis of 40A from Wittig salt 72 and aldehyde 42	113

Scheme 64. Synthesis of γ -carotene (6) according to the procedure by Ruegg <i>et. al.</i> ¹⁴⁷	113
Scheme 65. Possible epoxidation products of γ -carotene (6).	114

LIST OF ABBREVIATIONS

b.p.	boiling point
CARET	Carotene and Retinol Efficacy Trial
COSY	Correlation spectroscopy
<i>C. cohnii</i>	<i>Cryptosporidium cohnii</i>
2D	two dimensional
DHA	docosahexaenoic acid
DIBAL-H	diisobutylaluminum hydride
DMF	N,N-dimethylformamide
DMPU	dimethylpropylene urea
ESI+	electrospray ionization
EPP	erythropoietic protoporphyria
EtOAc	ethyl acetate
FDA	Food and Drug Association
GPx	glutathione peroxidase
h	hours
HMBC	heteronuclear multiple bond correlation
HDL	high density lipoprotein
HPLC	high performance liquid chromatography
HRMS	high resolution mass spectrometry
HSQC	heteronuclear single quantum correlation
HWE	Horner-Wadsworth-Emmons
IR	infrared

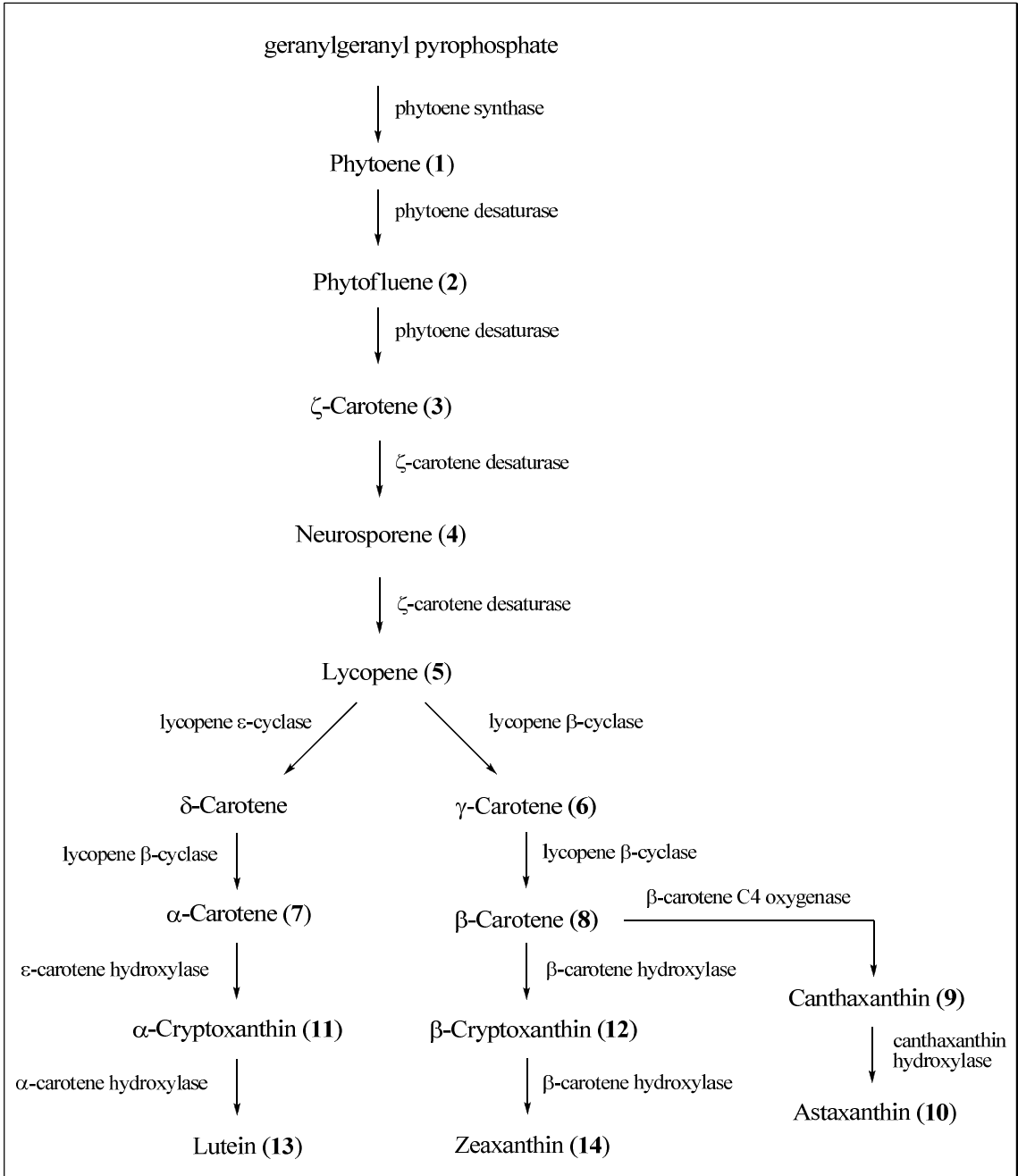
IU	International units
<i>J</i>	coupling constant
LAH	lithium aluminum hydride
LDL	low density lipoprotein
M ⁺	molecular ion
<i>m</i> -CPBA	meta-chloroperoxybenzoic acid
<i>m/z</i>	mass to charge ratio
m.p.	melting point
MS	mass spectrometry
NMR	nuclear magnetic resonance
NOESY	nuclear overhauser effect spectroscopy
PCC	pyridinium chlorochromate
PMA	phosphomolybdic acid
R.T.	room temperature
ROS	reactive oxygen species
SOD	superoxide dismutase
TEMPO	2,2,6,6-tetramethylpiperidine-1-nitroxide
TBHP	<i>tert</i> -butyl hydroperoxide
TBME	<i>tert</i> -butylmethyl ether
THF	tetrahydrofuran
TLC	thin layer chromatography

INTRODUCTION

To date, approximately 600 carotenoids have been identified in plants, animals, algae, and food.¹ These naturally occurring tetraterpenes are formed from the tail to tail linkage of two C-20 units. As such, they contain an extensively conjugated backbone composed of 40 carbon atoms with four isoprene units. End groups are either straight chain or cyclized. The most non-polar carotenoids contain only carbon and hydrogen and are classified as carotenes, whereas carotenoids with end groups containing hydroxyl and/or carbonyl groups are more polar and are classified as xanthophylls. Due to their extensive conjugation, carotenoids absorb light in the 400-500 nm region of the visible spectrum. This physical property imparts the characteristic yellow to red color observed in the skin and pulp of various fruits and vegetables, photosynthetic organisms, flowers, crustaceans, bird plumage and animal flesh.

Carotenoids are synthesized in the chloroplasts of plants and other photosynthetic organisms such as algae, bacteria and some types of fungus. The biosynthetic pathway of carotenoids is shown in Scheme 1.² Beginning with geranylgeranyl pyrophosphate, phytoene (**1**) is the first C₄₀ hydrocarbon formed. Successive enzymatic desaturations produce phytofluene (**2**), ζ -carotene (**3**), neurosporene (**4**) and lycopene (**5**), a straight chain carotene with 11 conjugated double bonds. The structures of these compounds are provided in Figure 1 with the conventional numbering system and definition of the ϵ -end group adopted for carotenoids. γ -Carotene (**6**), α -carotene (**7**) and β -carotene (**8**) are produced by enzymatic action of cyclases. Their structures are provided in Figure 2 along with the definition of the α - and β -end groups. Enzyme-mediated oxidation and hydroxylation further result in the production of xanthophylls such as canthaxanthin (**9**),

astaxanthin (10), α -cryptoxanthin (11), β -cryptoxanthin (12), lutein (13) and zeaxanthin (14). The structures of carotenoids 9-14 are shown in Figure 3.



Scheme 1. Enzymes in the carotenoid biosynthesis pathway in plants and algae.²

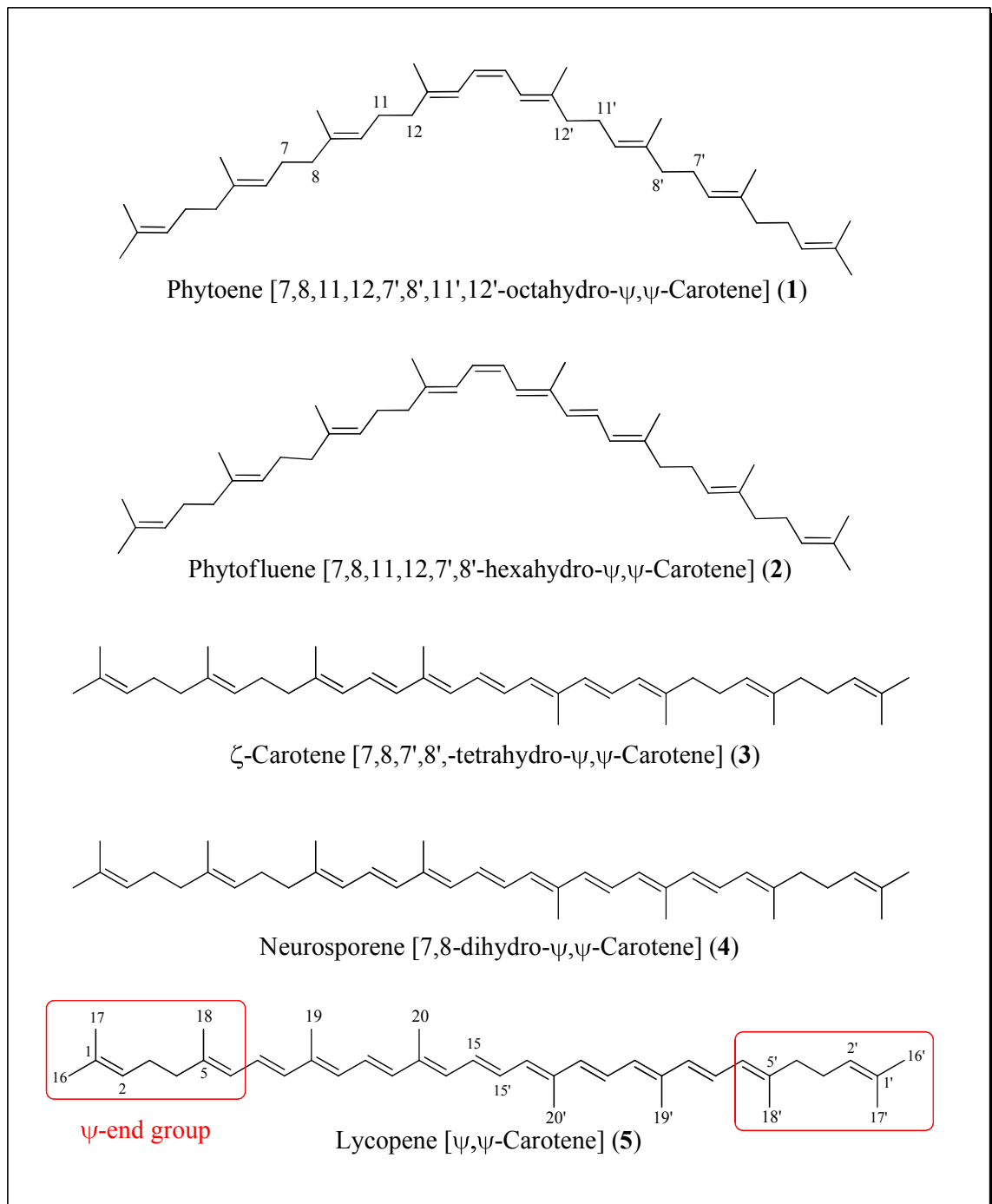


Figure 1. Structures of phytoene (1), phytofluene (2), ζ -carotene (3), neurosporene (4) and lycopene (5) with conventional numbering system and definition of ψ -end-group adopted for carotenoids.

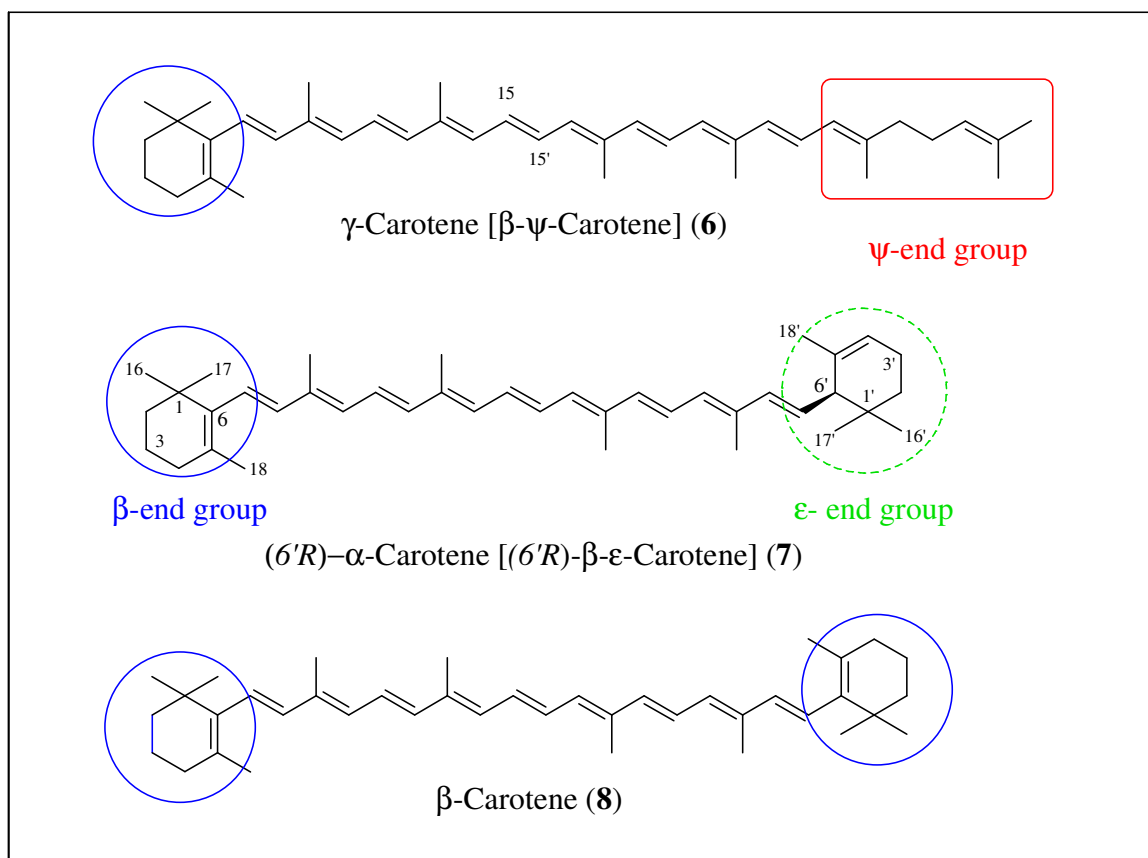


Figure 2. Structures of γ -carotene (6), α -carotene (7), and β -carotene (8) with conventional numbering system and definition of α -, β - and ϵ -end groups adopted for carotenoids.

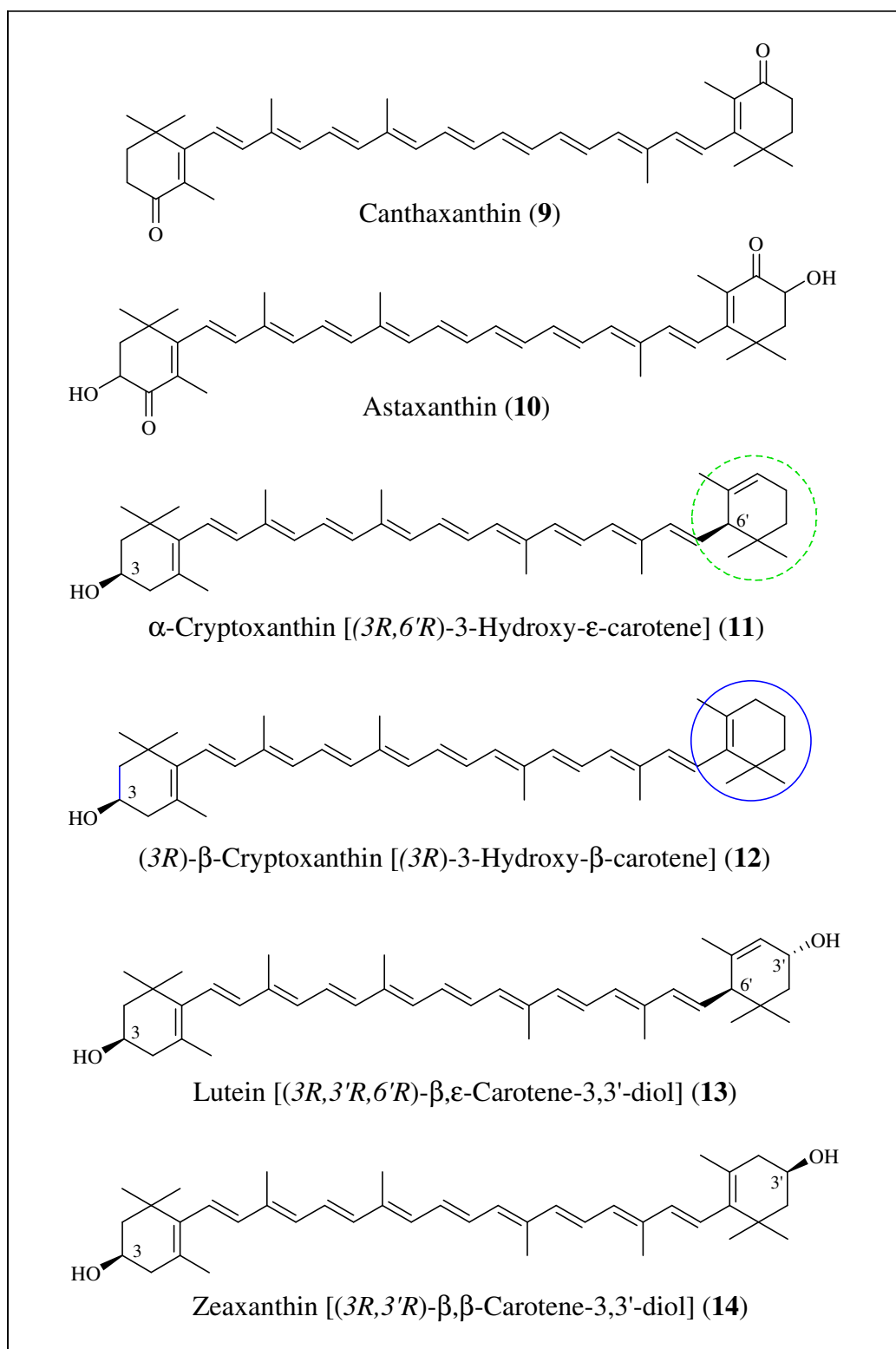


Figure 3. Structures of canthaxanthin (9), astaxanthin (10), α -cryptoxanthin (11), β -cryptoxanthin (12), lutein (13), and zeaxanthin (14).

As humans and animals cannot synthesize carotenoids *in vivo*, these must be obtained from the diet. Of the 40-50 carotenoids found in commonly consumed foods in the United States,³ only 12 dietary carotenoids and 8 of their metabolites have been identified in human serum and tissues.^{4,5} While carotenoids exist primarily in the *all-trans* form, processing conditions that require heat treatment result in the formation of lower levels of 9-, 13-, and 15-Z isomers, and these are absorbed into plasma to different extents.^{6,7} Dietary sources of γ -carotene (**6**) - the focus of this research - and other major dietary carotenoids are indicated in Table 1 along with their concentration in human plasma.

Table 1. Major dietary carotenoids and their concentration in human plasma.^{5,6,8-11}

Carotenoid	Dietary Source	Plasma Concentration (nM)
α -Carotene (7)	Pumpkin, carrots, squash, green beans, pea, lima beans, sweet potato, apricot, cantaloupe, green peas, prunes	81-192
β -Carotene (8)	Tomatoes and tomato-based products, carrot, squash, algae, broccoli, brussel sprouts, kale, spinach, green beans, sweet potato, apricot, cantaloupe, oranges, mango, honeydew melon, papaya, peaches, pumpkin, squash	132-332
β -Cryptoxanthin (12)	Orange, tangerine, mango, papaya, peaches, prunes, squash	149-371
γ -Carotene (6)	Apricot, tomatoes and tomato-based products, algae	71-140
Lycopene (5)	Tomatoes and tomato-based products, watermelon, pink grapefruit, guava, apricot	1041-1377
Lutein (13)	Dark green leafy vegetables, corn, green beans, broccoli, squash, brussel sprouts	135-266
Zeaxanthin (14)	Dark green leafy vegetables, peaches, kiwi, mango, papaya, green peas, pumpkin, squash, gogi fruit	35-50

The bioavailability from foods can vary widely, such that 5% of total carotenoids are absorbed from whole, raw vegetables whereas 50% or more can be absorbed from processed foods during consumption with some form of dietary fat. After ingestion, carotenoids are released from food in the intestinal lumen, incorporated into mixed micelles and absorbed into the intestine. Bile acids, dietary fat and protein all aid in this process. In the intestine, intact carotenoids are incorporated into the chylomicrons of low density lipoprotein (LDL) and transported to various organs and tissues *via* the lymph system and blood. Thereafter, carotenes are predominately distributed into LDL whereas xanthophylls are more equally distributed between LDL and high density lipoprotein (HDL).⁶

Carotenoids are generally measured and quantitated by normal- and reversed-phase HPLC with UV/Vis detection. Of the numerous methods published, Khachik *et al.* described a comprehensive approach capable of measuring eighteen carotenoids in the lipid soluble portion of human plasma.⁵ The *all-trans* forms of lycopene (**5**), α -carotene (**7**), β -carotene (**8**), β -cryptoxanthin (**12**), lutein (**13**) and zeaxanthin (**14**) were primarily detected. Minor amounts of *all-trans* phytoene (**1**), phytofluene (**2**), ζ -carotene (**3**), neurosporene (**4**), γ -carotene (**6**) and α -cryptoxanthin (**11**) were also detectable along with several *cis*- isomers of **5** and **8**, which can constitute up to 50% of the total form in serum.¹² In addition, oxidative metabolites of **5**, **13** and **14** were also measured by this method.

In addition to their presence in plasma, carotenoids are also distributed to various extents in the liver, colon, breast, adrenal gland, testes, ovary, corpus luteum, kidney, retina and adipose tissue.^{6,13} Distribution is thought to be largely influenced by preferential

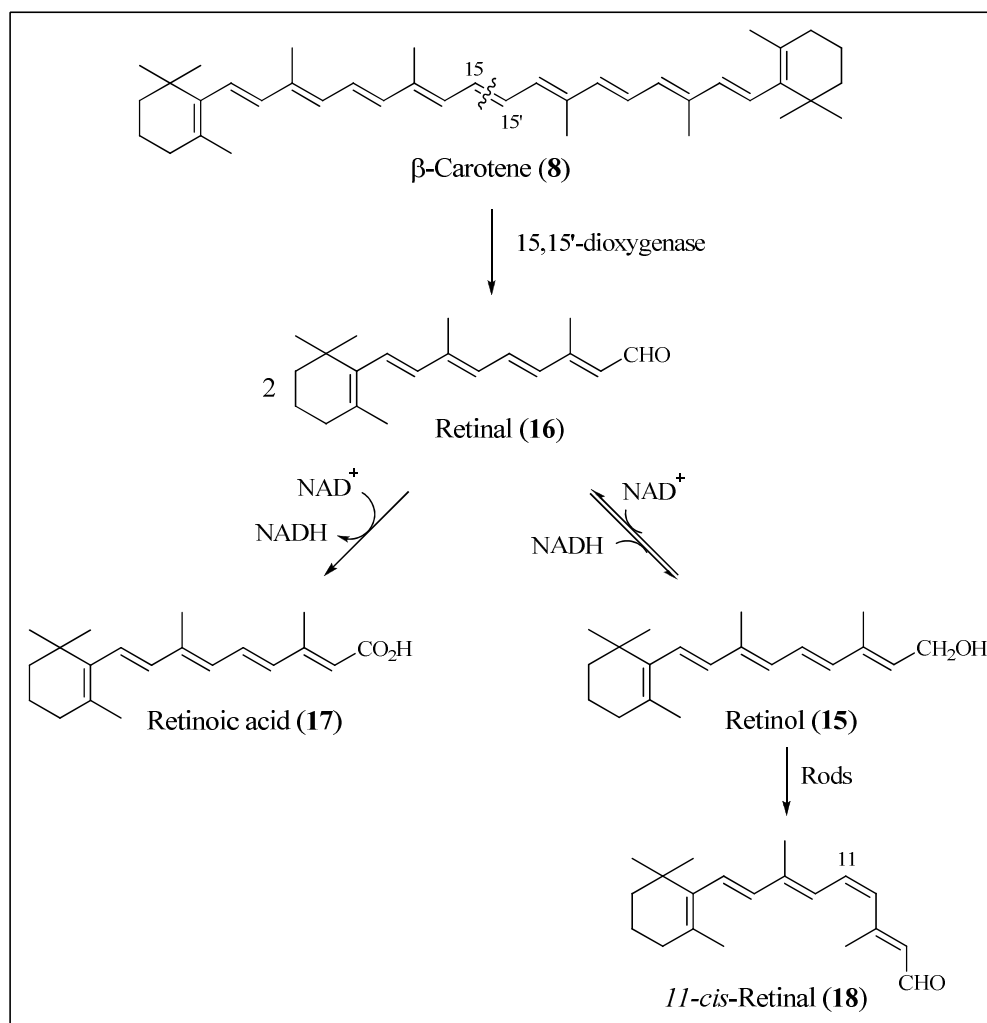
uptake into various cells as a function of structure and polarity.¹⁴ Further, individual carotenoids may have specialized, site-specific functions. For example, lycopene (**5**) is preferentially absorbed in the testes, and higher plasma levels of this carotene are uniquely associated with decreased risk for developing prostate cancer.¹⁵ The distribution of several carotenoids in tissues from human subjects living in Germany and the United States is shown in Table 2.

Table 2. Concentration of carotenoids measured in human tissues.^{6,13}

Tissue	β -Carotene (8) (nmol/g)	Lycopene (5) (nmol/g)	β -Crypto-xanthin (12) (nmol/g)	Lutein (13) (nmol/g)
Liver	0.8 – 8.0	1.3 – 5.7	0.1 – 3.5	0.1 – 12.2
Kidney	0.1 – 1.2	0.1 – 1.2	0.1 – 0.4	0.1 – 10.4
Adrenal	5.6 – 9.4	1.9 – 21.6		
Testes	2.7 – 4.6	4.3 – 21.4		
Ovary	0.4 – 1.0	0.2 – 0.3		
Adipose	0.4	0.2 – 1.3		
Lung	0.1 – 1.0	0.1 – 4.2	0.1 – 1.6	0.1 – 1.4
Colon	0.2	0.3		
Breast	0.7	0.8		
Skin	0.3	0.4		

Among the various carotenoids that are absorbed by humans, (*6'R*)- α -carotene (**7**), β -carotene (**8**), (*3R*)- β -cryptoxanthin (**12**), and γ -carotene (**6**) contain a β -end group. Only these carotenoids can be converted into vitamin A in the intestine, while lycopene (**5**) with a Ψ -end group is not a precursor to vitamin A. Vitamin A is a collective term for retinol (**15**) and its oxidized forms retinal (**16**) and retinoic acid (**17**), all of which play unique roles in human health and vision. While the mechanism employed by humans and non-primate animals such as quail and frogs to metabolize lutein (**13**) and zeaxanthin (**14**) in plasma, liver and ocular tissues has been reported by Khachik *et al.*,¹⁶ much attention has also been given to elucidating the pathway for conversion of pro-vitamin A carotenoids into vitamin A in humans. In 1960, Glover postulated that **8** could be

converted to **16** by central fission of the C15-15' bond in the polyene portion of the molecule.¹⁷ The theory was subsequently borne out experimentally when the enzyme β -carotenoid-15,15'-dioxygenase was isolated from the cytosol of rat liver and the intestinal mucosa of rats, rabbits, and human newborns.^{18,19} After partial purification, the enzyme was found to produce two molecules of retinal (**16**) as the major product from the central cleavage of β -carotene (**8**). Enzymatic transformation of **8** into vitamin A in the intestine is illustrated in Scheme 2.²⁰ This mechanism is thought to be operative for all pro-vitamin A carotenoids.



Scheme 2. Metabolic conversion of β -carotene (**8**) to vitamin A.²⁰

According to this process, central enzymatic cleavage of β -carotene (**8**) produces two molecules of retinal (**16**). After incorporation into chylomicrons, **16** is transported to the liver and oxidized irreversibly to retinoic acid (**17**) and/or reversibly reduced to *all-trans* retinol (**15**) by an enzyme using the coenzyme nicotinamide adenine dinucleotide (NADH/NAD⁺). The various forms of vitamin A are bound to retinol binding proteins, released from the liver, circulated in the blood and distributed to target cells. *All-trans* retinol (**15**) can be reversibly converted to retinyl esters for storage in the liver and adipose tissue or further converted to *11-cis*-retinal (**18**) in the rods of the eye. The binding of **18** to the visual pigment opsin is essential for vision, while retinoic acid (**17**) is required for cell differentiation and metabolic control.^{20,21} In addition to retinal, products resulting from the non-symmetrical, or excentric cleavage of β -carotene (**8**) have been isolated following incubation with intestinal mucosa homogenates from humans,²² and the excentric cleavage of provitamin A carotenoids is now also widely accepted. For a review on the nutritional and biological properties of vitamin A in humans, see the review by Ross and Harrison.²³

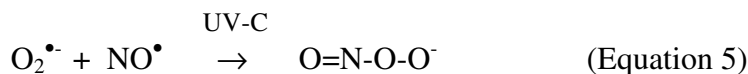
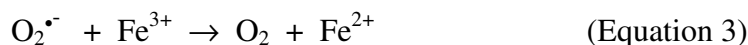
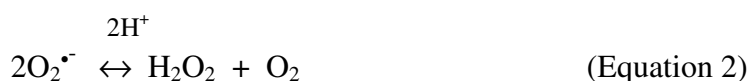
The focus of this dissertation is to develop a strategy for the synthesis of possible oxidation products of γ -carotene (**6**) that may be potentially formed in biological systems as a result of metabolism of this carotenoid. Because the structure of **6** is a hybrid of the structures of β -carotene (**8**) and lycopene (**5**), it is appropriate to describe the metabolism and biological activities of these carotenoids in prevention of chronic diseases. In addition, much of the biological activities of these carotenoids are based on their antioxidant mechanism of action. Therefore, the evidence for the interaction of carotenoids with reactive oxygen species (ROS) should first be considered.

Oxygen has damaging effects on aerobic organisms. Rodents exposed to 100% oxygen for periods ranging between several hours to one month exhibited mitochondrial damage of the heart and liver, degeneration of seminiferous epithelium, decreased sperm counts and inhibited erythroid cell development in bone marrow. Humans undergoing hyperbaric oxygen therapy developed haemorrhages in the inner ear and deafness. Plants exhibit diminished leaf growth at elevated oxygen concentrations. Molecular oxygen in its ground state is essentially unreactive toward non-radical species, leading Gershman and Gilbert to propose in 1954 that the damaging effects of oxygen could be attributed instead to the effects of ROS.²⁴

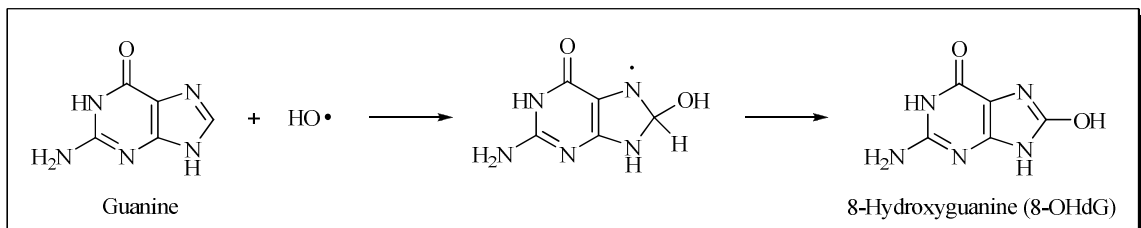
Biologically relevant ROS include the superoxide radical anion, hydrogen peroxide, hydroxyl radical, peroxyxynitrite anion, nitric oxide radical, nitrogen dioxide radical and singlet oxygen. In plants and algae, ROS are produced endogenously in chloroplasts during photosynthesis. In aerobic organisms, ROS are produced for useful purposes such as wound repair under typical conditions of oxygen metabolism as by-products of electron transport reactions occurring in mitochondria, and by neutrophils and macrophages during inflammation as a response to infection and by platelets involved in wound repair. ROS can also be generated during exposure to ionizing radiation, such as UV light and X-rays, while atmospheric pollution represents an exogenous source of ROS.²⁴

The *in vivo* formation of ROS begins with the reduction of oxygen to water by oxygen reductase in cytochrome a_3 in mitochondria and cytochrome P_{450} in microsomes to produce the superoxide radical anion $O_2^{\cdot-}$ (Equation 1).²⁵ Under physiological conditions, the superoxide radical anion can be protonated form hydrogen peroxide H_2O_2

(Equation 2). Detectable levels of hydrogen peroxide are present in the lens and breath of human subjects, and are also present in cigarette smoke.²⁶ Endogenous levels are capable of penetrating cell membranes and oxidizing sulfhydryl residues of proteins. The concentrations of superoxide radical anion and hydrogen peroxide must be rigorously controlled, otherwise iron can catalyze formation of the hydroxyl radical HO• by the superoxide-assisted Fenton reactions depicted in Equations 3 and 4.²⁴

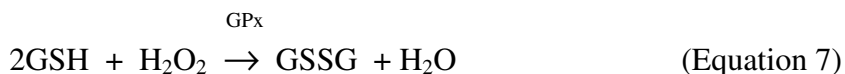


Another source of the hydroxyl radical is from the homolytic dissociation of the peroxyxynitrate anion, formed by reaction of the superoxide radical anion and the nitric oxide radical in the presence of UV-C light (Equation 5). The rapid, irreversible reaction of the hydroxyl radical makes this species the most reactive free radical towards many types of molecules found in living cells including phospholipids, sugars, amino acids and the nucleotides of DNA and RNA resulting in impaired function and strand breaks. The addition of hydroxyl radical to the purine base guanine to form 8-OHdG, one of the major products of DNA oxidation, is shown in Scheme 3.²⁴



Scheme 3. Reaction of hydroxyl radical with guanine to form 8-OHdG.

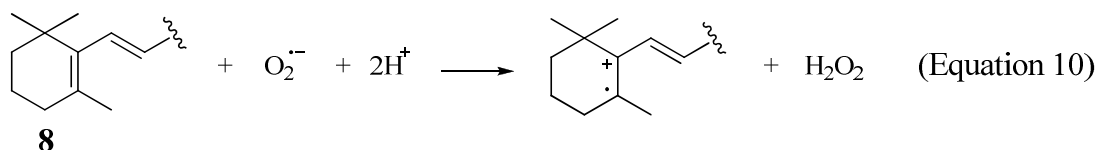
Biological systems employ antioxidant enzymes such as catalases, superoxide dismutase and glutathione to prevent accumulation of ROS that would otherwise damage cell structures.¹⁴ Hydrogen peroxide is decomposed by the catalase enzyme to water and oxygen,²⁷ and metabolized in mitochondrial and cytosolic compartments to water by the selenium-containing enzyme glutathione peroxidase (GPx), as shown in Equation 7. The active site of the enzyme contains glutathione (GSH), a tripeptide cofactor.



Mitochondrial superoxide dismutase (SOD) enzymes catalyze the dismutation of superoxide anion into oxygen and hydrogen peroxide by the processes shown in Equations 8 and 9 respectively. The cytosolic SOD enzyme requires manganese.²⁴



Carotenoids represent another class of essential, yet non-enzymatic micronutrients that can sequester free radicals. Truscott proposed that superoxide radical anion could be converted to hydrogen peroxide by β -carotene (**8**) in lung tissue exposed to cigarette smoke (Equation 10).²⁸



The peroxynitrite anion ONO_2^- is produced in plasma membranes and mitochondria by the reaction of nitric oxide ($\bullet\text{NO}$) and superoxide radical anion as shown in Equation 11.²⁹ Steady state concentrations are estimated to be in the nM range. Under physiological conditions the anion is protonated to peroxynitrous acid (ONOOH), which can cross cell membranes within 5-20 μm of its site of origin. Within the hydrophobic core, peroxynitrous acid can undergo homolytic dissociation to produce hydroxyl radicals and nitrogen dioxide radicals ($\bullet\text{NO}_2$) as shown in Equation 12. These ROS can in turn oxidize unsaturated lipids and LDL and modify proteins containing tyrosine residues by nitration.



Pathological conditions associated with endogenous peroxynitrite anion include vascular inflammation and dementia,²⁹ and coronary heart disease.³⁰ Results of *in vitro* studies provided evidence that carotenoids such as lycopene (**5**), β -carotene (**8**) and astaxanthin (**10**) can scavenge peroxynitrite anion directly to produce a series of apo-carotenal and nitration products. These observations suggest a possible role for carotenoids in mitigating the effects of peroxynitrite *in vivo*.³¹

Hydroxyl radicals formed by the Fenton reaction are mainly responsible for initiation of lipid oxidations.³² Lipid peroxidation is initiated by and propagated from uncontrolled reaction of alkyl and/or alkoxyl free radicals with essential unsaturated fatty acids to produce lipid hydroperoxides and lipid polymers. These events change the

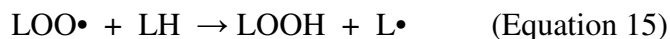
functionality of lipids which can lead to pathological conditions such as Alzheimer's disease.³³ The article by Cerutti summarizes supporting evidence for the roles played by lipid peroxidation in human carcinogenesis.³⁴

In tissues exposed to oxygen, lipid peroxidation can be represented as follows:²⁷

Initiation



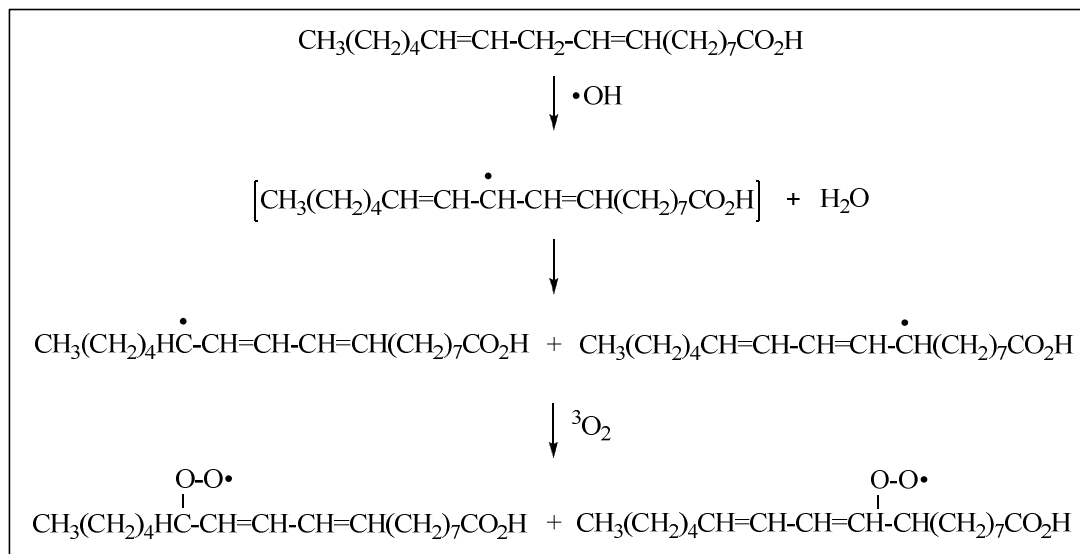
Chain Propagation



Termination

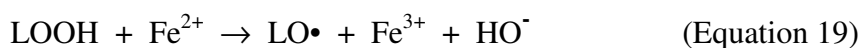
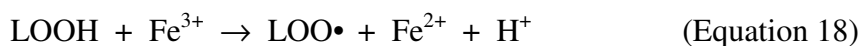


During initiation, the hydroxyl radical abstracts an allylic hydrogen atom from a lipid L to form a lipid radical L• (Equation 13). During the propagation phase, the lipid radical combines with oxygen to afford a lipid peroxy radical LOO• (Equation 14) which can in turn abstract a hydrogen atom from a vicinal lipid LH (Equation 15). In the absence of chain breaking antioxidants, lipid peroxidation can be terminated by the combination of radical species to form non-radical products such as dimerized lipids L-L (Equation 16) and lipid peroxides LOOL (Equation 17). To illustrate the processes of initiation and propagation, the hydroxyl radical-initiated oxidation of linoleic acid is shown in Scheme 4.

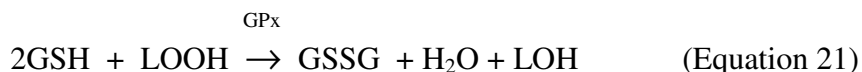


Scheme 4. Oxidation of linoleic acid by hydroxyl radical.³²

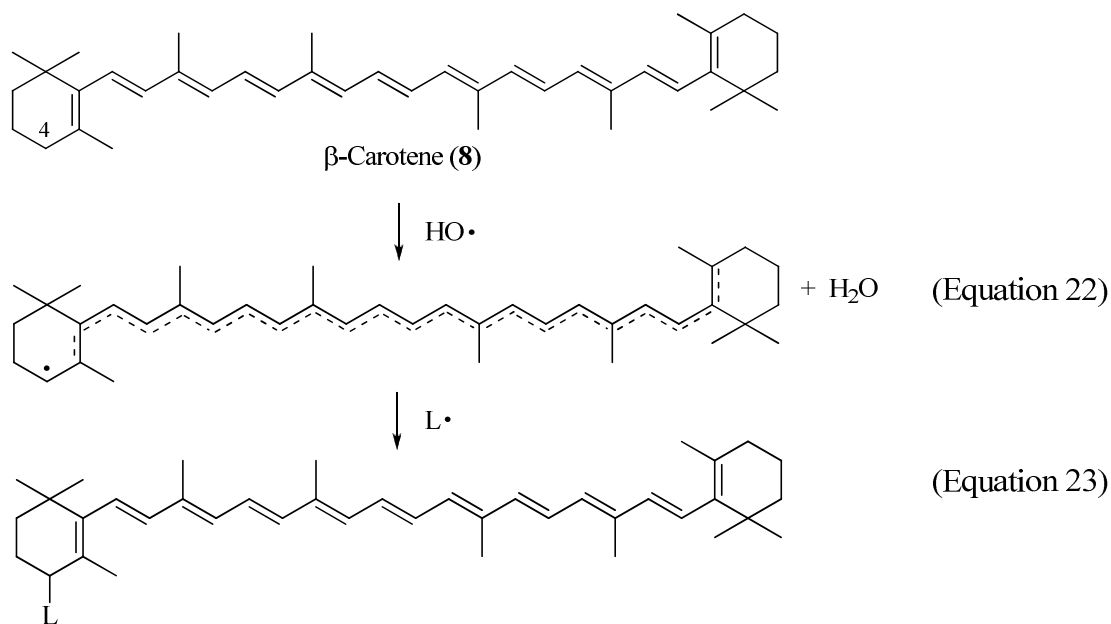
Lipid hydroperoxides formed in the membrane tend to adopt an orientation that allows the polar end of the molecule to move out of the hydrophobic core, and thus have the potential to disrupt the native architecture. Moreover, Diplock proposed that such events could activate a phospholipase enzyme that would cleave the peroxidized fatty acid (LOOH) from the phospholipid, rendering it susceptible to iron-catalyzed degradation to produce additional reactive radicals LOO• and LO• by the process shown in Equations 18 and 19.²⁵



Lipid peroxides (LOOH) can be decomposed by hydroperoxidases and glutathione to non-radical products such as alcohols (LOH) as shown in Equations 20 and 21, respectively.²⁷



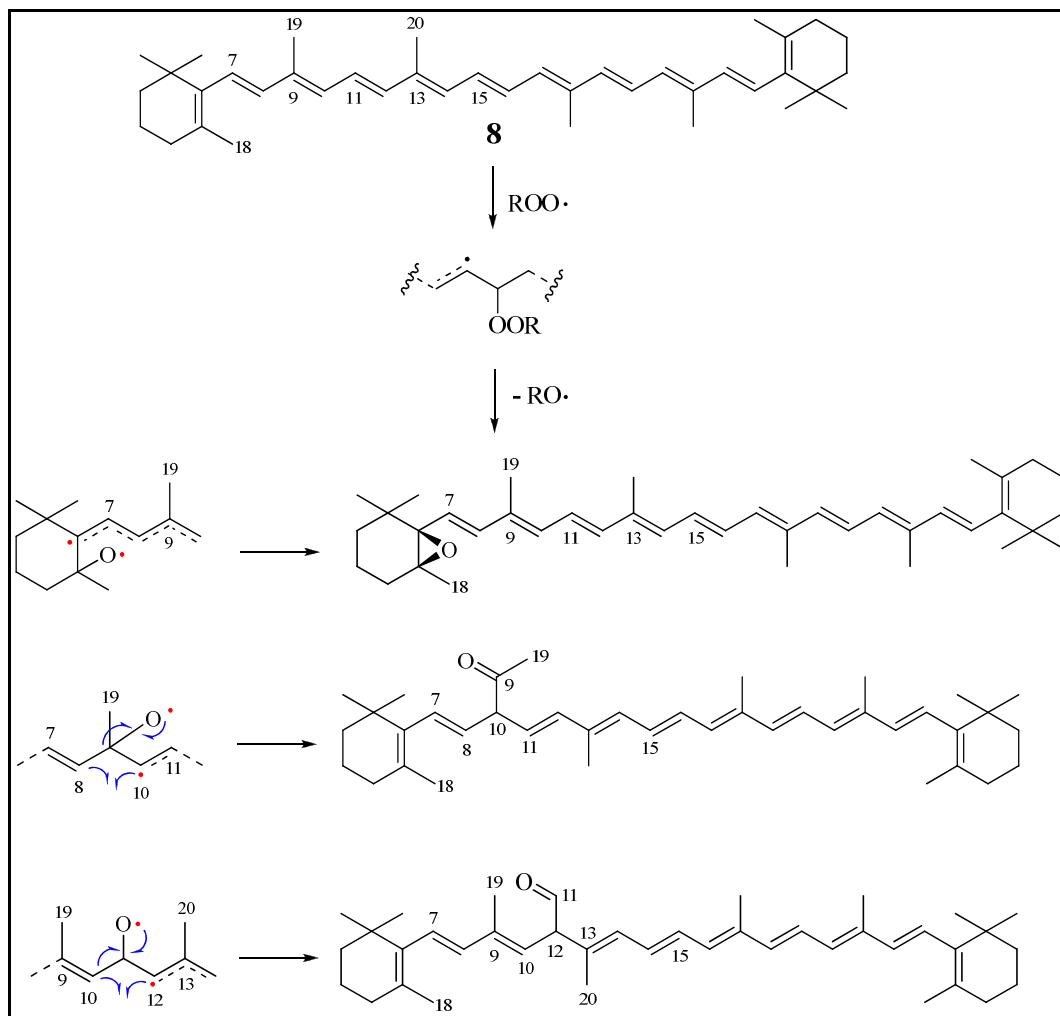
While vitamin E is the major lipid-soluble chain breaking antioxidant *in vivo*,³² carotenoids containing an allylic hydrogen atom at C4 such as β -carotene (**8**) and lycopene (**5**) can also attenuate lipid oxidation by intercepting the hydroxyl radical to form a resonance-stabilized free radical that is less reactive towards lipids and oxygen, as shown in Equation 22. Ultimately, carotenoids can terminate lipid peroxidation by combining with lipid free radicals $\text{L}\cdot$ to produce non-radical products as shown in Equation 23.^{26,32}



Experimental evidence from *in vitro* studies confirms that β -carotene (**8**), lycopene (**5**), zeaxanthin (**14**), astaxanthin (**10**) and canthaxanthin (**9**) are reactive towards hydroxyl radicals generated in a bulk phase.³⁵ Woodal and colleagues used a prototypical Fenton reaction to generate the hydroxyl radical from a mixture of ferric chloride, sodium ascorbate and hydrogen peroxide. The mixture was added to a solution

of carotenoid dissolved in alcoholic benzene. Reactions were monitored by visible absorption spectroscopy at the maximum wavelength of each carotenoid. Oxidation was evidenced by loss of absorbance and accompanied by rapid photobleaching. The slope of the initial tangent to the curve generated by plotting % residual pigment versus time was used to rank the antioxidant capacity of each carotenoid. Reactivity decreased in the order lycopene (**5**) > β -carotene (**8**) > zeaxanthin (**14**) > canthaxanthin (**9**) > astaxanthin (**10**). The electron withdrawing nature of the oxo group at C4 in canthaxanthin and astaxanthin was used to rationalize their decreased reactivity compared to that of lycopene and β -carotene. Semiempirical calculations confirmed that the electron density is substantially reduced at C4, C5 and C6 in astaxanthin.

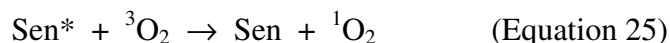
Reaction of β -carotene, lycopene, zeaxanthin, astaxanthin and canthaxanthin with alkyl peroxy radicals have also been modeled in benzene containing the free radical initiator 2,2'-azobis-2,4-dimethylvaleronitrile (AMVN) or 2,2'-azobis-isobutyronitrile (AIBN) and oxygen.^{35,36} The initiators dissociate at 37 °C to produce a steady supply of alkyl radicals (R•), which react with oxygen to form alkyl peroxy radicals (ROO•). These radicals reacted with carotenoids in the following decreasing order: Lycopene > β -carotene > zeaxanthin > canthaxanthin > astaxanthin. Reaction of **8** with AMVN produced a complex mixture of epoxides, apo-carotenones and apo-carotenals by a mechanism consistent with alkoxy radical addition to the conjugated polyene chain. Several of the products are shown in Scheme 5.³⁶



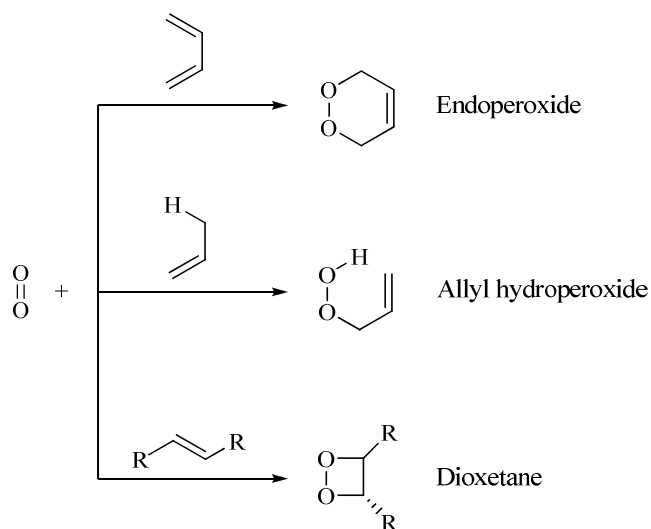
Scheme 5. Proposed pathway for formation of by-products obtained from the reaction of β -carotene (**8**) with alkylperoxyl radical ($\text{ROO}\cdot$).³⁶

The practical significance of alkyl radical scavenging properties exhibited by carotenoids was illustrated by *in vitro* studies where lycopene (**5**), β -carotene (**8**) and α -carotene (**7**) suppressed peroxidation of methyl linoleate fatty acid ester in a dose-dependent manner.^{35,38} The concentration of oxygen in tissues furthest from blood supply and in capillaries of active muscle is reportedly near 20 torr.²⁷ Therefore, carotenoids are theoretically capable of scavenging lipid peroxyl radicals that might be generated in tissues under physiological conditions.

Singlet oxygen is formed *in vivo* during the oxidation of unsaturated lipids by lipoxygenase, by neutrophils during respiratory burst where chloride or bromide ions are oxidized by myeloperoxidases needed for phagocytosis, and in living human eosinophils incubated in the presence of physiological concentrations of bromide ion.^{39,40} Upon exposure to UV light, singlet oxygen is generated in cells containing photosensitizers (Sen) such as chlorophyll, riboflavin, retinal, lipofuscin and dermal porphyrins. Light induces electronic transitions within these molecules, raising them to an excited state Sen* (Equation 24). The excess energy can be transferred to proximal ground-state oxygen molecules (³O₂) to produce singlet oxygen, while the photosensitized molecule Sen* returns to its ground state (Equation 25).

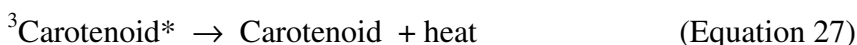


Unintercepted singlet oxygen can react with sensitizer molecules themselves and cause single-strand breaks in DNA. In biological tissue, singlet oxygen reacts with double bonds in unsaturated fatty acids and other biomolecules to produce endoperoxide, allyl hydroperoxide and dioxetane by-products as shown in Scheme 6.³² Being the more electrophilic species, singlet oxygen reacts with carbon-carbon double bonds 1500 times faster than ground state oxygen. Examples of destructive structural changes induced by singlet oxygen in humans are the development of macular degeneration and cataracts.²⁴



Scheme 6. Reaction products of singlet oxygen with olefins.³²

Endogenous carotenoids are able to play a protective role by absorbing the excess energy from singlet oxygen, thereby entering into an excited triplet state, $^3\text{Carotenoid}^*$ (Equation 26). Excited state carotenoids subsequently relax back to the ground state (Carotenoid) *via* loss of heat to the surroundings (Equation 27). In this process, known as physical quenching, the carotenoid is regenerated rendering it available to undergo further quenching cycles with singlet oxygen.



The direct reaction of β -carotene (**8**) with singlet oxygen occurs up to 0.1% of the time by a process known as chemical quenching.¹⁴ Apo-carotenals, apo-carotenones and endoperoxide by-products are obtained, as shown in Figure 4.⁴¹ Similar types of by-products from chemical quenching studies with lycopene (**5**) irradiated with UV light in the presence of methylene blue sensitizer have also been isolated and characterized.⁶

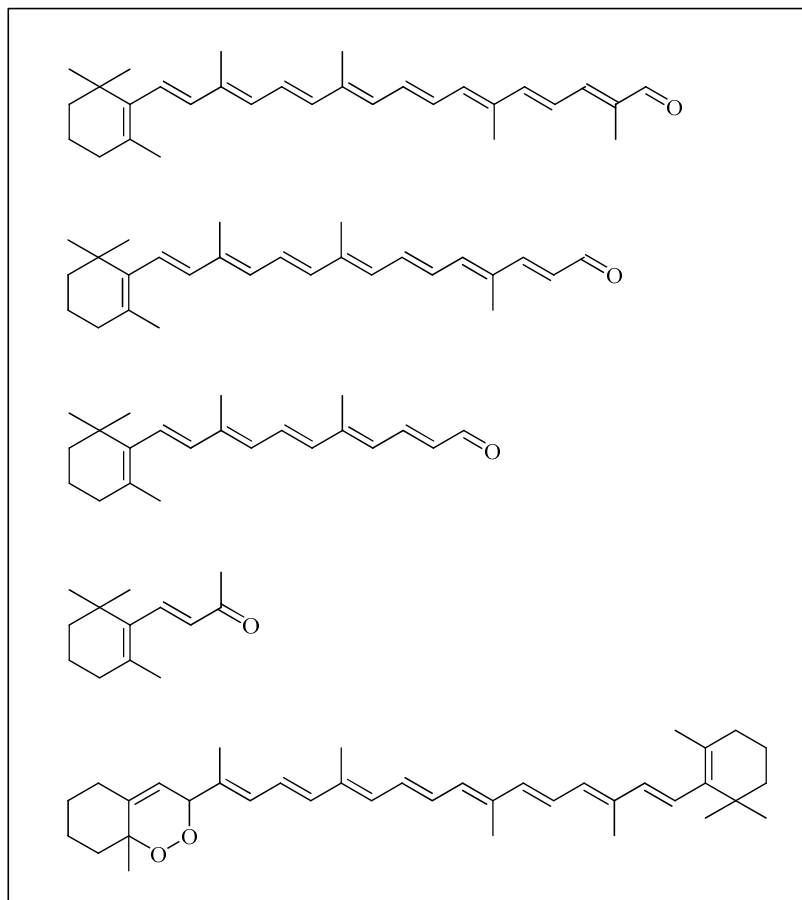


Figure 4. Products derived from chemical quenching of β -carotene (**8**) with singlet oxygen generated by illuminating a mixture of **8**/Rose Bengal/oxygen in organic solvent.⁴¹

The relationship between carotenoid structure and its reactivity towards singlet oxygen was gleaned from studies conducted by Di Mascio *et al.*⁴² Quenching rate constants were directly proportional to the length and planarity of the conjugated C=C chain. Compounds containing less than 8 double bonds such as retinoic acid (**17**) were incapable of quenching singlet oxygen. Lycopene (**5**) contains 11 conjugated planar double bonds, and exhibited the greatest quenching rate constant in a bulk phase, compared to the other carotenoids studied. Other studies also established **5** to be the most reactive carotenoid towards singlet oxygen.⁴³ Steric interactions between the C5 methyl group of the β -ionone ring and the vinylic proton on C8 in γ -carotene (**6**) cause the linear

portion of the conjugated backbone to rotate slightly out of the plane of the end group double bond, reducing orbital overlap on one end of the molecule. Orbital overlap is further decreased in β -carotene (**8**). Accordingly, quenching rate constants were found to decrease in the order lycopene (**5**) > γ -carotene (**6**) > β -carotene (**8**). Carotenoids with a keto group at C4 such as astaxanthin (**10**) and canthaxanthin (**9**) displayed enhanced quenching ability relative to **8**. The effect was attributed to the substituent's ability to lower the incipient triplet energy level of the carotenoid following energy transfer from the excited state of oxygen.⁴²

Evidence for a protective role of carotenoids against singlet oxygen was established from *in vitro* studies demonstrating that **8** could suppress the chlorophyll-sensitized photooxidation of methyl linoleate in solution.⁴⁴ Wagner *et al.* further demonstrated protective effects of carotenoids against singlet oxygen-mediated peroxidation of lipid residues in the LDL portion of human plasma. Thermal decomposition of a synthetic endoperoxide was used to generate singlet oxygen, which reacted with apo- β -protein at the hydrophilic interface of LDL, resulting in significant formation of phospholipid-hydroperoxides. Levels of lycopene (**5**) and β -carotene (**8**) versus lipid hydroperoxides in LDL were inversely correlated.⁴⁴ The ability of carotenoids to prevent singlet oxygen-mediated lipid oxidation was further demonstrated by Tinkler and colleagues. When human lymphoid cells were illuminated in the presence of the photosensitizer Rose Bengal and any of the carotenoids lycopene (**5**), β -carotene (**8**), astaxanthin (**10**) or canthaxanthin (**9**), membrane damage was significantly attenuated by the presence of carotenoids.⁴⁵ Efficacy decreased in the order lycopene (**5**) > β -

carotene (**8**) > astaxanthin (**10**) > canthaxanthin (**9**), as was also predicted by Di Mascio.⁴²

In vivo studies also provide evidence for a protective role of carotenoids against tissue damage from singlet oxygen in human subjects afflicted with the disease erythropoietic protoporphyria (EPP). EPP is caused by a deficiency of specific enzymes needed to produce and use porphyrins that are necessary for proper hemoglobin synthesis. The disease causes abnormal amounts of porphyrins sensitizers to build up in the body. Exposure to UV light triggers the formation of singlet oxygen in cutaneous skin, producing rashes, blistering, and scarring. However, oral supplementation with β -carotene (**8**) significantly increases the amount of time subjects can spend outdoors and is the only systemic treatment of EPP approved by the FDA.⁴⁶

The protective effect of lycopene (**5**) against chronic UV damage in humans has also been demonstrated. When skin from the forearm of 16 women was exposed to a single dose of UV radiation equal to three times the amount necessary to induce minimal erythema, the concentration of **5** decreased from 31-46% compared to levels of **5** in adjacent, non-exposed skin. Concentrations of β -carotene (**8**) were unaffected, suggesting that **5** is more protective than **8** against oxidative damage to tissues.⁴⁷

A broad range of *in vitro* studies have established that antioxidants can effectively mitigate damage to DNA and delay or significantly inhibit lipid peroxidation and a variety of malignant transformations.¹⁴ The extensively conjugated polyene chain of carotenoids can effectively absorb light and quench deleterious ROS generated endogenously, such as singlet oxygen, hydroxyl radicals, and lipid peroxy radicals.⁴¹ As such, carotenoids are effective antioxidants. As evidence for their ability to function as

antioxidants *in vivo*, oxidized metabolites of lutein, zeaxanthin and lycopene have been detected and identified in human serum and milk.³⁻⁵ Moreover, in a 4-week study to compare the bioavailability of lycopene from food versus supplements, the concentration of a lycopene metabolite was significantly higher in the plasma of human subjects relative to baseline concentrations after having consumed a controlled amount of lycopene twice per day from tomato juice, tomato oleoresin and lycopene beadlets.⁴⁸

Factors that influence the antioxidant activity of carotenoids in biological systems include their structure, cellular orientation, concentration, the partial pressure of oxygen and synergistic interaction with other antioxidants.²⁶ The hallmark feature of all carotenoids is the extensively conjugated double bond system. This structural element is necessary for energy transfer reactions that occur during photosynthesis and endows carotenoids with the special ability to quench singlet oxygen without being consumed. Their lipophilic nature restricts carotenoids to hydrophobic regions of cells, although polar substituents influence their solubility and orientation within membranes. For example, the hydroxyl end groups of zeaxanthin (**14**) tend to anchor this carotenoid vertically across a lipid bilayer membrane whereas more hydrophobic carotenes such as β -carotene (**8**) and lycopene (**5**) tend to be horizontally positioned within the hydrophobic core, as shown in Figure 5. Different orientations are expected to affect membrane fluidity and importantly, oxygen permeability, as lower levels of intracellular oxygen are expected to result in less lipid peroxidation. Orientation also influences the local environment within a cell, as evidenced by the unique effects of different carotenoids on the organization and function of pigment-protein complexes associated with light harvesting in plants.²⁶

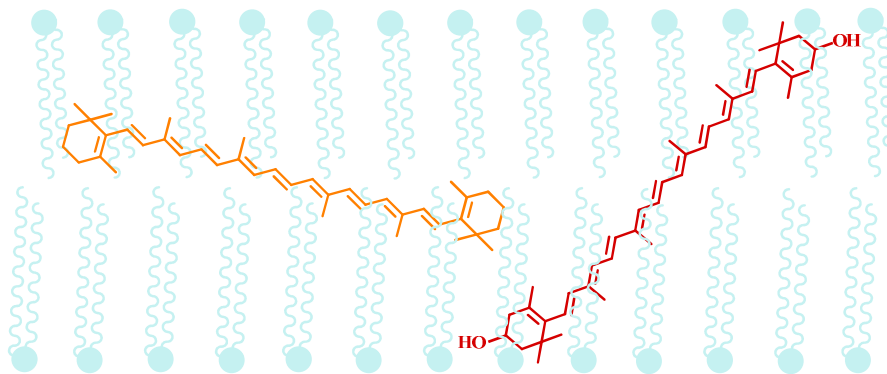


Figure 5. Schematic representation of β -carotene (**8**) and zeaxanthin (**14**) oriented across a lipid membrane.²⁶

Carotenoids appear to interact synergistically with other antioxidants, especially vitamins C and E. Evidence for the plausibility of this mechanism was provided by Jialal *et al.*, who demonstrated that ascorbate effectively preserved 76% and 95% of native tocopherols and β -carotene (**8**) present in human LDL during copper (II) mediated production of lipid peroxides, respectively. In the absence of vitamin C, **8** was undetected while 5% of the total tocopherols remained after the experiment.⁴⁹ Meanwhile, Palozza and Krinsky demonstrated that a combination of **8** and α -tocopherol could inhibit free radical induced lipid peroxidation of rat liver microsomes to a greater extent than the sum of the inhibition afforded by either compound alone.⁵⁰

While epidemiological studies have demonstrated an inverse correlation between increased consumption of dietary β -carotene (**8**) and the development of lung cancer, pro-oxidant effects have actually been observed in studies involving high doses of **8** administered in supplement form. The CARET (Carotene and Retinol Efficacy Trial) study was conducted in 18,000 high-risk smokers in the US. During the study, researchers found that consumption of a daily combination of 30 mg **8** and 25,000 international units (IU) retinyl palmitate resulted in a 28% increase in the incidence of

lung cancer and the trial was ended 21 months prematurely.⁵¹ Because cigarette smoke contains hydrogen peroxide and superoxide anion radical, these phenomenon were thought to result from pro-oxidative effects produced by extraordinary levels of oxidative by-products having formed in the presence of these ROS and oxygen in lung.¹⁴ It is interesting to note that lung tissue taken from ferrets exposed to cigarette smoke contained higher concentrations of oxidation by-products of β -carotene (**8**) compared to controls.²⁶

In support of this hypothesis, benzo[a]pyrene metabolites were found to bind more effectively to calf thymus DNA in the presence of oxidative products of BC while binding was inhibited by β -carotene itself.⁵² In an *in vitro* model, Lowe *et al.* demonstrated that higher levels of endogenous carotenoids can lose their antioxidant effects. Hydrogen peroxide was generated by the xanthine/xanthine oxidase system in the presence of HT29 cells, and either β -carotene (**8**) or lycopene (**5**). Both carotenoids protected cells against oxidative damage to DNA at concentrations up to 3 μ M, or typical levels that would be present in the plasma of human subjects consuming dietary carotenoids. However at concentrations three times this level, the protective effects of both **8** and **5** were lost.⁵³

The first observation of the biological activity of lycopene (**5**) was reported by Ernster and co-workers in 1959, who showed a significant increase in the survival rate among mice exposed to X-Rays after intraperitoneal injections with **5**/Tween-80/saline, compared to controls.⁵⁴ The same year, the authors also demonstrated a significant increase in the survival of mice receiving either β -carotene (**8**) or **5** by the same route of

administration, prior to infection by a highly virulent strain of *K. pneumonia* bacteria.⁵⁵ Other biological properties of **5** have been reviewed by Nguyen and Schwartz.³⁸

In 1968, the discovery by Foote and colleagues that **8** is capable of deactivating singlet oxygen stimulated further interest on the potential biological effects of this and other carotenoids.⁵⁶ In 1977, Epstein conducted the first experiment demonstrating a significant inverse correlation between the development and growth of UV induced skin tumors in mice receiving **8** by intraperitoneal injection.⁵⁷ These observations led Peto *et al.* to propose in 1981 that dietary β -carotene (**8**) could be associated with a decreased risk for cancer development in humans.⁵⁸ The hypothesis has been supported by results from many biological⁵⁹ and epidemiological studies that have consistently established an inverse correlation between consumption of carotenoid-rich fruits, vegetables and juices and the risk of developing cancers of the mouth and throat, epithelial, breast, cervix, bladder, pancreas and prostate gland.⁶⁰⁻⁶³ Beyond chemoprevention, dietary carotenoids have been shown to confer significant protection against developing age-related macular degeneration,⁶⁴ ischemic stroke,⁶⁵ and cardiovascular disease.^{66,67} Although these foods contain many nutritionally relevant vitamins and minerals, carotenoid content has often been correlated most strongly with decreased risk.⁶⁸

Beyond the value of carotenoids in mitigating tumor development in mice,^{3,6,57,69,70} results from an *in vitro* study showed that lycopene (**5**) was capable of inhibiting the proliferation of human endometrial, mammary and lung cancer cells seeded in culture media to a greater extent than α -carotene (**7**) and β -carotene (**8**). The enhanced effect of lycopene was attributed to its proven ability to suppress secretion of specific insulin-like growth factors that stimulate uncontrolled division in endometrial and breast

cancer cells.^{71,72} Strong evidence that dietary carotenoids can discourage development of cancer in humans was provided by results from a human intervention study led by Pool-Zobel.⁷³ In subjects consuming either lycopene from tomato juice, α -carotene and β -carotene from carrot juice or lutein from powdered spinach, the number of DNA strand breaks in peripheral blood lymphocytes was significantly lower than in controls.

Results from clinical trials have shown that retinoids can be used topically or administered orally to effect regression of premalignant lesions, reduce the number of primary lesions and prevent occurrence of secondary malignancies in basal and squamous cell skin cancers in humans.⁷⁴ While the provitamin A activity of β -carotene (**8**) and α -carotene (**7**) may be invoked to explain the tumor suppressive properties of these carotenoids, the proven efficacies of lycopene (**5**), lutein (**13**) and canthaxanthin (**9**) suggests that provitamin A activity is not a necessary condition for the tumor suppressive function of carotenoids. Nevertheless, dietary retinoids are generally recognized for their ability to prevent a variety of human cancers by increasing the expression of connexin 43, the most widely expressed member of the family of genes that codes for the transcription of a connexin, a gap junction protein necessary for direct transfer of signals, nutrients and waste products between contacting cells.^{75,76} In many studies, increased gap junction communication has been associated with increased control over cancerous growth.⁷⁷ In regards to this finding, several researchers showed that diverse carotenoids such as zeaxanthin (**14**), lycopene (**5**), β -carotene (**8**), and canthaxanthin (**9**) increased gap junctional communication in mouse embryo fibroblasts and cultured human keratinocytes in a dose-dependent manner.^{3,78}

In this regard, the ability to upregulate the expression of connexin 43 may be one mechanism by which carotenoids function as chemopreventive agents. As was the case for tumor suppression, provitamin A activity alone does not explain the enhanced gap junctional communication afforded by canthaxanthin, zeaxanthin and lycopene. Further, Stahl found no correlation between the singlet oxygen quenching ability of carotenoids and their ability to enhance gap junctional communication in mouse cells⁷⁹ while Zhang found no correlation between the ability of carotenoids to inhibit lipid peroxidation and GJC communication.⁷⁸ Therefore, carotenoids appear to be able to modulate the development of cancer by several mechanisms.

While catalases and peroxidases effectively control the amount of hydrogen peroxide and lipid peroxide that can accumulate intracellularly, epoxidation of lycopene might provide an alternative mechanism for scavenging hydrogen peroxide generated *in vivo*. In support of this hypothesis, a series of oxygenated carotenoids including lycopene-1,2-epoxide (**19**) have been isolated from red tomato fruit⁸⁰⁻⁸² and guava juice.⁸³ Identification of **19** was based on retention time by HPLC, properties of the UV-visible absorption spectra, and results of mass spectral analysis compared with a standard of lycopene-1,2-epoxide synthesized by reaction of lycopene with *m*-chloroperoxybenzoic acid (*m*-CPBA). The structure of **19** is shown in Figure 6.

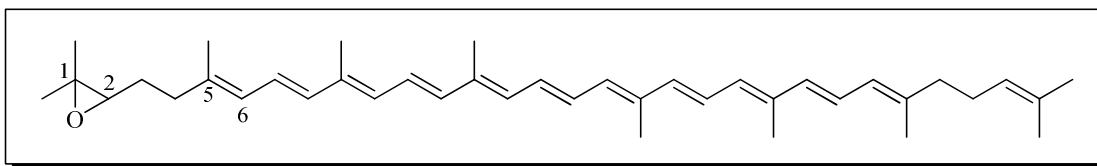


Figure 6. Lycopene-1,2-epoxide (**19**).

In a formal study conducted by Lu *et al.*, **19** was synthesized with either *m*-CPBA or acidified hydrogen peroxide reagents in 10% and 4% yields, respectively.⁸⁴

Significantly, a new oxidation product of lycopene was isolated from the reaction mixtures and given the name 1,5-epoxyiridanyl-lycopene (**20**), as shown in Figure 7.

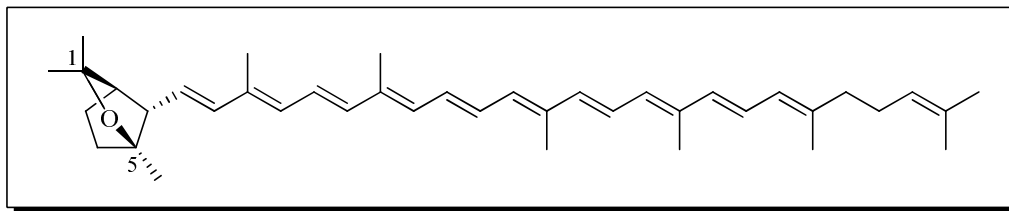


Figure 7. 1,5-Epoxyiridanyl-lycopene (**20**).⁸⁴

Compound **20** was produced in 2% and 6% yields when lycopene was treated with *m*-CPBA or acidified hydrogen peroxide, respectively. Both reactions were carried out in methylene chloride. The structural characterization and relative stereochemistry of **20** were assessed by molecular weight determination by mass spectral analysis, UV-visible absorption characteristics, IR spectra and 2D NMR experiments.

In 1997, Yokota *et al.*⁸⁵ also accomplished the synthesis of **19** and **20** in 4% and 6.5% yields respectively from the epoxidation of lycopene with acidified hydrogen peroxide in methylene chloride. Moreover, a novel hydrolyzed derivative of **20** was isolated in 3.3% yield from the chemical synthesis and named 1,5-dihydroxyiridanyl-lycopene (**21**). Yokota also isolated **21** from tomato puree in 0.0003%.⁸⁵ The structure of **21** is shown in Figure 8.

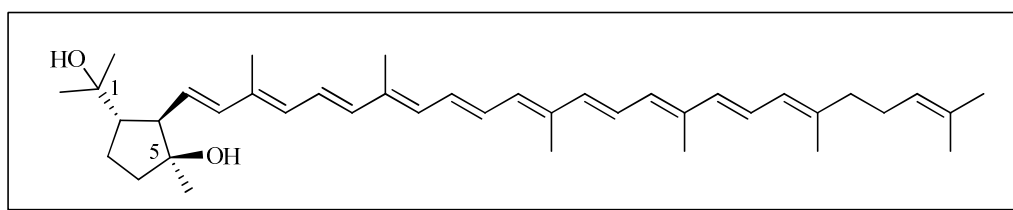


Figure 8. 1,5-Dihydroxyiridanyl-lycopene (**21**).⁸⁵

Structural characterization and relative stereochemistry of **21** were assessed by molecular weight determination by mass spectral analysis, UV-visible absorption characteristics, IR spectra and 2D NMR experiments.

Oxidized metabolites of lycopene have also been identified by Khachik *et al.* based on results of HPLC analyses. In 1992, lycopene-1,2-epoxide (**19**) was detected in tomatoes and tomato paste.⁸² In 1997, diol **21** and its diastereomer **22** were detected in the serum and milk of lactating mothers.⁴ The structure of **22** is shown in Figure 9.

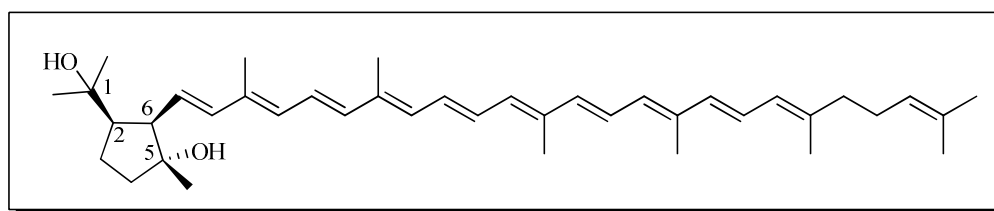


Figure 9. Structure of 2,6-Cyclolycopene-1,5-diol (**22**) identified by Khachik.⁴

Lycopene oxidation with *m*-CPBA was studied more extensively by Khachik *et al.* who proved that this compound is first oxidized at the 1,2- and the 5,6-positions to form lycopene-1,2-epoxide (**19**) and lycopene-5,6-epoxide (**23**), based on the reversed phase HPLC profile of the crude reaction.⁸⁶ The structure of **23** is shown in Figure 10.

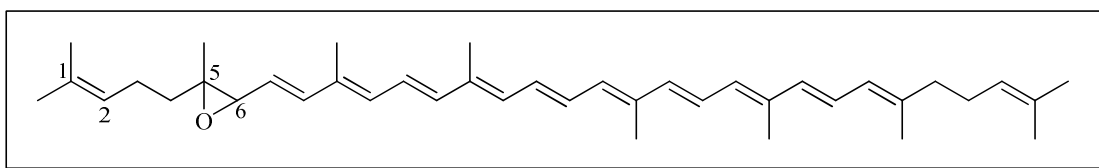


Figure 10. Lycopene-5,6-epoxide (**23**).

After purification by flash column chromatography on silica gel, **19** was found to be quite stable and was isolated in 15% yield. However, **23** was shown to be highly unstable in the presence of mildly acidic hydroxyl groups on silica and underwent intramolecular cyclization during normal phase HPLC and purification by flash column

chromatography to give a mixture of bicyclic oxides **20** and **24** in 12% and 2% respectively. The structure of **24** is shown in Figure 11, and has been given the name 2,6-cyclolycopene-1,5-epoxide.

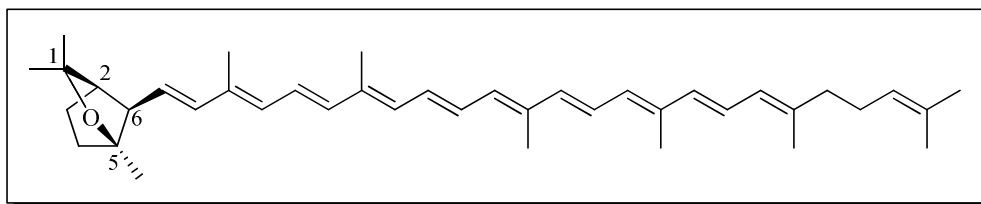
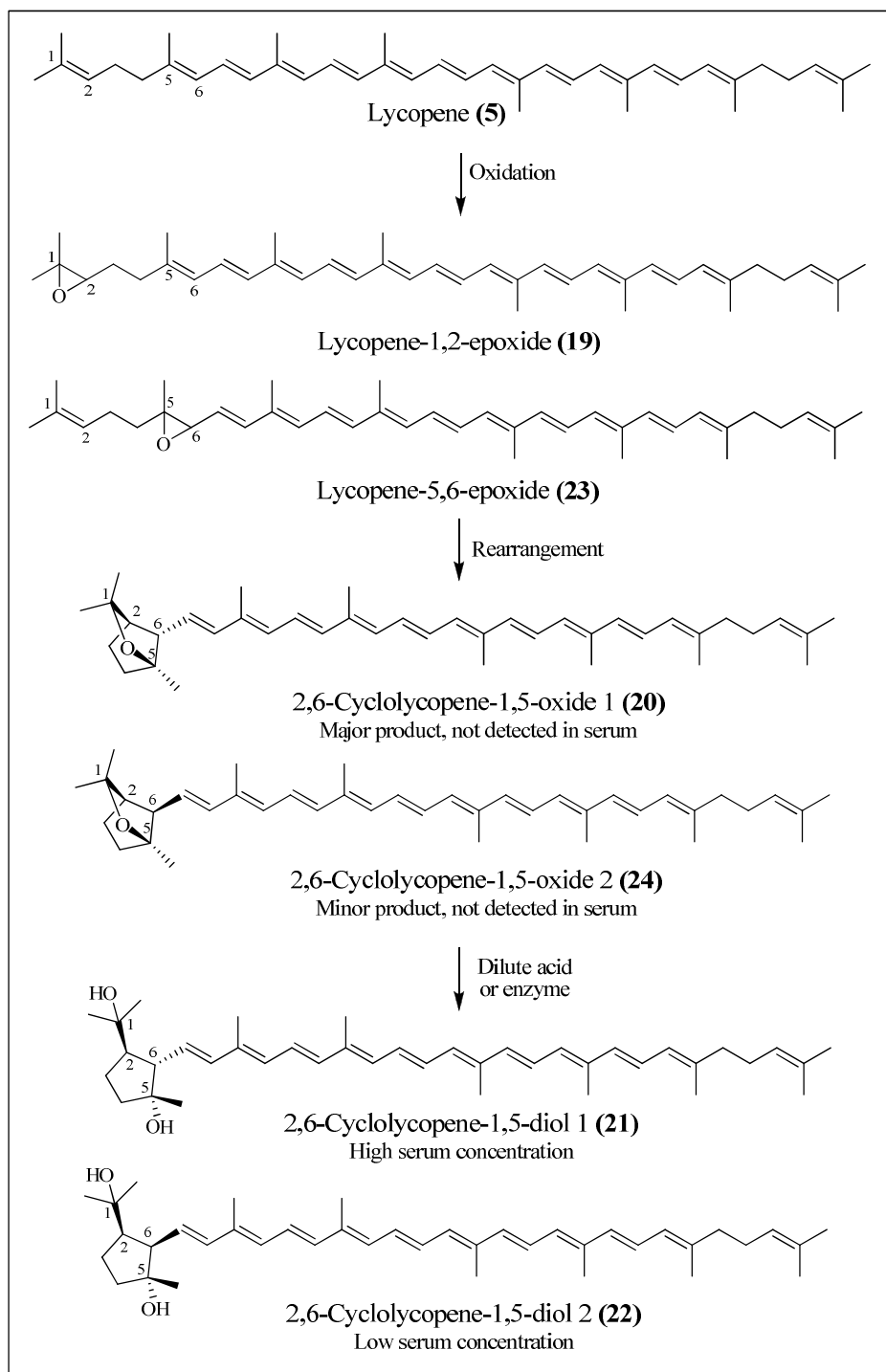


Figure 11. Structure of 2,6-cyclolycopene-1,5-epoxide (**24**) isolated by Khachik *et al.*⁸⁶

Diols **21** and **22** were also isolated in 12% and 4%, respectively. Bicyclic oxides **20** and **24** and 2,6-cyclolycopene-1,5-diols **21** and **22** were also identified in tomato paste, tomato juice and human serum. Their structures and relative stereochemistry were confirmed by comparison of the HPLC-UV/Vis-MS profiles with those of fully characterized synthetic compounds. Detailed structural assignments were based on results from COSY, DEPT-135, HMQC and HMBC NMR experiments. The diols contain three asymmetric centers at C2, C5, and C6. While the relative configurations at these centers were determined by a T-ROESY experiment, the absolute configurations of these diols were not established.⁸⁶

Based on results from the chemical oxidation of lycopene with *m*-CPBA and the detection of the 1,5-bicyclic oxide and 1,5-diol metabolites in tomato products, Khachik *et al.* proposed the metabolic pathway for lycopene shown in Scheme 7.⁸⁷ Accordingly, lycopene 1,2- and 5,6-epoxides (**19** and **23**) might be formed under typical conditions for metabolic oxidation in biological tissues. Intramolecular rearrangement of lycopene-5,6-epoxide (**23**) can afford bicyclic oxides **20** and **24** as intermediates under acidic conditions present in tomato fruit and during digestion, although neither bicyclic oxide

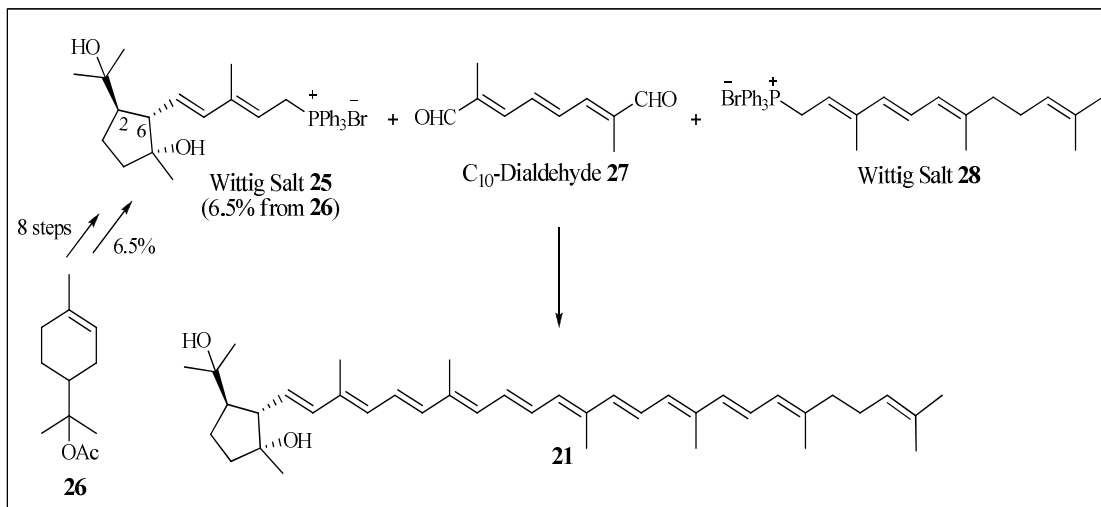
has been detected in human serum to date. Ultimately, the bicyclic oxides can undergo acid and/or enzyme-mediated ring opening to the respective diols **21** and **22**.⁸⁷



Scheme 7. Proposed metabolic pathway of lycopene in humans and tomato-based food products.⁸⁷

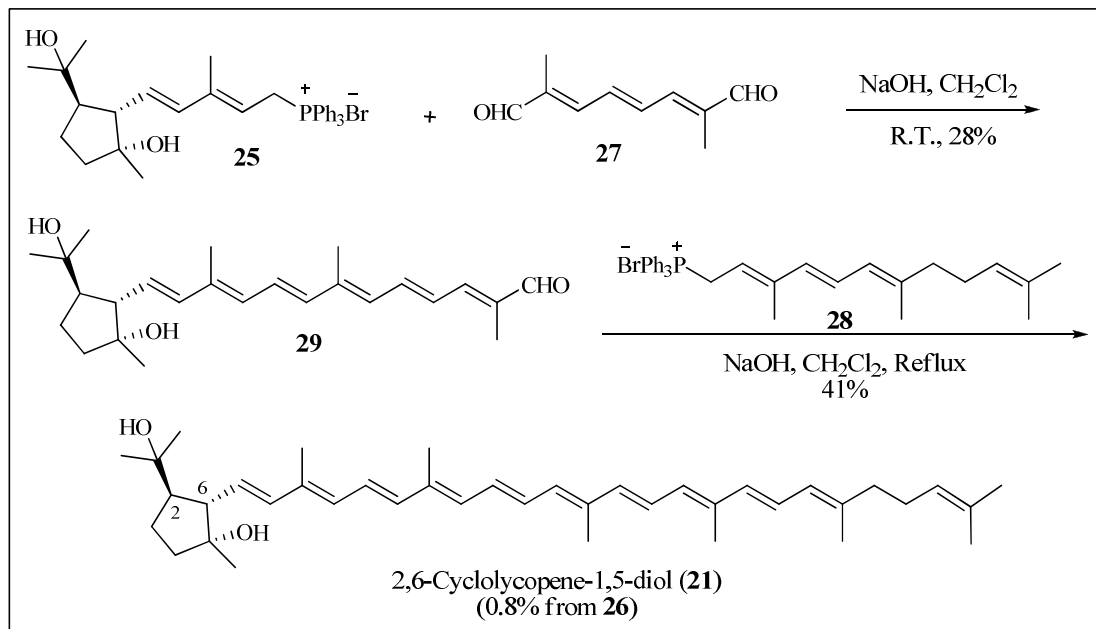
It is interesting to note that supplementation of healthy human subjects with purified lycopene was accompanied by increased serum levels of diols **21** and **22**.⁴⁸ Results of *in vitro* studies provide evidence for the biological activity of these diols. These metabolites were more effective than lycopene in up-regulating the transcription of connexin 43 in mouse embryonal fibroblasts and human keratinocytes at concentrations present in serum.^{3,68,88} Further, results from an *in vitro* study conducted by the Division of Cancer Treatment and Diagnosis at the National Cancer Institute demonstrated that diols **21** and **22** can inhibit the growth of solid human tumor cells of the breast, lung and central nervous system to 32% or less compared to untreated cells. The compounds were further tested over five concentration ranges in a 60-cell panel and found to moderately inhibit the growth of leukemia, non-small cell lung, colon, melanoma, ovarian, renal, kidney, central nervous system and prostate tumors in humans.⁸⁹ The biological activities of **21** and **22** may explain some of the chemopreventive effects associated with lycopene.

To date, the only total synthesis of diol **21** was accomplished by Traber and Pfander in 1998.⁹⁰ Their strategy was based on the C₁₅+C₁₀+C₁₅ double Wittig coupling reaction shown in Scheme 8. The novel Wittig salt **25** was prepared with defined relative stereochemistry from α -terpinylacetate (**26**) in 7 steps in 6.5% overall yield. The C₁₀-dialdehyde synthon **27** (2,7-dimethyl-2,4,6-octatrien-1,8-dial) was commercially available while Wittig salt **28** was prepared according to the procedure previously reported in high yield for the synthesis of lycopene⁹¹ and several Z-isomers of lycopene.⁹²



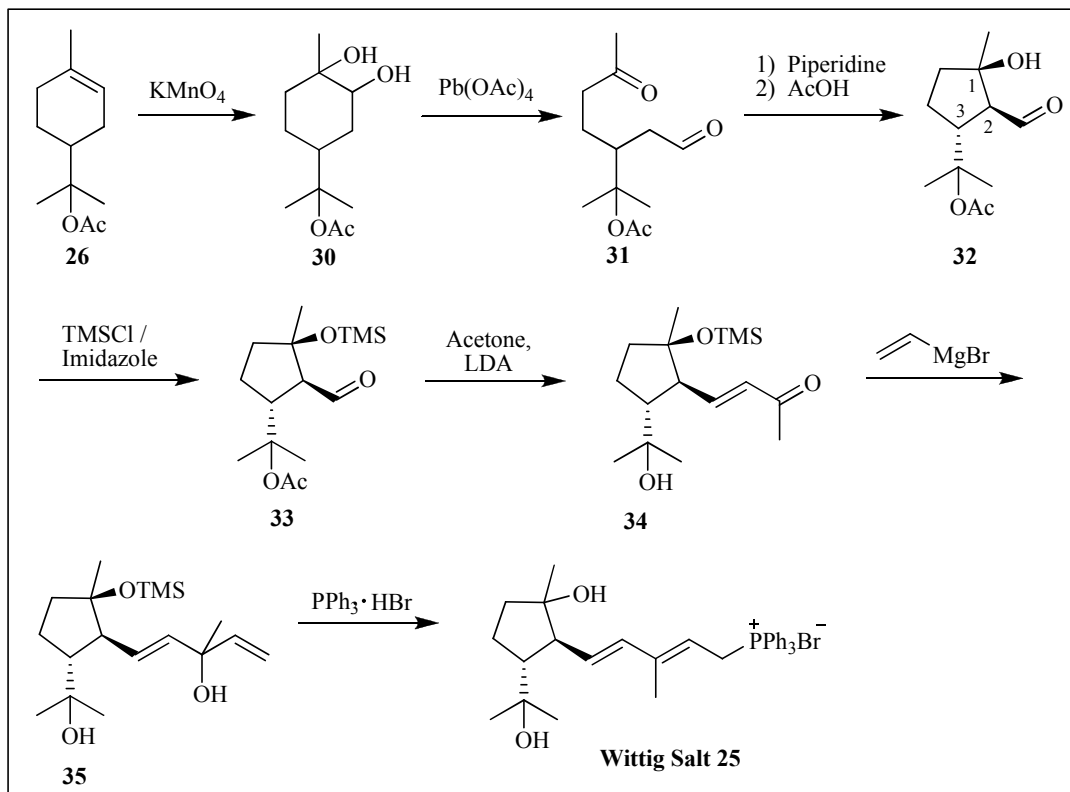
Scheme 8. C₁₅+C₁₀+C₁₅ Wittig olefination strategy used by Traber and Pfander.⁹⁰

The stepwise coupling of synthons **25**, **27** and **28** is illustrated in Scheme 9. Wittig salt **25** was first coupled with C₁₀-dialdehyde (**27**) under basic conditions in methylene chloride at room temperature to afford the C₂₅-cyclized aldehyde intermediate (**29**) in 28% yield. Use of a slight excess of **25** and the decreased reactivity of the longer chain aldehyde **29** encouraged formation of the monocondensation product. In the final step, **29** was coupled with Wittig salt **28** using sodium hydroxide in methylene chloride under reflux to produce **21** in 41% yield. The overall yield of 2,6-cyclolycopene-1,5-diol (**21**) was 0.8% from the alpha-terpinyl acetate (**26**).



Scheme 9. Double Wittig coupling of C₁₀-dialdehyde **27** with Wittig salts **25** and **28**.⁹⁰

To arrive at Wittig salt **25**, Traber and Pfander employed the strategy shown in Scheme 10. The starting material alpha-terpinyl acetate (**26**) was oxidized under neutral conditions with KMnO₄ to yield the vicinal diol **30**, which underwent oxidative cleavage with lead tetraacetate to ketoaldehyde **31**. Intramolecular aldol condensation of **31** in the presence of piperidine followed by treatment with acetic acid resulted in the formation of the formylcyclopentanol **32** with the indicated relative stereochemistry. After the alcohol moiety was protected with TMSCl to afford **33**, aldol condensation with the enolate anion of acetone produced the α,β -unsaturated ketone **34**. Alkylation with vinylmagnesium bromide produced allylic alcohol **35**. In the final step, reaction of **35** with Ph₃P·HBr afforded Wittig salt **25**. Traber and Pfander's synthesis of **25** was accomplished in just 6.5% overall yield from **26**.



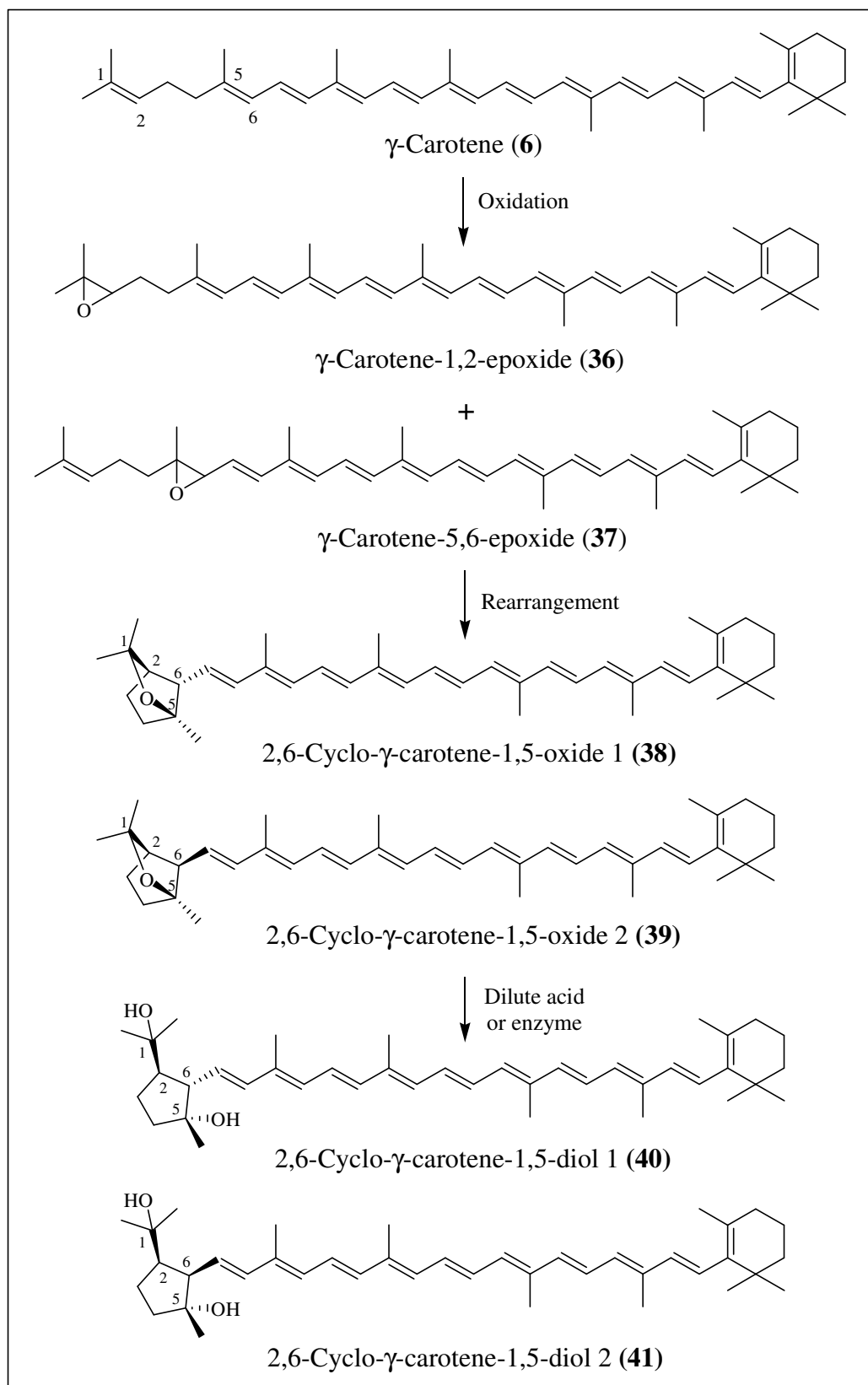
Scheme 10. Synthesis of Wittig salt **25** according to Traber and Pfander.⁹⁰

Upon formation of **32**, two new stereocenters were generated. The stereochemistry of **32** was established by proton NMR spectroscopy, where a large coupling constant of 9.9 Hz between protons at C2 and C3 suggested a dihedral angle near 180°. Moreover, the indicated conformation is expected to be the most thermodynamically stable arrangement, with the bulky acetoxyl substituent at C3 and the carbaldehyde at C2 in a *trans* relationship to one another. Further, the authors concluded that the *cis*-position of the hydroxyl group at C1 would allow intramolecular hydrogen bonding with the carbonyl group of the aldehyde. The relative stereochemistry of **32** was preserved in successive transformations to produce Wittig salt **25** and compound **21**. The relative stereochemistry of **21** was confirmed by comparing the chemical shift and

coupling constants of protons at C2 and C6 with those reported by Khachik *et al.* for this particular stereoisomer.²⁷

γ -Carotene (**6**) with a β -end group and a Ψ -end group is a structural hybrid of β -carotene (**8**) and lycopene (**5**), and would be expected to possess similar functional roles in living systems. While γ -carotene occurs in some of the same foods as these carotenoids, especially apricots and tomatoes,^{9,10} *Cryptocodinium cohnii* (*C. cohnii*) algae are a more obscure dietary source of this carotenoid.⁹³ This algal strain produces an abundance of γ -carotene along with a lower amount of β -carotene. Lipid soluble extracts of *C. cohnii* are added to many foods, beverages, infant formulas and nutritional supplements as a vegetarian source of docosahexaenoic acid (DHA). DHA is an omega-3 polyunsaturated fatty acid found to be essential for healthy brain and cardiovascular function.⁹⁴ Although γ -carotene is less prevalent in commonly consumed foods than other prominent carotenoids such as β -carotene and lycopene, it has been identified in the extracts from human serum and breast milk.⁴

Because of its structural similarities to lycopene, **6** would be expected to undergo metabolic transformations analogous to this carotenoid as proposed in Scheme 11.



Scheme 11. Proposed metabolic oxidation of γ -carotene (6).

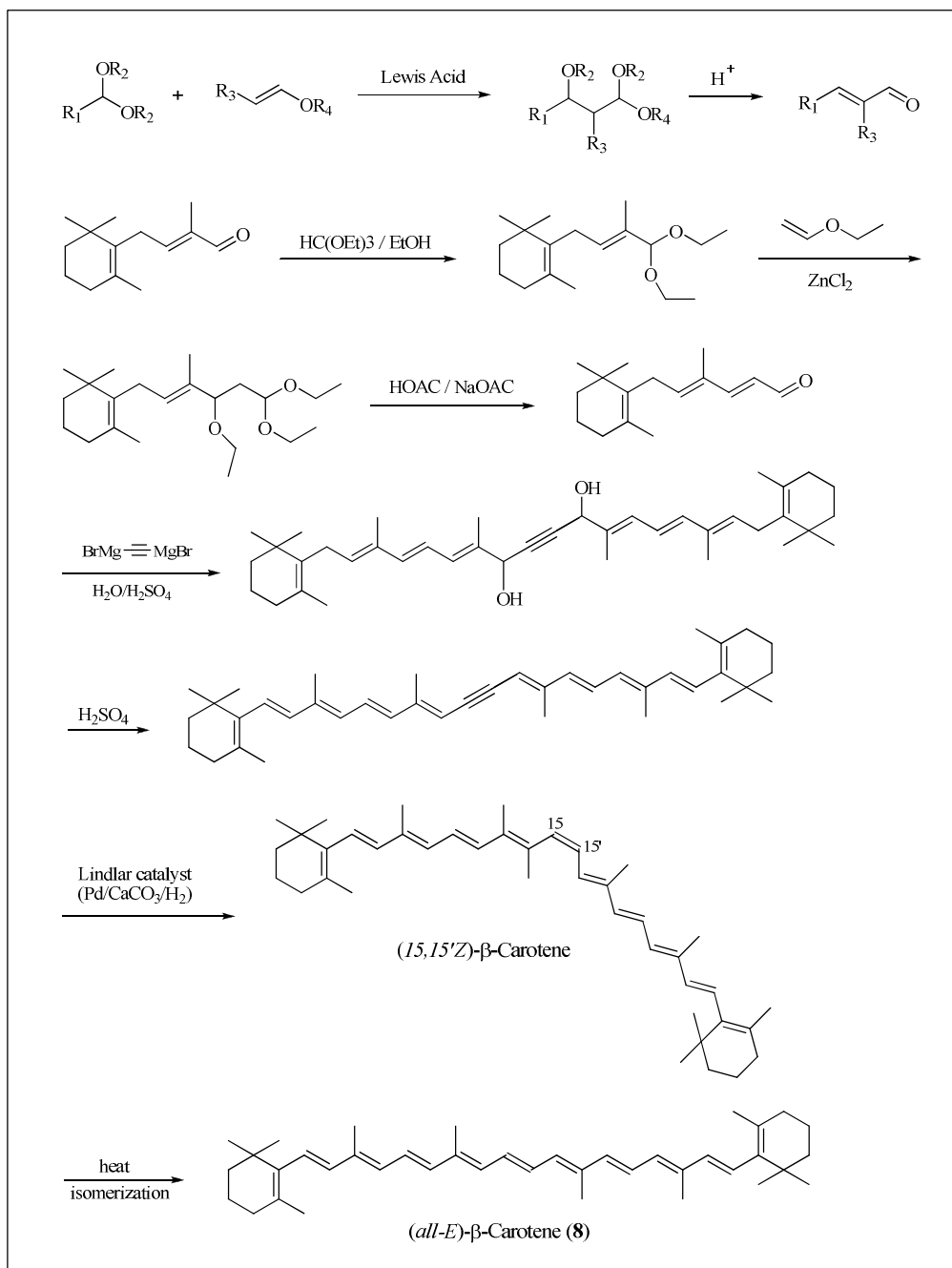
In fact, γ -carotene-1,2-epoxide (**36**) has been isolated from the Delta tomato mutant.⁹⁵ Therefore, one likely pathway for the metabolism of **6** is the oxidation of the Ψ -end group of this carotenoid at the 1,2- and 5,6-positions, resulting in the formation of **36** and **37** respectively. Similar to the established oxidative pathways for lycopene, **37** would be expected to undergo acid and/or enzyme catalyzed rearrangement to 2,6-cyclo- γ -carotene-1,5-oxides (**38**) and (**39**) followed by ring opening to 2,6-cyclo- γ -carotene-1,5-diols (**40**) and (**41**).

While the rate constant for singlet oxygen quenching by γ -carotene (**6**) has been studied in an *in vitro* model,⁴³ the metabolic fate of this dietary carotenoid in living systems is not known at present. In addition, the chemopreventive properties of **6** and/or its possible metabolite(s) in relation to their anti-inflammatory and antioxidant activities have not yet been explored. Therefore, the objectives of this research are to:

1. Develop a viable strategy for the total synthesis of the possible oxidative metabolites of γ -carotene (**6**), including 2,6-cyclo- γ -carotene-1,5-diols (**40**) and (**41**);
2. Accomplish this synthesis from an end-group that can serve as a precursor for the total synthesis of lycopene metabolites, namely, diols **21** and **22**;
3. Investigate the presence of the oxidation products of γ -carotene in human plasma, algal extracts and tomato products that are the major dietary sources of this carotenoid.

DISCUSSION

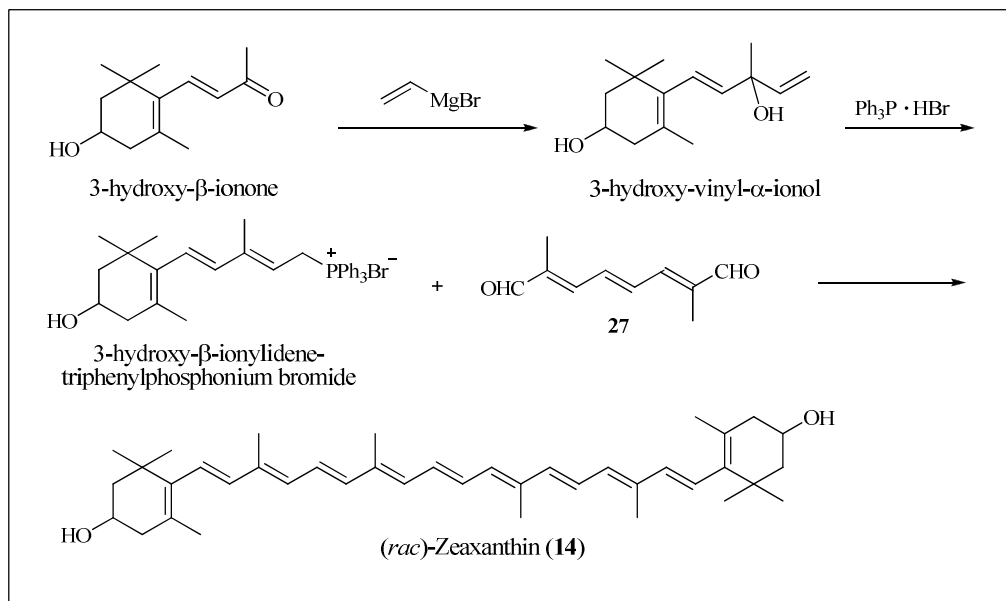
In 1950, Karrer,⁹⁶ Milas⁹⁷ and Inhoffen⁹⁸ independently accomplished the synthesis of the first carotenoid, β -carotene. By 1976, ninety-eight naturally occurring carotenoids had been synthesized by the general strategy of coupling various end-groups to a central, conjugated polyene synthon with the use of Grignard reactions, enol ether condensations, palladium and titanium-mediated C-C bond formations, Julia sulphone and Wittig coupling reactions. While aldol condensations between aldehydes and ketones have found application in the total synthesis of carotenoids that are not sensitive to bases,⁹⁹ a more common approach to C-C bond formation is the enol ether condensation. The process was discovered by Isler and colleagues in 1939, and has been used for the industrial synthesis of β -carotene (**8**).¹⁰⁰ Chain lengthening by two or more carbons occurs during the Lewis acid coupling of an alkyl enol ether with an acetal to produce an unsaturated aldehyde, which can then be coupled with a Grignard reagent. Acid-catalyzed dehydration followed by partial *cis*-reduction with the Lindlar catalyst afforded 15,15'-*Z*- β -carotene. After refluxing in an organic solvent such as heptane, the 15*Z*-isomer could be transformed into the thermodynamically more stable (*all-E*) form of **8** (Scheme 12). However, this approach cannot be employed in the synthesis of carotenoids with acid-sensitive end groups.



Scheme 12. Synthesis of (*all-E*)- β -carotene (**8**) via enol ether condensation.

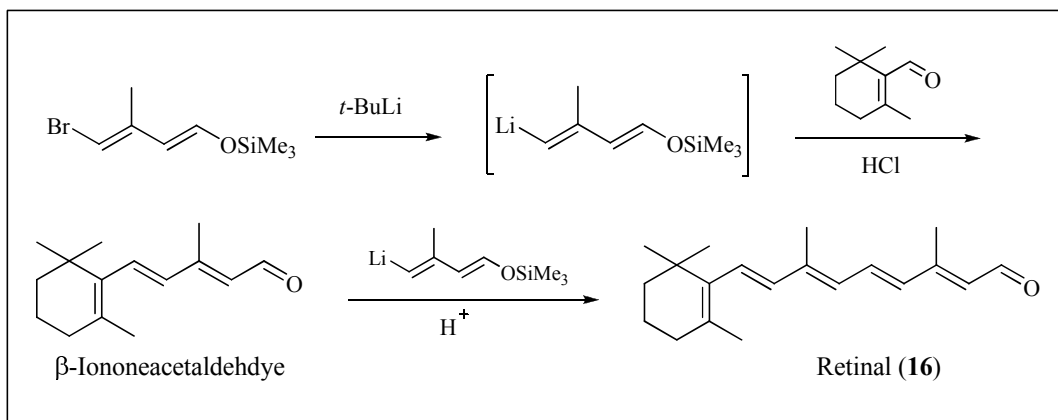
The combination of organometallic and Wittig reactions find application in the synthesis of carotenoids such as (*rac*)-zeaxanthin (**14**).¹⁰¹ For example, condensation of 3-hydroxy- β -ionone with vinyl magnesium bromide at sub-ambient temperatures affords 3-hydroxy-vinyl- α -ionol (Scheme 13). Reaction with triphenylphosphine hydrobromide

produces 3-hydroxy- β -ionylidetriphenylphosphonium bromide. The double Wittig reaction of the phosphonium salt with the C₁₀-dialdehyde (**27**) affords **14** in high yields.



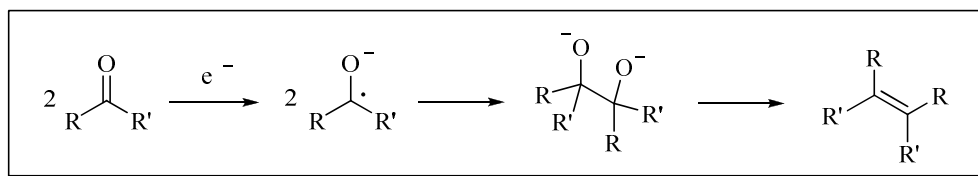
Scheme 13. Synthesis of (*rac*)-zeaxanthin (**14**) via organometallic and Wittig coupling reactions.¹⁰¹

Alkenyl lithium reagents are prepared by the Shapiro reaction and are often condensed with aldehydes and ketones to construct the polyene chain under mildly acidic conditions. An example of this is the synthesis of retinal (**16**) from β -iononeacetaldehyde. (Scheme 14).



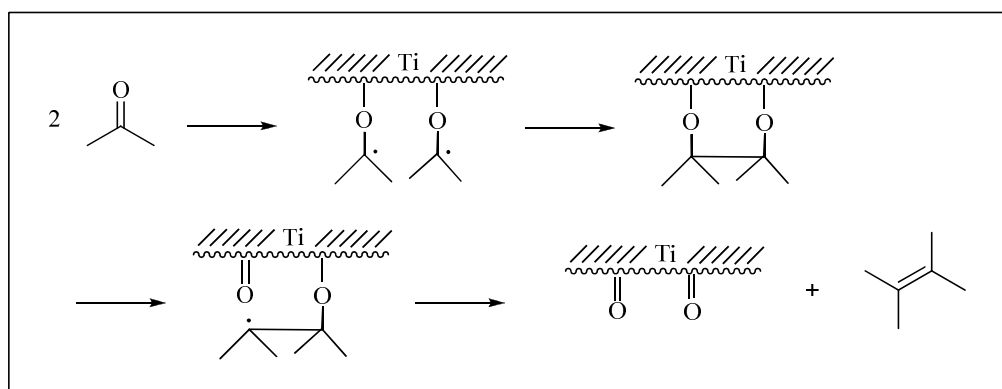
Scheme 14. Synthesis of retinal (**16**) via an alkenyl lithium reagent.¹⁰²

Low valent titanium (0) prepared from the reduction of TiCl_3 with LiAlH_4 , participates in the coupling of ketones and/or aldehydes to afford olefins in high yields.¹⁰³ β -Carotene (**8**) has been synthesized in 90% yield by coupling 2 moles of retinaldehyde (**16**) with TiCl_3 and LiAlH_4 in THF at room temperature. Coupling reportedly occurs in a stepwise manner from the reductive dimerization of the carbonyl compounds followed by deoxygenation of a 1,2-diolate intermediate, as illustrated in Scheme 15.



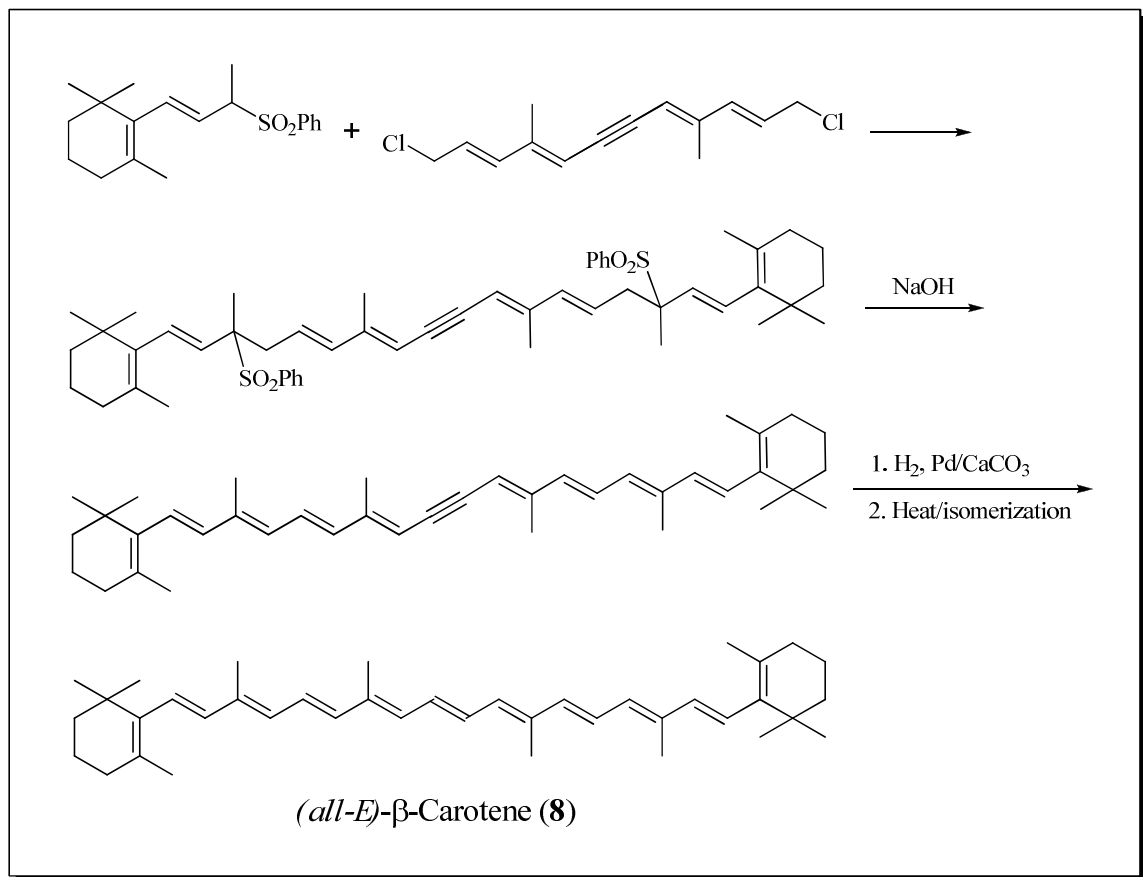
Scheme 15. Reductive coupling of carbonyl compounds in the presence of low valent titanium.

The role of the metal is illustrated in Scheme 16. Following coordination to the surface of titanium, stepwise cleavage of the C-O bonds of the diolate proceeds with formation of the olefin and oxide-coated titanium.



Scheme 16. Role of titanium metal in reductive coupling of carbonyl compounds.¹⁰³

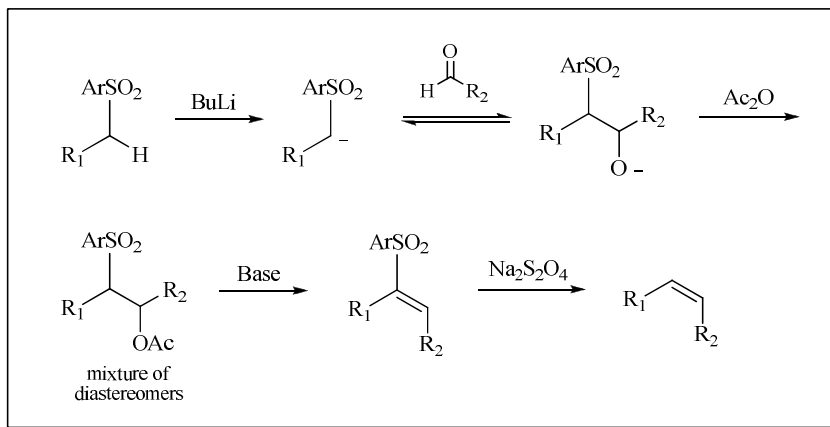
The formation of olefins *via* sulfone coupling with an alkyl halide followed by base-promoted elimination was pioneered by Julia in 1973 for the synthesis of vitamin A.¹⁰⁴ The general process has also been used to synthesize β -carotene (**8**) (Scheme 17).



Scheme 17. Synthesis of β -carotene (**8**) via Julia's sulphone coupling reaction.

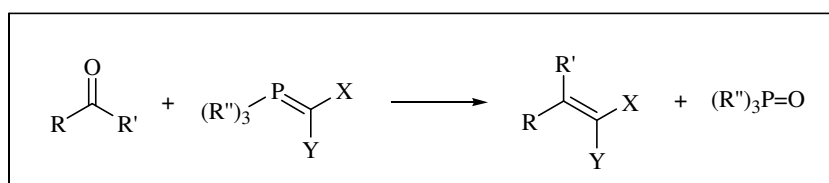
The anion of the C_{13} -sulphone was coupled to the dichloride after undergoing an S_N2 reaction. (*All-E*)- β -carotene (**8**) was obtained after partial reduction with the Lindlar catalyst and double bond isomerization during reflux.

In 1991, Bernhard and Mayer¹⁰⁵ further developed C-C bond formation via sulphone coupling with carbonyl compounds. The procedure incorporates reduction by sodium dithionite to liberate the olefin, as shown in Scheme 18. In addition to the synthesis of **8**, the process has been used to produce a variety of carotenoids, often with (*Z*)-stereochemistry, in high yields including lycopene (**5**), zeaxanthin (**14**), astaxanthin (**10**) and canthaxanthin (**9**).



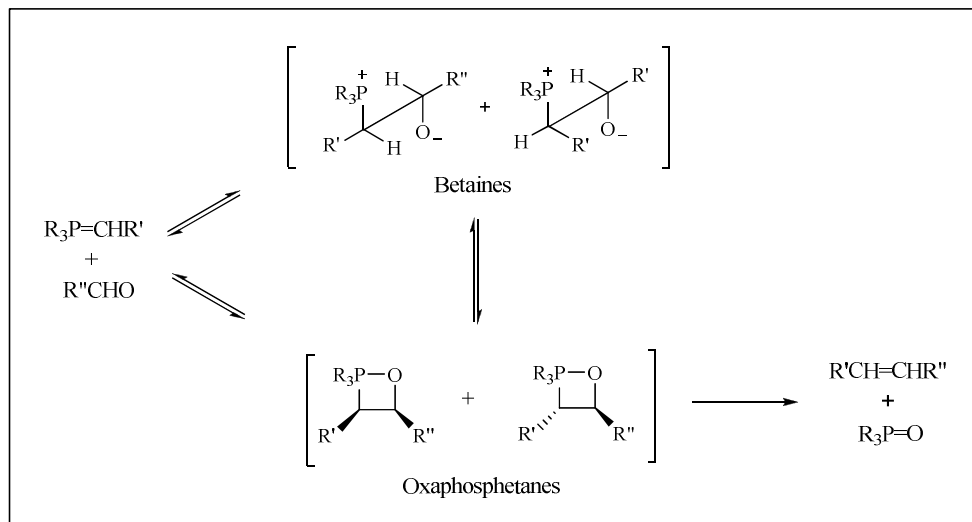
Scheme 18. Synthesis of *Z*-olefins by sulphone coupling with carbonyl compounds and reduction by sodium dithionite.¹⁰⁵

The convenient and effective coupling reaction between phosphorous ylides and carbonyl compounds to produce olefins with predictable placement of the double bond was discovered in the 1950's by Georg Wittig and colleagues.^{106,107} The Wittig reaction remains one of the most important reaction for preparing polyenes to date. In a prototypical reaction, a base is used to generate a phosphonium ylide; subsequent reaction with a carbonyl compound produces an alkene of uncertain stereochemistry and the by-product trialkyl- or triphenylphosphine oxide as shown in Scheme 19.



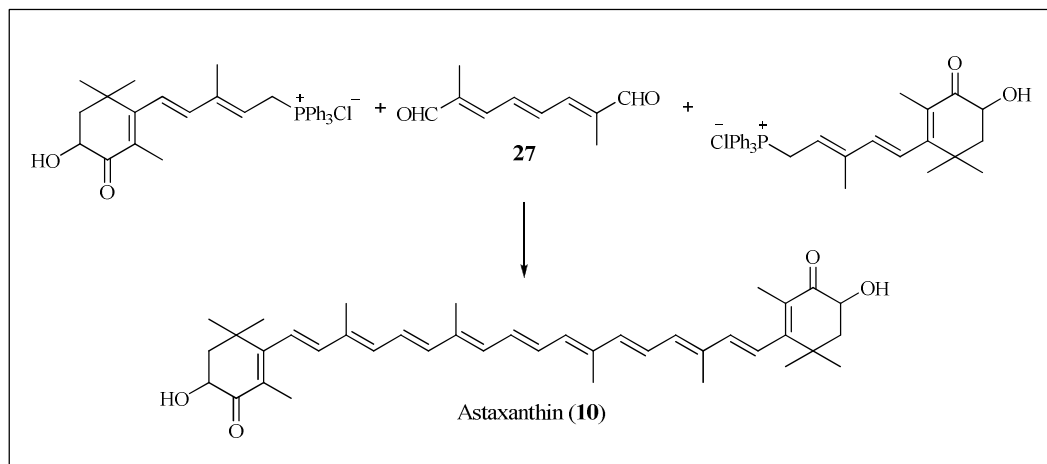
Scheme 19. Conventional Wittig Reaction.¹⁰⁸

The transformation proceeds according the mechanism shown in Scheme 20.¹⁰⁸ Wittig proposed that a four-membered 1,2-oxaphosphetane cyclic intermediate could exist in equilibrium with a betaine before irreversibly collapsing to form the olefin, although evidence for the existence of the betaine could not since be confirmed in ³¹P NMR studies conducted by Vedejs and colleagues.¹⁰⁹



Scheme 20. Proposed oxaphosphetane and betaine intermediates in a typical Wittig reaction.¹⁰⁸

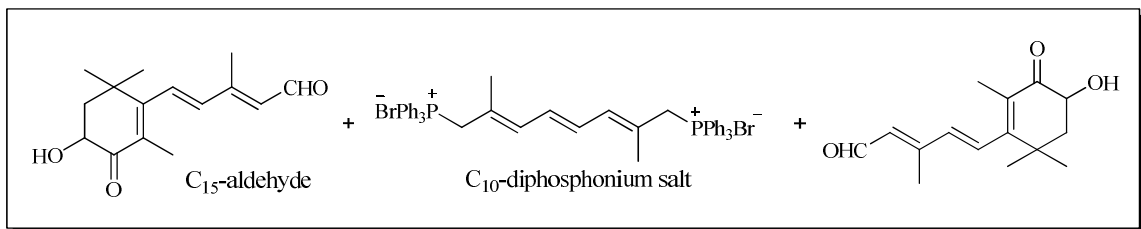
The Wittig reaction is one of the most effective coupling strategies to produce symmetrical C₄₀-carotenoids like astaxanthin (**10**),¹¹⁰ zeaxanthin (**14**) and β-carotene (**8**) where two identical C₁₅-phosphonium salt end- groups are coupled to the C₁₀-dialdehyde **27** in successive steps (Scheme 21).



Scheme 21. General Wittig coupling strategy for the synthesis of astaxanthin (**10**)¹¹⁰ and other symmetrical carotenoids.

Although a C₁₀-diphosphonium salt can be coupled with two molecules of C₁₅-aldehyde (Scheme 22), reactions have to be conducted at low temperature to minimize

the tendency for elimination of triphenylphosphine, thus decreasing the efficiency of this approach.



Scheme 22. Structures of C₁₅-aldehyde and C₁₀-phosphonium salt building blocks.

Formation of carotenoids with a polyene chain having an (*all-E*)-geometry is highly desirable, since the *all-E*-isomers can be crystallized during purification, in contrast to the *Z*-stereoisomers. The task of synthesizing carotenoids with an (*all-E*)-geometry is made difficult by the fact that *Z*-isomerization can occur at C9, C9', C13, C13' and C15 and C15' of the polyene chain following coupling reactions. On the other hand, steric interactions between Me-18 and Me-19 as well as H-10 and Me-20 arising from 7*Z*, 7'*Z*, 11*Z* and 11'*Z* orientations tend to guarantee the formation of *trans* double bonds at these locations (Figure 12).

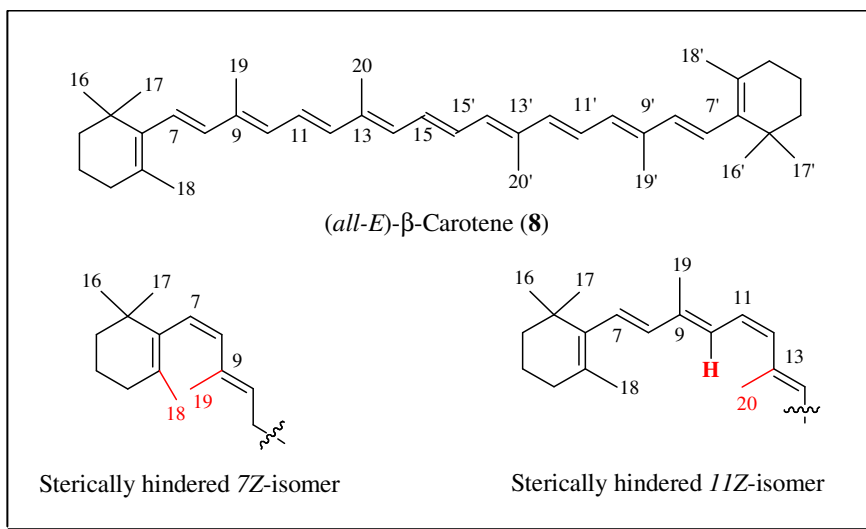
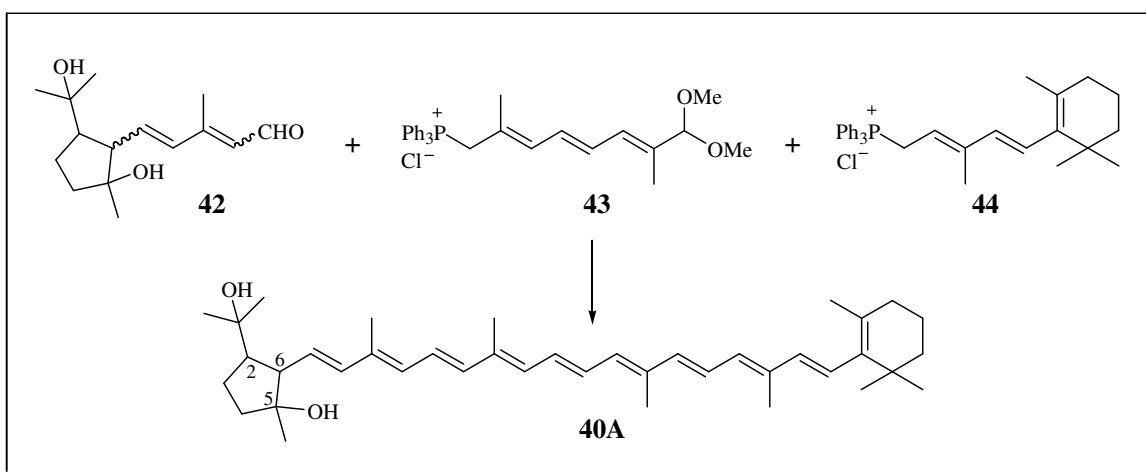


Figure 12. (*all-E*)- β -carotene (**8**) and two of its sterically hindered stereoisomers.

The C₁₅+C₁₀+C₁₅ coupling strategy employs bond formation at C11 and C11' and has been shown to be the method of choice for the synthesis of (*all-E*)-C₄₀-carotenoids containing cyclic end groups. Therefore, our approach for the total synthesis of the γ -carotene oxidation product was also based on the C₁₅+C₁₀+C₁₅ coupling strategy, where we used building blocks **42**, **43** and **44** to arrive at the targeted diol **40A** (Scheme 23). For compound **40A**, the relative stereochemistries at C2, C5 and C6 will be determined, and may be different than the relative stereochemistries predicted for **40** and **41**.



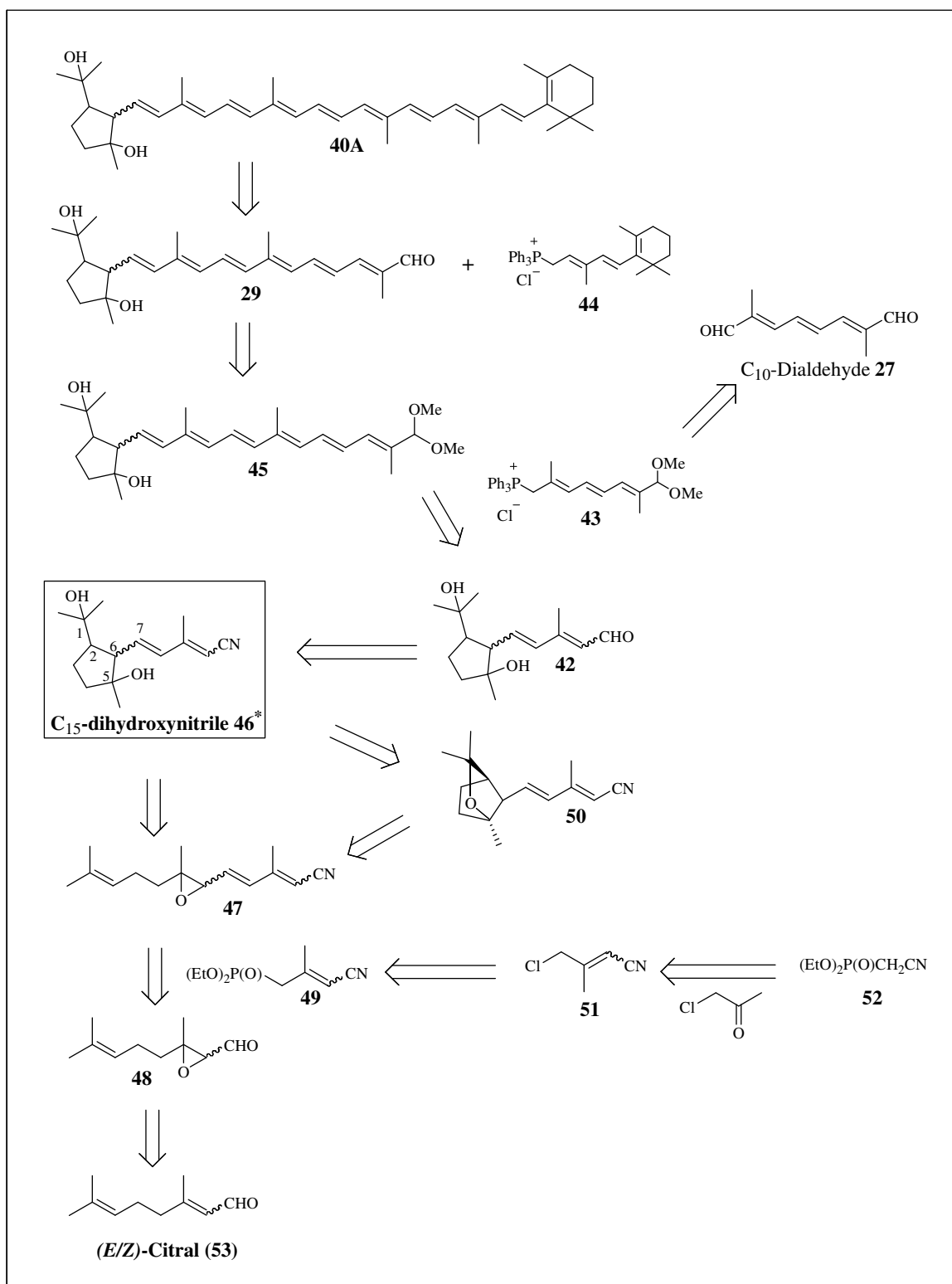
Scheme 23. Building blocks used for the synthesis of targeted diol **40A**. Stereochemistries at C2, C5 and C6 will be determined.

Retrosynthetic Analysis of γ -Carotene Oxidation Product **40A**.

To accomplish the synthesis of the target diol **40A**, we explored a slightly different strategy, based on the retrosynthetic pathway shown in Scheme 24. It was anticipated that the final step of our synthesis could be readily accomplished by elongation of the C₂₅-dihydroxyaldehyde **29** with the Wittig salt **44** that could be readily prepared according to known processes.^{111,112} We rationalized **29** could be prepared from deprotection of the corresponding dimethylacetal **45** under mild acidic conditions without

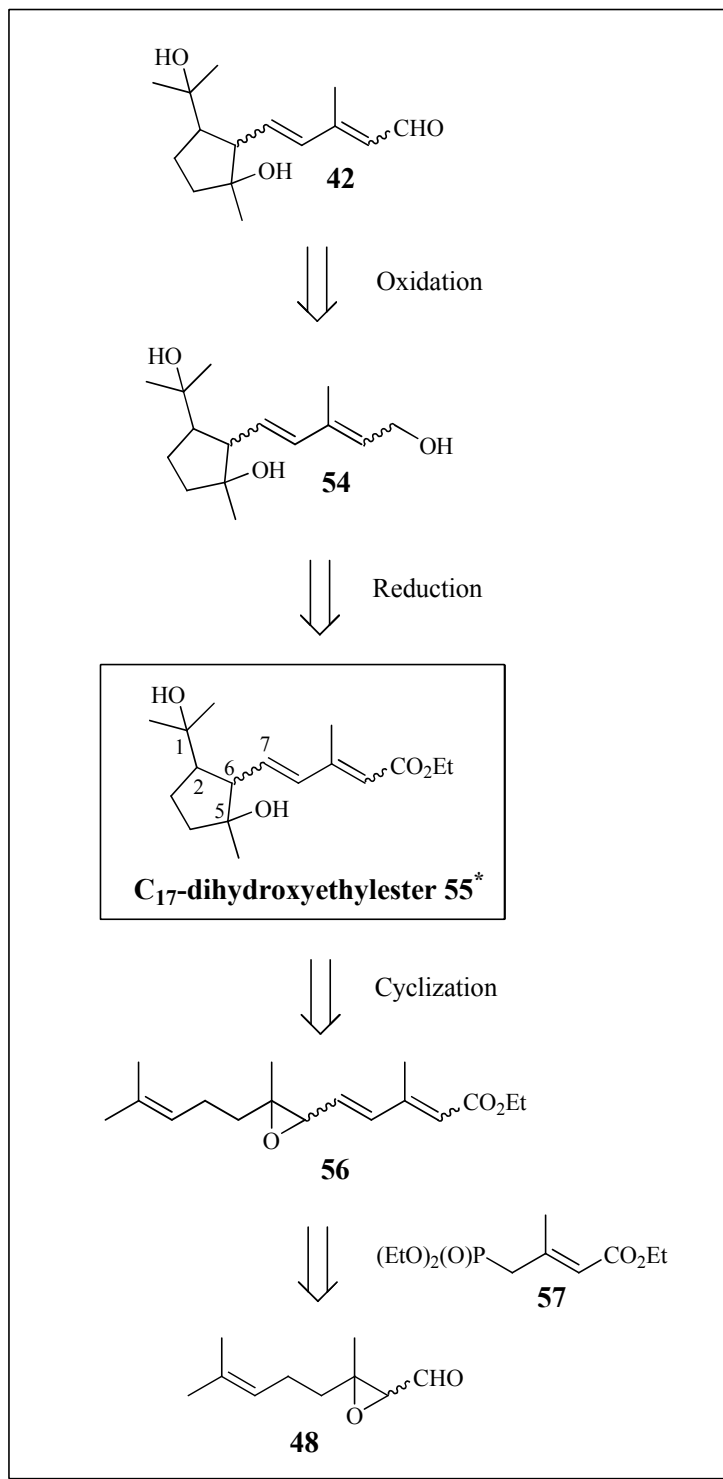
elimination of the tertiary hydroxyl groups at C1 and C5. The acetal **45** could in turn be prepared from the reaction of protected C₁₀-Wittig salt **43** with C₁₅-dihydroxyaldehyde **42**. The protected C₁₀-Wittig salt **43** is readily accessible according to published methods.^{113,114} Although application of **43** in the synthesis of unsymmetrical carotenoids with sensitive end-groups has been well documented in the literature,¹¹⁴⁻¹¹⁷ this building block has not been employed in the synthesis of the oxidation products of lycopene (**5**), γ -carotene (**6**), or their precursors.

The cyclized C₁₅-dihydroxynitrile **46**, prepared as a mixture of stereoisomers with known relative stereochemistries at C2, C5, C6 and C10 could in turn serve as the precursor to the cyclized C₁₅-dihydroxyaldehyde **42**. This aldehyde would be most likely prepared as a mixture of diastereomers. However, it was anticipated that due to the presence of polar hydroxyl groups, the diastereomeric aldehydes could be readily separated by column chromatography. The cyanoepoxide **47** could be prepared from elongation of citral epoxide **48** with synthon **49**. The cyclization of **47** to **46** would be expected to proceed in dilute H₂SO₄, similar to the reported rearrangement for lycopene-5,6-epoxide (**23**) to diols **21** and **22**. Alternatively, the C₁₅-dihydroxynitrile **46** might be obtained from the acid-catalyzed ring opening of bicyclic oxide **50** that could be generated by the lewis-acid catalyzed rearrangement of epoxide **47**. The preparation of **49** could be accomplished by reaction of 4-chloro-3-methyl-2-butenitrile (**51**) with triethyl phosphite. Horner-Wadsworth-Emmons (HWE) reaction of diethyl cyanomethylphosphonate **52** with chloroacetone was expected to afford **41** in useful yields.¹¹⁸ Commercially available (*E/Z*)-citral served as the precursor to citral epoxide (**48**).



Scheme 24. Retrosynthetic analysis of γ -carotene oxidation product **40A** via C_{15} -dihydroxynitrile **46**; *carotenoid numbering system has been used for compounds **40A-46**, **29** and **50**.

Alternatively, the C₁₅-dihydroxyaldehyde **42** could be prepared according to retrosynthetic pathway shown in Scheme 25. According to this strategy, the C₁₅-triol **54** could be oxidized to afford **42**. Triol **54** could in turn be prepared by reduction of the C₁₇-dihydroxyethylester **55**. We expected that **55** could be prepared from the intramolecular cyclization of the C₁₇-epoxyethylester **56** in dilute sulfuric acid. Epoxy ethylester **56** could be prepared by elongation of citral epoxide (**48**) with triethyl-3-methyl-4-phosphono-2-butenate **57**.

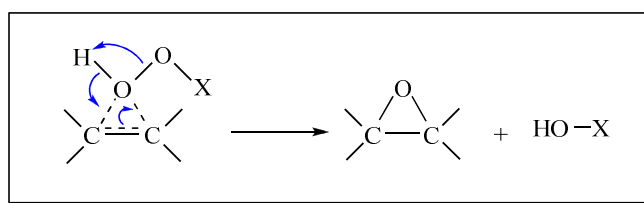


Scheme 25. Alternative route to the synthesis of C₁₅-dihydroxyaldehyde **42** via C₁₇-dihydroxyethyl ester **55**. *Carotenoid numbering system has been used for compounds **42**, **54** and **55**.

Synthesis of C₁₅-dihydroxyaldehyde 42 via C₁₅-epoxynitrile 47.

Citral (3,7-dimethyl-2,6-octadienal) is commercially available as a mixture of (2*E*)- and (2*Z*)-isomers. There are no known methods to separate these geometrical isomers, known as geranial and neral respectively. Although relatively pure forms of the corresponding alcohols geraniol and nerol are commercially available and could be subsequently oxidized to the aldehyde while preserving the stereochemistry at C2, we chose citral as a more affordable starting material.

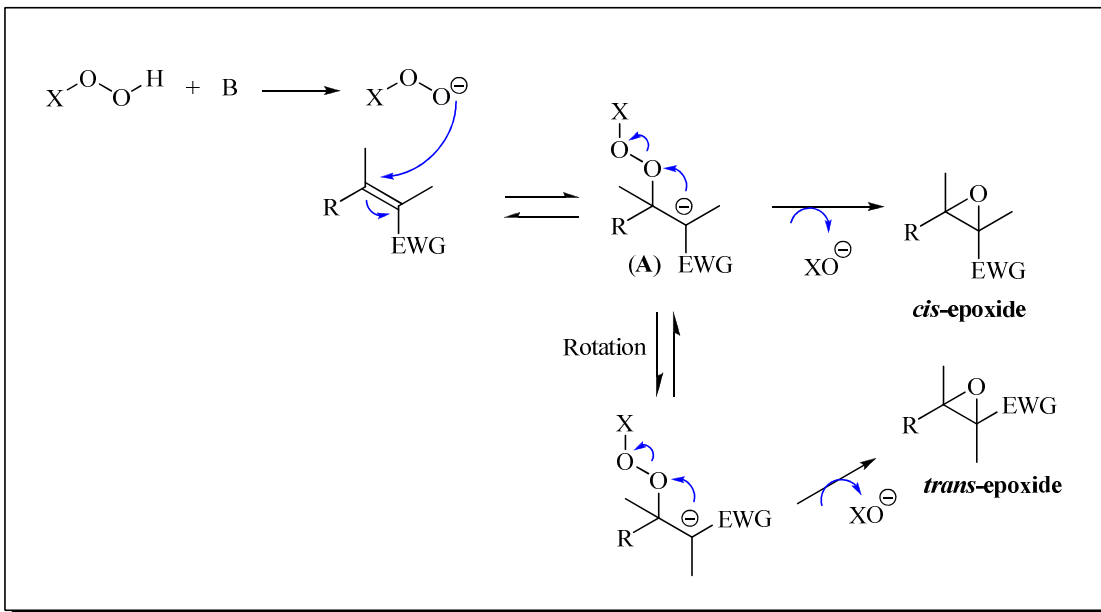
Peroxy-carboxylic acids are generally used to convert alkenes to epoxides. Useful reagents include *m*-chloroperoxybenzoic, peroxybenzoic, peroxyacetic acids and *tert*-butylhydroperoxide.¹¹⁹ Epoxidation is known to proceed by nucleophilic attack of the alkene on the peroxyacid in a concerted manner (Scheme 26). Because the rate of epoxidation is enhanced by electron-rich double bonds, we expected regioselective epoxidation of citral to produce the 6,7-epoxy derivative predominately, since the double bond at C2 is conjugated with an aldehyde.



Scheme 26. Epoxidation of alkenes by peroxide under neutral conditions.

Regiospecific epoxidation of alkenes conjugated with or adjacent to electron withdrawing substituents can be accomplished in a stepwise manner with hydrogen peroxide.¹²⁰ While α,β -unsaturated ketones¹¹⁹ and aldehydes such as acrolein have been shown to undergo epoxidation with H₂O₂ at pH = 8¹²¹ our attempted preparation of citral epoxide according to this method only gave a poor yield of this compound. Under basic

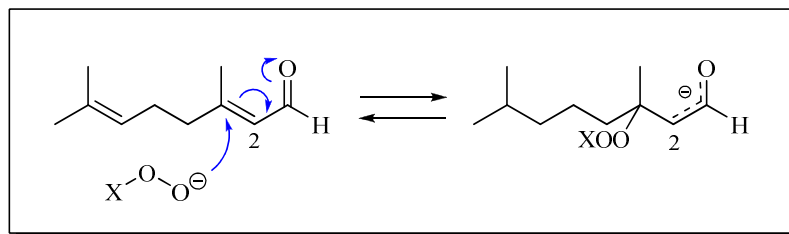
conditions, the usually accepted mechanism for epoxidation of electrophilic olefins is shown in Scheme 27.¹²⁰



Scheme 27. Epoxidation of olefins with peroxide under basic conditions.⁷¹

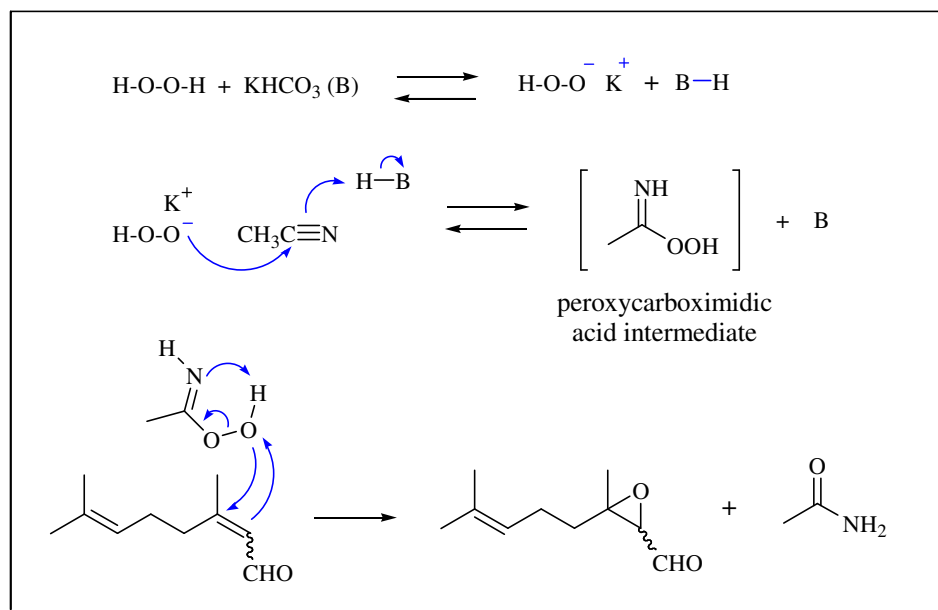
In contrast to the concerted mechanism shown in Scheme 26, the deprotonated form of the peroxide attacks the olefin to produce a stabilized carbanion **A**. The rate at which **A** evolves into the epoxide is highly dependent on the leaving group ability of the XO^- group.¹²² Accordingly, epoxidation of citral epoxide (**48**) at C2 would be expected to proceed more rapidly with *m*-CPBA than with hydrogen peroxide. With olefins containing non-conjugating electron withdrawing groups, choice of hydrogen peroxide is expected to increase the lifetime of adduct **A**, allowing for single bond rotation at C2 and ultimate formation of the thermodynamically more stable *trans*-epoxide. In our system however, nucleophilic epoxidation would produce an anion that is conjugated to the aldehydic carbon atom, which has the effect of reducing the single bond character and rotation about C2, as illustrated in Scheme 28. Regardless of the reagent used, we

expected the ratio of (*E/Z*)-citral epoxide isomers to be identical to that which was present in the starting material.



Scheme 28. Nucleophilic epoxidation of citral (**53**).

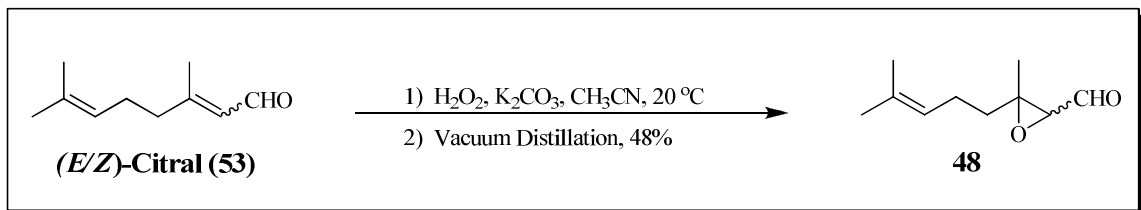
Hydrogen peroxide has been shown to react with nitriles in the presence of potassium bicarbonate to form a peroxy-carboximidic acid intermediate that can subsequently epoxidize alkenes under non-acidic conditions, as shown in Scheme 29.^{123,124}



Scheme 29. Epoxidation of citral (**53**) via a peroxy-carboximidic acid intermediate.

Synthesis of citral epoxide (**48**).

When (*E/Z*)-citral (**53**) was allowed to react with H₂O₂ in the presence of acetonitrile/K₂CO₃ at room temperature, **48** was obtained in 75% yield (Scheme 30).

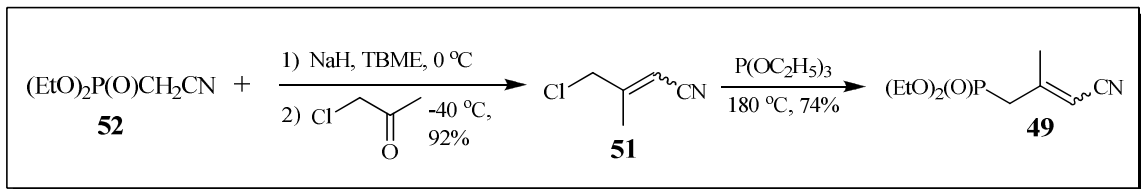


Scheme 30. Synthesis of citral epoxide (**48**).

However, after vacuum distillation, the isolated yield of **48** was 48%. The low yield was attributed to significant polymerization that occurred during distillation. The isomeric ratio of **48** was determined by NMR (*E:Z* = 1.2:1.0).

Preparation of 4-(diethylphosphono)-3-methyl-2-butenenitrile (**49**).

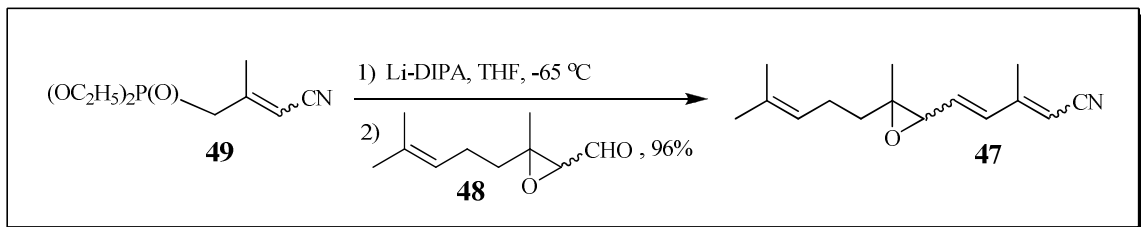
The preparation of **49** was accomplished in 74% overall yield in two steps according to a published procedure, as illustrated in Scheme 31.¹¹⁸ Horner-Wadsworth-Emmons (HWE) reaction of diethyl cyanomethylphosphonate (**52**) with chloroacetone gave (*E/Z*)-4-chloro-3-methyl-2-butenenitrile (**51**) in 92% yield after column chromatography. In an Arbuzov reaction,¹²⁵ nitrile **51** was then allowed to react with triethyl phosphite to afford **49** (*E/Z* = 1.1: 1.0) in 74% isolated yield after distillation.



Scheme 31. Synthesis of 4-(diethylphosphono)-3-methyl-2-butenenitrile (**49**).

Synthesis of C₁₅-epoxynitrile **47**.

A mixture of *E/Z*-epoxynitriles **47** was prepared by HWE reaction of phosphonate **49** with citral epoxide (**48**) as shown in Scheme 32.



Scheme 32. Synthesis of C₁₅-epoxynitrile **47**.

When sodium hydride was used as a base to generate the anion of **49**, a significant amount of precipitate was formed that prevented stirring. This resulted in 66% isolated yield of **47**. To circumvent this problem, we employed a modified procedure that has been reported by Wang *et al.*¹²⁶ Accordingly, the anion was first generated with lithium diisopropylamide (Li-DIPA) at -65 °C, resulting in a fluid mixture that could be magnetically stirred. After addition of citral epoxide (**48**) to the anion and purification by column chromatography, C₁₅-epoxynitrile **47** was obtained in 96% isolated yield as a mixture of 4 stereoisomers. These were separated by preparative TLC into two sets of isomers **47a** and **47b** as shown in Figure 13. The first set was identified by NMR to be a mixture of (*2E,4E*)-*trans*-6,7-epoxynitrile **47a1** and (*2Z,4E*)-*trans*-6,7-epoxynitrile (**47a2**), while the second set was tentatively identified to be a mixture of (*2E,4E*)-*cis*-6,7-epoxynitrile **47b1** and (*2Z,4E*)-*cis*-6,7-epoxynitrile **47b2**. The ratio of *trans/cis* epoxides **47a:47b** was approximately (1:1), based on HPLC area counts while the ratio of (*2E/2Z*) isomers was approximately 2:1, based on analysis by NMR. These stereoisomers would arise from coupling between (*E/Z*)-citral epoxides **48** and (*E/Z*)-phosphonate **49**.

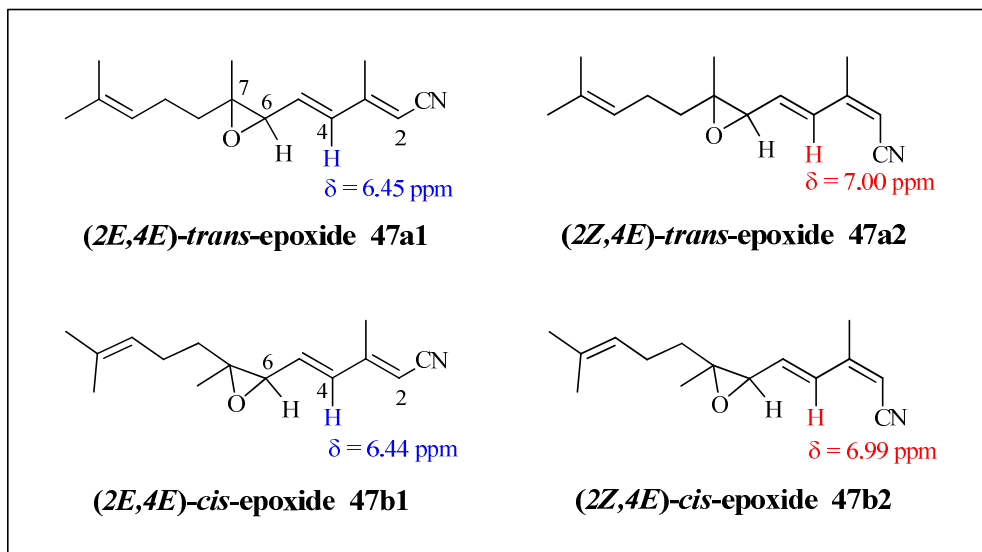
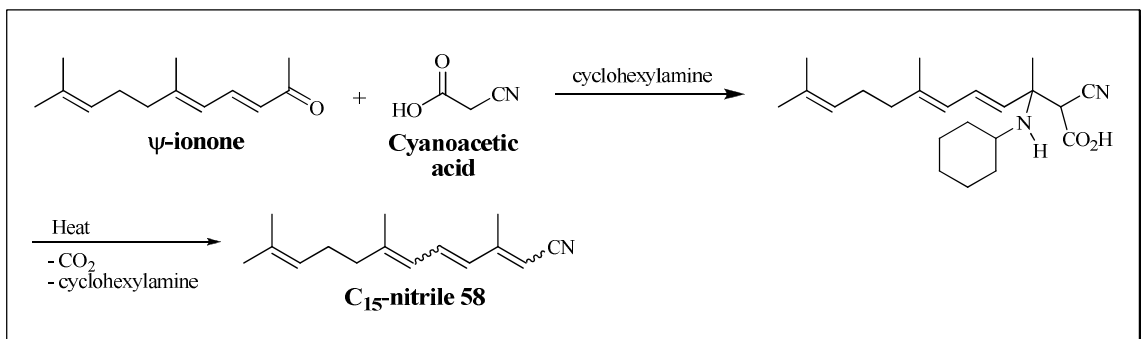


Figure 13. C₁₅-epoxynitriles **47a** and **47b**.

trans-Epoxides **47a1** and **47a2** and *cis*-epoxides **47b1** and **47b2** were analyzed by HRMS which gave rise to signals for the protonated molecular ion $[M+H]^+$ and its loss of water $[M+H-H_2O]^+$. ¹³C NMR data were acquired for these four stereoisomers of **47**. The stereochemistry of the cyano group at C2 was established from comparison of the proton NMR chemical shift of H4. It has been well documented that when H4 and an electron withdrawing group (EWG) are in a *cis*-geometry, the chemical shift of H4 is shifted measurably downfield in comparison with the chemical shift of this proton when it is in a *trans*-geometry with the EWG. Because the chemical shifts of H4 in epoxynitriles **47a2** and **47b2** was 7.0 ppm versus 6.5 ppm in epoxynitriles **47a1** and **47b1**, the stereochemistry of the cyano group at C2 could be assigned in these structures on this basis. We were unable to distinguish the difference between *cis/trans*-6,7-epoxynitriles **47a1** and **47b1** and **47a2** and **47b2** by proton NMR studies.

To avoid the formation of the *2Z*-epoxynitriles **47a2** and **47b2**, another route to **47** was investigated. This involved Knoevenagel condensation of ψ -ionone with cyanoacetic

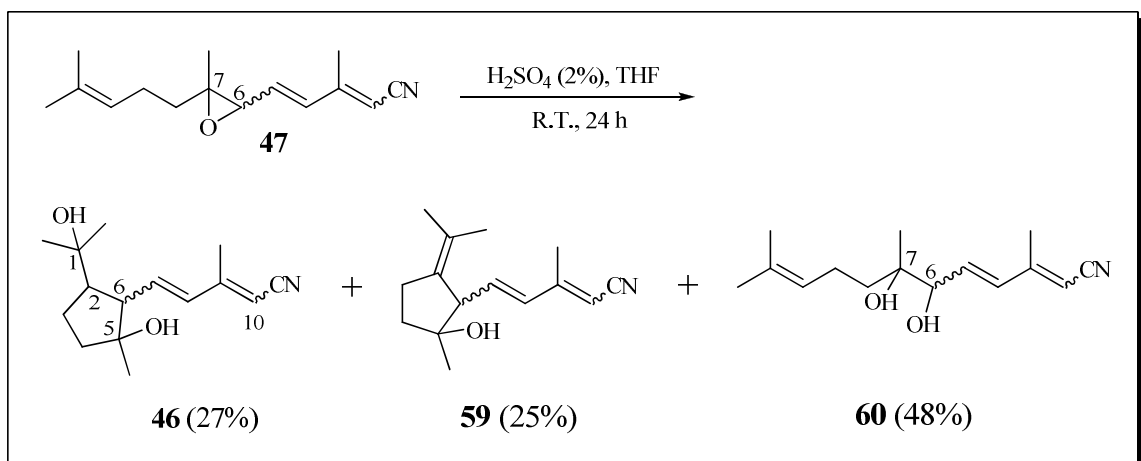
acid to yield C₁₅-nitrile **58** as an *all-E*-isomer (Scheme 33). Regioselective epoxidation of **58** at C6 could then produce **47** as a single isomer.¹²⁷ However, HPLC analysis of the product revealed a mixture of 4 isomers was obtained when ψ -ionone, cyanoacetic acid and cyclohexylamine were heated together at 85 °C for two hours. We therefore discontinued our attempt to produce **47** as a single product by this route.



Scheme 33. Synthesis of **58** by Knoevenagel condensation reaction.

Cyclization of C₁₅-epoxynitrile **47** in dilute H₂SO₄.

The following step of our synthesis involved cyclization of C₁₅-epoxynitrile **47** to C₁₅-dihydroxynitrile **46** at R.T. with dilute sulfuric acid in THF (Scheme 34).



Scheme 34. Acid-catalyzed cyclization of C₁₅-epoxynitrile **47**.

The target compound **46** was isolated in 27% yield, although competitive amounts of dehydrated hydroxynitrile product **59** and 6,7-dihydroxynitrile by-product (**60**) were also obtained in 25% and 48% yields, respectively. The product was purified by flash column chromatography. An isomeric mixture of **46** was further purified by semi-preparative HPLC. Four compounds **46a1**, **46a2**, **46b1** and **46b2** were isolated in relative yields 3.4:1.0:1.8:1.4 (Figure 14).

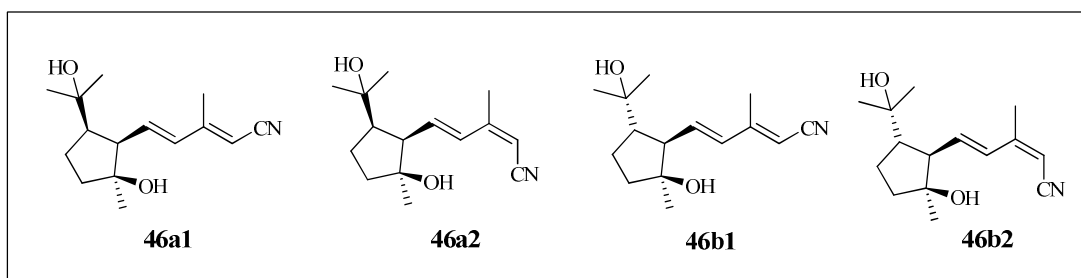


Figure 14. C₁₅-Dihydroxynitriles **46a1**, **46a2**, **46b1** and **46b2**.

The normal phase HPLC profile of the C₁₅-dihydroxynitriles is shown in Figure 15.

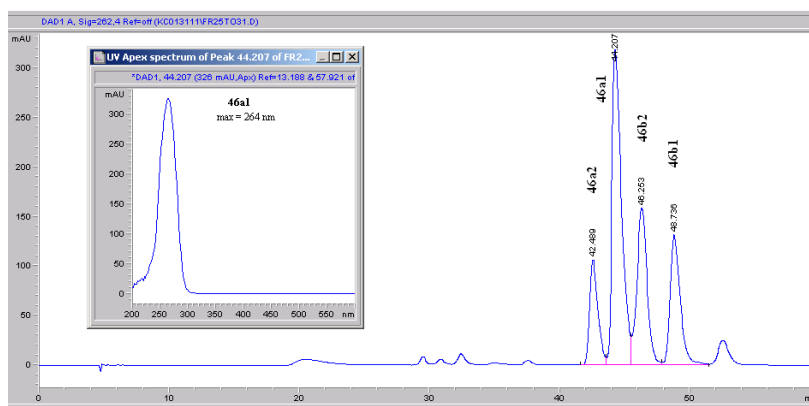


Figure 15. Normal phase HPLC profile of C₁₅-dihydroxynitriles **46a1**, **46a2**, **46b1**, and **46b2**. (HPLC condition K, Appendix I).

The C₁₅-dihydroxynitriles **46** were analyzed by HRMS which gave rise to signals for the protonated molecular parent ion and fragments associated with loss of one and two molecules of water.

The ^{13}C -NMR data obtained for the stereoisomers of **46** were consistent with the proposed structures (Figure 16).

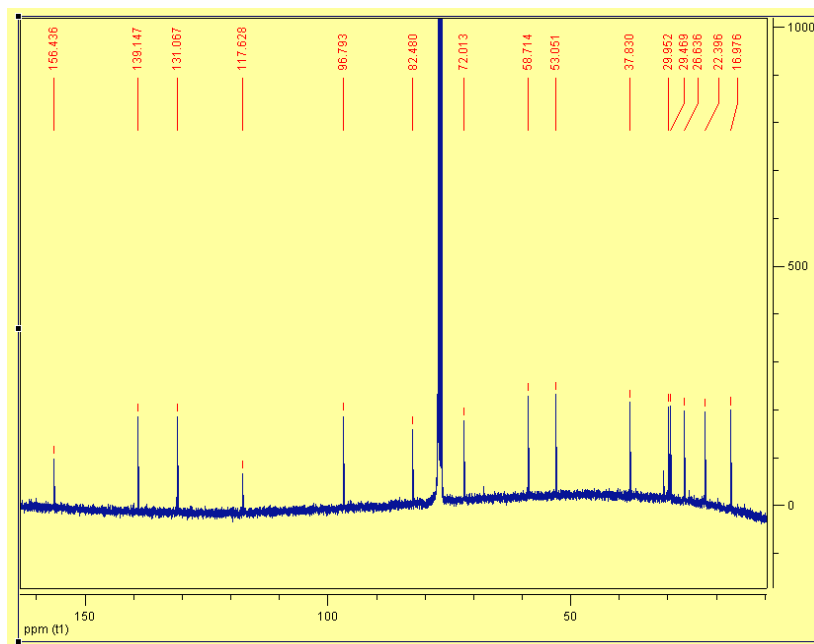


Figure 16. ^{13}C -NMR spectrum of C_{15} -dihydroxynitrile **46a1**.

Chemical shifts corresponding to C1 and C5 attached to hydroxyl groups occurred at 72 and 82 ppm, respectively. Three signals corresponding to substituted olefinic carbons were evident while another signal was observed for the olefinic carbon atom conjugated to the cyano group at approximately 97 ppm. The chemical shift of the nitrile carbon atom was evident at approximately 156 ppm.

The ^1H -NMR spectrum of **46a1** is shown in Figure 17.

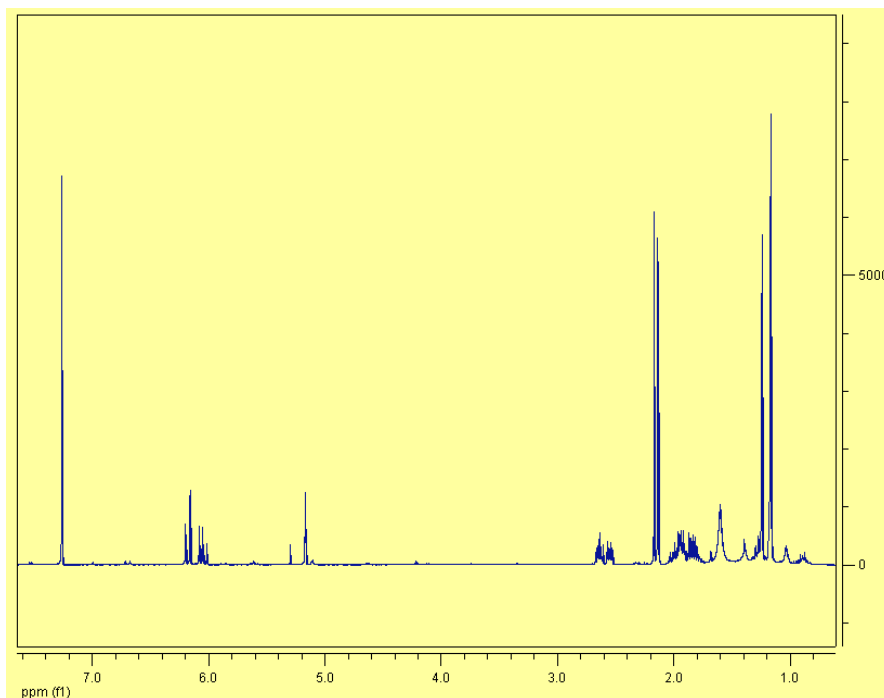


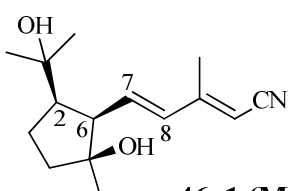
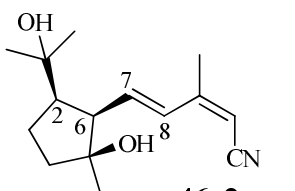
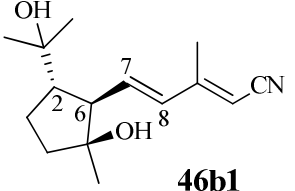
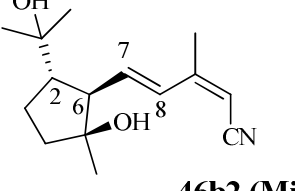
Figure 17. ^1H -NMR spectrum of C_{15} -dihydroxynitrile **46a1**.

The relative stereochemistry of the cyano group at C10 was established from comparison of the proton NMR chemical shift of H8. Analogous to the rationale used to establish the orientation of the cyano group in epoxide **47**, when H8 and the cyano group were in a *cis*-configuration, the chemical shift of H8 was shifted measurably downfield in comparison with the chemical shift of this proton when it was in a *trans*-configuration with respect to the cyano group. Because the chemical shifts of H8 in cyanodiols **46a2** and **46b2** were 6.7 ppm versus 6.1 ppm in epoxynitriles **46a1** and **46b1**, the stereochemistry of the cyano group at C10 could be assigned in these structures on this basis. Stereochemical differences between **46a** and **46b** were also evident from the differences in the chemical shift between H2 and H6. In diols **46a**, the chemical shift of H2 and H6 when these protons were in a *cis* relationship to each other were nearly

identical. When these protons were in a *trans* relationship to one another, the difference between the chemical shift of H2 and H6 was approximately 0.7 ppm.

Typical stereochemical differences for key protons in **46a1**, **46a2**, **46b1**, and **46b2** are shown in Table 3.

Table 3. Proton chemical shifts of C₁₅-dihydroxynitriles **46**.

Stereoisomer	H2 (ppm)	H6 (ppm)	H7 (ppm)	H8 (ppm)
 <p>46a1 (Major)</p>	2.65	2.56	6.06	6.19
 <p>46a2</p>	2.66	2.66	6.11	6.70
 <p>46b1</p>	1.92	2.57	5.86	6.13
 <p>46b2 (Minor)</p>	1.95	2.66	5.93	6.64

The structures of the stereoisomeric cyanodiols were unequivocally established by proton, COSY, NOESY, HSQC and HMBC NMR experiments. The HMBC spectrum of **46a1** is shown in Figure 18.

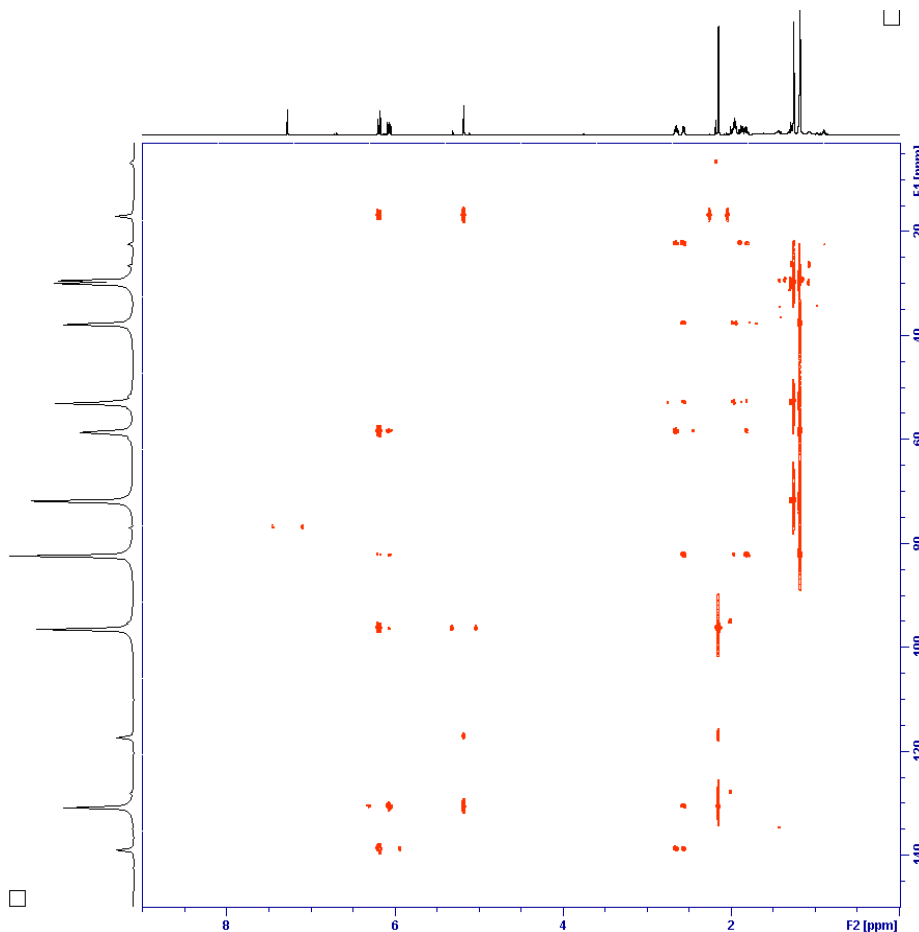


Figure 18. HMBC spectrum of C₁₅-dihydroxynitrile **46a1**.

Long-range connectivities between proton and carbon atoms for **46a1** are summarized in Table 4.

Table 4. Carbon-proton connectivities determined for **46a1** by HMBC NMR.

C Position	H Connectivities	C Position	H Connectivities
1	2, 6, 16, 17	9	7, 8, 10, 19
2	3, 4, 6, 7, 16, 17	10	8, 19
3	2, 4	11	10, 19
4	3, 6, 18	16	2, 17
5	2, 3, 4, 6, 7, 18	17	2, 16
6	2, 3, 4, 7, 8, 18	18	4, 6
7	2, 6, 8	19	8, 10
8	6, 7, 10, 19		

The relative stereochemistries of **46a1** at C2, C5 and C6 were determined by NOESY NMR (Figure 19).

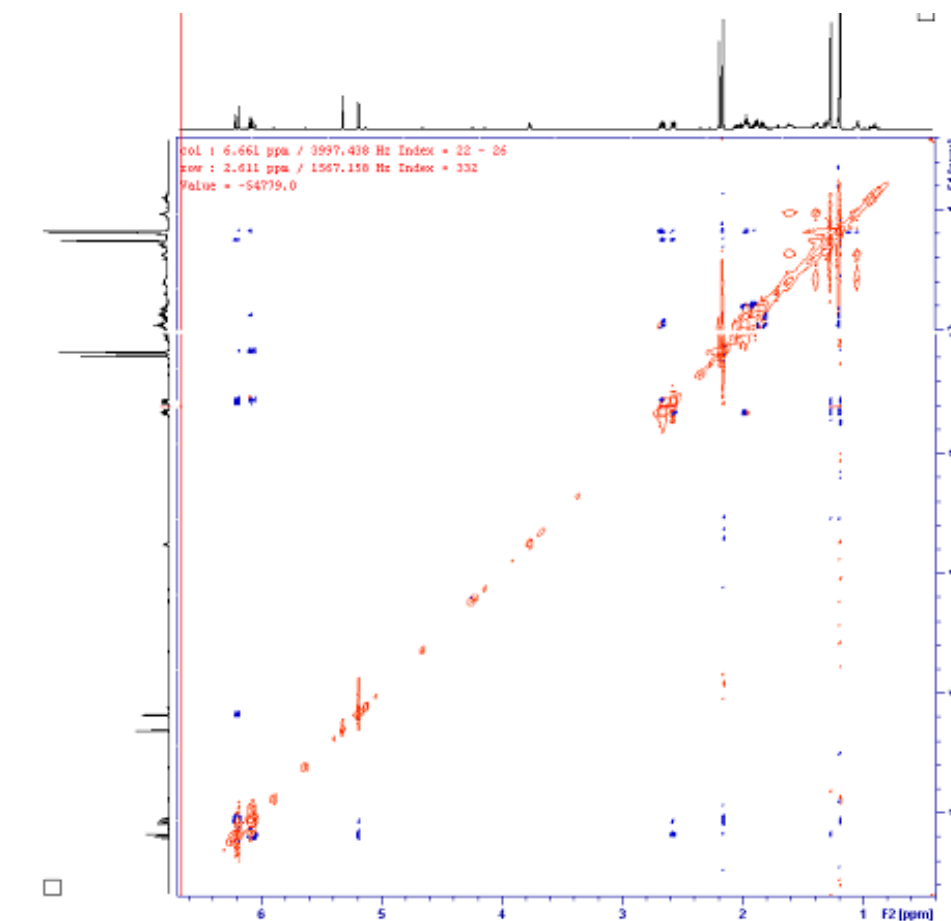


Figure 19. NOESY spectrum of C₁₅-dihydroxynitrile **46a1**.

For **46a1**, the major diol isolated, crosspeaks observed between the protons of Me16/17 and H7 and those between H2 and H6 indicated their *cis* relationship and established the orientation of the protons at C2 and C6. NOESY crosspeaks observed between the protons on Me18, H2 and H6 revealed a *cis* relationship and established the orientation of both the hydroxyl group at C5 and the side chain at C6. HMBC crosspeaks between the Me18 protons and C4 and C6 were used to distinguish Me18 from Me16 and

Me17. Further, Me17 can be distinguished from Me16 by the NOESY crosspeak with H7. Crosspeaks and relative stereochemical assignments for **46a1** are shown in Figure 20.

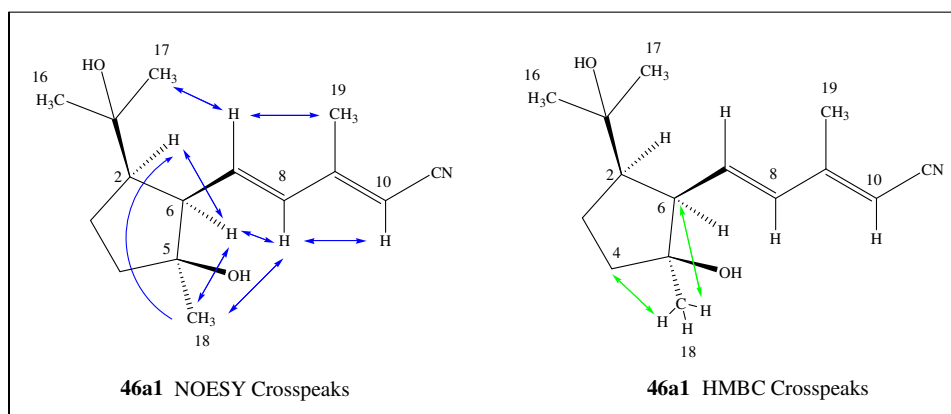


Figure 20. NOESY and HMBC crosspeaks and relative stereochemistry for **46a1**.

In addition to the same NOESY crosspeaks as diol **46a1**, an additional crosspeak between Me19 and H10 established the *cis*-orientation of the cyano group at C10 in diol **46a2**. It should be noted that the only difference in the relative stereochemistry between diols **46a1** and **46a2** is the orientation of the cyano group at C10 (Figure 21).

NOESY crosspeaks observed in diols **46b1** and **46b2** between the protons on Me18 and H6 indicated their *cis* relationship, and established the orientation of both the hydroxyl group at C5 and the side chain at C6 (Figure 21). A crosspeak was observed between H2 and H7 in both of these diols, indicating a *trans* relationship between the hydroxylated isopropyl group and the side chain at C6. Further evidence for the relative stereochemistry at C2 for **46b1** and **46b2** was provided by the NOESY crosspeaks observed between the protons of Me16/Me17 and H6. The relative stereochemistry of diols **46b1** and **46b2** differed only in the orientation of the cyano group at C10, where a crosspeak between the protons on Me19 and H10 indicated a *cis* orientation of the cyano group in **46b2**.

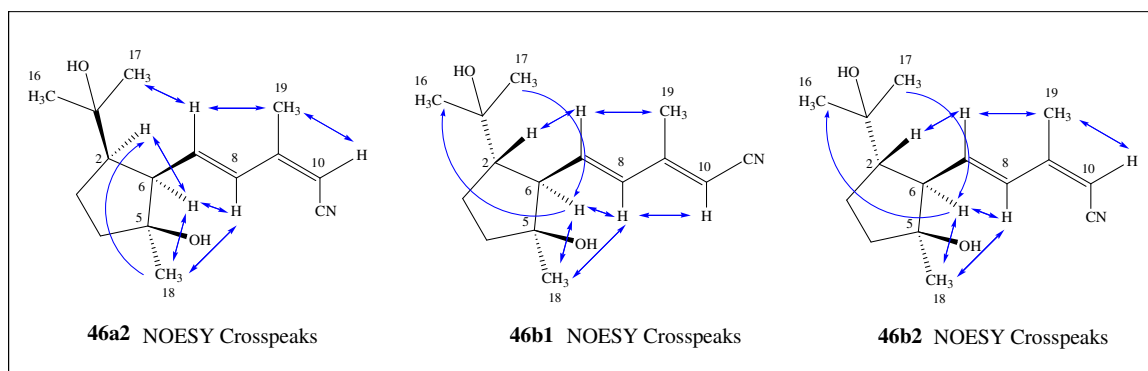
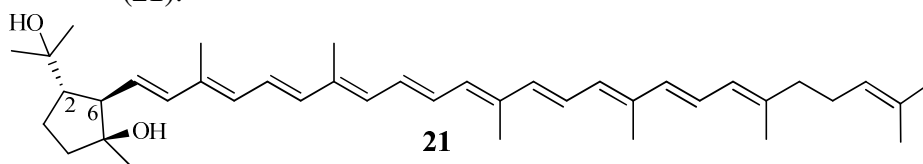


Figure 21. NOESY crosspeaks and relative stereochemistries for **46a2**, **46b1** and **46b2**.

The relative stereochemistries determined at C2 and C6 for diols **46b1** and **46b2** do not agree with those reported at these locations for the analogous compound 1,5-dihydroxy-2,6-cyclolycopene (**21**), as determined by Yokota,⁸⁵ Khachik,⁸⁶ and Pfander⁹⁰ (Table 5). However, the small differences between the chemical shifts of H2 and H6 that were reported by these authors are consistent with the relative stereochemistry we determined for diols **46a1** and **46a2**.

Table 5. Chemical shifts for H2 and H6 of 1,5-dihydroxy-2,6-cyclolycopene (**21**).^{85,86,90}



Reference	H2 (ppm)	H6 (ppm)
27	2.32	2.25
28	2.10	2.11
33	2.30	2.23

The dehydration product **59** was analyzed by HRMS. The protonated form of the molecular parent ion for this compound was observed in addition to a fragment resulting

from loss of one molecule of water. The NMR chemical shift for H2 at approximately 1.9 or 2.7 ppm was no longer evident in this dehydration product. The chemical shifts of Me16/17 were shifted downfield from 1.2 ppm to approximately 1.6 ppm, which is characteristic of geminal methyl groups attached to an sp² carbon atom. The chemical shift of Me16/17 in ¹³C-NMR were 21 and 24 ppm, near the expected value of 19 ppm.

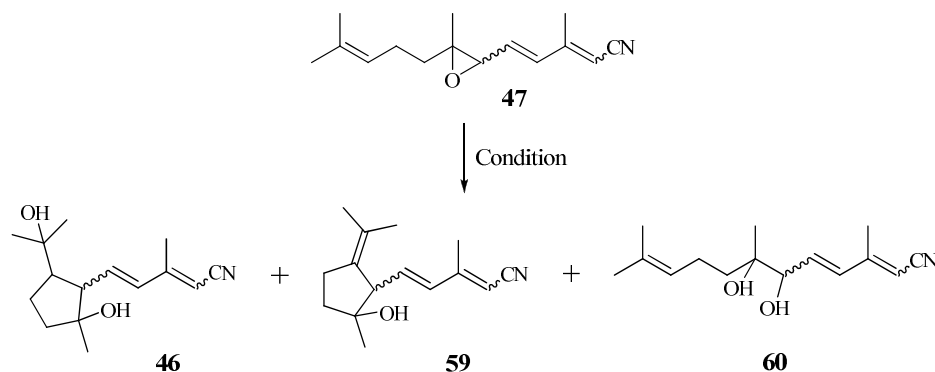
Only diol **60** was identified by mass spectral analysis, proton and carbon NMR. The protonated form of the molecular ion was observed in addition to fragments resulting from loss of one and two molecules of water. An isomeric mixture was isolated based on results of proton NMR (*E/Z* = 2:1). The chemical shift of H6 at 4.1 ppm was consistent with a hydroxyl substituent, in comparison the chemical shift of H6 of epoxide **47** at 3.3 ppm.

Various conditions were explored to optimize the yield of **46** (Table 6). When methylene chloride was used as solvent, only the starting material was isolated from the biphasic mixture after 24 h at R.T., whereas 20% of the desired product **46** was obtained when the water miscible solvent THF was used (entries 1 and 2). Nevertheless, 12% of the starting material **47** remained unreacted.

To drive the reaction to completion, the amount of acid was increased (entry 3). Under this condition, the yield of **46** increased to 26% after just 2 h at R.T. Although most of the starting material was consumed under these conditions, the dehydration product **59** and diol **60** were formed predominately and lowering the temperature to 0 °C (entry 4), had no effect on preventing the formation of these side products. The yield of **46** remained essentially the same when cyclization was carried out with increasing the

concentration of sulfuric acid (entry 5). Ultimately, differences in product ratios were not significantly influenced by changes in the amount of acid used or reaction temperature.

Table 6. Cyclization of C₁₅-epoxynitrile **47** with dilute sulfuric acid.

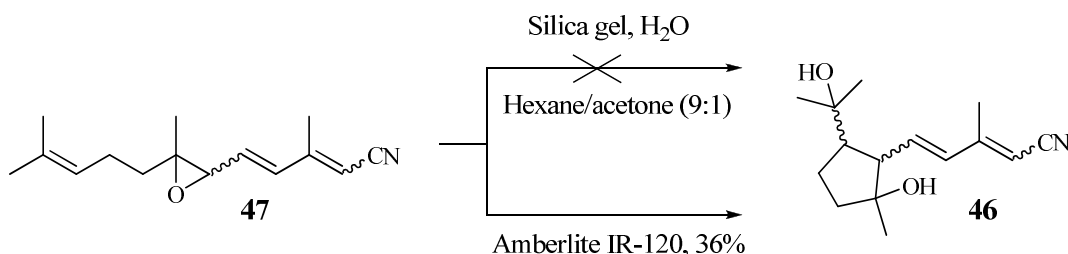


Entry	47 : H ₂ SO ₄ (mmol)	Conditions	Temp. Time (h)	Relative % ^a 46 : 59 : 60 : 47
1	0.1 : 0.015	0.05% H ₂ SO ₄ , 4 mL CH ₂ Cl ₂ , 2 mL	R.T. 24	0 : 0 : 0 : 100
2	0.1 : 0.015	0.05% H ₂ SO ₄ , 4 mL THF, 2 mL	R.T. 24	20 : 30 : 28 : 12
3	0.1 : 0.4	1.7 % H ₂ SO ₄ , 3 mL THF, 3 mL	R.T. 2	26 : 28 : 34 : 2
4	0.1 : 0.4	1.7 % H ₂ SO ₄ , 3 mL THF, 3 mL	0 °C 5	27 : 31 : 21 : 17
5	0.1 : 2.1	5 % H ₂ SO ₄ , (1 mL) THF (1 mL)	R.T. 2	24 : 19 : 34 : 1

^a Determined by HPLC peak area (condition B, Appendix I).

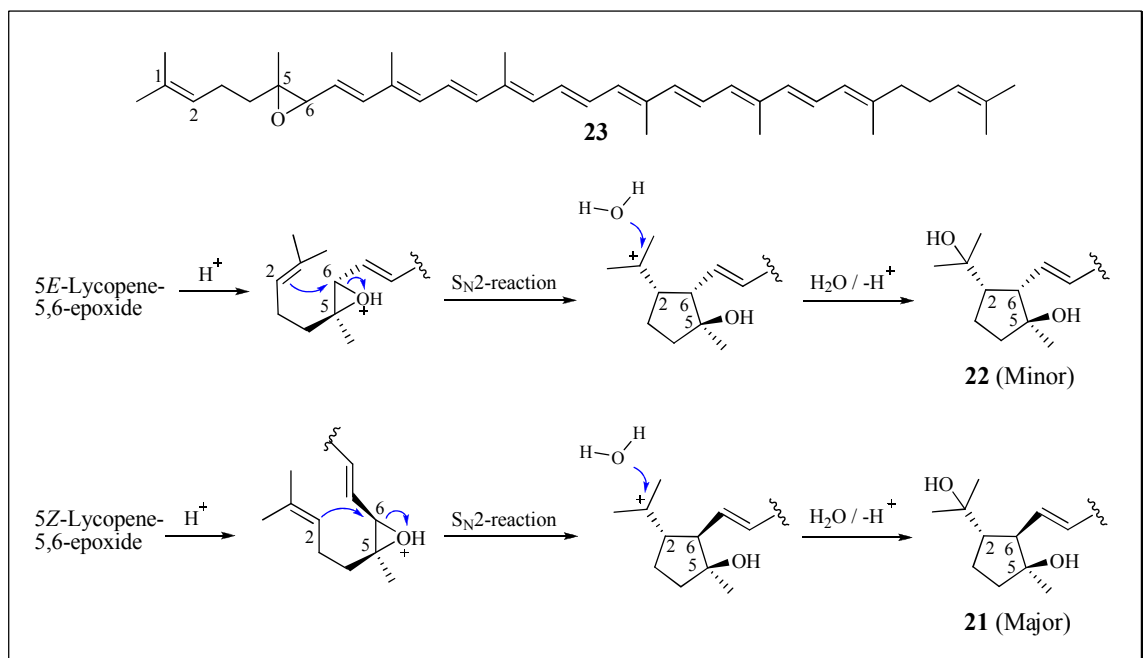
Although the C₁₅-dihydroxynitrile **46** could be prepared with dilute sulfuric acid in modest yields, we hoped to develop a condition under which the yield of the key synthon **46** would predominate over those of the dehydration product **59** and 6,7-diol **60** by-products. Recognizing the acidic nature of moist silica gel, cyanoepoxides **47** (**a1**, **a2**,

b1 and **b2**) (0.43 mmol) were passed through a small column containing 20 g silica gel treated with water (23 mmol). However, no reaction took place under these conditions. Gratifyingly, **46** could be prepared by stirring a solution of **47** with the acidic cation exchange resin (Amberlite IR-120), which is a sulfonated polystyrene/divinylbenzene copolymer. A solution of epoxynitriles **47** in hexane were treated with water and Amberlite IR-120. The mixture was stirred overnight at R.T. Based on area percent by normal phase HPLC, **46** was obtained as a mixture of 4 compounds in 36% yield, along with **60** (20%), **59** (32%) and starting material (11%) (Scheme 35).



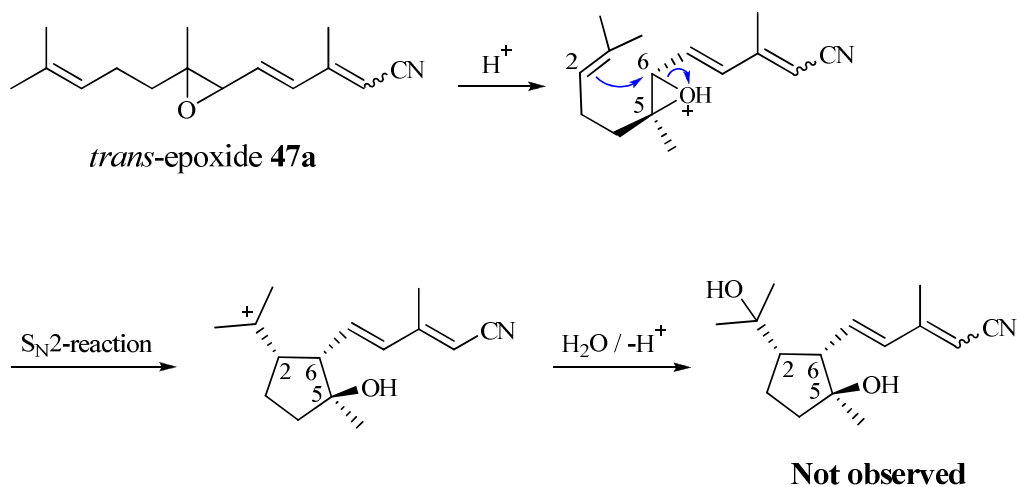
Scheme 35. Synthesis of C₁₅-dihydroxynitrile **46** by Amberlite IR-120 vs. silica gel.

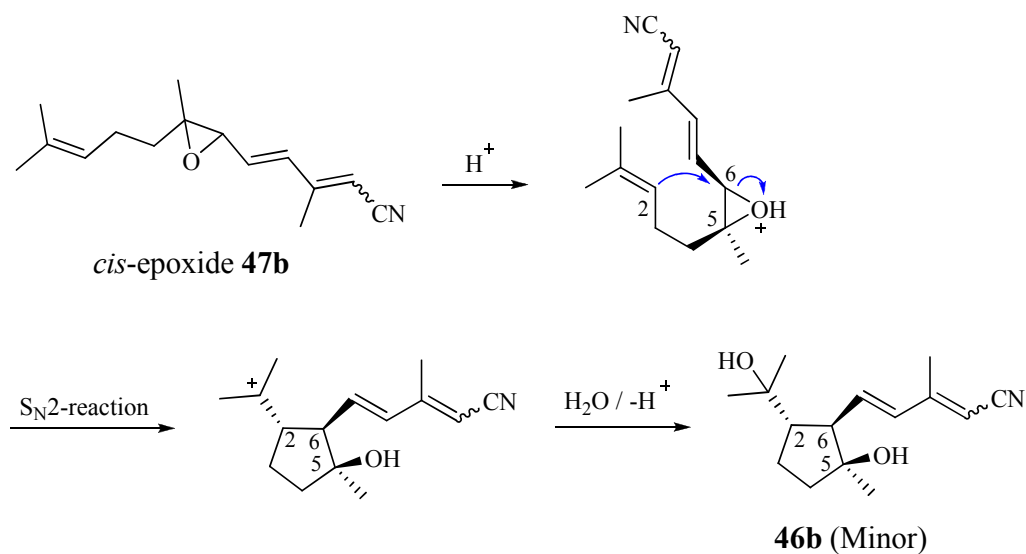
The mechanism for the acid-catalyzed rearrangement of 5*E*- and 5*Z*-lycopene-5,6-epoxides (**23**) has been proposed by Khachik *et al.* to occur *via* an S_N2 type mechanism (Scheme 36).⁸⁷ Protonation of the epoxide ring followed by nucleophilic attack of the C1/C2 double bond at C6 produced five-membered ring carbocation intermediates. Addition of water and subsequent loss of a proton afforded 2,6-cyclolycopene-1,5-diols (**22** and **21**) observed by Khachik *et al.* in minor and major amounts, respectively.



Scheme 36. Rearrangement of *5E*- and *5Z*-lycopene-5,6-epoxides (**23**) by an S_N2 mechanism.⁸⁷

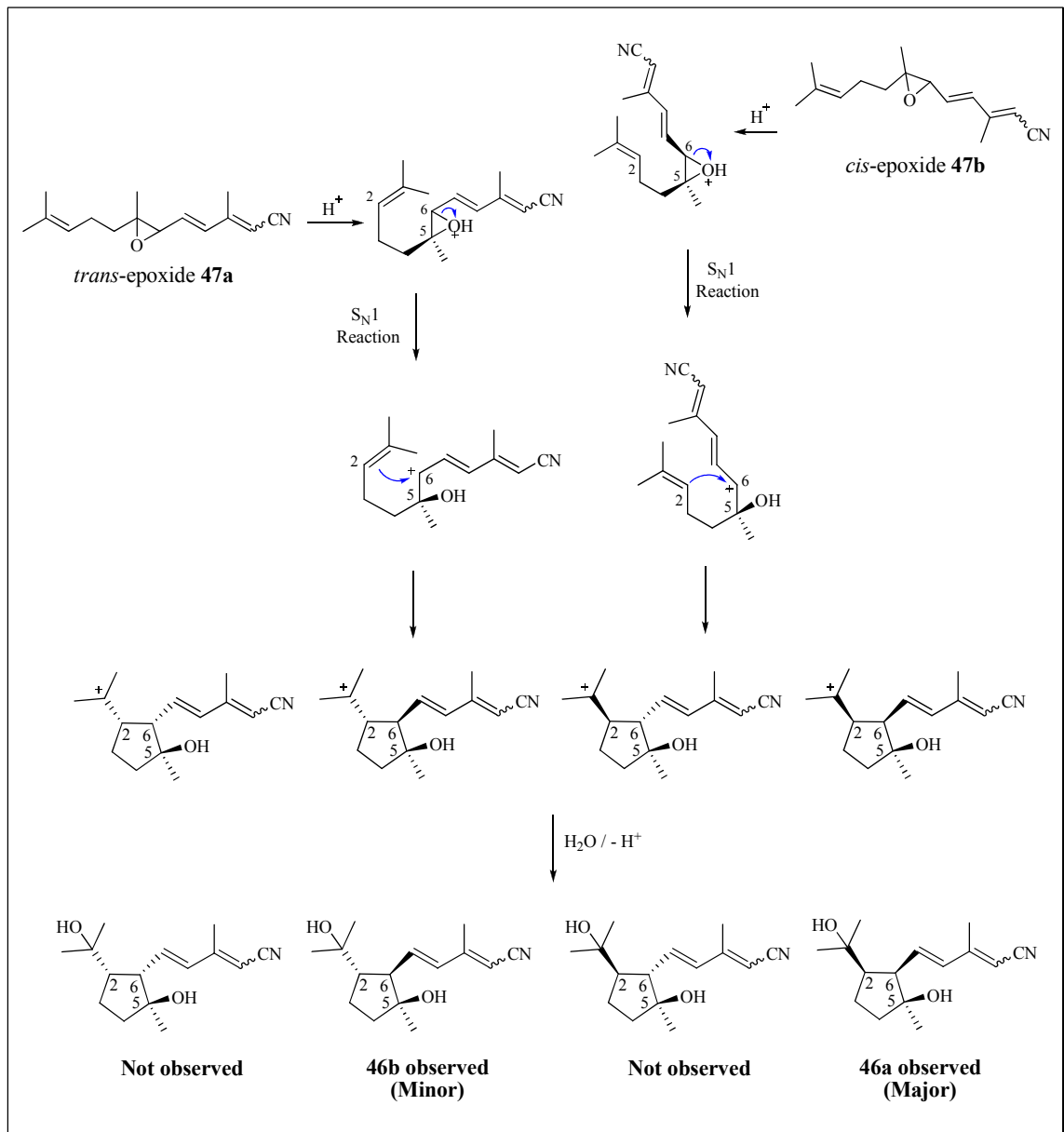
The major 2,6-cyclolycopene-1,5-diol (**21**) observed by Khachik corresponds to the minor C_{15} -dihydroxynitrile **46b2** observed in this research when the *cis*-epoxides **47b1** and **47b2** undergo an S_N2 -type reaction (Scheme 37).





Scheme 37. C₁₅-dihydroxynitrile **46b** formed from *cis*-epoxide **47b** via an S_N2-type reaction.

In an S_N1 type process, acid-catalyzed protonation of the *cis* and *trans* epoxide rings followed by ring opening would be accompanied by formation of a carbocation at C6. Intramolecular cyclization would produce four 5-membered rings with epimerization at C2 and C6. Reaction with water followed by loss of a proton would afford products with relative stereochemistries at C2, C5 and C6 observed for diols **46a** and **46b** (Scheme 38). The acid-catalyzed intramolecular cyclization of the *cis* and *trans*-epoxide **47a** and **47b** by an S_N1 pathway would account for both sets of diols **46a** and **46b** observed in this research.



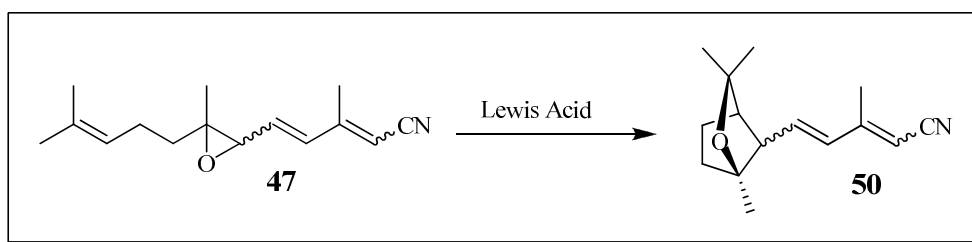
Scheme 38. Rearrangement of *cis* and *trans*-epoxides **47a** and **47b** by an S_N1 -type mechanism.⁸⁷

Cyclization of C_{15} -epoxynitrile **47** with $FeCl_3$ and $ZrCl_4$.

Meanwhile, a literature survey revealed similar Lewis acid-promoted cyclization of simple isoprenoid epoxyolefins such as geraniol and farnesol epoxides with $FeCl_3$ hexahydrate and $ZrCl_4$.^{128,129} Because the cyclization with these Lewis acids have been

shown to be regiochemically controlled, we then investigated the cyclization of **47** with these catalysts under a number of different conditions.

As described earlier, cyclization of lycopene 5',6'-epoxide (**23**) to diols **21** and **22** has been shown to proceed *via* bicyclic oxides **20** and **24**. Therefore, we anticipated that epoxynitrile **47** could similarly undergo cyclization in the presence of a Lewis acid to dihydroxynitrile **46** *via* nitrile **50** as shown in Scheme 39.



Scheme 39. Formation of bicyclic oxide **50**.

Zirconium tetrachloride, iron trichloride, boron trifluoride and acidic alumina were evaluated for their ability to cyclize epoxynitrile **47** to diol **46**, possibly *via* bicyclic oxide **50**. Solvent type, mol percent of Lewis acid and temperature were varied to optimize the formation of diol **46**; the results are listed in Table 7. In all reactions with ZrCl_4 and FeCl_3 , a substantial amount of compound **59**, a dehydration product of dihydroxynitrile **46**, was formed, along with a mixture of numerous unidentified side-products based on HPLC analysis.

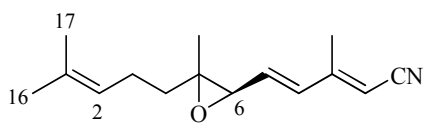
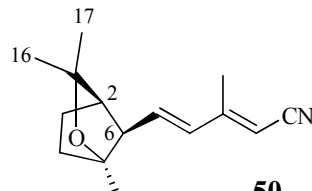
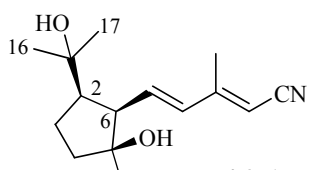
Table 7. Lewis acid-catalyzed reactions of C₁₅-epoxynitrile **47**.

Lewis Acid (LA)	mol% LA	Temp. (°C)	Solvent	Time (min)	47 : 59 (%)
ZrCl ₄	15	Ambient	CH ₂ Cl ₂	30	5 : 22
	10	-5	CH ₂ Cl ₂	30	28 : 26
	20	-5	CH ₂ Cl ₂	30	3 : 29
	20	-20	CH ₂ Cl ₂	30	15 : 26
	100	-20	CH ₂ Cl ₂	60	9 : 25
	20	-20	Hexane	60	2% conversion
	20	-20	THF	60	49 : 22
ZrCl ₄ , Na ₂ CO ₃ , excess	20	-20	CH ₂ Cl ₂	60	38 : 23
ZrCl ₄ , Et ₃ N, excess	100	-10	CH ₂ Cl ₂	60	No reaction
FeCl ₃ , anhydrous	20	-20	CH ₂ Cl ₂	60	43 : 24
	50	-20	CH ₂ Cl ₂	60	20 : 27
	100	-5	CH ₂ Cl ₂	20	3 : 26
	100	-20	CH ₂ Cl ₂	20	3 : 27
	100	0	Hexane	30	No reaction
BF ₃ ·Ether	20	-20	THF	60	No reaction
Alumina, acidic	Excess	Ambient	CH ₂ Cl ₂	120	No reaction
	Excess	60 °C	THF	120	No reaction

Addition of Na₂CO₃ did not seem to have any effect in preventing the formation of **59**, and in the presence of Et₃N no reaction was observed. Similar results were also obtained in the reactions of **47** with anhydrous FeCl₃. The solvent of choice with both catalysts was found to be dichloromethane, as it resulted in nearly complete conversion of the starting material. Lowering the temperature produced similar results but prolonged the reaction time. Further, varying the amounts of the catalysts and lowering the reaction temperature had no effect on relative composition of **59**. Attempted cyclization of **47** with BF₃ etherate in THF or in the presence of acidic alumina was also unsuccessful. We also attempted microwave heating of **47** in CH₂Cl₂ but only the starting material was recovered.

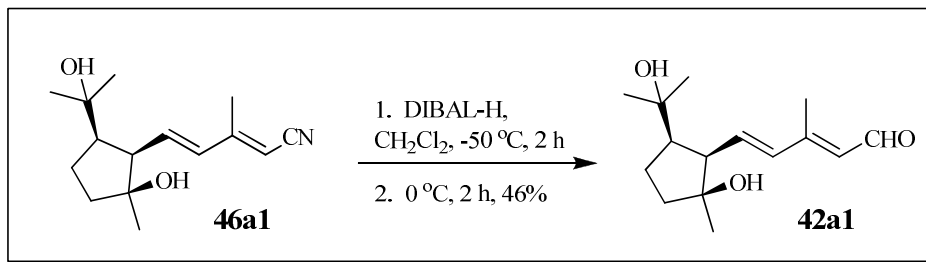
We were unable to identify the existence of **50** under any experimental condition employed based proton NMR spectrometry. Signature chemical shifts for H2, H6 and Me16/17 expected for the bicyclic oxide intermediate reported by Lu *et al.*⁸⁴ were not observed in the spectra of crude products. These are provided in Table 8 along with those of the epoxy nitrile starting material **47** and product **46**, which was also not present in the crude product, based on the HPLC profiles. As we were unable to isolate and identify **50** under any experimental condition employed, no attempt was made to further isolate and identify compounds in the crude product. This is because our initial goal was to optimize the reaction conditions that could prevent the formation of **59** that was most likely formed from dehydration of the desired diol **46**.

Table 8. Chemical shifts for the bicyclic oxide (**50**)⁸⁴, cyanoepoxide **47** and C₁₅-dihydroxynitrile **46a1**.

	H2 (ppm)	H6 (ppm)	Me 16 / 17 (ppm)
 <p style="text-align: center;">47</p>	5.1	3.4	1.7 / 1.6
 <p style="text-align: center;">50</p>	2.0	2.8	1.3 / 1.2
 <p style="text-align: center;">46a1</p>	2.7	2.6	1.3 / 1.2

DIBAL-H reduction of C₁₅-dihydroxynitrile **46**.

While reduction of C₁₅-dihydroxynitriles **46a** and **46b** with DIBAL-H afforded a mixture of aldehydes, stereochemically pure C₁₅-dihydroxynitrile **46a1** could be reduced to produce the corresponding isomer **42a1** in 46% yield when the temperature was maintained below -20 °C, as shown in Scheme 40.

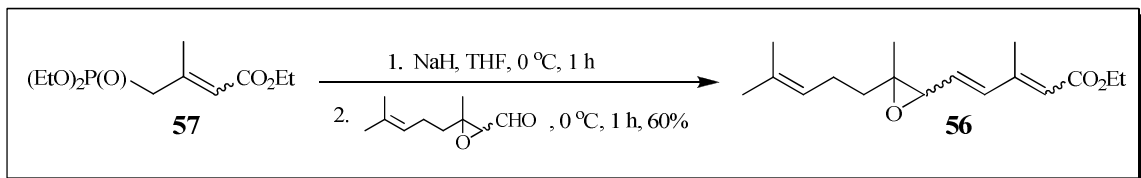


Scheme 40. DIBAL-H reduction of C₁₅-dihydroxynitrile **46a1**.

Although conjugated cyano compounds have been reduced with DIBAL-H at R.T. to aldehydes in good yields,^{130,131} the low temperature condition was expected to result in a higher isolated yield of the product, due to the tendency of the C₁₅-dihydroxyaldehyde **42** to decompose at room temperature and during purification by semi-preparative HPLC.

Alternate route to the synthesis of C₁₅-dihydroxyaldehyde **42**.

In an attempt to increase the yield of **42**, another route to this key intermediate was explored. This essentially involved the same route with the exception of replacing the cyano group with an ester function. With the hope that the cyclization could proceed much more efficiently, key synthon **42** was also prepared *via* the C₁₇-epoxyethyl ester **56** in a second route according to the process outlined in Scheme 41.



Scheme 41. Synthesis of C₁₇-epoxyethylester **56**.

In the first step, sodium hydride was used to generate the anion of the commercially available starting material triethyl-3-methyl-4-phosphono-2-butenoate (**57**). Formation of hydrogen gas was evident and ceased within one hour. Subsequent HWE coupling with citral epoxide (**48**) in the second step produced a dark colored product. The crude product was purified by flash column chromatography to afford **56** in 60% isolated yield. The product consisted of a mixture of *cis/trans*-epoxides with their corresponding *2E*- and *2Z*-stereoisomers. The ratio of *cis/trans*-epoxides **56a**:**56b** was approximately (1:1), based on HPLC area counts while the ratio of (*2E/2Z*) isomers was approximately 2:1, based on analysis by NMR. The mixture was further separated by semi-preparative normal phase HPLC into four stereoisomers (**56a1**, **56a2**, **56b1**, **56b2**) as shown in Figure 22. The structures and relative stereochemistries at C2, C4 and C6 were established by proton and NOESY NMR spectroscopy.

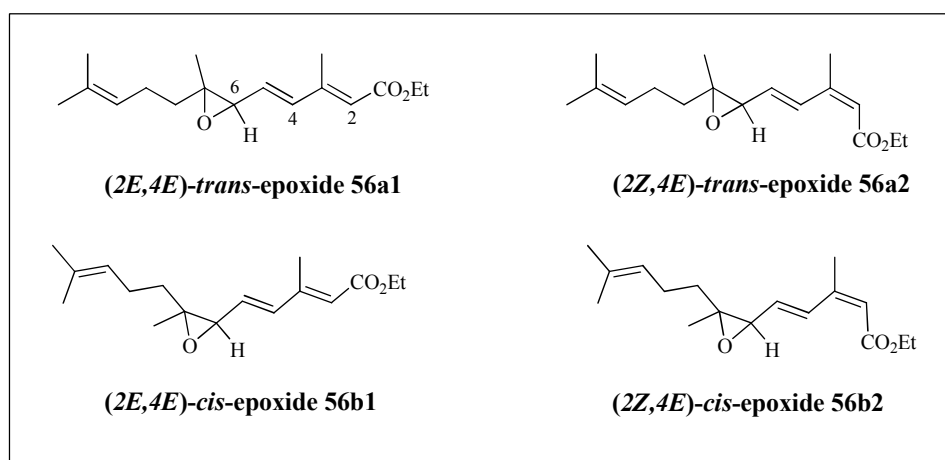
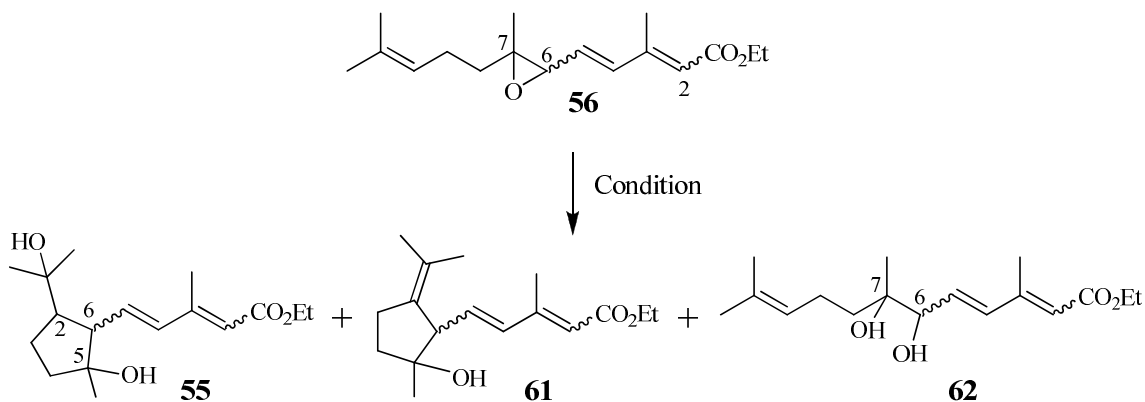


Figure 22. Structures of C₁₇-epoxyethylesters.

Cyclization of C₁₇-epoxyethylester **56** with dilute H₂SO₄.

The C₁₇-epoxyethylester epoxides **56a1**, **56a2** and **56b1**, **56b2** were converted to the cyclized C₁₇-epoxyethylesters **55** in dilute sulfuric acid in THF, as shown in Scheme 42. In addition to the product **55**, competitive amounts of the dehydration product **61** and 6,7-dihydroxy compound **62** were formed. The nature and relative amount of these products were influenced by temperature, solvent and the ratio of starting material to acid (Table 9). Reactions were monitored by normal phase HPLC; the relative percent of each product was based on area counts.



Scheme 42. Acid catalyzed intramolecular cyclization of C₁₇-epoxyethylesters **56**.

Table 9. The cyclization of C₁₇-epoxyethylesters **56** with dilute sulfuric acid.

Entry	56 : H ₂ SO ₄ (mmol)	Conditions	Temp Time (h)	Relative % ^a 55 : 61 : 62 : 56
1	1 : 0.09	0.025% H ₂ SO ₄ , 20 mL THF, 3 mL	R.T. 24	48 : 19 : 27 : 6
2	1 : 0.09	0.021% H ₂ SO ₄ , 24 mL THF, 13 mL	10 °C 24	29 : 26 : 6 : 39
3	1 : 0.05	0.01% H ₂ SO ₄ , 28 mL THF, 16 mL	R.T. 24	34 : 28 : 27 : 10
4	1 : 0.09	0.025% H ₂ SO ₄ , 20 mL acetone, 3 mL	R.T. 24	36 : 12 : 28 : 23

^a Determined by HPLC peak area (condition B, Appendix I).

Our observations indicate that the highest yield of product **55** could be obtained by stirring epoxide **56** with 0.1M sulfuric acid in water and THF at room temperature for 24 hours (entry 1). While formation of the diol **62** was suppressed when the reaction was conducted at 10°C, the amount of dehydration product **61** formed could not be minimized accordingly (entry 2). When half the amount of acid was used (entry 3), or when the solvent was changed from THF to acetone (entry 4), a greater amount of the starting material remained unreacted, and the formation of dehydration product **61** and diol **62** were still significant. Ultimately, differences in product ratios were not significantly influenced by changes in the amount of acid used or reaction temperature.

The C₁₇-dihydroxyethylesters **55** were synthesized under the conditions indicated for entry 1 (Table 9) and isolated by flash column chromatography in 42% overall yield along with the dehydration product **61** (15%) and 6,7-dihydroxyethylester **62** (23%). The protonated form of the molecular parent ion was observed in addition to fragments resulting from loss of one and two molecules of water by HRMS. **62** was characterized by proton NMR (*E/Z* = 1.5:1.0). The chemical shift of H6 at 4.1 ppm is consistent with a hydroxyl substituent at the allylic position, in comparison with the chemical shift of H6 of epoxide **56** at 3.3 ppm.

For the dehydration product **61**, the protonated form of the molecular ion was observed in addition to a fragment resulting from loss of one molecule of water by HRMS. Structural assignment of **61** was based on results of proton NMR. The chemical shift of H2 between 2.0 and 2.6 ppm was no longer evident. Chemical shifts of protons on Me16/17 were shifted downfield from 1.2 ppm to approximately 1.6 ppm, which is characteristic of geminal methyl groups attached to an sp² carbon atom.

Because the starting material consisted of four stereoisomers, the product was expected to consist of four stereoisomers as well. However, the target compound could only be separated into three diastereomeric compounds **55a1**, **55a2**, and **55b1** by semi-preparative normal phase HPLC in relative ratios **55a1** > **55a2** > **55b1** (4.9:3.2:1.0), Figure 23.

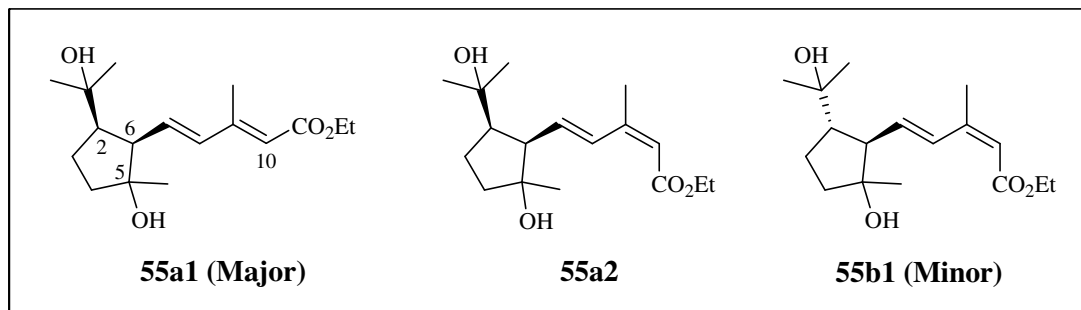


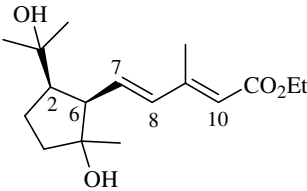
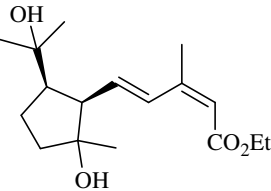
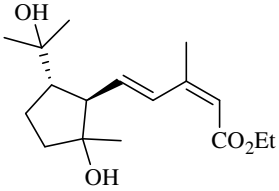
Figure 23. C₁₇-dihydroxyethyl esters **55a**, **55a2**, and **55b**.

The structures of **55a1**, **55a2**, and **55b** were established by proton NMR spectroscopy. The stereochemical assignments were based on the chemical shift patterns for H₂, H₇ and H₈ established for the analogous cyano-derivatives **46a1**, **46a2** and **46b1** by a NOESY experiment. The chemical shifts of H₂ and H₆ were approximately 2.6 ppm in **55a1** and **55a2**, which indicated their *cis* relationship to one another, whereas the chemical shift of H₂ in **55b1** was shifted upfield to approximately 2.0 ppm, indicating a *trans* relationship between H₂ and H₆ in this compound. Further, the chemical shift of H₈ was approximately 7.6 ppm in compounds **55a2** and **55b1** (Table 10). This established the *cis*-geometry of the ester group at C₁₀ in these compounds. By comparison, the chemical shift of H₈ in **55a1** was shifted upfield to approximately 6.2 ppm, indicating a *trans*-geometry of the ester group at C₁₀ in this compound.

¹³C NMR results for **55a1**, **55a2**, and **55b** showed signals corresponding to C₁ and C₅ attached to hydroxyl groups occurred at approximately 72 and 81 ppm,

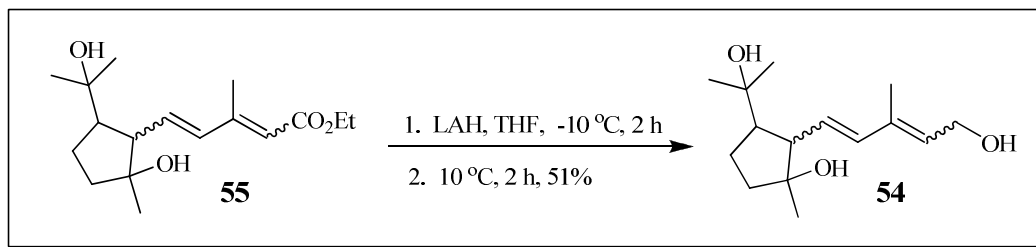
respectively. Four chemical shifts corresponding to substituted olefinic carbons were evident while another signal was observed for the carbonyl group of the ester at 167 ppm. Compounds **55a1**, **55a2**, and **55b** gave rise to signals for the protonated parent molecular ion and fragments associated with loss of one and two molecules of water by HRMS.

Table 10. Chemical shifts of key protons for C₁₇-dihydroxyethylesters **55a1**, **55a2**, and **55b**.

Stereoisomer	H2 (ppm)	H6 (ppm)	H7 (ppm)	H8 (ppm)
 <p>55a1 (Major)</p>	2.58	2.64	6.02	6.18
 <p>55a2</p>	2.64	2.64	6.00	7.65
 <p>55b1 (Minor)</p>	1.98	2.64	5.89	7.56

Reduction of C₁₇-dihydroxyethylesters **55** to C₁₅-triol **54** by LAH reduction

The C₁₅-cyclized triol **54** was prepared by reduction of the C₁₇-dihydroxyethylester **55** with lithium aluminum hydride (Scheme 43).



Scheme 43. Reduction of C₁₇-dihydroxyethylester **55** to C₁₅-triol **54**.

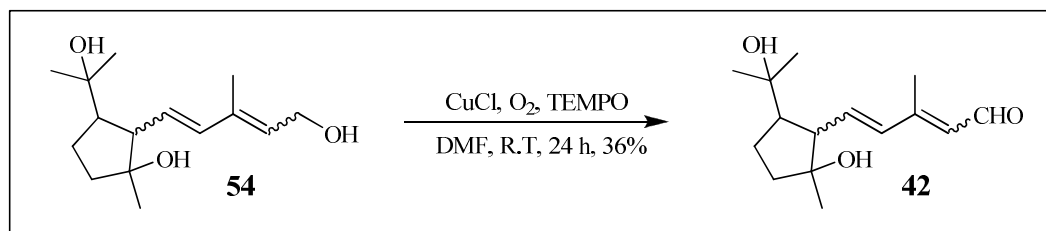
The crude triol product **54** was purified by flash column chromatography and isolated as a gummy, white crystalline solid in 51% isolated yield. Based on HPLC analysis, the product consisted of 2 isomeric products in a 1:1 ratio. The mixture was further separated using normal phase semi-preparative HPLC and analyzed by HRMS, which gave rise to signals for the parent ion paired with a sodium ion and fragments associated with loss of two and three molecules of water.

In the proton NMR spectrum of triol **54**, chemical shifts for three vinylic hydrogen atoms were evident, while a doublet corresponding to the methylene protons adjacent to the hydroxyl group appeared at 4.3 ppm. In the ¹³C NMR spectrum, chemical shifts corresponding to quaternary C1 and C5 attached to a hydroxyl group were observed at 72 and 83 ppm respectively, while a chemical shift for a secondary carbon atom attached to a hydroxyl group was evident at 59 ppm. Four chemical shifts corresponding to substituted olefinic carbon atoms were evident.

Although retinol (**15**) has been oxidized to retinal (**16**) with manganese dioxide in useful yields,¹³² attempts to produce key synthon C₁₅-dihydroxyaldehyde **42** from the oxidation of C₁₅-triol **54** with manganese dioxide in methylene chloride were unsuccessful. After 24 h at R.T., the starting material remained unreacted, based on TLC analysis. While primary alcohols can also be oxidized to the corresponding aldehydes

with pyridinium chlorochromate (PCC) in dichloromethane,¹³³ by Swern oxidation with dimethylchlorosulfonium ion,¹³⁴ or the Dess-Martin hypervalent iodine (V) reagent,^{135,136} one of the most common reagents for the oxidation of primary alcohols is 2,2,6,6-tetramethylpiperidine-1-nitroxide radical (TEMPO) that has been shown to be a highly selective oxidizing reagent for the exclusive preparation of aldehydes from primary allylic alcohols,¹³⁷ primary saturated alcohols¹³⁸ and sugars.¹³⁹ For a review on the industrial applications of TEMPO in the preparation of pharmaceuticals, flavors and fragrances and agrochemicals, see the review by Ciriminna and Pagliaro.¹⁴⁰

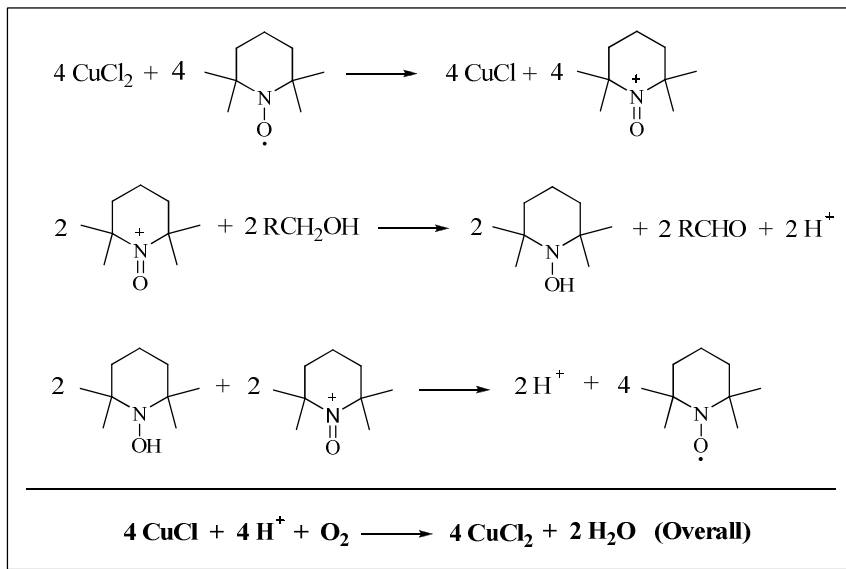
Based on the procedure adopted from Semmelhack *et al.*,¹⁴¹ the triol **54** was oxidized to the corresponding aldehyde **42** with 10 mole percent each TEMPO and cuprous chloride in the presence of oxygen at R.T in DMF solvent as shown in Scheme 44.



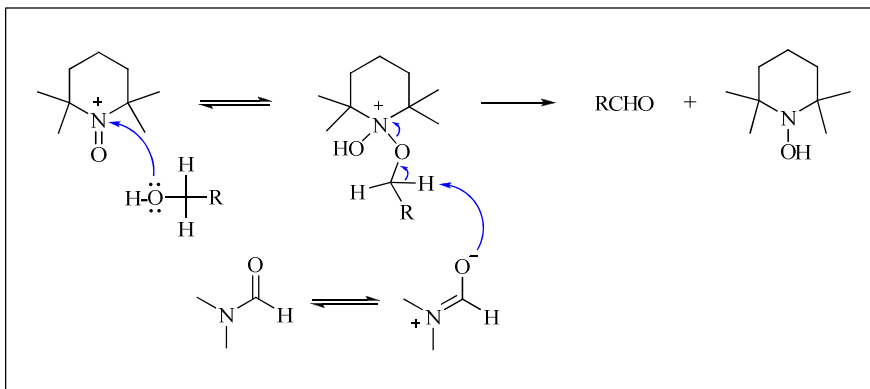
Scheme 44. TEMPO oxidation of C₁₅-triol **54** to C₁₅-dihydroxyaldehyde **42**.

In the overall process shown in Scheme 45, copper (I) is oxidized to copper (II) as oxygen is reduced to water. Cupric ions mediate the one electron oxidation of the nitroxyl radical to nitrosonium ion. Reaction between the nitrosonium ion and alcohol affords the aldehyde in a subsequent step according to the mechanism proposed in Scheme 46, where the solvent DMF may act as a base. During the process of *syn* disproportionation, redistribution of charge between the hydroxyl amine by-product and the

nitrosonium ion regenerates the TEMPO radical. In the net reaction, oxygen is consumed during the oxidation of alcohol to the aldehyde, with the concomitant formation of water.



Scheme 45. Sequence proposed for the organocatalytic oxidation of alcohols to aldehydes with TEMPO and oxygen.



Scheme 46. Mechanism proposed for the catalytic conversion of primary alcohols to aldehydes with TEMPO.^{140,141}

During the reaction, the solution took on the blue/green color of cuprous/cupric ions. After flash column chromatography, key synthon **42** was isolated in 36% yield as a light yellow oil and shown to consist of 4 stereoisomers by normal phase HPLC (Figure 24).

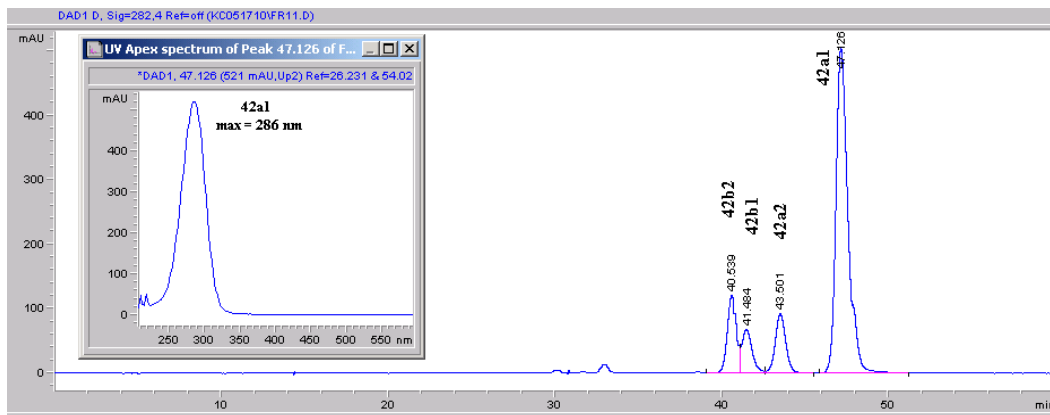


Figure 24. HPLC chromatogram of C₁₅-dihydroxyaldehydes **42a1**, **42a2**, **42b1**, and **42b2**. (Condition B, Appendix I).

The isomers **42a1**, **42a2**, **42b1** and **42b2** were separated by semi-preparative HPLC and isolated in the relative ratio (1.5:0.9:1.0:1.0). Compound **42a2** could be crystallized from the mixture in hexane/ethyl acetate solvent after storage for two weeks at -80 °C. The compounds were further isolated by semi-preparative normal phase HPLC and analyzed by ¹H-NMR (Figure 25).

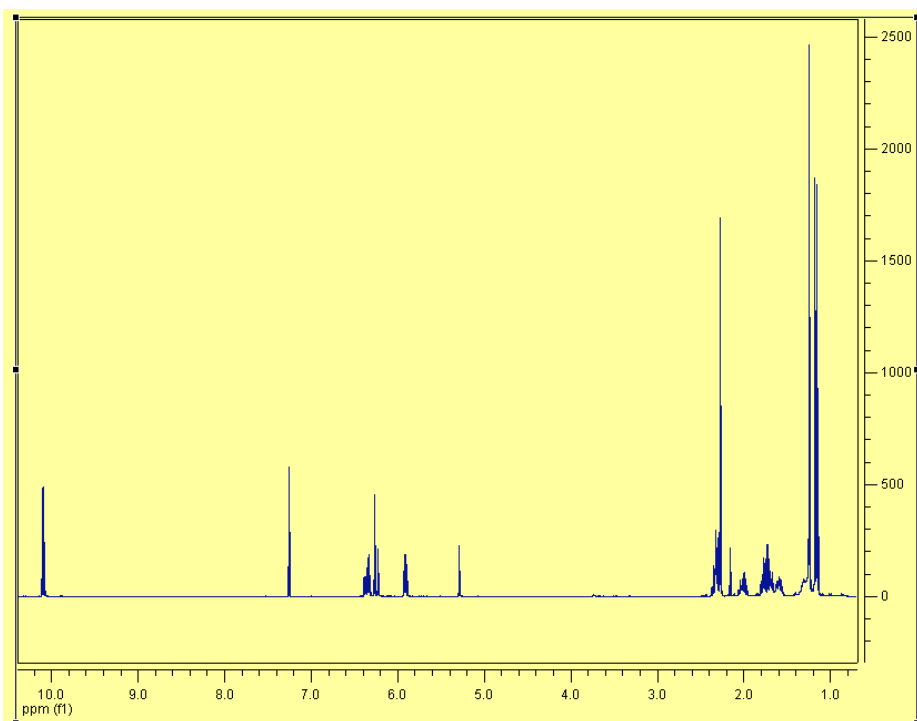
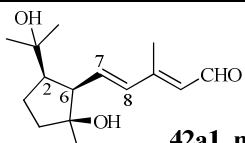
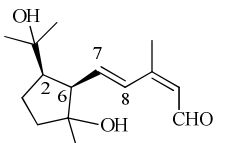
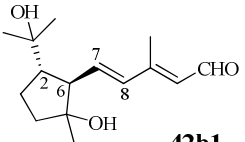
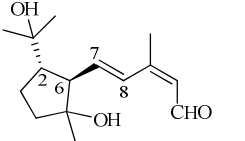


Figure 25. ¹H-NMR spectrum of C₁₅-dihydroxyaldehyde **42a1**.

Based on analogous chemical shift patterns observed for the structurally characterized isomer **42a1** and the C₁₅-dihydroxynitriles **46a** and **46b**, relative stereochemistries at C2, C6 and C10 were tentatively assigned for **42a2**, **42b1**, and **42b2**. However, only **42a1** was analyzed by NOESY NMR; while the relative stereochemistry of the hydroxyl group at C5 was determined for this isomer, the relative stereochemistry of the hydroxyl group at C5 was not confirmed for **42a2**, **42b1**, and **42b2**. Chemical shifts of H2, H6, H7 and H8 for the stereoisomers of **42** are shown in Table 11.

Table 11. Chemical shifts of key protons of C₁₅-dihydroxyaldehydes **42a1**, **42a2**, **42b1**, and **42b2**.

Stereoisomer	H2 (ppm)	H6 (ppm)	H7 (ppm)	H8 (ppm)
 42a1, major	2.32	2.29	6.36	6.25
 42a2	2.34	2.34	6.26	7.13
 42b1	1.97	2.63	6.03	6.20
 42b2	1.97	2.65	5.93	7.06

The ¹³C NMR results for the C₁₅-aldehydes of **42** were consistent with the reported structure (Figure 26). Chemical shifts corresponding to C1 and C5 attached to a hydroxyl group occurred at 72 and 81 ppm, respectively. Three signals corresponding to substituted olefinic carbons were evident while another signal was observed for the

olefinic carbon atom conjugated to an aldehyde at approximately 154 ppm. The chemical shift of the aldehydic carbon was evident at 190 ppm.

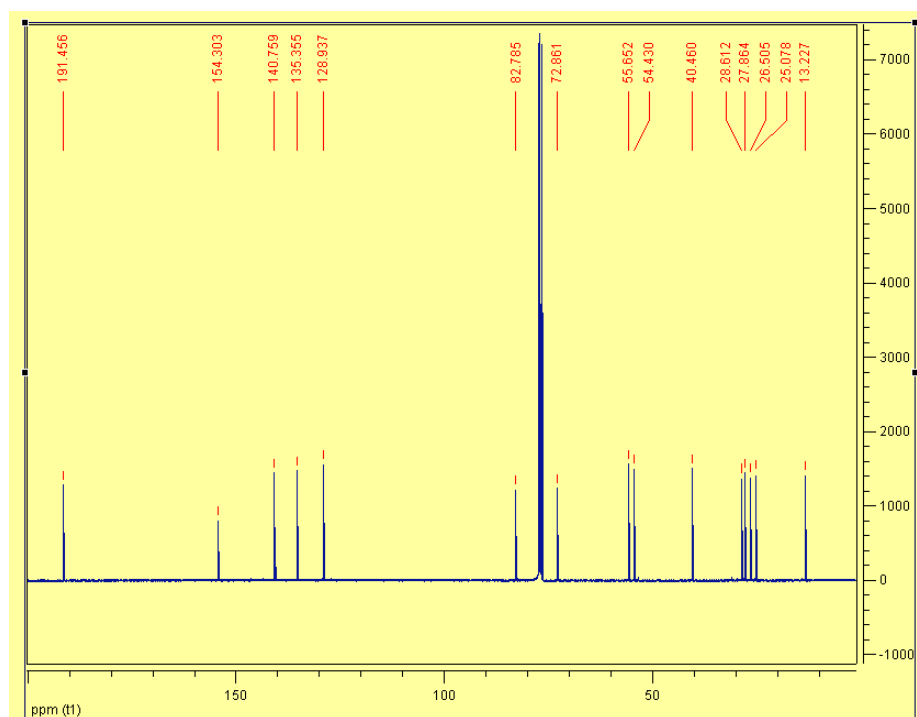


Figure 26. ^{13}C -NMR spectrum of C_{15} -dihydroxyaldehyde **42a1**.

The relative stereochemistries at C2, C5, C6 and C10 of **42a1** were determined by a NOESY experiment (Figure 27).

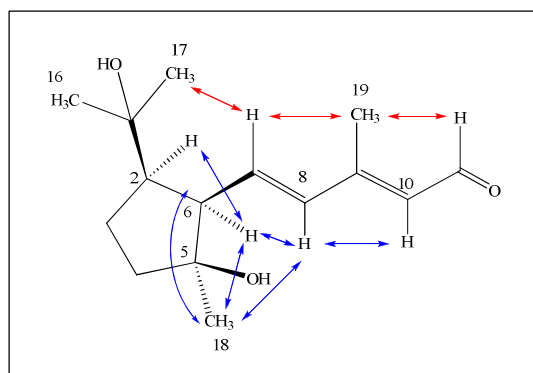


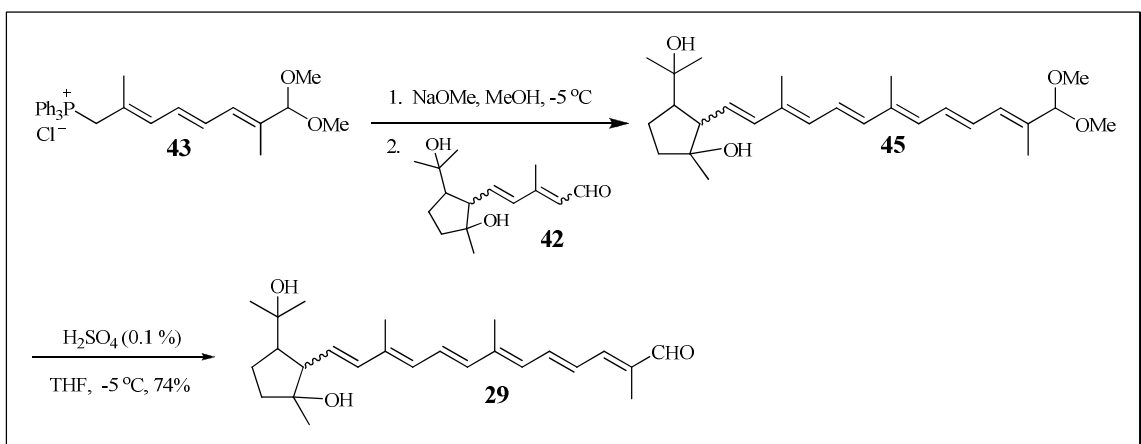
Figure 27. NOESY crosspeaks observed in key synthon **42a1**.

Crosspeaks between Me18, H2 and H6 demonstrated their *cis* relationship, thus establishing the relative orientations of the hydroxylated isopropyl group at C2, the hydroxyl group at C6 and side chain at C6. The *7E,9E* stereochemistry was established by crosspeaks between Me19 and H7 as well as Me19 and the aldehydic proton.

By HRMS, the protonated form of the molecular parent ion was observed in addition to fragments resulting from loss of one and two molecules of water for each of the four stereoisomers. Proton and carbon assignments were based on COSY and HSQC NMR experiments.

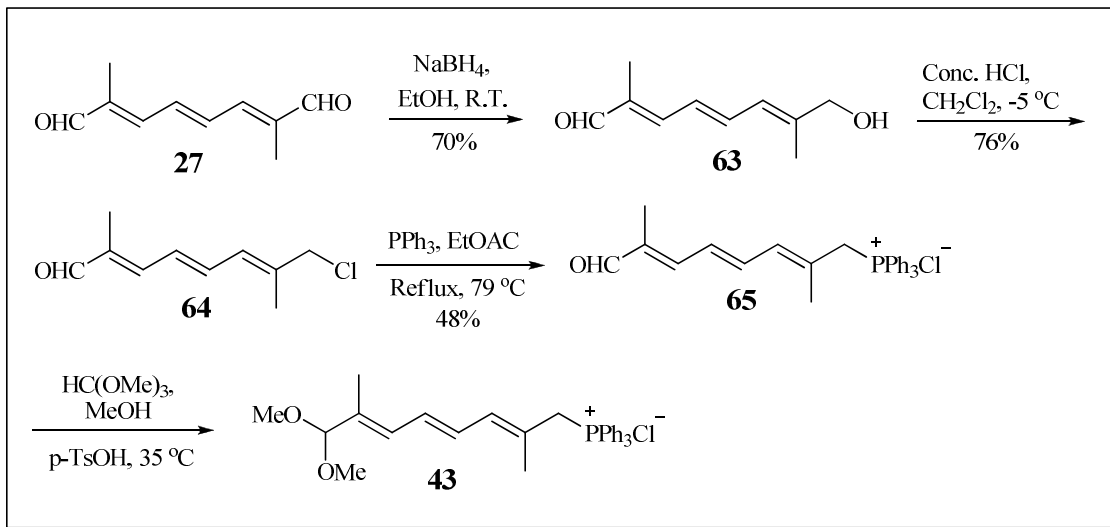
Synthesis of C₂₅-dihydroxyaldehyde **29**.

With key synthon **42** in hand, C₂₅-dihydroxyaldehyde **29** was prepared by a Wittig reaction. The stereoisomeric mixture of synthon **42** was first coupled with protected Wittig salt **43** in the presence of sodium methoxide to produce the C₂₅-acetal **45**, which without isolation, was deprotected *in-situ* with dilute sulfuric acid. Thus, **29** was obtained in 74% isolated yield after purification by column chromatography (Scheme 47).



Scheme 47. Synthesis of C₂₅-dihydroxyaldehyde **29**.

The protected Wittig salt **43** was prepared from C₁₀-dialdehyde **27** according to the procedure published by Bernhard *et al.*¹¹⁴ (Scheme 48).



Scheme 48. Synthesis of protected Wittig salt **43**.

The C₁₀-dialdehyde **27** is available by large scale industrial routes.¹⁴² Partial reduction of **27** with sodium borohydride in ethanol afforded the mono-ol **63** in 70% yield after purification by column chromatography. Concentrated HCl was used to transform **64** in 76% yield. Wittig salt **65** was prepared in 48% yield by refluxing **64** with triphenylphosphine in ethyl acetate overnight followed by recrystallization from ethyl acetate and methylene chloride. The protected Wittig salt **43** was prepared by gently heating **65** with trimethylformate in acidified methanol in the presence of silica gel.

Structural characterization of C₂₅-dihydroxyaldehyde **29**.

Aldehyde **29** was shown to consist of two isomers by normal phase HPLC. These were further separated by semi-preparative HPLC. The purified isomers of **29** were analyzed by HRMS where the protonated form of the molecular ion was observed in addition to fragments resulting from loss of one and two molecules of water. Proton and

carbon assignments for only one isomer were based on COSY, HSQC and HMBC NMR experiments. Relative stereochemistries at C2, C5, C6 and C12' were based on a NOESY experiment.

In the proton NMR spectrum of **29**, nine chemical shifts were evident for the vinylic protons. The chemical shift for the aldehydic proton occurred at 9.45 ppm. The chemical shifts for H2 and H6 were 1.96 and 2.53, respectively. This observation suggested these protons were in a *trans* relationship to one another, resulting in an *all-E* geometry for **29**. The *trans* relationship between H2 and H6 was further demonstrated by lack of a crosspeak between these protons in a NOESY experiment. NOESY crosspeaks were observed between Me18 and H6, which established their *cis* relationship to one another. A crosspeak between H14' and H12' established an *E*-geometry for the C14' double bond in relation to the aldehydic proton. Other crosspeaks observed are indicated in Figure 28.

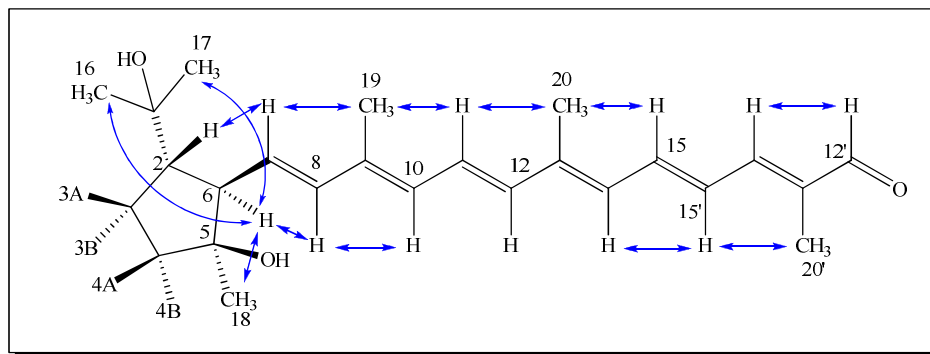


Figure 28. NOESY crosspeaks observed for C₂₅-dihydroxyaldehyde **29**.

The ¹³C NMR chemical shifts for **29** corresponding to C1 and C5 attached to hydroxyl groups appeared at approximately 72 and 81 ppm, respectively. Twelve signals corresponding to substituted olefinic carbons were evident. The chemical shift of the

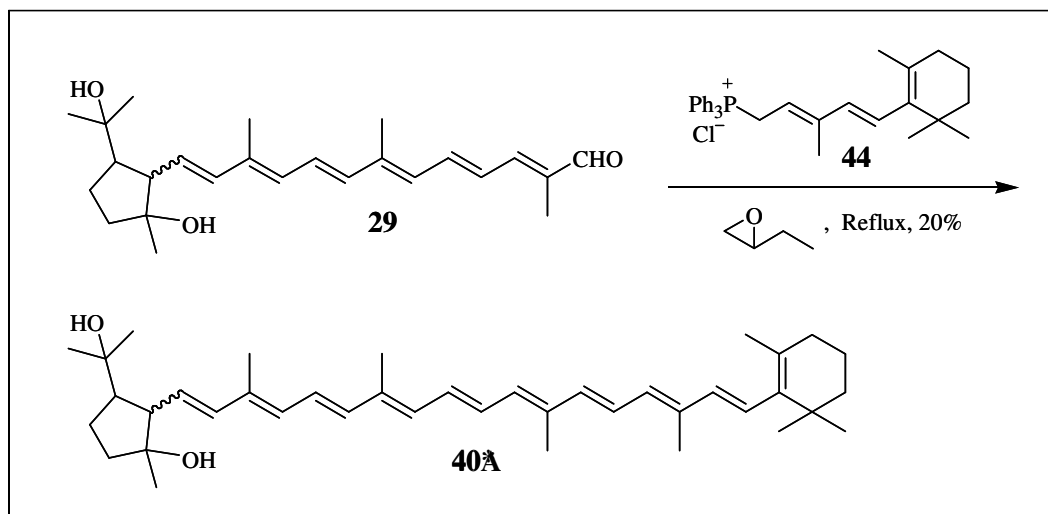
aldehydic carbon was evident at 194 ppm. Carbon-proton connectivities for **29** were determined by an HMBC experiment (Table 12).

Table 12. Carbon-proton connectivities determined for C₂₅-dihydroxyaldehyde **29** by HMBC NMR.

C Position	H Connectivities	C Position	H Connectivities
1	2, 6, 16, 17	13	11, 12, 15, 20
2	3AB, 4A, 6, 7	13'	12', 20'
3	2, 4AB	14	12, 15', 20
4	3AB, 6, 18	14'	12', 15, 20'
5	2, 3, 4, 6, 7	15	14'
6	2, 3, 7, 8	15'	14
7	2, 6, 8	Me16	2, 17
8	6, 10, 19	Me17	2, 16
9	7, 8, 19	Me18	None
10	8, 12, 19	Me19	8, 10
11	10, 12	Me20	12, 14
12	10, 11, 14, 20	Me20'	12', 14'
12'	15' 20'		

Synthesis of 40A by Wittig coupling reaction between C₂₅-dihydroxyaldehyde **29 and Wittig salt **44**.**

In the final step of the synthesis of γ -carotene oxidation product **40A**, C₂₅-dihydroxyaldehyde **29** was coupled with Wittig salt **44** in a refluxing solution of 1,2-epoxybutane (Scheme 49).



Scheme 49. Final step of the synthesis of γ -carotene oxidation product **40A**.

When the coupling reaction was attempted with sodium methoxide in methylene chloride at R.T., a significant amount of starting material **29** remained after 24 h. However, when the reactants were refluxed in 1,2-ethoxybutane for 24 h, the target compound **40A** was obtained in 20% isolated yield following purification by column chromatography. Based on HPLC analysis, the target compound **40A** was prepared as a mixture of *EZ*-isomers (*E/Z* = 1.9:1.0). These were further separated by normal phase semi-preparative HPLC. The *all-E* final isomer was isolated as an orange/red oil. The HPLC chromatogram is shown in Figure 29. **40A** was analyzed by HRMS, ^1H , ^{13}C , NOESY, HSQC and HMBC NMR.

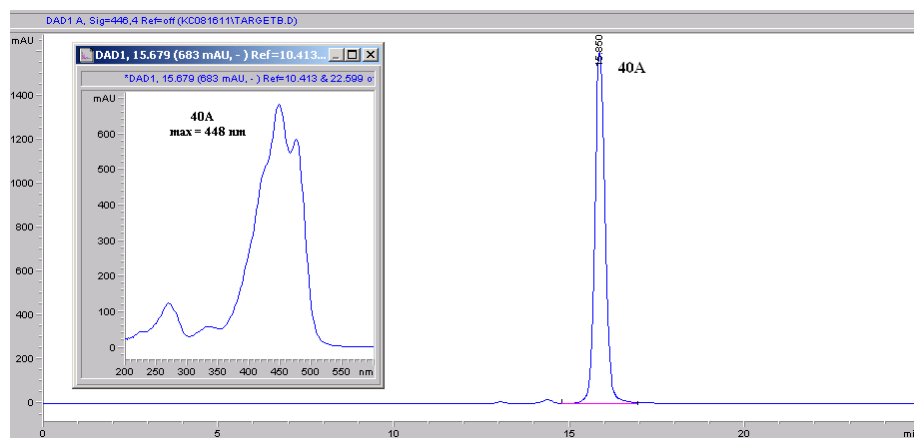
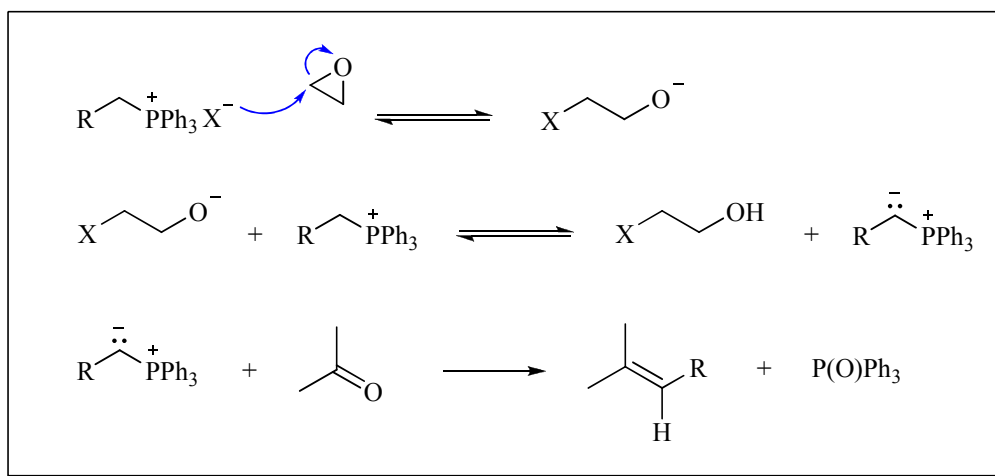


Figure 29. HPLC chromatogram and spectra of target carotenoid **40A** following purification by flash column chromatography and semi-preparative HPLC. (HPLC condition B, Appendix I).

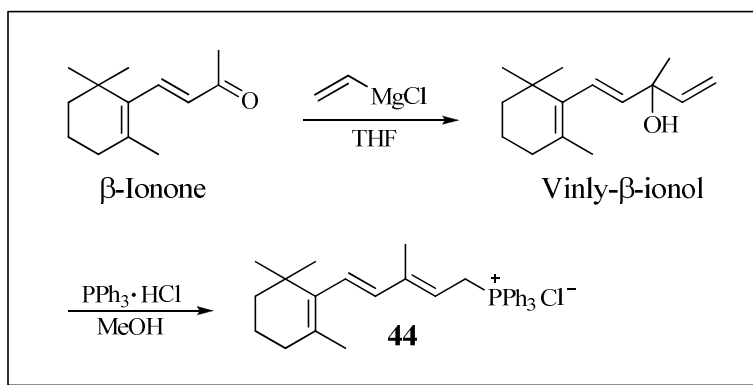
The mechanism proposed by Buddrus for epoxyalkane mediated Wittig coupling reactions is shown in Scheme 50.¹⁴³



Scheme 50. Mechanism proposed for epoxyalkane mediated Wittig coupling reactions.¹⁴³

The chloride counterion from the Wittig salt effects ring opening of the epoxide to generate a soft alkoxide base which is used to form the anion of the Wittig salt in the coupling reaction with the aldehyde.

Wittig salt **44** was prepared according to a published process, shown in Scheme 51.¹⁴⁴ The reaction between β -ionone and vinyl magnesium bromide afforded vinyl- β -ionol in 91% yield. Reaction of vinyl- β -ionol with triphenylphosphine hydrochloride produced (β -ionylideneethyl)triphenylphosphonium chloride, or Wittig salt **44**.^{111,112} The bromide salt can also be prepared.



Scheme 51. Synthesis of Wittig salt **44**.^{111,112}

As expected, the HRMS of the target compound showed the protonated form of the molecular parent ion. The proton and carbon assignments were established by COSY, HSQC and HMBC NMR experiments.

The chemical shifts and coupling constants exhibited by protons in the polyene chain were in agreement with those determined for (3*R*)- β -cryptoxanthin¹⁴⁵ and 2,6-cycloycopene-1,5-diol.⁸⁶ Chemical shifts were observed for the fourteen vinylic protons. Most coupling constants between the *trans*-vinylic protons in the polyene chain were 15 Hz, near the predicted value of 17 Hz. Chemical shifts observed for H2 and H6 were evident at 2.3 and 2.2 ppm, respectively, indicating their *cis* relationship to one another. The ¹H-NMR spectrum of **40A** is shown in Figure 30.

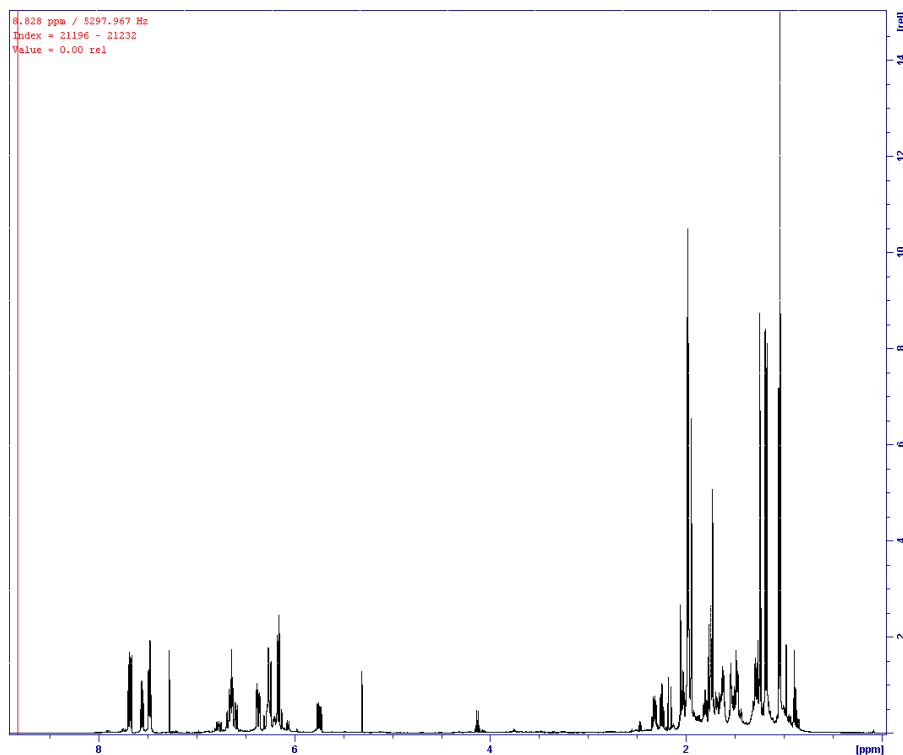


Figure 30. $^1\text{H-NMR}$ spectrum of γ -carotene oxidation product **40A**.

The relative stereochemistries of **40A** at C2, C5 and C6 were determined by a NOESY experiment. The NOESY spectrum is shown in Figure 31.

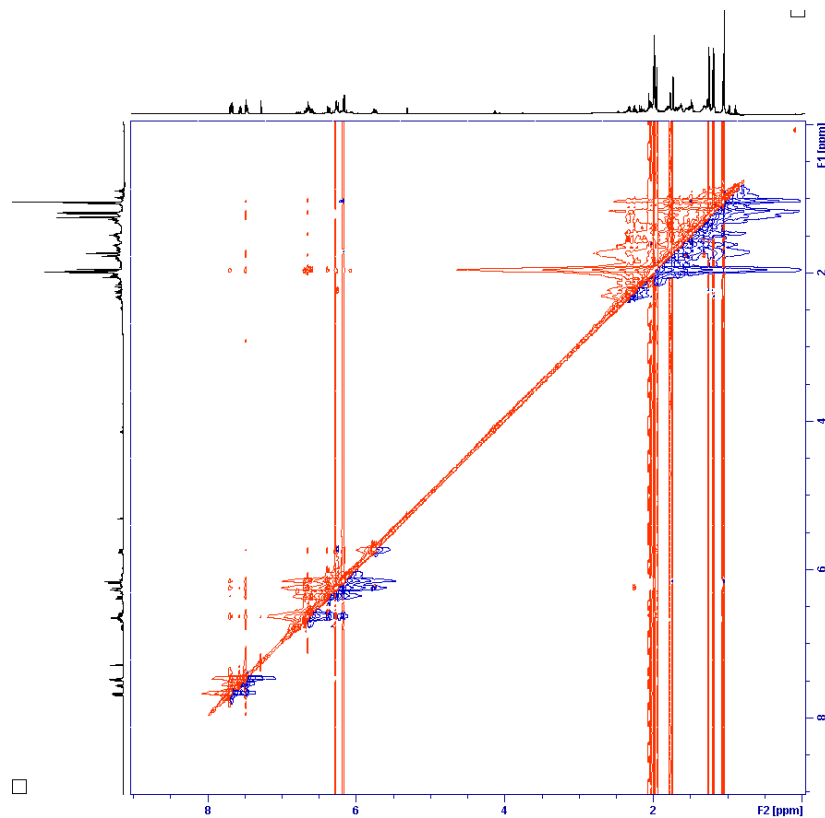


Figure 31. NOESY spectrum of γ -carotene oxidation product **40A**.

NOESY crosspeaks and the relative stereochemical assignments for **40A** are shown in Figure 32.

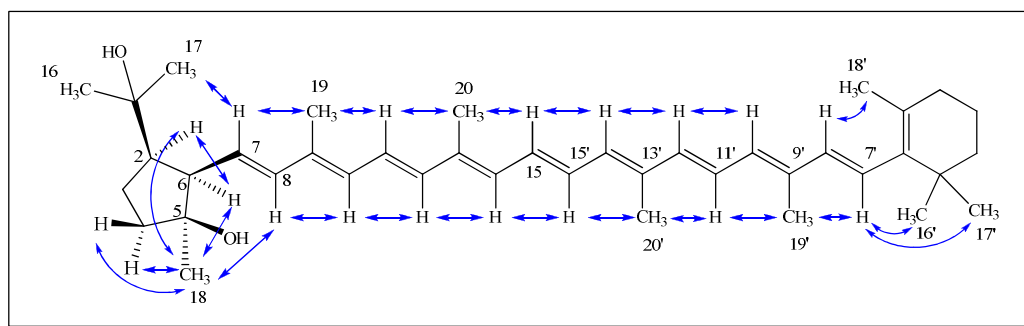


Figure 32. Structure of 1,2,5,6-tetrahydro-2,6-cyclo- γ -carotene-1,5-diol **40A** and observed NOESY crosspeaks.

Further evidence for the *cis* relationship between H2 and H6 was gleaned from results of the NOESY experiment. Crosspeaks were observed between the protons on

Me16/17 and H7 which indicated their *cis* relationship to each other and established the orientation of the protons H2 and H6 as *cis* relative to one another. NOESY crosspeaks observed between the protons on Me18, H2 and H6 revealed their *cis* relationship and established the orientation of the hydroxyl group at C5 and the side chain at C6. An HMBC crosspeak between the Me18 protons and C4 was used to distinguish Me18 from Me16 and Me17. Further, Me17 could be distinguished from Me16 by the NOESY crosspeak with H7.

^{13}C NMR chemical shifts for C1 and C5 attached to hydroxyl groups appeared at approximately 73 and 82 ppm, respectively (Figure 33). Twenty chemical shifts corresponding to substituted olefinic carbon atoms were evident. The ^{13}C NMR chemical shifts for the carbons in the five-membered ring diol as well as the in-chain olefinic carbons were consistent with those of 2,6-cycloycopene-1,5-diol.⁸⁶

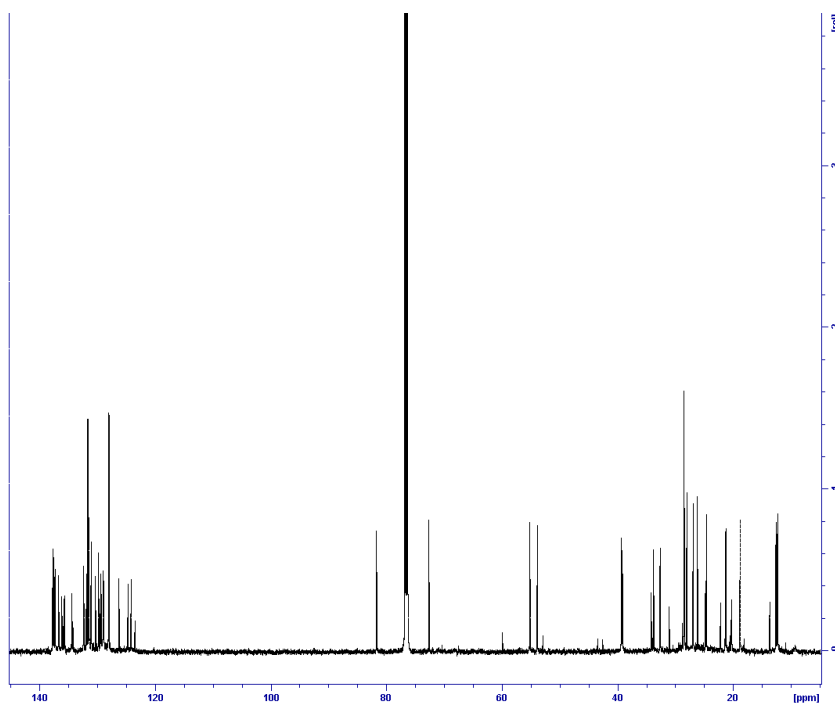


Figure 33. ^{13}C -NMR spectrum of γ -carotene oxidation product **40A**.

The HMBC NMR spectrum of γ -carotene oxidation product **40A** is shown in Figure 34.

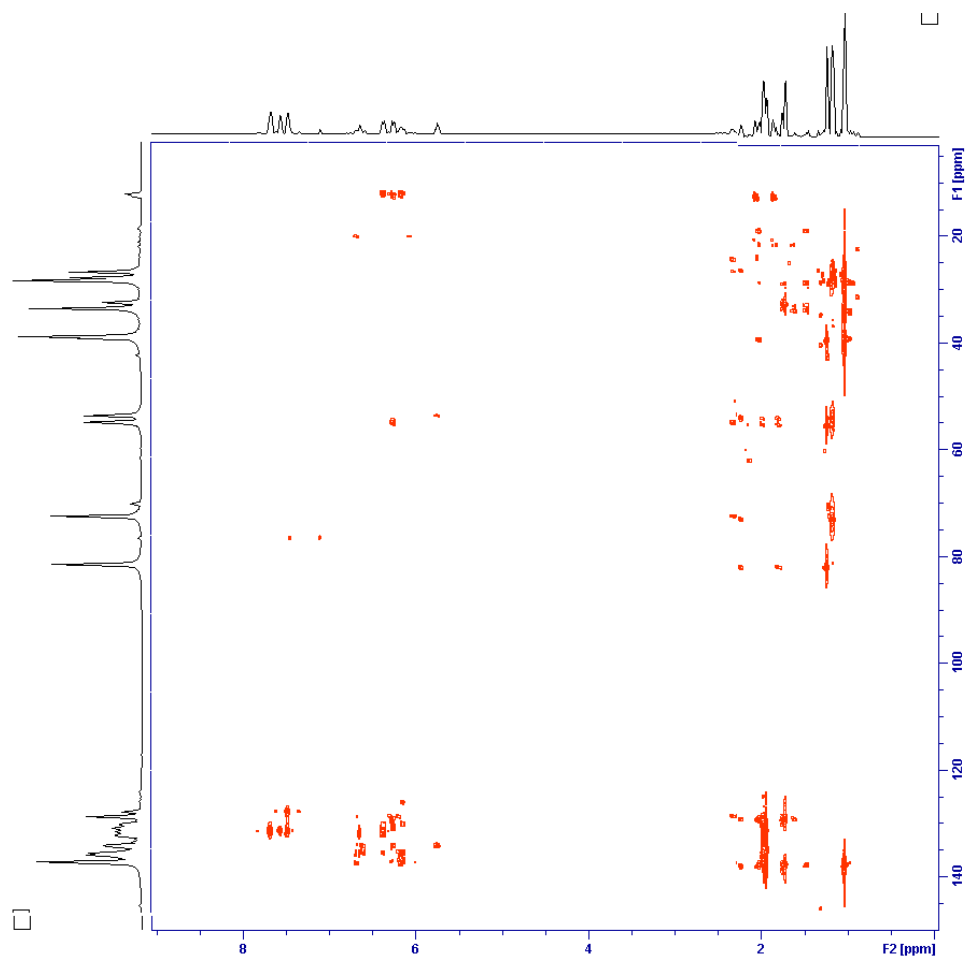


Figure 34. HMBC spectrum of γ -carotene oxidation product **40A**.

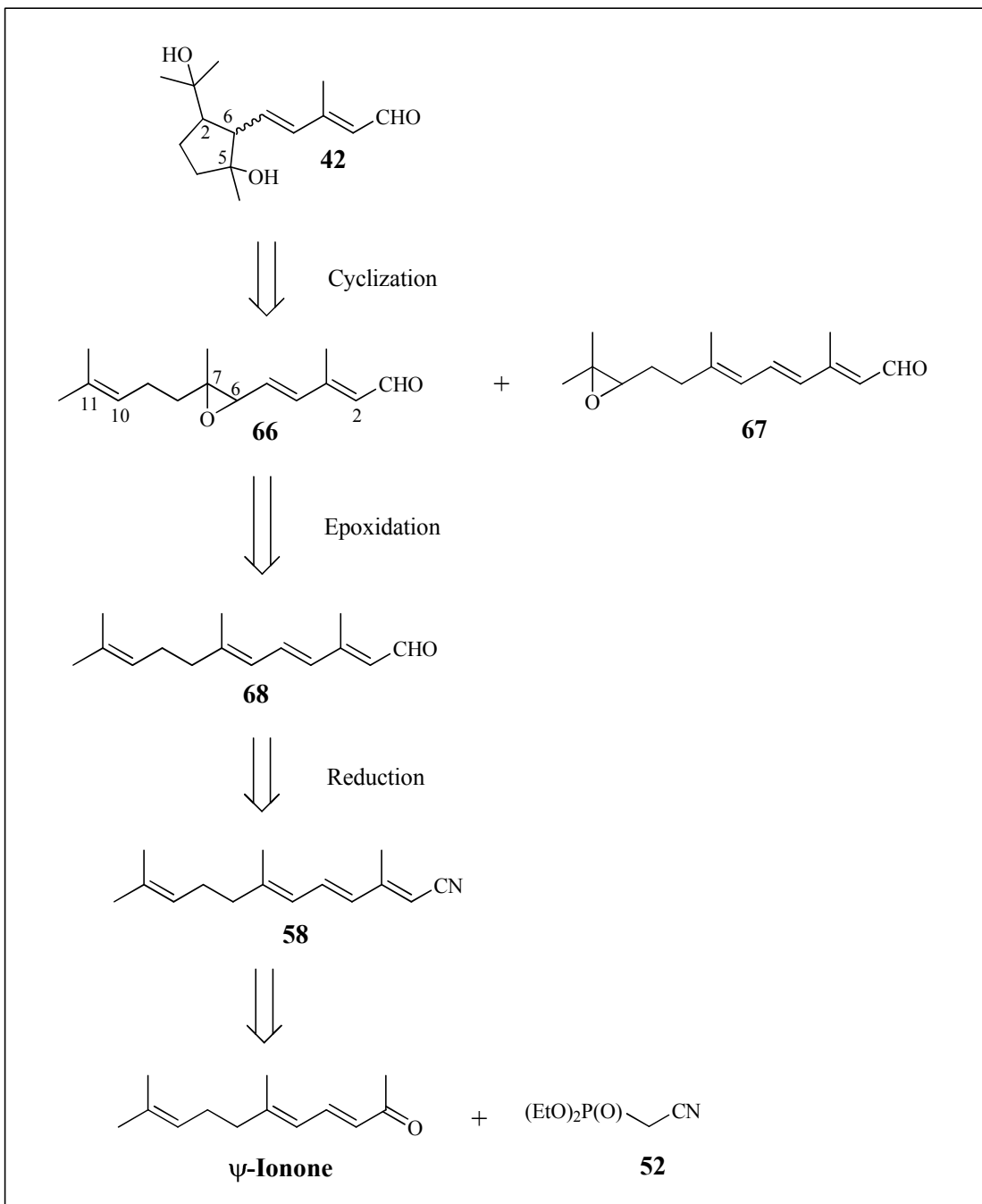
Long-range connectivities between protons and carbons for **40A** are summarized in Table 13.

Table 13. Carbon-proton connectivities determined for the target carotenoid **40A** by HMBC NMR.

C Position	H Connectivities	C Position	H Connectivities
1	2, 6, 16, 17	20'	12', 14'
2	3, 4A, 6, 7, 16, 17	19'	8', 10'
3	2, 4B	18'	4'
4	3, 18	17'	2', 16'
5	3, 4AB, 6, 7, 18	16'	2', 17'
6	2, 3, 4A, 7, 8, 18	15'	14
7	2, 6, 8	14'	12', 15, 20'
8	6, 7, 10, 19	13'	11', 12', 15', 20'
9	7, 8, 11, 19	12'	10', 11', 14', 20'
10	8, 12, 19	11'	10'
11	10	10'	8', 12', 19'
12	10, 11, 14, 20	9'	7', 8', 10', 11', 19'
13	11, 12, 15, 20	8'	7', 10', 19'
14	12, 15', 20	7'	8'
15	14'	6'	2', 4', 7', 8', 16', 17', 18'
16	2, 17	5'	3', 4', 18'
17	2, 16	4'	2', 3', 18'
18	4B, 6	3'	2', 4'
19	8, 10	2'	3', 4', 16', 17'
20	12, 14	1'	2', 3', 7', 16', 17'

Partial Synthesis of C₁₅-dihydroxyaldehyde **42**.

Synthesis of the C₁₅-dihydroxyaldehyde **42** was also attempted according to the retrosynthesis outlined in Scheme 52.



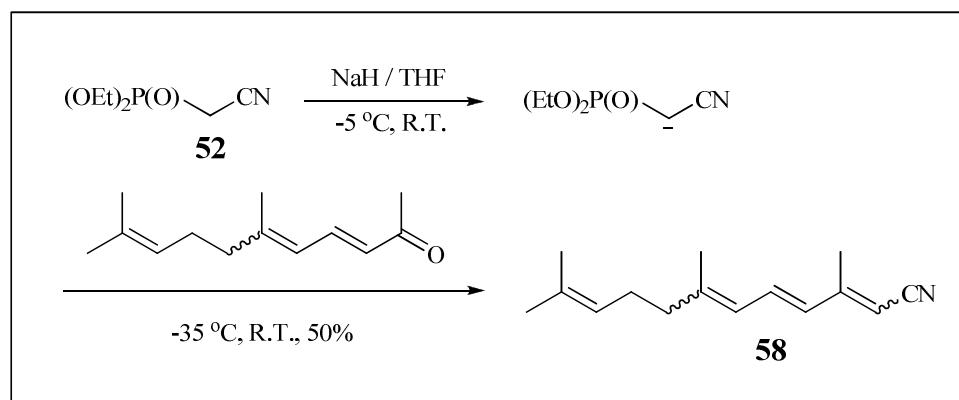
Scheme 52. Partial synthesis of C₁₅-dihydroxyaldehyde **42**. Carotenoid numbering system has been used for compound **42**.

Compound **42** could be obtained from the intramolecular cyclization of 6,7-epoxy-3,7,11-trimethyldodeca-2,4,10-trienal (**66**), based on results previously obtained with the cyano- and ethyl ester analogues. A mixture of 6,7- and 10,11-epoxides **66** and

67 would be synthesized by epoxidation of the C₁₅-aldehyde **68**. DIBAL-H reduction of the corresponding C₁₅-cyano compound **58** was expected to produce **68** in good yield. HWE coupling between the commercially available ψ -ionone and diethyl (cyanomethyl)phosphonate **52** could be used to prepare **58**. The C₁₅-nitrile **58** has been previously prepared by this route.¹²⁷

Synthesis of C₁₅-nitrile **58**.

3,7,11-Trimethyldodeca-2,4,6,10-tetraenitrile (**58**) was synthesized by HWE coupling between diethyl (cyanomethyl) phosphonate (**52**) and ψ -ionone according to a reported procedure shown in supporting Scheme 53.¹²⁷



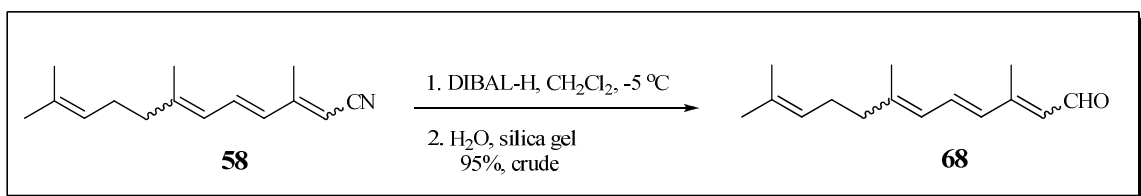
Scheme 53. HWE synthesis of C₁₅-nitrile **58**.

Following purification by column chromatography, **58** was isolated in 50% yield as a light- yellow oil. Because the ratio of 5-(*E/Z*) isomers in ψ -ionone was approximately (1:2)⁹² and HWE reactions tend to produce products with variable levels of (*E/Z*)-isomerization, **58** was obtained as a mixture of *E/Z* isomers at C7 and C2. While these could be partially separated by normal phase HPLC, the stereoisomers were not

further separated or characterized. However, the ^1H NMR spectrum of the isomeric mixture was in agreement with the published values.¹²⁷

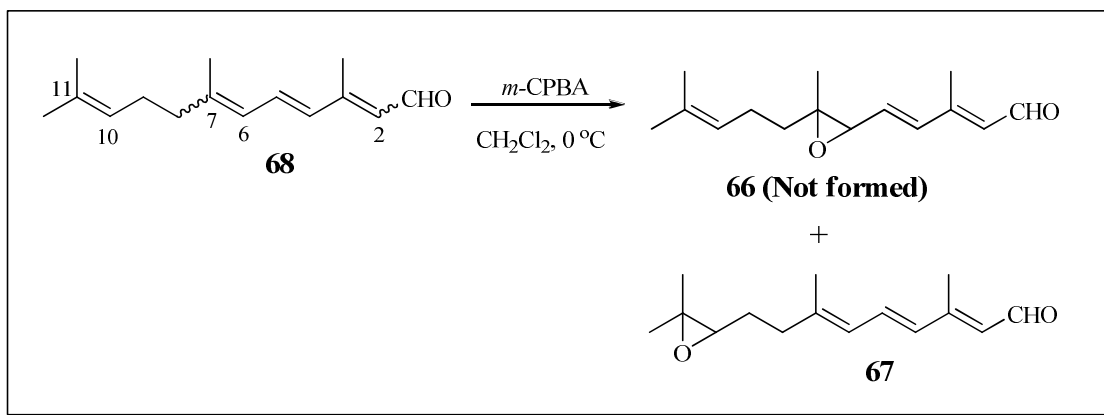
DIBAL-H reduction of C_{15} -nitrile **58**.

Purified **58** was reduced with DIBAL-H to produce the C_{15} -aldehyde **68** as shown in Scheme 54.



Scheme 54. Reduction of C_{15} -nitrile **58**.

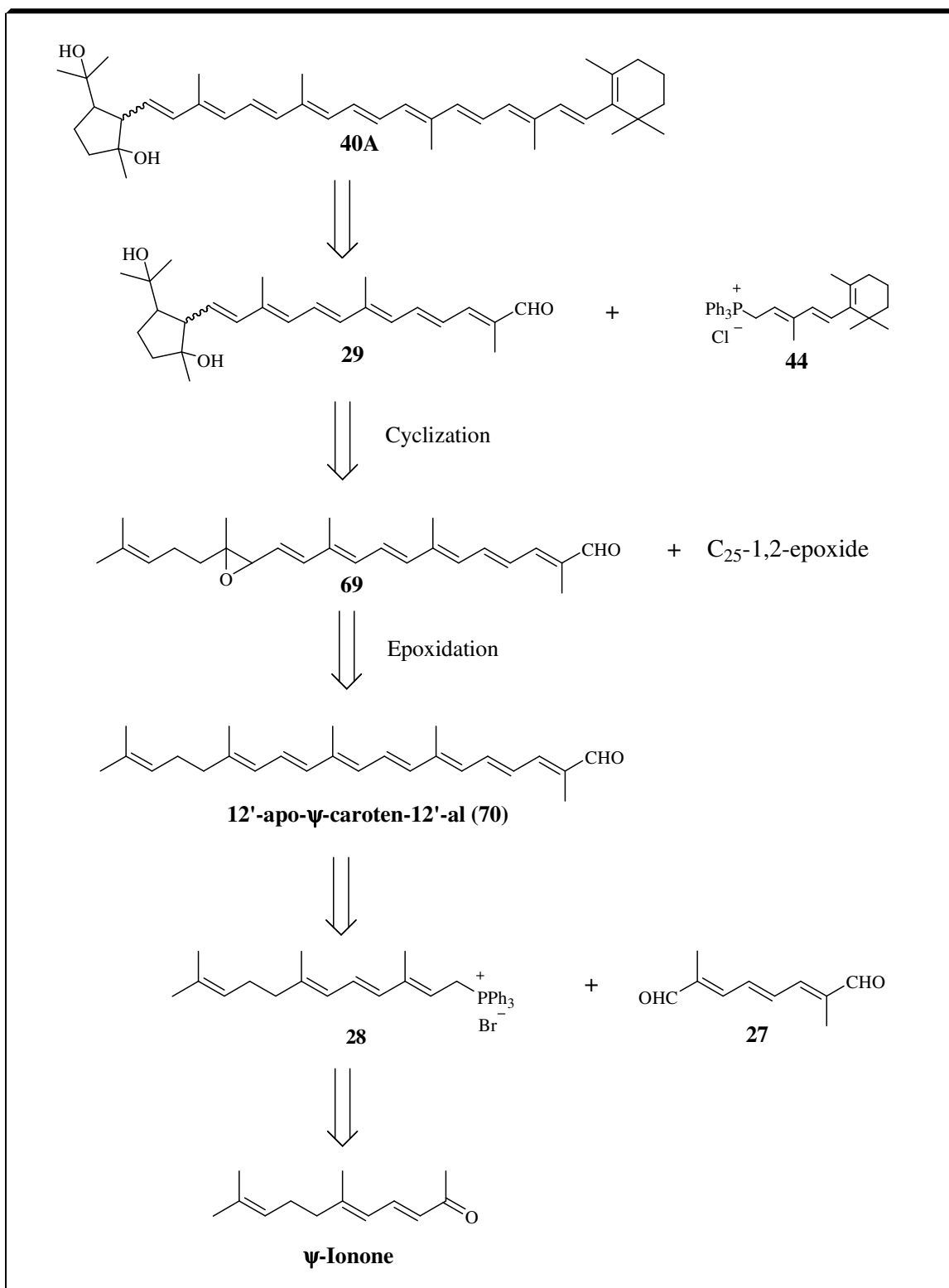
After column chromatography, *m*-CPBA epoxidation of **68** afforded only the 10,11-epoxy aldehyde **67** (Scheme 55). Because the analogous aldehyde **66** could not be isolated, further attempts to synthesize the C_{15} -dihydroxyaldehyde **42** by this route were not further pursued.



Scheme 55. Epoxidation of C_{15} -aldehyde **68** with *m*-CPBA.

Synthesis of target carotenoid **40A** via alternative route to C₂₅-dihydroxyaldehyde **29**.

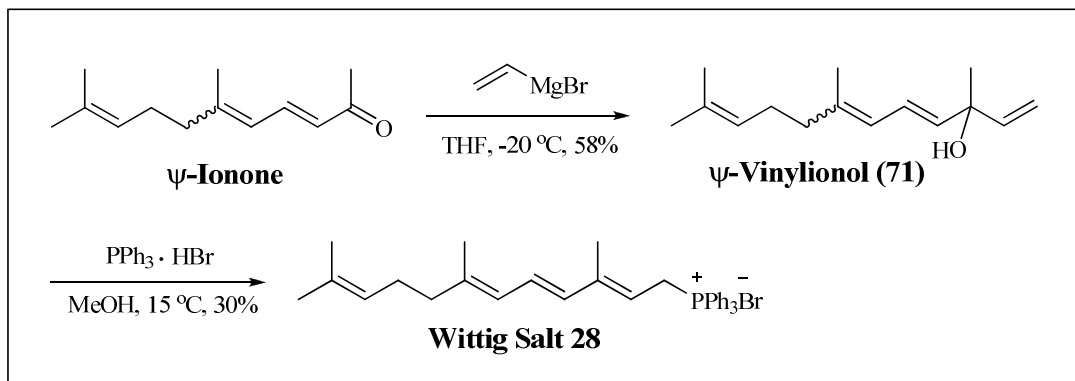
Another strategy to arrive at the target compound **40A** is illustrated by the retrosynthesis shown in Scheme 56. The final step of this synthesis involved elongation of **29** with Wittig salt **44** as described previously. However, compound **29** could be synthesized from the acid-catalyzed intramolecular cyclization and hydrolysis of the C₂₅-5,6-epoxide **69**, similar to the procedure described earlier. The 5,6-epoxy-aldehyde **69** and its 1,2-epoxy analogue could in turn be prepared from the *m*-CPBA epoxidation of the C₂₅-aldehyde apo-12'- ψ -caroten-12'-al (**70**), while **70** could be prepared according to a published procedure⁹² by the coupling of the C₁₅-Wittig salt **28** and the C₁₀-dialdehyde **27**. Wittig salt **28** has been successfully employed in the total synthesis of lycopene (**5**),⁹¹ and could be synthesized from ψ -ionone by C2 elongation with vinyl magnesium bromide followed by reaction with triphenylphosphine hydrobromide according to a known procedure.⁹²



Scheme 56. Synthesis of target carotenoid **40A** via C_{25} -aldehyde **70**.

Synthesis of C₁₅-Wittig salt **28**.

Wittig salt **28** was synthesized in two steps according to a reported procedure (Scheme 57).⁹²



Scheme 57. Synthesis of C₁₅-Wittig salt **28**.⁹²

ψ -ionone containing a 1:2 mixture of 5-(*E/Z*) isomers was elongated with vinyl magnesium bromide to produce ψ -vinylionol in 58% yield with a similar *E/Z* ratio at C7, based on analysis by ¹H NMR spectroscopy. Subsequent reaction with triphenylphosphine hydrobromide afforded **28**. The *all-E* isomer was crystallized from ethyl acetate and methanol according to the published procedure by Hengartner⁹² in 30% yield.

Synthesis of C₂₅-dihydroxyaldehyde **29** via C₂₅-aldehyde **70**.

Coupling of Wittig salt **28** and C₁₀-dialdehyde **27** afforded the acyclic C₂₅-aldehyde **70** in 78% isolated yield as a dark red oil after flash column chromatography (Scheme 58). Of this, approximately 98% was obtained as the *all-E* isomer, based on results of HPLC analysis and ¹H NMR spectroscopy.

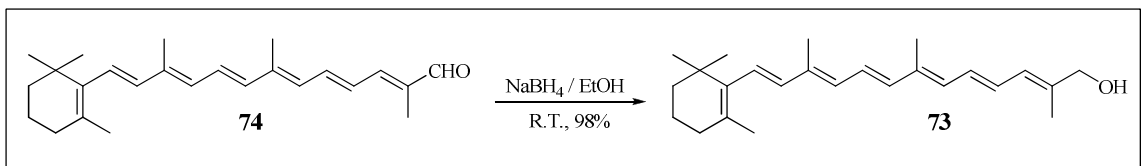
to dihydroxyaldehyde **29** which was isolated in 30% yield. The HPLC profile and proton NMR spectrum of this compound was identical with the reference sample of **29** prepared earlier.

A simplified procedure for the synthesis of target carotenoid 40A from dihydroxy aldehyde 42.

The synthesis of target compound **40A** could also be accomplished by a simplified procedure as outlined in the retrosynthetic pathway shown in Scheme 64. This would involve coupling of the previously prepared C₁₅-dihydroxyaldehyde **42** with the C₂₅-Wittig salt **72**. This Wittig salt has been previously prepared from 12'-apo- β -caroten-12'-ol (**73**) and triphenylphosphine hydrobromide.¹⁴⁶ The C₂₅-alcohol **73** has been prepared from NaBH₄ reduction of 12'-apo- β -caroten-12'-al (**74**) which is commercially available from BASF. This aldehyde is readily accessible from elongation of Wittig salt **44** with C₁₀-dialdehyde **27**.¹⁴⁶ Aldehyde **74** was provided to use by BASF (Ludwigshafen, Germany).

Reduction of (*all-E*)-12'-apo- β -caroten-12'-al (**74**) with NaBH₄.

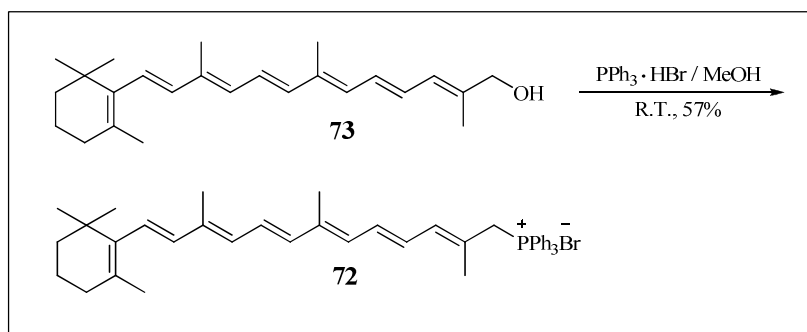
(*all-E*)-12'-Apo- β -carotenal (**74**) was reduced with sodium borohydride in ethanol according to a published procedure (Scheme 61).¹⁴⁶ The alcohol **73** was isolated as an orange oil in 98% yield, and was used in the next step without further purification.



Scheme 61. Reduction of (*all-E*)-12'-apo- β -caroten-12'-al (**74**).

Synthesis of C₂₅-Wittig salt **72**.

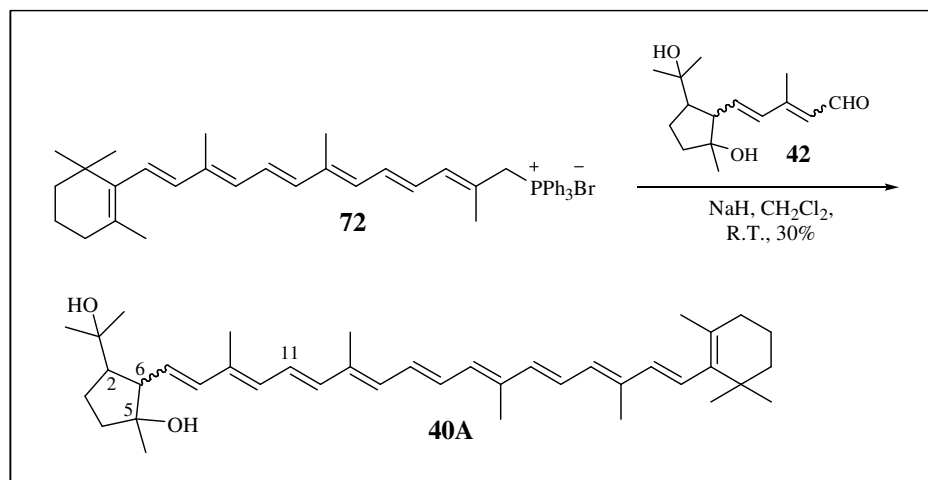
Subsequent reaction of **73** with triphenylphosphine hydrobromide in methanol afforded Wittig salt **72** after nearly 2 days at R.T. under argon (Scheme 62). The product was recrystallized from methanol/ethyl acetate (1:5) at -15 °C for several days, and was obtained as orange crystals in 57% isolated yield.



Scheme 62. Synthesis of C₂₅-Wittig salt **72**.

Synthesis of 40A from Wittig salt **72** and C₁₅-dihydroxyaldehyde **42**.

HWE coupling of **72** with the C₁₅-dihydroxyaldehyde **42** was accomplished similar to a reported procedure by Haugan and Liaanen-Jensen¹⁴⁶ (Scheme 63).

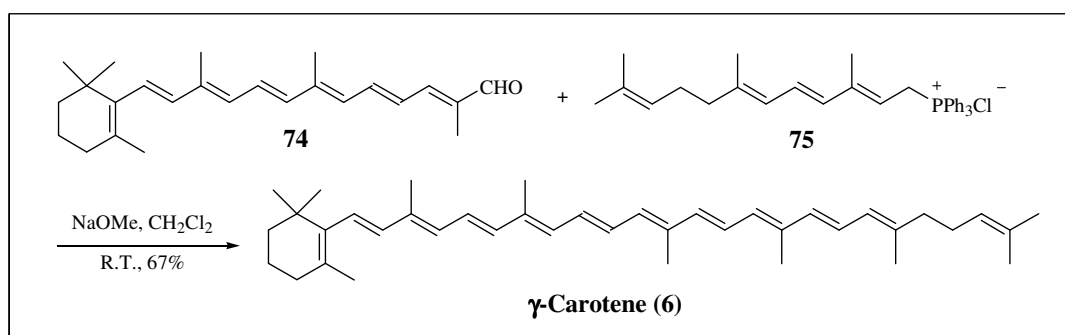


Scheme 63. Synthesis of **40A** from Wittig salt **72** and aldehyde **42**.

A small sample of **40A** was purified by preparative TLC. The HPLC profile of this purified sample consisted of a mixture of *all-E*-**40A** as well as two *Z*-stereoisomers and was consistent with the HPLC profile of the standard sample of **40A** prepared earlier.

Direct synthesis of target carotenoid 40A from γ -carotene (6).

γ -carotene (**6**) was synthesized according to a known method¹⁴⁷ as shown in Scheme 64.

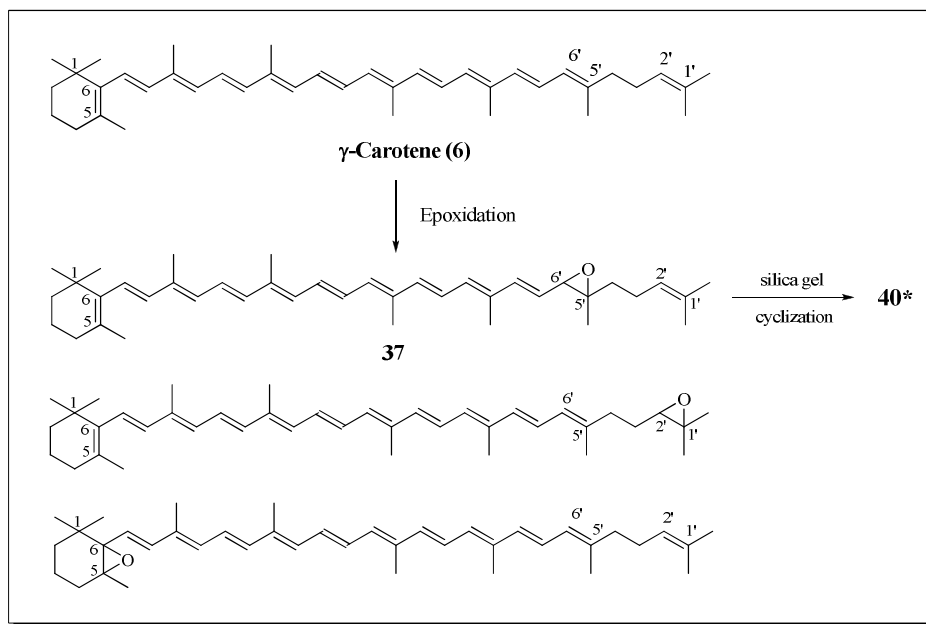


Scheme 64. Synthesis of γ -carotene (**6**) according to the procedure by Ruegg *et. al.*¹⁴⁷

After purification by flash column chromatography, γ -carotene (**6**) was isolated in 67% yield as a dark red viscous oil. The identity of the product was confirmed by

comparison of the HPLC retention time and ^1H NMR spectrum with those of a standard sample of **6**.

Because lycopene 5,6-epoxide (**23**) underwent intramolecular rearrangement to 2,6-cyclolycopene-1,5-diols **21** and **22** during silica gel chromatography, identical treatment of γ -carotene-5,6-epoxide (**37**) was expected to produce the target compound **40A**. However, the major difficulty with this approach was the fact that γ -carotene (**6**) could undergo epoxidation not only at 1',2'- and 5',6'-positions but also at the 5,6-position in the β -end group as shown in Scheme 65.



Scheme 65. Possible epoxidation products of γ -carotene (**6**).

Among these, only γ -carotene-5',6'-epoxide (**37**) could be converted to the target carotenoid **40A** by acid promoted cyclization by silica gel chromatography. In addition, this route could be even further complicated by possible formation of diepoxides. Nonetheless, we were interested to explore the partial synthesis of compound **40A** by this route because of the ease with which γ -carotene (**6**) could be prepared. Unfortunately, as

expected, *m*-CPBA epoxidation of **6** under various conditions produced a mixture of numerous epoxides. As a result, this approach was not further studied.

Investigation of the possible presence of γ -carotene oxidation product 40A in extracts of human plasma, tomato paste and algal biomass.

Human plasma was obtained from the American Red Cross. Proteins were denatured with 100% ethanol. After extraction and the usual work-up,⁸⁶ the HPLC analysis did not reveal the presence of **40A** in the extract from human plasma. However, it should be noted that the oxidation product of **6** would only be expected if this carotenoid were to be present at high concentrations in plasma. Therefore, the fact that **6** was not present even in modest concentration in the Red Cross plasma could account for the lack of detection of compound **40A**. This is consistent with the observation that oxidation products of major dietary carotenoids such as lutein and lycopene are only present in minute quantities in human plasma.

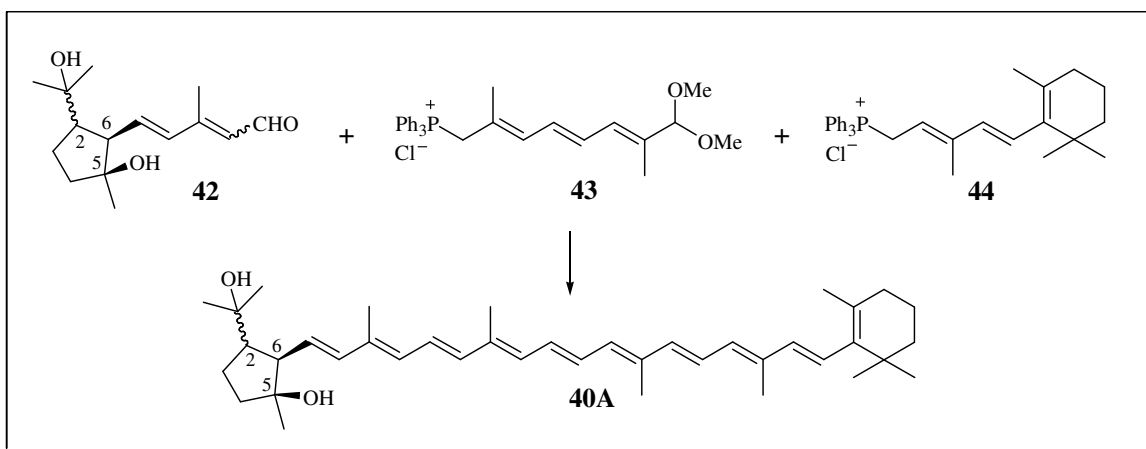
Hunt's tomato paste was purchased at a local grocery store and extracted with THF. The dark red, pasty extract was analyzed by normal phase HPLC. Several closely eluting signals eluted in the retention time window of the target carotenoid **40A**. However, the λ_{max} of all spectra taken across the signals was 450-454 nm, in contrast to the λ_{max} expected for the oxidized product of γ -carotene (**6**) (444 nm). Based on this observation, this batch of tomato paste was not found to contain the γ -carotene oxidation product **40A**.

Algal biomass was obtained from Martek Biosciences Corporation, and extracted with THF. The predominant carotenoids in the oil consisted of approximately 400 ppm

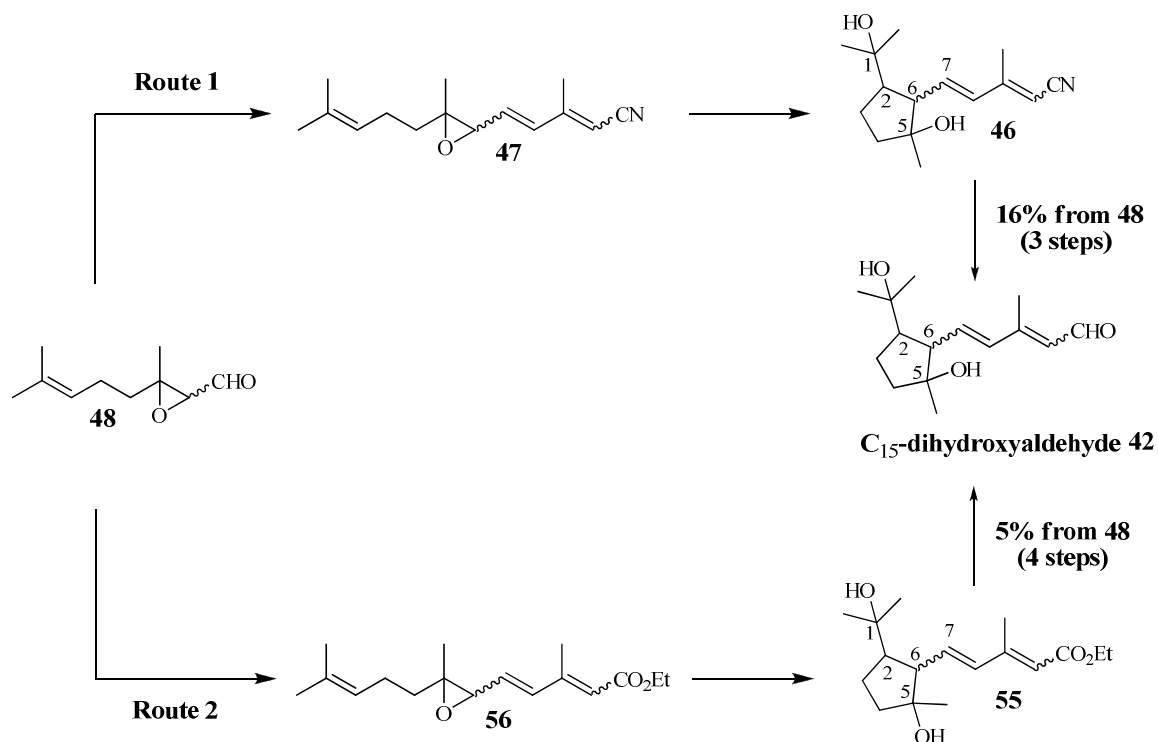
γ -carotene (**6**) and 200 ppm β -carotene (**8**), in addition to minor amounts of more polar, unidentified pigment. Several fractions of the polar material were further isolated by semi-preparative HPLC and evaluated. Based on results of normal phase HPLC, one fraction tentatively contains the target carotenoid in trace amounts, based on comparison of retention time and spectral characteristics. Unfortunately, the low concentration of this fraction did not allow structural elucidation by NMR.

CONCLUSION

Several strategies for the total and partial synthesis of a possible metabolic oxidation product of gamma-carotene, namely, 1,2,5,6-tetrahydro-2,6-cyclo- γ -carotene-1,5-diol (**40A**) have been explored. Among these, the total synthesis of **40A** has been accomplished by a C₁₅+C₁₀+C₁₅ double Wittig coupling using key synthon **42**, the protected Wittig salt **43**, and the well known Wittig salt **44** as shown below.



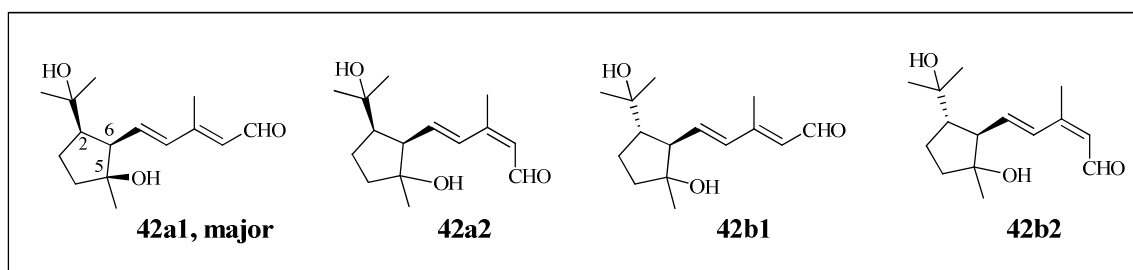
While the Wittig salts **43** and **44** could be readily prepared in high yields according to published procedures, the access to synthon **42** with a known relative stereochemistry was the most challenging features of this synthesis. Regioselective epoxidation of commercially available (*E/Z*)-citral afforded (*E/Z*)-citral 2,3-epoxide (**48**) that was elongated to C₁₅-dihydroxynitrile **47** (Route 1, see also Scheme 24). Cyclization of this nitrile to the C₁₅-dihydroxynitrile **46** followed by reduction gave synthon **42** in 16% overall yield. The low yield of this transformation was because of the cyclization of **47** to **46**.



In another approach, (*E/Z*)-citral 2,3-epoxide (**48**) was transformed into C₁₇-epoxyester **56** which is the ester analog of **47** that was similarly cyclized to synthon **42** in four steps in an overall yield of only 5% (Route 2, see also Scheme 25). The efficiency of the alternate Route 2 was further decreased by the additional step that was required to reduce ester **55** to triol **54** before subsequent oxidation to synthon **42**.

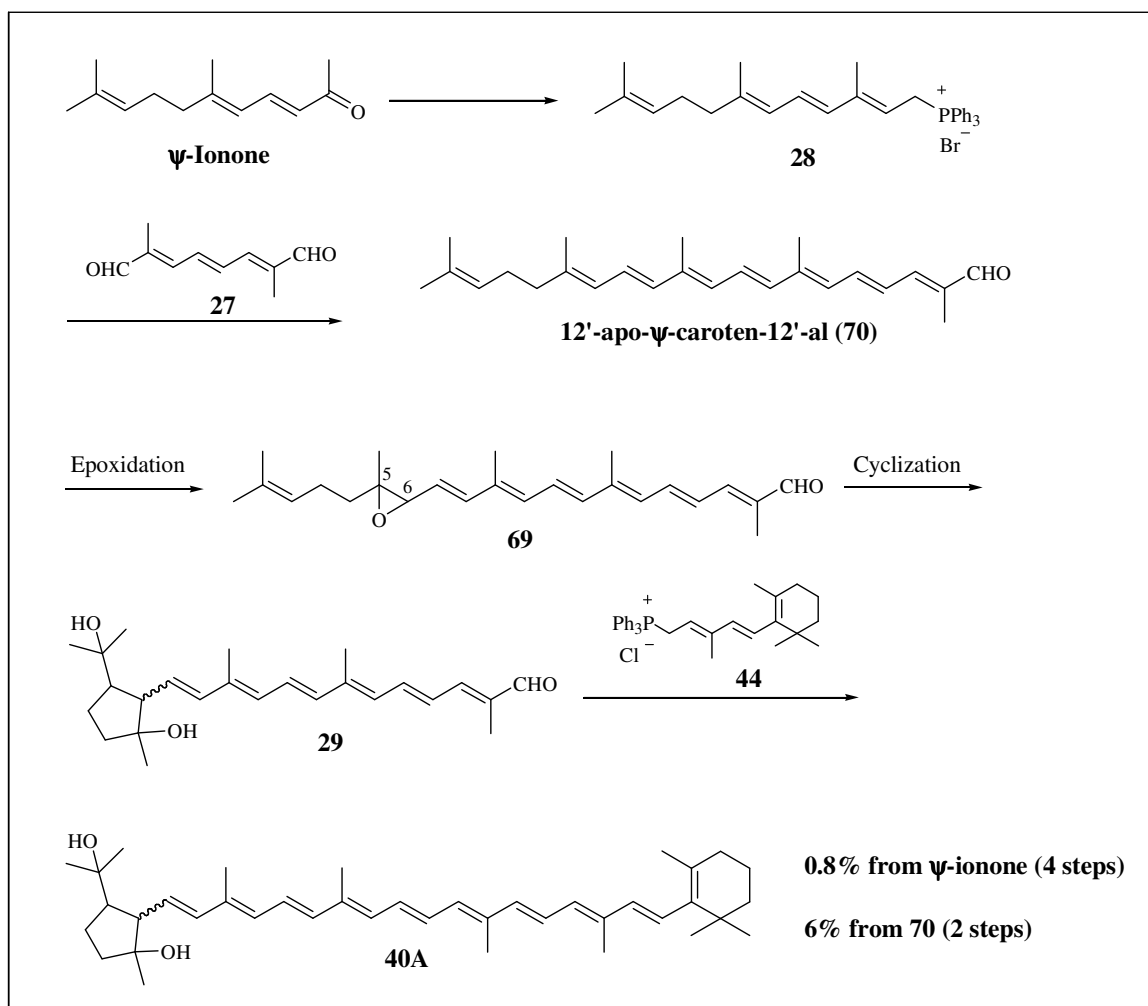
The major challenges with these two routes were the fact that separation of (*E*)-citral and (*E*)-citral epoxide from their corresponding *Z*-stereoisomers could not be accomplished on a gram scale and consequently the elongation of **48** to epoxy nitrile **47** and epoxyester **56** resulted in a *E/Z*-geometry for these epoxides. This was further complicated by the *E/Z*-geometry of the dienitrile and dieneester at the C2 double bonds resulting in a mixture of four stereoisomers for each **47** and **56**. Although with both routes the *all-E*-epoxides were obtained as the major products, the presence of the other stereoisomers contributed to the low yield of these key epoxides.

Another deficiency of this synthesis was due to the low yield of cyclization of **47** and **56** and their transformation to synthon **42** that was obtained as a mixture of *E/Z*-stereoisomers. Therefore, routes 1 and 2 each afforded four stereoisomer of **42** with the same relative stereochemistries at C2, C5 and C6 as shown below.

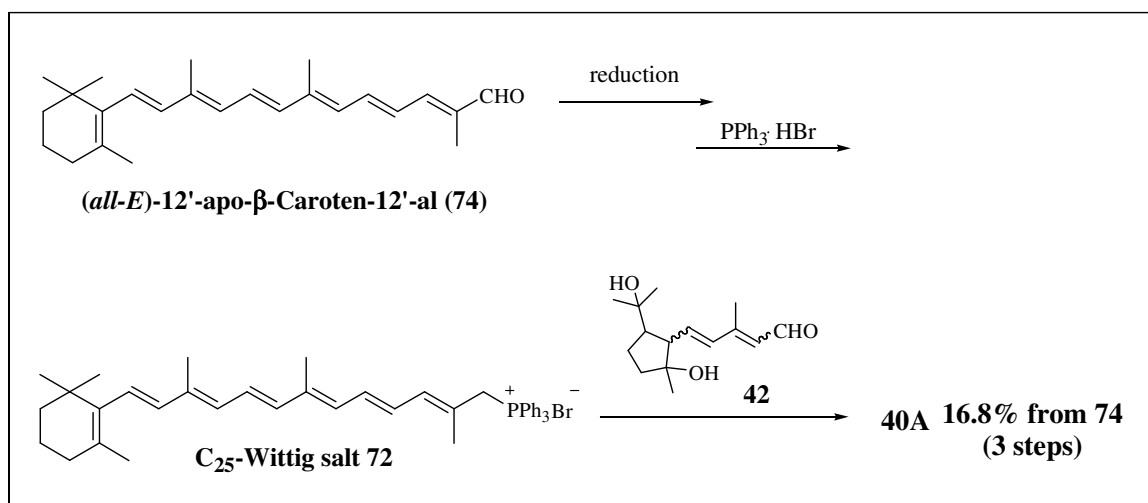


These relative stereochemistries were established by extensive NMR studies. The overall yield of **40A** that could be obtained from Routes 1 and 2 was 2.4% and 0.8%, respectively.

In the semi-synthetic approach outlined below (see also Scheme 56), ψ -ionone was used to prepare 12'-apo- ψ -carotene-12'-al (**70**). *m*-CPBA epoxidation of **70** afforded a mixture of C₂₅-1,2- and 5,6-epoxide (**69**). The latter was cyclized to C₂₅-dihydroxyaldehyde **29** upon silica gel chromatography. Final coupling of **29** with Wittig salt **44** could produce **40A** in 4 steps in an overall yield of 0.8% from ψ -ionone. However, it should be noted that 12'-apo- ψ -carotene-12'-al (**70**) is an intermediate product in the commercial synthesis of lycopene by DSM Nutritional Products (Basel, Switzerland) and BASF (Ludwigshafen, Germany) and could be available for the synthesis of **40A** on a large scale. Therefore employing aldehyde **70** as the starting material in this synthesis avoids the need to produce the C₁₅-dihydroxyaldehyde synthon **42** and is by far the most practical route to this carotenoid **40A**.



Another efficient strategy to **40A** was *via* the simplified procedure shown below (see also Scheme 60), where this carotenoid was prepared in just 3 steps in 16.8% yield from the readily available starting material (*all-E*)-12'-apo- β -caroten-12'-al (**74**). This is provided that the yield of the key synthon **42** could be improved.



The present methodologies provide novel access to a possible oxidation product of γ -carotene that could be potentially formed in humans or biological systems. While our attempt to direct chemical oxidation of γ -carotene resulted in complex mixture of products, the oxidation of this carotenoid in biological systems might provide a much less complicated profile and provide an insight into the function of γ -carotene as an antioxidant. Therefore, future studies in this area should investigate the oxidation of γ -carotene in various *in vitro* cell cultures in the presence of biological oxidants such as hydroxyl radicals ($\text{HO}\bullet$), singlet oxygen ($^1\text{O}_2$), hydrogen peroxide (H_2O_2), and peroxynitrite anion (ONOO^-). These studies can reveal the nature of oxidation products of this carotenoid.

Further, supplementation studies with γ -carotene from food sources or with dietary supplements would be expected to provide insight into possible metabolic oxidation of this carotenoid to **40A** or other metabolites of this carotenoid. In view of the well-established health benefits of lycopene and β -carotene in the prevention of chronic

diseases, investigation of the metabolism and γ -carotene that has structural features of both of these carotenoids is essential.

EXPERIMENTAL SECTION

All operations and HPLC analyses were conducted under yellow laboratory lights to prevent photo-isomerization and degradation of carotenoids and their precursors. Unless noted, experiments were carried out under anhydrous conditions under argon; reaction glassware were dried in an oven prior to use.

Reactions were monitored by using thin-layer chromatography (TLC) on Merck silica-coated glass plates treated with UV-active binder. Compounds were detected by UV (254 nm) and/or an ethanolic phosphomolybdic acid indicator solution. Reactions were also monitored by normal-phase chromatography under the conditions described below. The HPLC system (Agilent 1100 series) was equipped with a quaternary solvent delivery system (model G1311A), an autosampler (model G1313A), a thermostatted column compartment (model G1316A) and a photodiode array detector (model G1315B). The data were stored and processed by computer (Dell with Windows 2000 and HP Chem-Station software).

Normal phase HPLC separations were carried out on a Waters Spherisorb, silica-based nitrile bonded column (250 mm length x 4.6 mm internal diameter; 5 μ m particle size). Reversed phase HPLC separations were carried out on a Varian C₁₈-Microsorb column, (250 mm length x 4.6 mm internal diameter; 5 μ m particle size). Semipreparative HPLC separations were carried out on a Regis Spherisorb silica-based nitrile bonded column (250 mm length x 10 mm internal diameter; 5 μ m particle size).

Mass Spectral Analysis. High resolution mass spectra were obtained on a JEOL SX102 Time of Flight mass spectrometer with electrospray ionization source. All compounds were determined to be >95% pure by ¹H-NMR and HPLC analysis unless

otherwise noted. All new compounds were minimally characterized using ^1H -NMR, ^{13}C -NMR, HSQC-NMR, COSY-NMR, UV/Vis spectra and mass spectrometry. Stereochemical assignments were based on NOESY-NMR.

^1H , ^{13}C , COSY, and HSQC NMR spectra were recorded on a Bruker AV-400 spectrometer. HMBC and NOESY spectra were recorded on a Bruker AV-600 spectrometer. NMR spectra were referenced to the solvent resonance (CDCl_3 ; ^1H δ 7.24 ppm, ^{13}C δ 77.1 ppm).

COSY NMR spectra were recorded with average spectral widths of 2800 Hz in each domain and with 1024 data points in the F_2 dimension. A ^1H pulse width of 7 μs (90°) and a 1-s relaxation delay time were used to acquire 512 incremented proton NMR spectra of 8 scans each. Free-induction decays were processed as a 1024 x 1024 matrix with appropriate zero filling and sinebell weighting.

Phase-sensitive NOESY NMR spectra were recorded with average spectral widths of 2800 Hz in each domain and with 1024 data points in the F_2 dimension. A ^1H pulse width of 7 μs (90°) and a 2-s relaxation delay time were used to acquire 512 incremented proton NMR spectra of 16 scans each. Mixing times of 1 s were employed. Free-induction decays were processed as a 1024 x 1024 matrix with appropriate zero filling and Gaussian weighting.

HSQC NMR spectra were obtained with average spectral widths of 17,000 and 2800 Hz in the carbon and proton dimensions, respectively, and with 1024 data points in the ^1H dimension; 128 incremented ^1H spectra of 8 scans each were acquired by using 7- μs (90°) ^1H pulse widths and a 1-s relaxation delay time. Free-induction decays in both dimensions were processed as a 1024 x 256 matrix with appropriate zero filling and

Gaussian weighting. The value $^1J(\text{CH}) = 145$ Hz was used for calculating the delay Δ , which is then equal to 3.5 ms.

HMBC NMR spectra were recorded with average spectral widths of 28,000 and 2800 Hz in the carbon and proton dimensions, respectively, and with 1024 data points in the ^1H dimension; 128 incremented ^1H spectra of 128 scans each were acquired by using 7- μs (90°) ^1H pulse widths and a 1-s relaxation delay time. Free-induction decays in both dimensions were processed as a 1024 x 256 matrix with appropriate zero filling and Gaussian weighting. The value $^nJ(\text{CH}) = 7.5$ Hz was used for calculating the delay Δ_{LR} , which is then equal to approximately 60 ms, and $^1J(\text{CH}) = 145$ Hz was used for Δ in the J -filter.

Synthesis of citral epoxide (48). Hydrogen peroxide (30%, 70 mL, 700 mmol) was added dropwise to a mixture of *E/Z*-citral (86.0 g, 542 mmol) and potassium bicarbonate (76.0 g, 760 mmol) in acetonitrile (36.8 mL, 700 mmol) and methanol (280 mL) at R.T. After stirring overnight, the product was filtered and extracted with aqueous ammonium chloride and ethyl acetate. The organic layer was dried over Na_2SO_4 and concentrated. Vacuum distillation (62-66 °C and 0.1 mm Hg) gave a mixture of *E/Z*-citral epoxide (**48**) (43.8 g, 260 mmol; 48%) as a light yellow oil; TLC ($R_f = 0.41$ and 0.32, hexane:acetone, 9:1, n-Si). The (*E/Z*)-isomeric ratio of the products (*E/Z* = 1.0/0.8) was determined by ^1H -NMR. Results were in agreement with reported literature values.¹⁴⁸ ^{13}C NMR (400 MHz, CDCl_3) δ 17.3, 21.8, 25.4, 23.9, 33.1, 64.2, 64.3, 122.2, 132.9, 198.5.

***cis*-citral epoxide (48):** ^1H -NMR (400 MHz, CDCl_3) δ 1.39 (s, 3H), 1.56 (s, 3H), 1.63 (s, 3H), 1.78 (m, 2H), 2.06 (m, 2H), 3.12 (d, $J = 5.1$, 1H), 5.02 (m, 1H), 9.39 (d, $J = 5.1$, 1H).

trans-citral epoxide (48): $^1\text{H-NMR}$ (400 MHz, CDCl_3) δ 1.42 (s, 3H), 1.58 (s, 3H), 1.66 (s, 3H), 1.78 (m, 2H), 2.06 (m, 2H), 3.16 (d, $J = 5.0$, 1H), 5.02 (m, 1H), 9.43 (d, $J = 5.0$, 1H).

Synthesis of 4-chloro-3-methyl-2-butenenitrile (51). Sodium hydride (60% suspension in mineral oil, 10.8 g, 271 mmol) was washed with hexane (3 x 100 mL) in a 3-neck flask equipped with an addition funnel and a thermometer. Anhydrous *tert*-butyl methyl ether (TBME, 160 mL) was added under argon and the mixture was cooled down to 0 °C. Diethyl (cyanomethyl) phosphonate (36.2 mL, 226 mmol) in 20 mL TBME was added dropwise to sodium hydride with stirring. The mixture was cooled down to -40 °C and chloroacetone (21.8 g, 226 mmol) in TBME (10 mL) was added dropwise in 20 minutes. The crude product was allowed to warm up to R.T. and quenched with brine. The organic layer was washed twice with water, dried over Na_2SO_4 and concentrated, yielding 26.8 g of a yellow oil. Purification by column chromatography on silica (100% hexane to hexane:acetone, 9:1) afforded a mixture of (*E/Z*)-**51** (24.0 g, 200 mmol; 92%). The (*E/Z*)-isomeric ratio was determined by $^1\text{H-NMR}$ (*E/Z* = 2.6/1.0); the NMR data were in agreement with literature values.¹¹⁸

(E)-4-chloro-3-methyl-2-butenenitrile (51): $^1\text{H-NMR}$ (400 MHz, CDCl_3) δ 2.14 (d, $J = 1.2$, 3H), 4.07 (s, 2H), 5.51 (d, $J = 1.2$, 1H).

(Z)-4-chloro-3-methyl-2-butenenitrile (51): $^1\text{H-NMR}$ (400 MHz, CDCl_3) δ 2.05 (d, $J = 1.5$, 3H), 4.26 (s, 2H), 5.29 (d, $J = 1.5$, 1H).

Preparation of 4-(diethylphosphono)-3-methyl-2-butenenitrile (49). Triethyl phosphite (60 mL, 350 mmol) and (*E/Z*)-4-chloro-3-methyl-2-butenenitrile (**51**) (30.3 g, 262 mmol) were heated to 100 °C for 30 minutes without a condenser to boil off ethyl

chloride. The mixture was subsequently refluxed at 180 °C for 2 h. Vacuum distillation gave **49** (42.1 g, 190 mmol; 74%) as a colorless oil, b.p. 115-118 °C at 0.1 mm Hg. The (*E/Z*)-isomeric ratio was determined by ¹H-NMR (*E/Z* = 1.1/1.0); the NMR data were in agreement with literature values.¹¹⁸

(E-49): ¹H-NMR (400 MHz, CDCl₃) δ 1.31 (t, 6H), 2.18 (m, 3H), 2.95 (d, *J*_{P-H} = 23.9, 2H), 4.11 (m, 4H), 5.26 (s, 1H).

(Z-49): δ 1.31 (t, 6H), 2.08 (m, 3H), 2.70 (d, *J*_{P-H} = 23.6, 2H), 4.11 (m, 4H), 5.25 (s, 1H).

Synthesis of 6,7-epoxy-3,7,11-trimethyldodeca-2,4,10-trienitrile (47). Sodium hydride (60% suspension in mineral oil, 0.80 g, 20 mmol) was washed three times with small portions of hexane under argon. Anhydrous THF (5 mL) was added, and the mixture was cooled down to -8 °C. A solution of (diethylphosphono)-3-methyl-2-butenitrile (**49**) (2.6 g, 12 mmol) in 5 mL THF was added dropwise with stirring. The color changed from colorless to red/brown as the temperature rose to 0 °C during the addition. The mixture was cooled down to -35 °C and a solution of citral epoxide (**48**) (2.5 g, 15 mmol) in anhydrous THF (5 mL) was added dropwise in 10 minutes. The mixture was allowed to warm up to -20 °C, and was kept at this temperature for 1 h, and then maintained at 0 °C for 2 h. The reaction mixture was quenched with water and extracted with ethyl acetate. The organic layer was washed twice with dilute brine, dried over Na₂SO₄ and concentrated. After purification by column chromatography on silica (100% hexane to hexane:acetone, 99:1), **47** was obtained as a light yellow oil (1.8 g, 8 mmol; 66%), and was identified as a mixture of 4 stereoisomers. An analytical sample of these stereoisomers was separated by preparative TLC (hexane/ethylacetate, 9:1) into a mixture of two sets of stereoisomers (**47a** and **47b**). The first set was tentatively

identified by $^1\text{H-NMR}$ to be a mixture of $(2E,4E)$ -*trans*-6,7-epoxynitrile (**47a1**) and $(2Z,4E)$ -*trans*-6,7-epoxynitrile (**47a2**), while the second set was tentatively identified to be a mixture of $(2E,4E)$ -*cis*-6,7-epoxynitrile (**47b1**) and $(2Z,4E)$ -*cis*-6,7-epoxynitrile (**47b2**). UV/Vis $\lambda_{\text{max}} = 264$ nm (hexane). The ratio of *trans/cis* epoxides **47a:47b** was approximately (1:1), based on HPLC area counts while the ratio of $(2E/2Z)$ isomers was approximately 2:1, based on analysis of the chemical shift of H4 by $^1\text{H-NMR}$.

(47a1, 47a2): HRMS (ESI $^+$) m/z calculated for $\text{C}_{15}\text{H}_{22}\text{NO}$ $[\text{M}+\text{H}]^+$ 232.1701, found 232.1726; m/z calculated for $\text{C}_{15}\text{H}_{20}\text{N}$ $[\text{M}+\text{H}-\text{H}_2\text{O}]^+$ 214.1596, found 214.1606; ^{13}C NMR (400 MHz, CDCl_3) δ 16.6, 17.6, 22.0, 24.1, 25.7, 32.9, 63.4, 64.1, 98.6, 117.3, 123.1, 132.4, 133.1, 133.8, 155.5.

(47b1, 47b2): HRMS (ESI $^+$) m/z calculated for $\text{C}_{15}\text{H}_{22}\text{NO}$ $[\text{M}+\text{H}]^+$ 232.1701, found 232.1744; m/z calculated for $\text{C}_{15}\text{H}_{20}\text{N}$ $[\text{M}+\text{H}-\text{H}_2\text{O}]^+$ 214.1596, found 214.1600; ^{13}C NMR (400 MHz, CDCl_3) δ 16.6, 16.6, 17.6, 23.7, 25.7, 38.4, 62.4, 64.0, 98.6, 117.3, 123.2, 132.3, 133.2, 134.0, 155.5.

$(2E,4E)$ -epoxide (47a1, 47b1**):** $^1\text{H-NMR}$ (400 MHz, CDCl_3) δ 1.40 (s, 3H), 1.47 (m, 2H), 1.59 (s, 3H), 1.67 (s, 3H), 2.09 (m, 2H), 2.16 (d, 3H), 3.29 (d, $J = 6.8$, 1H), 5.07 (m, 1H), 5.25 (s, 1H), 6.00 (dd, $J = 15.8$ and $J = 6.8$, 1H), 6.45 (d, $J = 15.8$, 1H).

$(2Z,4E)$ -epoxide (47a2, 47b2**):** $^1\text{H-NMR}$ (400 MHz, CDCl_3) δ 1.41 (s, 3H), 1.47 (m, 2H), 1.60 (s, 3H), 1.68 (s, 3H), 2.02 (d, 3H), 2.09 (m, 2H), 3.35 (d, $J = 7.7$, 1H), 5.05 (m, 1H), 5.20 (s, 1H), 5.99 (dd, $J = 15.7$ and $J = 7.7$, 1H), 7.00 (d, $J = 15.7$, 1H).

Synthesis of 47 employing LDA as base. n-Butyl lithium (1.6 M in hexane, 17.5 mL, 28 mmol) was added to diisopropylamine (4.0 mL, 2.9 g, 29 mmol) at -65 °C and the mixture was stirred for 15 minutes under argon. A solution of **49** (6.0 g, 28 mmol) in

anhydrous THF (15 mL) was added. The reaction mixture was allowed to warm up to –20 °C and kept at this temperature for 2 h. A solution of **48** (5.0 g, 30 mmol) in anhydrous THF (10 mL) was added to the pre-formed anion at –20 °C and the mixture was stirred for 1 h, warmed to R.T. and stirred for an additional 30 minutes. The product was quenched with saturated NH₄Cl and extracted with ethyl acetate. The organic layer was washed with water to neutral pH, dried over Na₂SO₄ and concentrated to yield 7.3 g of a yellow oil. The product was purified by column chromatography (100% hexane to hexane/ethyl acetate, 95:5) on silica to give epoxynitrile **47** (6.2 g, 27 mmol; 96%).

Synthesis of 3,7,11-trimethyldodeca-2,4,6,10-tetraen-nitrile (58) by Knoevenagel condensation reaction. ψ -Ionone (10.0 g, 52 mmol), cyanoacetic acid (5.3 g, 62 mmol) and cyclohexylamine (20 mL, 170 mmol) were stirred under argon at 85 °C for 1 h, then for another 1 h at 85 °C while open to the atmosphere. Progress of the reaction was monitored by TLC (hexane:acetone, 95:5). The mixture was cooled down to R.T. and transferred to a separatory funnel. Water (50 mL) and hydrochloric acid (30 mL, 2M) were added. The product was extracted into ethyl acetate, dried over Na₂SO₄ and evaporated to dryness. The crude product (13.7 g) was obtained as a dark brown oil and was not further purified. The isomeric ratio of **58** (2*E*/2*Z* = 1.0/1.5) was determined by normal phase HPLC (condition I, Appendix 1) and ¹H NMR. The NMR data were in agreement with literature values.¹²⁷

Cyclization of (cis/trans)-6,7-epoxy-3,7,11-trimethyldodeca-2,4,10-trienenitrile (47) with dilute H₂SO₄. Sulfuric acid (5% v/v in water, 150 mL) was added to a stereoisomeric mixture of **47** (6.5 g, 28 mmol) in THF (30 mL) at 0 °C. The reaction was warmed up to R.T. and stirred for 2 h. Progress of the reaction was monitored by

disappearance of the signal for the starting material by normal phase HPLC (condition B, Appendix I). The reaction mixture was neutralized with saturated NaHCO₃ and extracted twice with hexane/CH₂Cl₂ (75/25). The organic layer was dried over Na₂SO₄ and concentrated to yield 6.2 g of yellow oil. The product was purified by flash column chromatography on silica (hexane:acetone, 9:1). Three fractions were collected and individually subjected to semi-preparative normal phase HPLC (condition E, Appendix I). These were identified as 3-methyl-5-[3-(1-hydroxyl-1-methylethyl)-1-hydroxy-1-methyl-2-cyclopent-2-yl]-penta-2,4-dienitrile (**46**) (27%), monool dehydration product (**59**) (25%) and 6,7-dihydroxy-3,7,11-trimethyldodeca-2,4,10-trienitrile (**60**) (48%). A small sample of C₁₅-dihydroxynitrile **46** was further separated into 4 stereoisomers (**46a1**, **46a2**, **46b1** and **46b2**) by normal phase semi-preparative HPLC (condition E, Appendix I) in relative yields 3.4:1.0:1.8:1.4. The structures were assigned based on results of HRMS and proton, carbon, COSY, HSQC and HMBC NMR (400 MHz, CDCl₃). The relative stereochemistries were determined by NOESY NMR (600 MHz, CDCl₃).

(2E,4E)-3-methyl-5-[3-(1-hydroxyl-1-methylethyl)-1-hydroxy-1-methyl-2-cyclopent-2-yl]-penta-2,4-dienitrile (46a1): HRMS (ESI⁺) *m/z* calculated for C₁₅H₂₂NO [M+H-H₂O]⁺ 232.1701, found 232.1708; *m/z* calculated for C₁₅H₂₀N [M+H-2H₂O]⁺ 214.1596, found 214.1613. UV λ_{max} = 262 nm (hexane). ¹H-NMR (400 MHz, CDCl₃) δ 1.18 (s, 3H), 1.19 (s, 3H), 1.25 (s, 3H), 1.84 (m, 2H), 1.95 (m, 1H), 2.14 (d, 3H), 2.56 (dd, *J* = 10.8, *J* = 5.7, 1H), 2.65 (dt, *J* = 9.7, *J* = 5.7, 1H), 5.18 (s, 1H), 6.06 (dd, *J* = 15.5, *J* = 10.8, 1H), 6.19 (d, *J* = 15.5, 1H). ¹³C NMR (400 MHz, CDCl₃) δ 17.0, 22.4, 26.6, 29.5, 29.9, 37.8, 53.0, 58.7, 72.0, 82.4, 96.8, 117.6, 131.1, 139.1, 156.4.

(2Z,4E)-3-methyl-5-[3-(1-hydroxyl-1-methylethyl)-1-hydroxy-1-methyl-2-cyclopent-2-yl]-penta-2,4-dienitrile (46a2): HRMS (ESI⁺) *m/z* calculated for C₁₅H₂₂NO [M+H–H₂O]⁺ 232.1701, found 232.1689; *m/z* calculated for C₁₅H₂₀N [M+H–2H₂O]⁺ 214.1596, found 214.1616. UV λ_{max} = 264 nm (hexane). ¹H-NMR (400 MHz, CDCl₃) δ 1.18 (s, 3H), 1.19 (s, 3H), 1.28 (s, 3H), 1.83 (m, 2H), 1.94 (m, 2H), 1.99 (d, 3H), 2.66 (m, 1H), 2.67 (m, 1H), 5.11 (s, 1H), 6.11 (dd, *J* = 15.5, *J* = 10.5, 1H), 6.70 (d, *J* = 15.5, 1H). ¹³C NMR (600 MHz, CDCl₃) δ 19.7, 22.4, 26.73, 29.5, 30.0, 37.6, 53.1, 58.9, 72.1, 82.5, 95.3, 116.9, 128.4, 140.1, 156.0.

(2E,4E)-3-methyl-5-[3-(1-hydroxyl-1-methylethyl)-1-hydroxy-1-methyl-2-cyclopent-2-yl]-penta-2,4-dienitrile (46b1): HRMS (ESI⁺) *m/z* calculated for C₁₅H₂₂NO [M+H–H₂O]⁺ 232.1701, found 232.1687; *m/z* calculated for C₁₅H₂₀N [M+H–2H₂O]⁺ 214.1596, found 214.1590. UV λ_{max} = 262 nm (hexane). ¹H-NMR (400 MHz, CDCl₃) δ 1.14 (s, 3H), 1.21 (s, 3H), 1.22 (s, 3H), 1.65 (m, 2H), 1.84 (m, 2H), 1.93 (m, 1H), 2.13 (d, 3H), 2.57 (dd, *J* = 10.2, *J* = 3.8, 1H), 5.17 (s, 1H), 5.86 (dd, *J* = 15.4, *J* = 10.2, 1H), 6.13 (d, *J* = 15.4, 1H). ¹³C NMR (600 MHz, CDCl₃) δ 24.0, 16.8, 24.5, 28.4, 29.5, 40.1, 55.3, 56.3, 72.3, 81.2, 97.1, 117.6, 130.3, 141.3, 156.6.

(2Z,4E)-3-methyl-5-[3-(1-hydroxyl-1-methylethyl)-1-hydroxy-1-methyl-2-cyclopent-2-yl]-penta-2,4-dienitrile (46b2): HRMS (ESI⁺) *m/z* calculated for C₁₅H₂₂NO [M+H–H₂O]⁺ 232.1701, found 232.1687; *m/z* calculated for C₁₅H₂₀N [M+H–2H₂O]⁺ 214.1596, found 214.1593. UV λ_{max} = 262 nm (hexane). ¹H-NMR (400 MHz, CDCl₃) δ 1.16 (s, 3H), 1.22 (s, 3H), 1.26 (s, 3H), 1.76 (m, 2H), 1.84 (m, 2H), 1.95 (m, 1H), 2.00 (d, 3H), 2.66 (dd, *J* = 10.1, *J* = 4.5, 1H), 5.11 (s, 1H), 5.93 (dd, *J* = 15.4, *J* = 10.1, 1H), 6.64 (d, *J* = 15.4, 1H).

59: HRMS (ESI⁺) m/z calculated for C₁₅H₂₂NO [M+H]⁺ 232.1701, found 232.1686; m/z calculated for C₁₅H₂₀N [M+H-H₂O]⁺ 214.1596, found 214.1574. λ_{\max} = 262 nm (hexane). ¹H-NMR (400 MHz, CDCl₃) δ 1.26 (s, 3H), 1.57 (s, 3H), 1.68 (s, 3H), 1.77 (m, 2H), 2.14 (d, 3H), 2.39 (m, 1H), 2.48 (mm, 2H), 3.10 (d, J = 9.0, 1H), 5.17 (s, 1H), 5.82 (dd, J = 15.5, J = 9.0, 1H), 6.10 (d, J = 15.5, 1H). ¹³C NMR (100 MHz, CDCl₃) δ 16.8, 21.0, 21.2, 24.5, 27.6, 38.1, 58.8, 81.8, 96.9, 117.7, 128.1, 130.5, 134.4, 137.7.

6,7-dihydroxy-3,7,11-trimethyldodeca-2,4,10-trienitrile (60): HRMS (ESI⁺) m/z calculated for C₁₅H₂₄NO₂ [M + H]⁺ 250.1807, found 250.1808; m/z calculated for C₁₅H₂₂NO [M+H-H₂O]⁺ 232.1701, found 232.1701; m/z calculated for C₁₅H₂₀N [M+H-2H₂O]⁺ 214.1596, found 214.1601. UV/VIS λ_{\max} = 258 nm (hexane). ¹H-NMR (400 MHz, CDCl₃) δ 1.12 (s, 3H), 1.64 (s, 3H), 1.71 (s, 3H), 1.99 (s, 1H), 2.18 (d, 3H), 2.40 (d, 1H), 4.11 (m, 1H), 5.14 (m, 1H), 5.26 (s, 1H), 6.12 (dd, J = 15.7, 1H), 6.43 (d, J = 15.7, 1H). ¹³C NMR (100 MHz, CDCl₃) δ 16.8, 17.7, 21.5, 22.0, 25.7, 38.7, 98.7, 117.4, 123.9, 132.2, 132.3, 135.7, 156.1.

Synthesis of 46 by cyclization of 47 with Amberlite IR-120. A solution of **47** (128 mg, 0.55 mmol) in hexane (6 mL) was sequentially treated with water (0.5 mL) and Amberlite IR-120 (40 mg). The mixture was stirred at R.T. for 5 h. Additional Amberlite (60 mg) and water (0.5 mL) were added. After stirring at R.T. overnight, the product was extracted into ethyl acetate and analyzed by normal phase HPLC (condition K, Appendix I). Based on area counts, **46** was produced in 36% yield, along with **60** (20%), **59** (32%) and starting material **47** (11%).

Lewis acid-catalyzed cyclization of 47. A mixture of Lewis acid in solvent (0.08 M) was cooled down to the appropriate temperature and added to a solution of **47** (20 mg,

0.090 mmol) in solvent with stirring. The products were extracted with dilute NaHCO₃ and hexane/CH₂Cl₂ (3:1). The organic layer was washed with water, dried over Na₂SO₄ and analyzed by normal phase HPLC (condition E, Appendix I).

For alumina mediated reactions, excess acidic alumina powder (100 mg) was added to a solution of **47** (20 mg, 0.090 mmol) dissolved in either CH₂Cl₂ or THF (5 mL) and the mixture was heated at the reflux temperature for 2 h. The product was filtered and analyzed by HPLC (condition E, Appendix I).

In the microwave heating experiment, a solution of **47** (20 mg, 0.090 mmol) in CH₂Cl₂ (2 mL) was sealed in a pressure resistant and temperature controlled glass tube and placed in a microwave designed for laboratory use. In three separate experiments, the samples were heated at 60 °C and 100 °C for 5 minutes, and at 100 °C for 10 minutes. In all experiments, the starting material was recovered quantitatively.

Synthesis of stereochemically pure (4E,2E)-3-methyl-5-[3-(1-hydroxy-1-methylethyl)-1-hydroxy-1-methyl-2-cyclopent-2-yl]-penta-2,4-dienal (42a1) from (2E,4E)-3-methyl-5-[3-(1-hydroxyl-1-methylethyl)-1-hydroxy-1-methyl-2-cyclopent-2yl]-penta-2,4-dienitrile (46a1) by reduction with DIBAL-H. (2E,4E)-C₁₅-dihydroxynitrile **46a1** (0.2 g, 0.8 mmol) was dissolved in CH₂Cl₂ (10 mL). The solution was cooled down to -50 °C in an acetone/dry ice bath. DIBAL-H solution (3 mL, 1.0 M in CH₂Cl₂, 3 mmol) was added dropwise with stirring over 30 minutes. The reaction was kept at -20 °C for 2 h before warming to 0 °C for 2 h. Progress of the reaction was monitored by normal phase HPLC (condition A, Appendix I). The reaction was worked up by cooling the mixture down to -10 °C. Dilute sulfuric acid was added (0.5%, 50 mL). The crude product (0.2 g) was extracted into CH₂Cl₂ from dilute brine, dried over Na₂SO₄

and concentrated to produce a viscous yellow oil. After purification by flash column chromatography on silica (hexane:ethyl acetate, 4:1 to 1:1), **42a1** (0.92 g, 3.6 mmol; 46%) was recovered as a light yellow oil. Retention time by normal phase HPLC (condition A, Appendix I) and ^1H , ^{13}C , COSY, HSQC, NOESY NMR experiments were used to establish the relative stereochemistry of the product.

Synthesis of 6,7-epoxy-3,7,11-trimethyldodeca-2,4,10-trienoic ethylester (56).

Sodium hydride (60% suspension in mineral oil, 2.7 g, 67.5 mmol) was washed three times with small portions of hexane under argon. Anhydrous THF (100 mL) was added, and the mixture was cooled down to 0 °C. A solution of triethyl-3-methyl-4-phosphono-2-butenolate (**57**) (11.6 g, 43.9 mmol) in THF (15 mL) was added dropwise with stirring. After 1 h, a solution of citral epoxide (**48**) (7.4 g, 43.9 mmol) in anhydrous THF (15 mL) was added dropwise in 10 minutes. Based on TLC analysis (hexane:acetone = 95:5), after 45 minutes at 0 °C, the starting material had been completely converted to the product. The reaction mixture was quenched with dilute brine and extracted into ethyl acetate. The organic layer was washed twice with dilute brine, dried over Na_2SO_4 and concentrated. After purification by column chromatography on silica (100% hexane to hexane:acetone, 95:5), **56** was obtained as a light yellow oil (7.4 g, 27 mmol; 60%), consisting of a mixture of four stereoisomers. The ratio of *trans/cis* epoxides **56a:56b** was approximately (1:1), based on HPLC area counts while the ratio of (*2E/2Z*) isomers was approximately 2:1, based on analysis by NMR. These were further separated by normal phase semi-preparative HPLC (condition F, Appendix I). NOESY NMR was used to assign the relative stereochemistry at C2, C4 and C6. HRMS (ESI⁺) *m/z* calculated for $\text{C}_{17}\text{H}_{27}\text{O}_3$ [M+H]⁺ 279.1960, found 279.1943.

(2E,4E)-trans-6,7-epoxy-3,7,11-trimethyldodeca-2,4,10-trienoic ethylester (56a1):

$^1\text{H-NMR}$ (400 MHz, CDCl_3) δ 1.31 (s, 3H), 1.46 (m, 2H), 1.53 (s, 3H), 1.60 (s, 3H), 2.04 (m, 2H), 2.21 (d, 3H), 3.24 (d, $J = 7.0$, 1H), 5.04 (m, 1H), 5.74 (s, 1H), 5.92 (dd, $J = 15.6$ and $J = 7.0$, 1H), 6.37 (d, $J = 15.6$, 1H).

(2Z,4E)-trans-6,7-epoxy-3,7,11-trimethyldodeca-2,4,10-trienoic ethylester (56a2):

UV $\lambda_{\text{max}} = 270$ nm (hexane). $^1\text{H-NMR}$ (400 MHz, CDCl_3) δ 1.31 (s, 3H), 1.46 (m, 2H), 1.53 (s, 3H), 1.60 (s, 3H), 1.94 (d, 3H), 2.04 (m, 2H), 3.29 (d, $J = 8.0$, 1H), 5.02 (m, 1H), 5.65 (s, 1H), 5.85 (dd, $J = 16.0$ and $J = 8.0$, 1H), 7.91 (d, $J = 16.0$, 1H).

(2E,4E)-cis-6,7-epoxy-3,7,11-trimethyldodeca-2,4,10-trienoic ethylester (56b1): $^1\text{H-}$

NMR (400 MHz, CDCl_3) δ 1.27 (s, 3H), 1.42 (m, 2H), 1.49 (s, 3H), 1.56 (s, 3H), 2.02 (m, 2H), 2.18 (d, 3H), 3.19 (d, $J = 7.0$, 1H), 5.00 (m, 1H), 5.70 (s, 1H), 5.88 (dd, $J = 15.7$ and $J = 7.0$, 1H), 6.33 (d, $J = 15.7$, 1H).

(2Z,4E)-cis-6,7-epoxy-3,7,11-trimethyldodeca-2,4,10-trienoic ethylester (56b2): $^1\text{H-}$

NMR (400 MHz, CDCl_3) δ 1.27 (s, 3H), 1.42 (m, 2H), 1.49 (s, 3H), 1.56 (s, 3H), 1.90 (d, $J = 1.2$, 3H), 2.02 (m, 2H), 3.25 (d, $J = 8.0$, 1H), 4.98 (m, 1H), 5.61 (s, 1H), 5.82 (dd, $J = 16.0$ and $J = 8.0$, 1H), 7.88 (d, $J = 16.0$, 1H).

Cyclization of 56 with dilute H_2SO_4 . A solution of **56** (12.7 g, 45.6 mmol) in THF (90 mL) was treated with water (650 mL) and sulfuric acid (0.1% v/v, 220 mL). The mixture was stirred under argon at R.T. for 24 h. Progress of the reaction was monitored by normal phase HPLC (condition B, Appendix I). The product was worked up with saturated sodium bicarbonate solution (200 mL) and extracted into ethyl acetate (200 mL). The organic layer was washed once with water and dried over Na_2SO_4 and concentrated to yield 11.5 g of pale yellow oil. The crude product was purified by flash column

chromatography on silica (hexane:ethyl acetate, 95:5 to 80:20 to 70:30). Four fractions were collected, analyzed by ^1H NMR and found to consist of starting material **56** (0.6 g, 2.1 mmol; 5%), 3-methyl-5-[3-(1-hydroxy-1-methylethyl)-1-hydroxy-1-methyl-2-cyclopent-2-yl]-penta-2,4-dieneoic acid ethyl ester (C_{17} -dihydroxyethylester **55**) (4.8 g, 16.2 mmol; 42%) consisting of isomers at C2 ($E/Z = 1.2/1.0$), dehydration product **61** (1.7 g, 6.1 mmol; 15%) consisting of isomers at C2 ($E/Z = 1.2/1.0$), and 6,7-dihydroxyethylester **62** (2.6 g, 8.8 mmol; 23%) consisting of isomers at C2 ($E/Z = 1.5/1.0$). The fraction containing **55** was further purified by semi-preparative normal phase HPLC (condition F, Appendix I). Three stereoisomeric compounds (**55a1**, **55a2** and **55b1**) were isolated and formed in relative amounts **55a1** > **55a2** > **55b1** (4.9:3.2:1.0). The stereoisomers were analyzed by HRMS, ^1H , ^{13}C , COSY and HSQC NMR.

(4E,2E)-3-methyl-5-[3-(1-hydroxy-1-methylethyl)-1-hydroxy-1-methyl-2-cyclopent-2-yl]-penta-2,4-dieneoic acid ethylester (55a1): UV $\lambda_{\text{max}} = 268$ nm (hexane: CH_2Cl_2 , 75:25). HRMS (ESI^+) m/z calculated for $\text{C}_{17}\text{H}_{29}\text{O}_4$ $[\text{M}+\text{H}]^+$ 297.2066, found 297.2080; m/z calculated for $\text{C}_{17}\text{H}_{27}\text{O}_3$ $[\text{M}+\text{H}-\text{H}_2\text{O}]^+$ 279.1960, found 279.1987; m/z calculated for $\text{C}_{17}\text{H}_{25}\text{O}_2$ $[\text{M}+\text{H}-2\text{H}_2\text{O}]^+$ 261.1854, found 261.1844. ^1H -NMR (400 MHz, CDCl_3) δ 1.17 (s, 3H), 1.18 (s, 3H), 1.27 (s, 3H), 1.29 (t, $J = 7.1$, 3H), 1.95 (m, 2H), 1.95 (m, 2H), 2.27 (d, 3H), 2.58 (m, 1H), 2.64 (m, 1H), 4.18 (q, $J = 7.1$, 2H), 5.76 (s, 1H), 6.02 (dd, $J = 15.5$, 1H), 6.18 (d, $J = 15.5$, 1H). ^{13}C NMR (400 MHz, CDCl_3) δ 14.1, 14.3, 22.4, 26.6, 29.6, 29.6, 37.8, 53.1, 58.7, 59.8, 72.1, 82.5, 118.7, 135.0, 136.2, 151.4, 167.0.

(4E,2Z)-3-methyl-5-[3-(1-hydroxy-1-methylethyl)-1-hydroxy-1-methyl-2-cyclopent-2-yl]-penta-2,4-dieneoic acid ethylester (55a2): UV $\lambda_{\text{max}} = 270$ nm (hexane: CH_2Cl_2 ,

75:25). HRMS (ESI⁺) m/z calculated for C₁₇H₂₉O₄ [M+H]⁺ 297.2066, found 297.2067; m/z calculated for C₁₇H₂₇O₃ [M+H-H₂O]⁺ 279.1960, found 279.1952; m/z calculated for C₁₇H₂₅O₂ [M+H-2H₂O]⁺ 261.1854, found 261.1850. ¹H-NMR (400 MHz, CDCl₃) δ 1.16 (s, 3H), 1.19 (s, 3H), 1.28 (t, $J = 7.1$, 3H), 1.30 (s, 3H), 1.85 (m, 2H), 1.93 (m, 2H), 1.98 (d, 3H), 2.64 (m, 1H), 2.64 (m, 1H), 4.16 (q, $J = 7.1$, 2H), 5.65 (s, 1H), 6.00 (dd, $J = 15.8$, 1H), 7.65 (d, $J = 15.8$, 1H). ¹³C NMR (400 MHz, CDCl₃) δ 14.3, 21.3, 22.4, 26.7, 29.5, 29.7, 37.6, 53.3, 59.0, 59.7, 72.2, 82.5, 116.8, 129.2, 137.7, 150.1, 166.2.

(4E,2Z)-3-methyl-5-[3-(1-hydroxy-1-methylethyl)-1-hydroxy-1-methyl-2-cyclopent-2-yl]-penta-2,4-dieneic acid ethylester (55b1): UV $\lambda_{\max} = 268$ nm (hexane:CH₂Cl₂, 75:25). HRMS (ESI⁺) m/z calculated for C₁₇H₂₉O₄ [M+H]⁺ 297.2066, found 297.2059; m/z calculated for C₁₇H₂₅O₂ [M+H-2H₂O]⁺ 261.1854, found 261.1848. ¹H-NMR (400 MHz, CDCl₃) δ 1.17 (s, 3H), 1.21 (s, 3H), 1.27 (s, 3H), 1.28 (t, $J = 7.1$, 3H), 1.68 (m, 2H), 1.82 (m, 2H), 1.98 (d, 3H), 1.98 (m, 1H), 2.64 (dd, $J = 9.0$ and $J = 4.7$, 1H), 4.16 (q, $J = 7.1$, 2H), 5.64 (s, 1H), 5.89 (dd, $J = 15.7$ and $J = 9.9$, 1H), 7.56 (d, $J = 15.7$, 1H). ¹³C NMR (400 MHz, CDCl₃) δ 14.3, 21.2, 24.0, 24.4, 28.4, 29.4, 40.0, 55.2, 56.4, 59.7, 72.4, 81.3, 116.3, 116.8, 127.7, 140.4, 150.4.

(2E)-C₁₇-dehydration product 61: UV $\lambda_{\max} = 268$ nm (hexane: CH₂Cl₂, 75:25). ¹H-NMR (400 MHz, CDCl₃) δ 1.20 (s, 3H), 1.28 (t, $J = 7.1$, 3H), 1.53 (s, 3H), 1.61 (s, 3H), 1.72 (m, 1H), 1.80 (m, 1H), 2.21 (d, 3H), 2.33 (m, 1H), 2.43 (m, 1H), 3.04 (d, $J = 8.7$, 1H), 4.17 (q, $J = 7.1$, 2H), 5.68 (s, 1H), 5.77 (dd, $J = 15.5$ and $J = 8.7$, 1H), 6.01 (d, $J = 15.5$, 1H).

(2Z)-C₁₇-dehydration product 61: UV $\lambda_{\max} = 268$ nm (hexane: CH₂Cl₂, 75:25). ¹H-NMR (400 MHz, CDCl₃) δ 1.20 (s, 3H), 1.28 (t, $J = 7.1$, 3H), 1.57 (s, 3H), 1.61 (s, 3H),

1.72 (m, 1H), 1.80 (m, 1H), 1.92 (d, 3H), 2.33 (m, 1H), 2.43 (m, 1H), 3.10 (d, $J = 9.1$, 1H), 4.17 (q, $J = 7.1$, 2H), 5.57 (s, 1H), 5.73 (dd, $J = 15.8$ and $J = 9.1$, 1H), 7.48 (d, $J = 15.8$, 1H).

(2E)-6,7-dihydroxyethylester 62: UV $\lambda_{\max} = 262$ nm (hexane: CH₂Cl₂, 75:25). ¹H-NMR (400 MHz, CDCl₃) δ 1.20 (s, 3H), 1.28 (t, $J = 7.1$ Hz, 3H), 1.43 (m, 2H), 1.55 (s, 3H), 1.61 (s, 3H), 2.03 (m, 2H), 2.20 (s, 3H), 3.99 (d, $J = 7.1$ Hz, 1H), 4.17 (q, $J = 7.1$, 2H), 5.04 (m, 1H), 5.71 (s, 1H), 6.05 (dd, $J = 15.5$ and $J = 7.1$, 1H), 6.28 (d, $J = 15.5$, 1H).

(2Z)-6,7-dihydroxyethylester 62: UV $\lambda_{\max} = 262$ nm (hexane: CH₂Cl₂, 75:25). ¹H-NMR (400 MHz, CDCl₃) δ 1.20 (s, 3H), 1.28 (t, $J = 7.1$, 3H), 1.43 (m, 2H), 1.55 (s, 3H), 1.61 (s, 3H), 1.94 (s, 3H), 2.03 (m, 2H), 4.03 (d, $J = 7.1$, 1H), 4.17 (q, $J = 7.1$, 2H), 5.03 (m, 1H), 5.63 (s, 1H), 6.09 (dd, $J = 16.1$ and $J = 7.1$, 1H), 7.65 (d, $J = 16.1$, 1H).

Conversion of C₁₇-dihydroxyethyl ester 55 to C₁₅-triol 54 by LAH reduction.

3-methyl-5-[3-(1-hydroxy-1-methylethyl)-1-hydroxy-1-methyl-2-cyclopent-2-yl]-penta-2,4-dieneic acid ethylester (**55**) (5.2 g, 17.5 mmol) was dissolved in THF (60 mL). The solution was cooled down to -10 °C in an ice/salt bath. LAH (14 mL, 2.0 M in THF) was added dropwise over 2 h. The mixture was stirred for 30 minutes then allowed to warm to 9 C° and stir for another 2 h. TLC analysis demonstrated complete conversion of the starting material (hexane:ethyl acetate, 4:6). The reaction was worked up by cooling the mixture down to 0 °C and adding ethyl acetate, dilute brine solution and 0.5% HCl (20 mL). After vacuum filtration through Celite, the organic phase was separated, dried over Na₂SO₄ and evaporated to dryness. The crude product was recovered as a yellow oil (4.2) and further purified by flash column chromatography on silica (hexane:ethyl acetate, 7:3). **54** was recovered as a mixture of white crystals and yellow oil (2.3 g, 9.0 mmol; 51%),

and was shown to consist of two isomers in a nearly 1:1 ratio, based on HPLC analysis (condition C, Appendix I). These were further separated by semi-preparative normal phase HPLC and isolated as white solids (condition F, Appendix I). Structural characterization of **54** was determined by ^1H , ^{13}C , COSY, HSQC NMR and HRMS.

3-methyl-5-[3-(1-hydroxy-1-methylethyl)-1-hydroxy-1-methyl-2-cyclopent-2-yl]-

penta-2,4-diene-1-ol (54): m.p. 120-133 °C. UV $\lambda_{\text{max}} = 238$ nm (MeOH). HRMS (ESI⁺) m/z calculated for $\text{C}_{15}\text{H}_{26}\text{O}_3\text{Na}$ $[\text{M}+\text{Na}]^+$ 277.1780, found 277.1729; m/z calculated for $\text{C}_{15}\text{H}_{23}\text{O}$ $[\text{M}+\text{H}-2\text{H}_2\text{O}]^+$ 219.1750, found 219.1744; m/z calculated for $\text{C}_{15}\text{H}_{21}$ $[\text{M}+\text{H}-3\text{H}_2\text{O}]^+$ 201.1643, found 201.1675. ^1H -NMR (400 MHz, CDCl_3) δ 1.16 (s, 3H), 1.19 (s, 3H), 1.29 (s, 3H), 1.80 (m, 2H), 1.85 (d, 3H), 1.89 (m, 2H), 2.55 (dd, $J = 10.7$, 1H), 2.62 (m, 1H), 4.30 (d, $J = 7.1$, 2H), 5.55 (t, $J = 7.1$, 1H), 5.66 (dd, $J = 10.7$ and $J = 15.5$, 1H), 6.52 (d, $J = 15.5$, 1H). ^{13}C NMR (400 MHz, CDCl_3) δ 20.7, 22.3, 26.5, 29.3, 29.8, 37.7, 52.9, 58.3, 58.8, 72.3, 82.5, 125.6, 128.5, 131.4, 134.7.

Synthesis of C_{15} -dihydroxyaldehyde **42 by TEMPO oxidation of 3-methyl-5-[3-(1-hydroxy-1-methylethyl)-1-hydroxy-1-methyl-2-cyclopent-2-yl]-penta-2,4-dieneic acid ethylester (**54**).** C_{15} -triol **54** (2.0 g, 7.9 mmol) was dissolved in DMF (30 mL). CuCl (0.08 g, 0.79 mmol) and 2,2,6,6-tetramethylpiperidine-1-nitroxide free radical (TEMPO, 0.12 g, 0.79 mmol) were added simultaneously. Oxygen was bubbled through the mixture at R.T. for 15 h. The product was extracted from dilute brine into ethyl acetate. The organic layer was dried over Na_2SO_4 and concentrated, affording crude product (2.3 g) as a yellow oil. After purification by flash column chromatography on silica (hexane:ethyl acetate, 4:1 to 1:1), **42** was recovered as a light yellow oil (0.71 g, 2.8 mmol; 36%). Analysis by normal phase HPLC (condition B, Appendix I) showed that

the product consisted of 4 stereoisomers **42a1**, **42a2**, **42b1** and **42b2**. The isomers were separated by semi-preparative HPLC and isolated in the relative ratio (1.5:0.9:1.0:1.0). Compound **42a2** was separated from the mixture by crystallization (hexane:ethyl acetate, 6:4) at -80 °C. The broad melting point was 115-128 °C. Isomers of **42** were isolated by semi-preparative HPLC (condition G, Appendix I).

(4E,2E)-3-methyl-5-[3-(1-hydroxy-1-methylethyl)-1-hydroxy-1-methyl-2-cyclopent-2-yl]-penta-2,4-dienal (42a1): UV λ_{\max} = 286 nm (hexane:CH₂Cl₂:methanol 75:25:1.2). HRMS (ESI⁺) m/z calculated for C₁₅H₂₅O₃ [M+H]⁺ 253.1804, found 253.1840; m/z calculated for C₁₅H₂₃O₂ [M+H-H₂O]⁺ 235.1698, found 235.1709; m/z calculated for C₁₅H₂₁O [M+H-2H₂O]⁺ 217.1592, found 217.1606. ¹H-NMR (400 MHz, CDCl₃) δ 1.16 (s, 3H), 1.18 (s, 3H), 1.25 (s, 3H), 1.60 (m, 1H), 1.74 (m, 2H), 2.00 (m, 1H), 2.28 (d, 3H), 2.32 (m, 1H), 2.33 (m, 1H), 5.91 (d, J = 8.1, 1H), 6.25 (d, J = 15.8, 1H), 6.36 (dd, J = 15.8, J = 8.5, 1H), 10.10 (d, J = 8.1, 1H). ¹³C NMR (400 MHz, CDCl₃) δ 13.2, 25.1, 26.5, 27.9, 28.6, 40.5, 54.4, 55.7, 72.9, 82.8, 128.9, 135.3, 140.8, 154.3, 191.5.

3-methyl-5-[3-(1-hydroxy-1-methylethyl)-1-hydroxy-1-methyl-2-cyclopent-2-yl]-penta-2,4-dienal (42a2): UV λ_{\max} = 284 nm (hexane:CH₂Cl₂:MeOH 75:25:1.2). HRMS (ESI⁺) m/z calculated for C₁₅H₂₅O₃ [M+H]⁺ 253.1804, found 253.1800; m/z calculated for C₁₅H₂₃O₂ [M+H-H₂O]⁺ 235.1698, found 235.1700; m/z calculated for C₁₅H₂₁O [M+H-2H₂O]⁺ 217.1592, found 217.1598. ¹H-NMR (400 MHz, CDCl₃) δ 1.18 (s, 3H), 1.20 (s, 3H), 1.28 (s, 3H), 1.60 (m, 2H), 1.75 (m, 2H), 2.10 (d, 3H), 2.34 (m, 1H), 2.35 (m, 1H), 5.85 (d, J = 7.7, 1H), 6.26 (dd, J = 15.7, 1H), 7.13 (d, J = 15.7, 1H), 10.18 (d, J = 7.7, 1H). ¹³C NMR (400 MHz, CDCl₃) δ 21.6, 25.1, 26.6, 27.9, 28.7, 40.5, 54.5, 55.8, 72.9, 82.8, 127.4, 127.7, 141.9, 154.5, 190.1.

3-methyl-5-[3-(1-hydroxy-1-methylethyl)-1-hydroxy-1-methyl-2-cyclopent-2-yl]-

penta-2,4-dienal (42b1): UV λ_{\max} = 284 nm (hexane:CH₂Cl₂:methanol 75:25:1.2).

HRMS (ESI⁺) m/z calculated for C₁₅H₂₅O₃ [M+H]⁺ 253.1804, found 253.1819; m/z calculated for C₁₅H₂₃O₂ [M+H-H₂O]⁺ 235.1698, found 235.1692; m/z calculated for C₁₅H₂₁O [M+H-2H₂O]⁺ 217.1592, found 217.1586. ¹H-NMR (400 MHz, CDCl₃) δ 1.17 (s, 3H), 1.22 (s, 3H), 1.25 (s, 3H), 1.68 (m, 2H), 1.85 (m, 2H), 1.97 (m, 1H), 2.25 (d, 3H), 2.63 (dd, J = 10.1, 1H), 5.93 (d, J = 8.1, 1H), 6.03 (dd, J = 15.5, J = 10.1, 1H), 6.20 (d, J = 15.5, 1H), 10.11 (d, J = 8.1, 1H). ¹³C NMR (400 MHz, CDCl₃) δ 13.3, 24.0, 24.5, 28.4, 29.5, 40.1, 55.3, 56.5, 72.3, 81.3, 129.0, 133.2, 141.1, 154.1, 191.3.

3-methyl-5-[3-(1-hydroxy-1-methylethyl)-1-hydroxy-1-methyl-2-cyclopent-2-yl]-

penta-2,4-dienal (42b2): UV λ_{\max} = 282 nm (hexane:CH₂Cl₂:methanol 75:25:1.2).

HRMS (ESI⁺) m/z calculated for C₁₅H₂₅O₃ [M+H]⁺ 253.1804, found 253.1863; m/z calculated for C₁₅H₂₃O₂ [M+H-H₂O]⁺ 235.1698, found 235.1703; m/z calculated for C₁₅H₂₁O [M+H-2H₂O]⁺ 217.1592, found 217.1593. ¹H-NMR (400 MHz, CDCl₃) δ 1.18 (s, 3H), 1.23 (s, 3H), 1.26 (s, 3H), 1.67 (m, 2H), 1.85 (m, 2H), 1.97 (m, 1H), 2.06 (d, 3H), 2.65 (dd, J = 10.2, 1H), 5.84 (d, J = 8.1, 1H), 5.93 (dd, J = 15.3, J = 10.2, 1H), 7.06 (d, J = 15.3, 1H), 10.16 (d, J = 8.1, 1H). ¹³C NMR (400 MHz, CDCl₃) δ 21.5, 24.1, 24.5, 28.4, 29.5, 40.2, 55.4, 56.7, 72.3, 81.2, 125.2, 128.0, 142.3, 154.4, 190.1.

Synthesis of 2,7-dimethyl-8-hydroxy-2,4,6-octatrienal (63). C₁₀-dialdehyde **27** (2.0 g, 12.2 mmol) was dissolved in ethanol (150 mL). A solution of sodium borohydride (155.2 mg, 4.1 mmol) in ethanol (50 mL) was added dropwise with stirring at R.T. over 3 h. The reaction was monitored by reversed-phase chromatography (condition J, Appendix D). The mixture was acidified with water (200 mL) containing hydrochloric acid (5 mL,

0.5%) and sulfuric acid (2 mL, 5%) and extracted into methylene chloride. The organic layer was dried over Na₂SO₄ and evaporated to dryness, affording an amber-colored oil (2.1 g). After purification by flash column chromatography on silica (hexane:ethyl acetate 9:1 to 8:2), **63** was recovered as a light yellow oil (1.4 g, 8.4 mmol; 70%).

Synthesis of 2,7-dimethyl-8-chloro-2,4,6-octatrienal (64). Mono-hydroxy aldehyde **63** (4.5 g, 27.0 mmol) was dissolved in methylene chloride (45 mL). The mixture was cooled down to -5 °C in an ice-salt bath. Concentrated hydrochloric acid (6.8 mL, 81.6 mmol) was added dropwise, producing a dark brown/black solution. The reaction was monitored by reversed-phase chromatography (condition J, Appendix I). Saturated sodium bicarbonate solution was added and the product was extracted into methylene chloride. The organic layer was washed with cold water to neutral pH, dried over Na₂SO₄ and evaporated to dryness. The product was recrystallized from the dark brown crude mixture with diisopropyl ether at -15 °C overnight affording **64** as dark brown solid (3.8 g, 20.5 mmol; 76%).

Synthesis of 7-formyl-2-methyl-2,4,6-octatrienyl-triphenylphosphonium chloride (65). Triphenylphosphine (8.1 g, 31 mmol) and **64** (5.0 g, 27 mmol) were dissolved in ethyl acetate (90 mL). The solution was refluxed overnight at 79 °C under argon. The mixture was cooled down to 0 °C in an ice bath. Solids were filtered and dried under vacuum overnight, affording crude **65** as a light brown solid (4.6 g). The product was recrystallized from methylene chloride (30 mL) and ethyl acetate (50 mL) at -10 °C for two days, affording **65** as a light brown, free flowing solid (4.4 g, 9.8 mmol; 48%). UV $\lambda_{\text{max}} = 332 \text{ nm}$ (methanol).

Protection of 7-formyl-2-methyl-2,4,6-octatrienyl-triphenylphosphonium chloride

(65). A solution of C₁₀ Wittig salt **65** (0.14 g, 0.31 mmol), trimethyl formate (80 μ L, 0.73 mmol) and methanolic p-toluenesulfonic acid (0.1 mL, 1% w/v) in methanol (5 mL) was heated to 40 °C for 4 h. The solution became red/brown in color. Progress of the reaction was monitored by UV spectroscopy. The protected Wittig salt **43** was not further isolated. UV λ_{max} = 294 nm (methanol).

Synthesis of protected C₂₅-dihydroxyaldehyde (45). A solution of protected C₁₀ Wittig salt **43** in methanol (4.8 mL, 0.073 M, 0.35 mmol) was cooled down to -5 °C in an ice-salt bath under argon. Sodium methoxide (20.7 mg, 0.38 mmol) was dissolved in methanol (2 mL) and added dropwise. After 20 minutes, a solution of C₁₅-dihydroxyaldehyde **42** (80.0 mg, 0.32 mmol) in methylene chloride (20 mL) was added dropwise. The reaction was allowed to stir at R.T. overnight. The reaction was monitored by normal phase HPLC (condition A, Appendix I).

Synthesis of C₂₅-dihydroxyaldehyde (29). The acetal **45** was extracted into methylene chloride from dilute brine and evaporated to dryness before dissolving in THF (15 mL). The solution was cooled down to -5 °C in an ice-salt bath under argon. **45** was treated with dilute sulfuric acid (2 mL, 0.5% v/v). After stirring for 2 h, crude product **29** was recovered as a dark red oil (300 mg). After purification by flash column chromatography on silica (hexane:ethyl acetate 8:2 to 6:4), **29** was recovered as a yellow oil (101 mg, 0.26 mmol; 74%). The product was shown to consist of two isomers by normal phase HPLC (condition A, Appendix 1). These were further separated by semi-preparative HPLC (condition D, Appendix 1) and isolated as orange solids.

(29-1): m.p. 60-66 °C. UV λ_{max} = 401 nm (hexane). HRMS (ESI⁺) m/z calculated for C₂₅H₃₇O₃ [M+H]⁺ 385.2743, found 385.2756; m/z calculated for C₂₅H₃₅O₂ [M+H-H₂O]⁺ 367.2637, found 367.2653. ¹H-NMR (600 MHz, CDCl₃) δ 1.16 (s, 3H), 1.21 (s, 3H), 1.24 (s, 3H), 1.67 (m, 1H), 1.73 (m, 1H), 1.80 (m, 2H), 1.88 (s, 3H), 1.92 (s, 3H), 1.96 (ddd, J = 10.0, 8.5 and 5.0, 1H), 2.03 (s, 3H), 2.53 (dd, J = 5.0 and 10.0, 1H), 5.54 (dd, J = 15.5 and 10.0, 1H), 6.15 (d, J = 11.0, 1H), 6.15 (d, J = 15.5, 1H), 6.30 (d, J = 12.0, 1H), 6.37 (d, J = 15.0, 1H), 6.69 (dd, J = 14.0 and 12.0, 1H), 6.74 (dd, J = 15.0 and 11.0, 1H), 6.95 (d, J = 12.0, 1H), 7.02 (dd, J = 14.0 and 12.0, 1H), 9.45 (s, 1H). ¹³C NMR (500 MHz, CDCl₃) δ 9.6, 13.0, 13.1, 24.2, 24.4, 28.3, 29.3, 40.0, 55.6, 56.6, 72.4, 81.4, 127.3, 127.5, 130.7, 131.0, 133.0, 135.1, 136.8, 136.9, 137.0, 137.6, 141.5, 148.7, 194.4.

(29-2): HRMS (ESI⁺) m/z calculated for C₂₅H₃₇O₃ [M+H]⁺ 385.2743, found 385.2751; m/z calculated for C₂₅H₃₅O₂ [M+H-H₂O]⁺ 367.2637, found 367.2641; m/z calculated for C₂₅H₃₃O [M+H-2H₂O]⁺ 349.2531, found 349.2525.

Synthesis of 1,2,5,6-tetrahydro-2,6-cyclo- γ -carotene-1,5-diol (40A).

C₂₅-dihydroxyaldehyde **29** (1.3 g, 3.5 mmol) and C₁₅-phosphonium Wittig salt **44** (4.1 g, 8.2 mmol) were dissolved in 1,2-ethoxybutane solvent (25 mL) and refluxed at 65 °C under argon for 24 h. Progress of the reaction was monitored by normal phase HPLC (condition A, Appendix I). Rotary evaporation of solvent afforded 5.6 g of dark red oil. Purification by flash column chromatography on silica (hexane:ethyl acetate 100:0 to 40:60) afforded **40A** as a dark red oil (0.4 g, 0.7 mmol; 20%), consisting of a mixture of *cis/trans* isomers based on the results of HPLC and spectral analysis of signals (condition A, Appendix I). The mixture was further purified by semi-preparative normal phase chromatography (condition H, Appendix I). The all-*trans* form of **40A** (15 mg, 0.03

mmol) was obtained as an orange-red solid. UV/VIS $\lambda_{\text{max}} = 444$ nm (hexane). HRMS (ESI⁺) m/z calculated for C₄₀H₅₉O₂ [M+H]⁺ 571.4515, found 571.4521. Proton and carbon assignments were established by COSY, HSQC and HMBC experiments. The relative stereochemistry of *all-trans* **40A** was determined by a NOESY experiment. ¹H-NMR (600 MHz, CDCl₃) δ 1.03 (s, 3H), 1.03 (s, 3H), 1.16 (s, 3H), 1.18 (s, 3H), 1.23 (s, 3H), 1.48 (m, 2H), 1.62 (m, 2H), 1.68 (m, 1H), 1.72 (s, 3H), 1.79 (m, 1H), 1.94 (s, 3H), 1.97 (s, 3H), 1.98 (s, 3H), 1.98 (s, 3H), 1.98 (m, 2H), 2.02 (m, 2H), 2.23 (dd, $J = 10.0$ and 9.0), 2.31 (ddd, 2H, $J = 10.0$, 10.0 and 7.2), 5.73 (dd, $J = 15.8$ and 9.0 , 1H), 6.15 (d, $J = 10.7$, 1H), 6.24 (d, $J = 15.8$, 1H), 6.25 (m, 1H), 6.25 (m, 1H), 6.35 (d, $J = 15.0$, 1H), 6.36 (d, $J = 15.0$, 1H), 6.59 (dd, $J = 15.0$ and 10.7 , 1H), 6.63 (m, 1H), 6.63 (m, 1H), 6.64 (dd, $J = 15.0$ and 10.7 , 1H). ¹³C NMR (500 MHz, CDCl₃) δ 12.7, 12.8, 12.8, 13.1, 19.3, 21.7, 25.1, 26.7, 27.4, 28.5, 29.0, 29.0, 33.1, 34.3, 39.7, 39.8, 54.3, 55.6, 73.1, 82.2, 124.6, 125.2, 126.7, 129.4, 129.4, 129.9, 130.3, 130.8, 131.6, 132.3, 132.8, 134.9, 136.1, 136.2, 136.7, 137.2, 137.8, 137.9, 138.0, 138.2.

Synthesis of 3,7,11-trimethyldodeca-2,4,6,10-tetraen-nitrile (58). Sodium hydride (60% suspension in mineral oil, 7.5 g, 0.19 mol) was washed two times with hexane under argon. THF (160 mL) was added and the mixture was cooled down to -5 °C in an ice-salt bath. A solution of diethyl (cyanomethyl)phosphonate (**52**) (23.5 g, 0.13 mol) in THF (40 mL) was added dropwise to sodium hydride while stirring. Additional THF (20 mL) was added to aid stirring of the preformed anion. The mixture was allowed to warm to R.T. and stir for 90 minutes. The mixture was cooled down to -35 °C in an acetone/dry ice bath. A solution of ψ -ionone (23.2 g, 0.12 mol) in THF (20 mL) was

added dropwise. The reaction was allowed to warm to R.T. and stir overnight under argon before quenching with dilute brine. Progress of the reaction was monitored by normal phase HPLC (condition C, Appendix I). The crude product was extracted into ethyl acetate. The organic layer was washed with additional brine to neutral pH, dried over Na₂SO₄ and evaporation, affording a dark, brown oil. After flash column chromatography on silica (hexane:ethyl acetate 95:5), **58** (13.1 g, 60.8 mmol; 50%) was recovered as a light yellow oil. UV λ_{max} = 308 nm (hexane/methylene chloride/methanol 75/24.2/0.8). The ¹H NMR data were in agreement with literature values.¹²⁷

Synthesis of 3,7,11-trimethyldodeca-2,4,6,10-tetraenal (68). A solution of C₁₅-nitrile **58** (13.1 g, 61 mmol) in methylene chloride (70 mL) was cooled down to -5 °C under argon. DIBAL-H (1.0 M in methylene chloride, 75 mL, 75 mmol) was added dropwise over 1 h. Progress of the reaction was monitored by normal phase HPLC (condition C, Appendix I). After 30 minutes, the reaction was cooled down to -20 °C and quenched with water (50 mL) and silica gel (36 g). After filtration through Celite, the product was taken up into methylene chloride. The organic phase was washed with water to neutral pH, dried over Na₂SO₄ and evaporated to dryness. The crude product **68** (12.6 g; 95%) was isolated as a light orange oil and stored at -80 °C. UV λ_{max} = 308 nm (hexane/methylene chloride/methanol 75/24.2/0.8).

Synthesis of ψ -vinyl ionol; 3,7,11-Trimethyldodeca-1,4,6,10-tetraen-3-ol (71). ψ -Ionone (15.9 g, 83 mmol) was dissolved in anhydrous THF (100 mL) under argon. The solution was cooled down to -20 °C in an ice-salt bath. Vinyl magnesium bromide (100 mL, 1M in THF, 100 mmol) was added dropwise. Progress of the reaction was monitored by TLC (hexane:ethyl acetate, 85:15). After stirring for 2 h at -10 °C, the

reaction was quenched with saturated ammonium chloride (100 mL). The crude product was extracted into ethyl acetate. The organic layer was washed with dilute brine to neutral pH, then dried over Na₂SO₄ and concentrated. The crude product (18.3 g) was obtained as a yellow oil. After purification by column chromatography on silica (100% hexane to hexane:ethyl acetate, 85:15), **71** (1.6 g, 7.3 mmol; 58%) was obtained as a light yellow oil. The isomeric ratio was determined by ¹H NMR (*7E/7Z* = 1:2). The NMR data were in agreement with literature values.⁶¹

(all E)-ψ-vinyl ionol; 3,7,11-Trimethyldodeca-1,4,6,10-tetraen-3-ol (71): ¹H-NMR (400 MHz, CDCl₃) δ 1.41 (s, 3H), 1.61 (s, 3 H), 1.68 (s, 3H), 1.77 (s, 3H), 2.10 (m, 2H), 2.10 (m, 2H), 5.07 (d, *J*=10.6, 1H), 5.11 (m, 1H), 5.26 (d, *J* = 17.3, 1H), 5.69 (d, *J* = 15.3, 1H), 5.84 (d, *J* = 10.6, 1H), 5.99 (dd, *J* = 17.3 and 10.9, 1 H), 6.47 (dd, *J* = 15.3 and 10.9, 1H).

(7Z)-3,7,11-Trimethyldodeca-1,4,6,10-tetraen-3-ol (71): ¹H-NMR (400 MHz, CDCl₃) δ 1.40 (s, 3H), 1.61 (s, 3 H), 1.68 (s, 3H), 1.78 (s, 3H), 2.10 (m, 2H), 2.10 (m, 2H), 5.07 (d, *J*=10.6, 1H), 5.13 (m, 1H), 5.25 (d, *J*=17.3, 1H), 5.66 (d, *J* = 15.3, 1H), 5.84 (d, *J* = 10.9, 1H), 5.98 (dd, *J* = 17.3 and 10.6, 1 H), 6.45 (dd, *J* = 15.3 and 10.9, 1H).

Synthesis of triphenyl [(2E,4E,6E)-3,7,11-trimethyldodeca-2,4,6,10-tetraenyl]phosphonium bromide, C₁₅-Wittig Salt (28). Triphenylphosphine hydrobromide (16.8 g, 49 mmol) was dissolved in methanol (95 mL) at R.T. under argon. After all solids dissolved, the mixture was cooled down to 15 °C. A solution of ψ-vinyl ionol (**71**) (10.7 g, 49 mmol) in methanol (30 mL) was added dropwise. The reaction was allowed to warm up to R.T. and stir for 20 h. Progress of the reaction was monitored by TLC (hexane:ethyl acetate, 85:15). The mixture was evaporated to dryness at 45 °C

under vacuum, affording crude product (30.4 g) as a yellow oil. Recrystallization from ethyl acetate (90 mL) at -10 °C for 3 days afforded **28** (0.9 g, 1.6 mmol; 4%) as a gummy white solid. The ¹H NMR results were in agreement with those reported in the literature.⁹²

Synthesis of (*all-E*)-12'-apo- ψ -carotene-12'-al (70**).** C₁₅-Wittig salt **44** (0.54 g, 0.99 mmol) and C₁₀-dialdehyde **27** (0.15 g, 0.91 mmol) were dissolved in CH₂Cl₂ (60 mL). The solution was cooled down to -10 °C in an ice-salt bath. A solution of sodium metal (0.13 g, 5.8 mmol) dissolved in methanol (10 mL) was added dropwise. The reaction was monitored by normal phase HPLC (condition B, Appendix I). After stirring for 3 h, dilute brine was added and the crude product was extracted into CH₂Cl₂. The organic layer was dried over Na₂SO₄ and evaporated to dryness to give 1.3 g dark red, viscous oil. After purification by flash column chromatography on silica (hexane:ethyl acetate, 100:0 to 98:2), **70** (0.4 g, 1.1 mmol; 78%) was recovered as a viscous, dark red oil in the *all-E* form, based on HPLC analysis and results of ¹H NMR which agreed with those reported in the literature.⁹²

70: UV λ_{max} = 436 nm (hexane:CH₂Cl₂:methanol 75:25:0.8). ¹H-NMR (400 MHz, CDCl₃) δ 1.62 (s, 3H), 1.69 (s, 3H), 1.83 (s, 3H), 1.88 (s, 3H), 1.98 (s, 3H), 2.04 (s, 3H), 2.18 (m, 2H), 2.24 (m, 2H), 5.15 (t, J = 7.1, 1H), 5.95 (d, J = 11.0, 1H), 6.19 (d, J = 12.0, 1H), 6.27 (d, J = 15.7, 1H), 6.30 (d, J = 12.0, 1H), 6.37 (d, J = 15.0, 1H), 6.54 (dd, J = 11.0 and 15.0, 1H), 6.68 (dd, J = 12.0 and 14.0, 1H), 6.78 (dd, J = 12.0 and 15.0, 1H), 6.96 (d, J = 12.0, 1H), 7.03 (dd, J = 12.0 and 14.0, 1H), 9.45 (s, 1H). ¹³C NMR (400 MHz, CDCl₃) δ 9.6, 12.9, 13.0, 17.7, 24.2, 25.7, 26.9, 32.8, 123.9, 125.7, 126.4, 127.3, 127.8, 130.9, 131.9, 132.1, 134.8, 136.3, 136.8, 137.8, 138.1, 140.7, 141.8, 148.9, 194.5.

Synthesis of C₂₅-aldehyde-5,6-epoxide (69). C₂₅-aldehyde **70** (82.6 mg, 0.24 mmol) was dissolved in methylene chloride (15 mL) at 0 °C under argon. *m*-CPBA (39.8 mg, 0.24 mmol) was dissolved in methylene chloride (10 mL) and added dropwise. Progress of the reaction was monitored by normal phase HPLC (condition B, Appendix I). After 40 minutes, the reaction was quenched with dilute sodium meta bisulfite and diluted with brine. The crude products were extracted into hexane:methylene chloride (75:25). The organic layer was evaporated to dryness and passed through silica (100% ethyl acetate). The product **69** (30.3 mg, 0.087 mmol; 35%) was recovered as a dark red oil, and was further purified by semi-preparative HPLC to afford **69** in two stereoisomeric forms **69a** and **69b** (condition D, Appendix I). UV λ_{\max} = 406 nm and 414 nm (Hexane:CH₂Cl₂:MeOH 75:23.8:1.2). **69a**: HRMS (ESI⁺) *m/z* calculated for C₂₅H₃₅O₂ [M+H]⁺ 367.2637, found 367.2616. **69b**: HRMS (ESI⁺) *m/z* calculated for C₂₅H₃₅O₂ [M+H]⁺ 367.2637, found 367.2625.

Synthesis of γ -carotene (6). Wittig salt **72** (2.0 g, 4.0 mmol) and β -apo-12'-carotenal (**74**) (1.0 g, 2.9 mmol) were dissolved in methylene chloride (35 mL). The solution was cooled down to -5 °C in an ice-salt bath. A solution of sodium methoxide (0.2 g, 4.1 mmol) in methanol (20 mL) was added dropwise with stirring. After one h, the reaction was warmed up to R.T. and allowed to stir for 24 h. Progress of the reaction was monitored by TLC (hexane:acetone, 9:1). Brine (50 mL) was added, and the product was extracted with methylene chloride (3 x 30 mL). The organic layer was dried over Na₂SO₄ and evaporated, affording 3.7 g of dark red, viscous oil. After purification by flash column chromatography on silica (hexane:ethyl acetate 100:0 to 98:2), **6** was obtained as a dark red oil (1.0 g, 1.9 mmol; 68%). UV λ_{\max} = 460 nm (hexane).

APPENDIX I

Condition	HPLC Column	HPLC eluent and flow rate	Compounds separated, monitoring wavelength (nm)
A	Silica-based nitrile bonded, 250 x 4.6 mm, 5 μ m (Analytical)	70% Hexane, 30% Ethyl acetate, 0.7 mL/min	45 , 374 nm; 42 , 286 nm; 29 , 410 nm; 40 , 446 nm
B	Silica-based nitrile bonded, 250 x 4.6 mm, 5 μ m (Analytical)	75% Hexane, 25% CH ₂ Cl ₂ , 1.2% MeOH, 0.7 mL/min	46 , 262 nm; 42 , 282 nm; 70 , 430 nm; 69 , 410 nm; 55 , 56 , 61 , 62 , 270 nm; 40A , 446 nm.
C	Silica-based nitrile bonded, 250 x 4.6 mm, 5 μ m (Analytical)	75% Hexane, 25% CH ₂ Cl ₂ , 0.8% MeOH, 0.7 mL/min	68 , 338 nm; 54 , 270 nm; 58 , 310 nm; 55 , 56 , 61 , 62 , 270 nm.
D	Silica-based nitrile bonded, 25 cm x 10 mm, 5 μ m (semi-preparative)	75% Hexane, 25% CH ₂ Cl ₂ , 0.5% MeOH, 3.0 mL/min	70 , 430 nm; 69 , 410 nm; 29 , 410 nm
E	Silica-based nitrile bonded, 25 cm x 10 mm, 5 μ m (semi-preparative)	75% Hexane, 25% CH ₂ Cl ₂ , 1.2% MeOH, 3.0 mL/min	46 , 262 nm
F	Silica-based nitrile bonded, 25 cm x 10 mm, 5 μ m (semi-preparative)	75% Hexane, 25% CH ₂ Cl ₂ , 0.7% MeOH, 2.5 mL/min (600-603); 3.5 mL/min	54-56 , 61 , 62 , 270 nm
G	Silica-based nitrile bonded, 25 cm x 10 mm, 5 μ m (semi-preparative)	75% Hexane, 25% CH ₂ Cl ₂ , 1.0% MeOH, 2.8 mL/min	42 , 282 nm
H	Silica-based nitrile bonded, 25 cm x 10 mm, 5 μ m (semi-preparative)	80% Hexane, 20% Ethyl acetate, 2.3 mL/min	40 , 446 nm
I	Silica-based nitrile bonded, 250 x 4.6 mm, 5 μ m (Analytical)	95% Hexane, 5% CH ₂ Cl ₂ , 0.7 mL/min	58 , 306 nm
J	C18 column, 250 x 4.6 mm, 5 μ m (Analytical).	70% acetonitrile, 30% water, 0.7 mL/min	63 , 64 , 330 nm.
K	C18 column, 250 x 4.6 mm, 5 μ m (Analytical).	80% acetonitrile, 20% water, 0.7 mL/min	46 , 262 nm

REFERENCES

1. Straub, O. In *Key to Carotenoids*, 2nd Ed; Pfander, H., Ed.; Birkhauser: Basel, 1987.
2. Hirschberg, J.; Cohen, M.; Harker, M.; Lotan, T.; Mann, V.; Pecker, I. Molecular Genetics of the Carotenoid Biosynthesis Pathway in Plants and Algae. *Pure Appl. Chem.* **1997**, *69*, 2151-2158.
3. Khachik, F.; Bertram, J.; Huyang, M.; Fahey, J.; Talalay, P. Dietary Carotenoids and their Metabolites as Potentially Useful Chemoprotective Agents Against Cancer. In *Antioxidant Food Supplements in Human Health*; Packer, L., Hiramatsu, M., and Yoshikawa, T., Eds.; Academic Press: San Diego, 1999; Chapter 14, 203-229.
4. Khachik, F.; Spangler, C.; Smith, J.; Canfield, L.; Pfander, H.; Steck, A. Identification, Quantification and Relative Concentrations of Carotenoids and their Metabolites in Human Milk and Serum. *Anal. Chem.* **1997**, *69*, 1873-1881.
5. Khachik, F.; Beecher, G.; Goli, M.; Lusby, W.; Smith, J. Separation and Identification of Carotenoids and their Oxidation Products in Extracts of Human Plasma. *Anal. Chem.* **1992**, *64*, 2111-2122.
6. Stahl, W.; Sies, H. Perspectives in Biochemistry and Biophysics. Lycopene: A Biologically Important Carotenoid for Humans? *Arch. Biochem. Biophys.* **1996**, *339*, 1-9.
7. Olson, J. Absorption, Transport, and Metabolism of Carotenoids in Humans. *Pure Appl. Chem.* **1994**, *66*, 1011-1016.
8. Khachik, F. Distribution and Metabolism of Dietary Carotenoids in Humans as a Criterion for Development of Nutritional Supplements. *Pure Appl. Chem.* **2006**, *78*, 1551-1557.
9. Tonnucci, L.; Holden, J.; Beecher, G.; Khachik, F.; Davis, C.; Mulokozi, G. Carotenoid Content of Thermally Processed Tomato-Based Food Products. *J. Agric. Food Chem.* **1995**, *43*, 579-586.
10. Khachik, F. Carotenoids in Food. In *Carotenoids*, Volume 5; Britton, G., Liaaen-Jensen, S., Pfander, H., Eds.; Birkhauser: Basel, 2009.
11. Khachik, F.; Beecher, G.; Smith, C. Lutein, Lycopene and their Oxidative Metabolites in Chemoprevention of Cancer. *J. Cell. Biochem. Suppl.* **1995**, *22*, 236-246.

12. Stahl, W.; Schwarz, W.; Sundquist, A.; Sies, H. *cis-trans* Isomers of Lycopene and β -carotene in Human Serum and Tissues. *Arch. Biochem. Biophys.* **1992**, *294*, 173-177.
13. Schimitz, H.; Poor, C.; Wellman, R.; Erdman, J. Concentrations of Selected Carotenoids and Vitamin A in Human Liver, Kidney and Lung Tissue. *J. Nutr.* **1991**, *121*, 1613-1621.
14. Sies, H.; Stahl, W. Vitamins E and C, Beta-Carotene and Other Carotenoids as Antioxidants. *Am. J. Clin. Nutr.* **1995**, *62*, 1315S-1321S.
15. Gann, P.; Ma, J.; Giovannucci, E.; Willett, W.; Sacks, F.; Hennekens, C.; Stampfer, M. Lower Prostate Cancer Risk in Men with Elevated Plasma Lycopene Levels: Results of a Prospective Analysis. *Cancer Res.* **1999**, *59*, 1225-1230.
16. Khachik, F.; Moura, F.; Zhao, D.; Aebischer, C.; Bernstein, P. Transformations of Selected Carotenoids in Plasma, Liver and Ocular Tissues in Humans and in Non-Primate Animals. *Invest. Ophthalmol. Vis. Sci.* **2002**, *43*, 3383-3392.
17. Glover, J. The Conversion of β -Carotene into Vitamin A. *Vitam. Horm.* **1960**, *18*, 371-386.
18. Lakshman, M.; Mychkovsky, I.; Attlesey, M. Enzymatic Conversion of *all-trans*- β -Carotene to Retinal by a Cytosolic Enzyme from Rabbit and Rat Intestinal Mucosa. *Proc. Natl. Acad. Sci. U.S.A.* **1989**, *86*, 9124-9128.
19. Lakshman, M.; Johnson, L.; Okoh, C.; Attlesey, M.; Mychkovsky, I.; Bhagavan, H. Conversion of *all-trans*- β -Carotene to Retinal by an Enzyme from the Intestinal Mucosa of Human Neonates. *J. Nutr. Biochem.* **1993**, *4*, 659-663.
20. *Nutritional Biochemistry and Metabolism*. 2nd Edition; Lindler, M., Ed.; Appleton and Lange: Connecticut, 1991; Chapter 5, p 153.
21. Von Lintig, J. Colors with Functions: Elucidating the Biochemical and Molecular Basis of Carotenoid Metabolism. *Ann. Rev. Nutr.* **2010**, *30*, 35-56.
22. Tang, G.; Wang, X.; Russell, R.; Krinsky, N. Characterization of β -Apo-13-Carotenone and β -Apo-14'-Carotenal as Enzymatic Products of the Excentric Cleavage of β -Carotene. *Biochemistry* **1991**, *30*, 9829-9834.
23. Ross, C., Harrison, E. Vitamin A: Nutritional aspects of retinoids and carotenoids. In *The Handbook of Vitamins*, 4th Edition; Zempleni, J., Ed.; CRC Press, LLC: Florida, 2007; pp 1-39.
24. *Free Radicals in Biology and Medicine*, 3rd Edition; Halliwell, B., Gutteridge, J., Eds.; Oxford University Press: New York, 1999.

25. Diplock, A. Antioxidant Nutrients and Disease Prevention: An overview. *Am. J. Clin. Nutr.* **1991**, *53*, 189S-193S.
26. Young, A.; Lowe, A. Antioxidant and Prooxidant Properties of Carotenoids. *Arch. Biochem. Biophys.* **2001**, *385*, 20-27.
27. Burton, G.; Ingold, K. β -Carotene: An Unusual Type of Lipid Antioxidant. *Science* **1984**, *224*, 569-573.
28. Truscott, T. β -Carotene and Disease: A Suggested Pro-Oxidant and Anti-Oxidant Mechanism and Speculations Concerning its Role in Cigarette Smoking. *J. Photochem. Photobiol. B.* **1996**, *35*, 233-235.
29. Szabo, C.; Ischiropoulos, H.; Radi, R. Peroxynitrite: Biochemistry, Pathophysiology and Development of Therapeutics. *Nature Rev. Drug Disc.* **2007**, *6*, 662-680.
30. Turko, I.; Murad, F. Protein Nitration in Cardiovascular Disease. *Pharmacol. Rev.* **2002**, *54*, 619-634.
31. Yokota, T.; Ohtake, H.; Ishikawa, H.; Inakuma, T.; Ishiguro, Y.; Terao, J.; Nagao, A.; Etoh, H. Quenching of Peroxynitrite by Lycopene *in vitro*. *Chem. Lett.* **2004**, *33*, 80-81.
32. *Lipid Oxidation Pathways*, Volume 2; Kamal-Eldin, A., Min, D., Eds.; AOCS Press: Illinois, 2008; Chapter 1.
33. Montine, T.; Neely, M.; Quinn, J.; Beal, M.; Markesbery, W.; Roberts, L.; Morrow, J. Lipid Peroxidation in Aging Brain and Alzheimer's Disease. *Free Radical Biol. Med.* **2002**, *33*, 620-626.
34. Cerutti, P. Prooxidant States and Tumor Promotion. *Science* **1985**, *227*, 375-381.
35. Woodall, A.; Lee, S.; Weesie, R.; Jackson, M.; Britton, G. Oxidation of Carotenoids by Free Radicals: Relationship Between Structure and Reactivity. *Biochim. Biochim. Biophys. Acta* **1997**, *1336*, 33-42.
36. Yamauchi, R.; Miyake, N.; Inoue, H.; Kato, K. Products Formed by Peroxyl Radical Oxidation of β -carotene. *J. Agric. Food Chem.* **1993**, *41*, 708-713.
37. Anguelova, T.; Warthesen, J. Degradation of Lycopene, Alpha-Carotene and Beta-Carotene During Lipid Peroxidation. *J. Food Sci: Food Chem. Toxicol.* **2000**, *65*, 71-75.
38. Nguyen, M.; Schwartz, S. Lycopene: Chemical and Biological Properties. *Food Tech.* **1999**, *53*, 38-34.

39. Steinbeck, M.; Khan, A.; Karnovsky, M. Intracellular Singlet Oxygen Generation by Phagocytosing Neutrophils in Response to Particles Coated with a Chemical Trap. *J. Biol. Chem.* **1992**, *267*, 13425-13438.
40. Kanofsky, J.; Hoogland, H.; Wever, R.; Weiss, S. Singlet Oxygen Production by Human Eosinophils. *J. Biol. Chem.* **1988**, *263*, 9692-9696.
41. Martin, H.; Ruck, C.; Schmidt, M.; Sell, S.; Beutner, S.; Mayer, B.; Walsh, R. Chemistry of Carotenoid Oxidation and Free Radical Reactions. *Pure Appl. Chem.* **1999**, *71*, 2253-2262.
42. Di Mascio, P.; Kaiser, S.; Sies, H. Lycopene: The Most Efficient Biological Carotenoid Singlet Oxygen Quencher. *Arch. Biochem. Biophys.* **1989**, *274*, 532-538.
43. Conn, P.; Schalch, W.; Truscot, T. The Singlet Oxygen and Carotenoid Interaction. *J. Photochem. Photobiol B: Biology* **1991**, *11*, 41-47.
44. Wagner, J.; Motchnik, P.; Stocker, R.; Sies, H.; Ames, B. The Oxidation of Blood Plasma and Low Density Lipoprotein Components by Chemically Generated Singlet Oxygen. *J. Biol. Chem.* **1993**, *268*, 18502-18506.
45. Tinkler, J.; Bohm, F.; Schalch, W.; Truscott, T. Dietary Carotenoids Protect Human Cells from Damage. *J. Photochem. Photobiol. B.* **1994**, *26*, 283-285.
46. Mathews-Roth, M. Treatment of Cutaneous Porphyrias. *Clin. Dermatol.* **1998**, *16*, 295-298.
47. Ribaya-Mercado, J.; Garmyn, M.; Gilcrest, B.; Russell, R. Skin Lycopene is Destroyed Preferentially over β -Carotene During Ultraviolet Irradiation in Humans. *J. Nutr.* **1995**, *125*, 1854-1859.
48. Paetau, I.; Khachik, F.; Brown, E.; Beecher, G.; Kramer, T.; Chittams, J.; Clevidence, B. Chronic Ingestion of Lycopene-Rich Tomato Juice or Lycopene Supplements Significantly Increases Plasma Concentrations of Lycopene and Related Tomato Carotenoids in Humans. *Am. J. Clin. Nutr.* **1998**, *68*, 1187-1195.
49. Jialal, I.; Grundy, S. Preservation of the Endogenous Antioxidants in Low Density Lipoprotein by Ascorbate but not Probucol During Oxidative Modification. *J. Clin. Invest.* **1991**, *87*, 597-601.
50. Palozza, P.; Krinsky, N. β -Carotene and α -Tocopherol are Synergistic Antioxidants. *Arch. Biochem. Biophys.* **1992**, *297*, 184-187.
51. Omenn, G.; Goodman, G.; Thornquist, M.; Balmes, J.; Cullen, M.; Glass, A.; Keogh, J.; Valanis, B.; Williams, J.; Barnhart, S.; Cherniack, M.; Brodtkin, C.; Hammar, S. Risk Factors for Lung Cancer and for Intervention Effects in

- CARET, the Beta-Carotene and Retinol Efficacy Trial. *J. Natl. Cancer Inst.* **1996**, *88*, 1550-1559.
52. Salgo, M.; Cueto, R.; Winston, G.; Pryor, W. β -Carotene and its Oxidation Products Have Different Effects on Microsome Mediated Binding of Benzo[a]Pyrene to DNA. *Free Radical Biol. Med.* **1999**, *26*, 162-173.
 53. Lowe, G.; Booth, L.; Young, A.; Bilton, R. Lycopene and β -Carotene Protect Against Oxidative Damage in HT29 Cells at Low Concentrations but Rapidly Lose this Capacity at Higher Concentrations. *Free Radical Res.* **1999**, *30*, 141-151.
 54. Forsberg, A.; Lingen, C.; Ernster, L.; Lindberg, O. Modification of the X-Irradiation Syndrome by Lycopene. *Exp. Cell Res.* **1959**, *16*, 7-14.
 55. Lingen, C.; Ernster, L.; Lindberg, O. The Promoting Effect of Lycopene on the Non-Specific Resistance of Animals. *Exp. Cell Res.* **1959**, *16*, 384-393.
 56. Foote, C.; Denny, R. Chemistry of Singlet Oxygen. VII. Quenching by β -Carotene. *J. Am. Chem. Soc.* **1968**, *90*, 6233-6235.
 57. Epstein, J. Effects of β -Carotene on Ultraviolet Induced Cancer Formation in the Hairless Mouse. *Photochem. Photobiol.* **1977**, *25*, 211-213.
 58. Peto, R.; Doll, R.; Buckley, J.; Sporn, M. Can Dietary Beta-Carotene Materially Reduce Human Cancer Rates? *Nature* **1981**, *290*, 201-208.
 59. Krinsky, N. Effects of Carotenoids in Cellular and Animal Systems. *Am. J. Clin. Nutr.* **1991**, *53*, 238S-246S.
 60. Mayne, S. *FASEB J.* Beta-Carotene, Carotenoids and Disease Prevention in Humans. **1996**, *10*, 690-701.
 61. Micozzi, M.; Beecher, G.; Taylor, P.; Khachik, F. Carotenoid Analyses of Selected Raw and Cooked Foods Associated with a Lower Risk for Cancer. *J. Natl. Cancer Inst.* **1990**, *82*, 282-285.
 62. Freudenheim, J.; Marshall, J.; Vera, R.; Laughlin, J.; Swanson, M.; Nemoto, T.; Graham, S. Premenopausal Breast Cancer Risk and Intake of Vegetable, Fruits and Related Nutrients. *J. Natl. Cancer Inst.* **1996**, *88*, 340-348.
 63. VanEenwyk, J.; Davis, F.; Bowen, P. Dietary and Serum Carotenoids and Cervical Intraepithelial Neoplasia. *Int. J. Cancer* **1991**, *48*, 34-38.
 64. Seddon, J.; Ajani, U.; Sperduto, R.; Hiller, R.; Blair, N.; Burton, T.; Farber, M.; Gragoudas, E.; Haller, J.; Miller, D. Dietary Carotenoids, Vitamins A, C, and E and Advanced Age-Related Macular Degeneration. Eye Disease Case-Control Study Group. *J. Am. Med. Assoc.* **1994**, *272*, 1413-1420.

65. Joshipura, K.; Ascherio, A.; Manson, J.; Stampfer, M.; Rimm, E.; Speizer, F.; Hennekens, C.; Spiegelman, D.; Willett, W. Fruit and Vegetable Intake in Relation to Risk of Ischemic Stroke. *J. Am. Med. Assoc.* **1999**, *282*, 1233-1239.
66. Ness, A.; Powles, J. Fruit and Vegetables, and Cardiovascular Disease: A Review. *Int. J. Epidemiol.* **1997**, *26*, 1-13.
67. Prakash, D.; Gupta, K. The Antioxidant Phytochemicals of Nutraceutical Importance. *Open Nutraceuticals J.* **2009**, *2*, 20-35.
68. Bertram, J.; King, T.; Fukushima, L.; Khachik, F. Enhanced Activity of an Oxidation Product of Lycopene Found in Tomato Products and Human Serum Relevant to Cancer Prevention. In *Antioxidant and Redox Regulation of Genes*: Sen, C., Sies, H., Baeuerle, P., Eds.; Academic Press: San Diego, 2000; 409-423.
69. Bertram, J.; Pung, A.; Churley, M.; Kappock, T.; Wilkins, L.; Cooney, Robert V. Diverse Carotenoids Protect Against Chemically Induced Neoplastic Transformations. *Carcinogenesis* **1991**, *12*, 671-678.
70. Nagasawa, H.; Mitamura, T.; Sakamoto, S.; Yamamoto, K. Effects of Lycopene on Spontaneous Mammary Tumor Development in SHN Virgin Mice. *Anticancer Res.* **1995**, *15*, 1173-1178.
71. Levy, J.; Bosin, E.; Feldman, B.; Giat, Y.; Minster, A.; Danilenko, M.; Sharoni, Y. Lycopene is a More Potent Inhibitor of Human Cancer Cell Proliferation than Either α -Carotene or β -Carotene. *Nutr. and Cancer.* **1995**, *24*, 257-26.
72. Palozza, P. Carotenoids and Modulation of Cancer: Molecular Targets. *Curr. Pharmacogenomics* **2004**, *2*, 35-45.
73. Pool-Zobel, B.; Bub, A.; Muller, H.; Wollowski, I.; Rechkemmer, G. Consumption of Vegetables Reduces Genetic Damage in Humans: First Results of a Human Intervention Trial with Carotenoid-Rich Foods. *Carcinogenesis* **1997**, *18*, 1847-1850.
74. Harwood, C.; Leedhan-Green, M.; Leigh, I.; Proby, C. Low Dose Retinoids in the Prevention of Cutaneous Squamous Cell Carcinomas in Organ Transplant Recipients. *Arch. Dermatol.* **2005**, *141*, 456-464.
75. Bertram, J.; Vine, A. Cancer Prevention by Retinoids and Carotenoids: Independent Action on a Common Target. *Biochim. Biophys. Acta* **2005**, *1740*, 170-178.
76. Bertram, J. Dietary Carotenoids, Connexins and Cancer: What is the Connection? *Biochem. Soc. Trans.* **2004**, *32*, 985-989.

77. Neveu, M.; Bertram, J. Gap junctions and Neoplasia. In *Gap Junctions: Advances in Molecular and Cellular Biology*; Hertzberg, E. Ed.; JAI Press: Greenwich, 1999.
78. Zhang, L.; Cooney, R.; Bertram, J. Carotenoids Enhance Gap Junctional Communication and Inhibit Lipid Peroxidation in C3H/10T1/2 Cells: Relationship to their Cancer Chemopreventive Action. *Carcinogenesis* **1991**, *12*, 2109-2114.
79. Stahl, W.; Swantje, N.; Briviba, K.; Hanusch, M.; Broszeit, R.; Peters, M.; Martin, H.; Sies, H. Biological Activities of Natural and Synthetic Carotenoids: Induction of Gap Junctional Communication and Singlet Oxygen Quenching. *Carcinogenesis* **1997**, *18*, 89-92.
80. Ben-Aziz, A.; Britton, G.; Goodwin, T. Carotene Epoxides of Lycopersicon Esculentum. *Phytochemistry* **1973**, *12*, 2759-2764.
81. Kamber, M.; Pfander, H.; Noack, K. 1,2-Epoxycarotenoids. 4. Synthesis, Proton NMR and CD Studies of (*S*)-1,2-Epoxy-1,2-Dihydrolycopene and (*S*)-1',2'-Epoxy-1',2'-Dihydro- γ -Carotene. *Helv. Chim. Acta* **1984**, *67*, 968-985.
82. Khachik, F.; Goli, M.; Beecher, G.; Holen, J.; Lusby, W.; Tenorio, M.; Barrera, M. Effect of Food Preparation on Qualitative and Quantitative Distribution of Major Carotenoid Constituents of Tomatoes and Several Green Vegetables. *J. Agric. Food Chem.* **1992**, *40*, 390-398.
83. Rodriguez, E, Rodriguez-Amaya, D. Lycopene Epoxides and Apo-Lycopenals Formed by Chemical Reactions and Autoxidation in Model Systems and Processed Foods. *J. Food Sci.* **2009**, *74*, C674-C682.
84. Lu, Y.; Etoh, H.; Watanabe, N.; Ina, K.; Ukai, N.; Oshima, S.; Ojima, F.; Sakamoto, H.; Ishiguro, Y. A New Carotenoid; Hydrogen Peroxide Oxidation Products from Lycopene. *Biosci. Biotechnol. Biochem.* **1995**, *59*, 2153-2155.
85. Tadashi, Y.; Etoh, H.; Ukai, N.; Oshima, S.; Sakamoto, H. 1,5-Dihydroxyiridanyl-lycopene in Tomato Puree. *Biosci. Biotechnol. Biochem.* **1997**, *61*, 549-550.
86. Khachik, F.; Steck, A.; Niggli, U.; Pfander, H. Partial Synthesis and Structural Elucidation of the Oxidative Metabolites of Lycopene Identified in Tomato Paste, Tomato Juice and Human Serum. *J. Agric. Food Chem.* **1998**, *46*, 4874-4884.
87. Khachik, F.; Pfander, H.; Traber, B. Proposed Mechanisms for the Formation of Synthetic and Naturally Occurring Metabolites of Lycopene in Tomato Products and Human Serum. *J. Agric. Food Chem.* **1998**, *46*, 4885-4890.

88. King, T.; Khachik, F.; Borkiewicz, H.; Fukushima, L.; Marioka, S.; Bertram, J. Metabolites of Dietary Carotenoids as Potential Cancer Preventive Agents. *Pure Appl. Chem.* **1997**, *69*, 2135-2140.
89. Monks, A.; Scudiero, D.; Skehan, P.; Shoemaker, R.; Paul, K.; Vistica, D.; Hose, C.; Langley, J.; Cronise, P. Feasibility of a High Flux Anticancer Drug Screen Using a Diverse Panel of Cultured Human Tumor Cell Lines. *J. Natl. Cancer Inst.* **1991**, *83*, 757-766.
90. Traber, B.; Pfander, H. 2,6-Cyclolycopene-1,5-diol: Total Synthesis of a Naturally Occurring Oxidation Product of Lycopene. *Tetrahedron* **1998**, *54*, 9011-9022.
91. Manchand, P.; Ruegg, P.; Schwieter, U.; Siddons, P.; Weedon, B. Carotenoids and Related Compounds. XI. Synthesis of δ -Carotene and ϵ -Carotene. *J. Chem. Soc.* **1965**, 2019-2026.
92. Hengartner, U.; Bernhard, K., Meyer, K., Englert, G., Glinz, E. Synthesis, Isolation and NMR-Spectroscopic Characterization of Fourteen (Z)-Isomers of Lycopene and of Some Acetylenic Didehydro- and Tetradehydrolycopenes. *Helv. Chim. Acta* **1992**, *75*, 1848-1865.
93. Withers, N.; Tuttle, R. Effects of Visible and Ultraviolet Light on Carotene-Deficient Mutants of *Cryptocodium Cohnii*. *J. Eukaryotic Microbiol.* **2007**, *26*, 120-122.
94. Horrocks, L.; Yeo, Y. Health Benefits of Docosahexaenoic Acid (DHA). *Pharmacol. Res.* **1999**, *40*, 211-225.
95. Britton, G.; Goodwin, T. Carotene Epoxides from the Delta Tomato Mutant. *Phytochemistry* **1975**, *14*, 2530-2532.
96. Karrer, I.; Eugster, C. Synthesis of Carotenoids. II. Total Synthesis of β -carotene. *Helv. Chimica Acta* **1950**, *33*, 1172-1174.
97. Milas, N.; Davis, P.; Belic, I.; Fles, D. Synthesis of β -carotene. *J. Am. Chem. Soc.* **1950**, *72*, 4844.
98. Inhoffen, H.; Pommer, H.; Bohlmann, F. Syntheses in the Carotenoid Series. XIV. Synthesis of β -carotene. *Just. Liebigs Annal. Chem.* **1950**, *569*, 237-246.
99. *Carotenoids, Volume 2: Synthesis*. Britton, G.; Liaen-Jensen, S.; Pfander, H., Eds.; Birkhauser, 1996. Basel, Switzerland. Chapter 2: Coupling Reactions. Part I: Enol Ether and Aldol Condensations. Ludvik Labler, August Ruttimann and Alfred Giger. Page 27.
100. *Carotenoids*; Isler, O., Ed.; Birkhauser: Basel, 1971.

101. Widmer, E.; Soukup, M.; Zell, R.; Broger, E.; Lohri, B.; Marbet, R.; Lukac, T. Technical Procedures for the Synthesis of Carotenoids and Related Compounds from 6-Oxoisophorone. VI. Synthesis of Rhodoxanthin and (3*RS*,3'*RS*)-Zeaxanthin; Routes to the C₁₅-Ring Component *via* 3-Oxoionone Derivatives. *Helv. Chim. Acta* **1982**, *65*, 944-957.
102. Duhamel, L.; Duhamel, P.; Lecouve, J. A New Prenylation Reagent: 1-Lithio-2-Methyl-4-(Trimethylsiloxy) Butadiene. *Tetrahedron* **1987**, *43*, 4339-4342.
103. McMurry, J. Carbonyl-Coupling Reactions using Low-Valent Titanium. *Chem. Rev.* **1989**, *89*, 1513-1524.
104. Julia, M.; Arnould, D. Use of Sulfones in Synthesis. III. Synthesis of Vitamin A *Bull. Soc. Chim. Fr.* **1973**, *2*, 746-750.
105. Bernhard, K.; Mayer, H. Recent Advances in the Synthesis of Achiral Carotenoids. *Pure Appl. Chem.* **1991**, *63*, 35-44.
106. Wittig, G.; Geissler, G. Course of Reactions of Pentaphenylphosphorus and Certain Derivatives. *Liebigs Ann. Chem.* **1953**, *580*, 44-57.
107. Wittig, G.; Scholkopf, U. Triphenylphosphinemethylene as an Olefin-Forming Reagent. I. *Chem. Ber.* **1954**, *87*, 1318-1330.
108. Maryanoff, B.; Reitz, A. The Wittig Olefination Reaction and Modifications Involving Phosphoryl-Stabilized Carbanions. Stereochemistry, Mechanism, and Selected Synthetic Aspects. *Chem. Rev.* **1989**, *89*, 863-927.
109. Vedejs, E.; Snoble, K. Direct Observation of Oxaphosphetanes from Typical Wittig Reactions. *J. Am. Chem. Soc.* **1973**, *95*, 5778-5780.
110. Widmer, E.; Zell, R.; Broger, E.; Cramer, Y.; Wagner, P.; Dinkel, J.; Schlageter, M.; Lukac, T. Technical Procedures for the Synthesis of Carotenoids and Related Compounds from 6-Oxoisophorone. II. A Novel Concept for the Synthesis of (3*RS*,3'*RS*)-Astaxanthin. *Helv. Chim. Acta* **1981**, *64*, 2436-2446.
111. Widmer, E.; Soukup, M.; Zell, R.; Broger, E.; Wagner, H.; Imfeld, M. Technical Procedures for the Synthesis of Carotenoids and Related Compounds from 6-Oxoisophorone. Synthesis of (3*R*,3'*R*)-Zeaxanthin. Part I. *Helv. Chim. Acta* **1990**, *73*, 861-867.
112. Soukup, M.; Widmer, E.; Lukac, T. Technical Procedures for the Synthesis of Carotenoids and Related Compounds from 6-Oxoisophorone. Synthesis of (3*R*,3'*R*)-Zeaxanthin. Part II. *Helv. Chim. Acta* **1990**, *73*, 868-873.
113. Makin, S. The Enol Ether Synthesis of Polyenes. *Pure Appl. Chem.* **1976**, *47*, 173-181.

114. Bernhard, K.; Kienzle, F.; Mayer, H.; Müller, R. Synthesis of Optically Active Natural Carotenoids and Structurally Related Natural Products. VIII. Synthesis of (3*S*,3'*S*)-7,8,7',8'-Tetrahydroastaxanthin and (3*S*,3'*S*)-7,8-Didehydroastaxanthin (Asterinic Acid). *Helv. Chim. Acta* **1980**, *63*, 1473-1490.
115. Khachik, F.; Chang, A. Total Synthesis of (3*R*,3'*R*,6'*R*)-Lutein and its Stereoisomers. *J. Org. Chem.* **2009**, *74*, 3875-3885.
116. Haag, A.; Eugster, C. Synthesis of Optically Active Carotenoids with (*R*)-4-Hydroxy- β -Endgroups. *Helv. Chim. Acta* **1985**, *68*, 1897-1906.
117. Yamano, Y.; Sakai, Y.; Yamashita, S.; Ito, M. Synthesis of Zeaxanthin- and Cryptoxanthin- β -D-Glucopyranosides. *Heterocycles* **2000**, *52*, 141-146.
118. Creemers, A.; Lugtenburg, J. The Preparation of *all-trans* Uniformly ¹³C-Labeled Retinal *via* a Modular Total Organic Synthetic Strategy. Emerging Central Contribution of Organic Synthesis Toward the Structure and Function Study with Atomic Resolution in Protein Research. *J. Am. Chem. Soc.* **2002**, *124*, 6324-6334.
119. *Advanced Organic Chemistry, Part B: Reactions and Synthesis*, 5th Edition; Carey, F., Sundberg, R., Eds.; Springer Science and Business Media, LLC: New York, 2007; Chapter 12, section 12.2.
120. Ruano, J.; Fajardo, C.; Fraile, A.; Martín, M. *m*-CPBA/KOH: An Efficient Reagent for Nucleophilic Epoxidation of *gem*-Deactivated Olefins. *J. Org. Chem.* **2005**, *70*, 4300-4306.
121. Payne, G.; Reactions of Hydrogen Peroxide. V. Alkaline Epoxidation of Acrolein and Methacrolein. *J. Am. Chem. Soc.* **1959**, *81*, 4901-4904.
122. Curci, R.; DiFuria, F. The Influence of the Oxidizing Nucleophile on Stereochemistry in the Alkaline Epoxidation of α,β -Unsaturated Sulfones. *Tetrahedron Lett.* **1974**, *47*, 4085-4086.
123. Fieser, L.; Fieser, M. Naphthoquinone Antimalarials. XII. The Hooker Oxidation Reaction. *J. Am. Chem. Soc.* **1948**, *70*, 3215-3222.
124. Payne, G.; Deming, P.; Williams, P. Reactions of Hydrogen Peroxide. VII. Alkali-Catalyzed Epoxidation and Oxidation Using a Nitrile as Co-Reactant. *J. Org. Chem.* **1961**, *26*, 659-663.
125. Bhattacharya, A.; Thyagarajan, G. The Michaelis-Arbuzov Rearrangement. *Chem. Rev.* **1981**, *81*, 415-430.
126. Wang, Y.; Woo, W.; Hoef, I.; Lugtenburg, J. 9-Demethyl-9-Haloretinals by Wadsworth-Emmons Coupling – Easy Preparation of Pure (*all-E*), (*9Z*) and (*11Z*) Isomers. *Eur. J. Org. Chem.* **2004**, 2166-2175.

127. Valla, A.; Valla, B.; Guillou, R.; Cartier, D.; Dufosse, L., Labia, R. New Synthesis of Retinal and its Acyclic Analog Gamma-Retinal by an Extended Aldol Reaction with a C₆ Building Block that Incorporates a C₅ Unit after Decarboxylation. A Formal Route to Lycopene and Beta-Carotene. *Helv. Chim. Acta* **2007**, *90*, 512-520.
128. Vidari, G.; Beszant, S.; Marabet, J.; Bovolenta, M.; Zanoni, G. FeCl₃ and ZrCl₄ Regiochemically Controlled Biomimetic-like Cyclizations of Simple Isoprenoid Epoxyolefins. *Tetrahedron Lett.* **2002**, *43*, 2687-2690.
129. Bovolenta, M.; Castronovo, F.; Vadala, A., Zanoni, G.; Vidari, G. A Simple and Efficient Highly Enantioselective Synthesis of α -Ionone and α -Damascone. *J. Org. Chem.* **2004**, *69*, 8959-8962.
130. Stevens, R.; Lai, J. General Methods of Alkaloid Synthesis. X. The Total Synthesis of the Scelletium Alkaloids (\pm)-Joubertiamine, (\pm)-*O*-Methyljoubertiamine, and (\pm)-Dihydrojoubertiamine. *J. Org. Chem.* **1972**, *37*, 2138-2140.
131. Trofimenko, S. 1,1,2,2-Ethanetetracarboxaldehyde and its Reactions. *J. Org. Chem.* **1964**, *29*, 3046-3049.
132. Surmatis, J.; Walser, A.; Gibas, J.; Schwieter, U.; Thommen, R. Synthesis of Oxygenated Carotenoids. *Helv. Chim. Acta* **1970**, *53*, 974-990.
133. Corey, E.; Suggs, J. Pyridinium Chlorochromate: Efficient Reagent for Oxidation of Primary and Secondary Alcohols to Carbonyl Compounds. *Tetrahedron Lett.* **1975**, *31*, 2647-2650.
134. *Organic Chemistry*, 5th Edition; Bruice, P., Ed.; Pearson Prentice Hall: New Jersey, 2007; Chapter 19, p 918.
135. Dess, D; Martin, J. Readily Accessible Oxidant for the Conversion of Primary and Secondary Alcohols to Aldehydes and Ketones. *J. Org. Chem.* **1983**, *48*, 4155-4156.
136. Hu, T.; Schaus, J.; Lam, K.; Palfreyman, M.; Wuonola, M.; Gustafson, G.; Panek, J. Total Synthesis and Preliminary Antibacterial Evaluation of the RNA Polymerase Inhibitors (\pm)-Myxopyronin A and B. *J. Org. Chem.* **1998**, *63*, 2401-2406.
137. Piancatelli, G.; Leonelli, F. Oxidation of Nerol to Neral with Iodobenzene and TEMPO. *Organic Synthesis*, **2006**, *83*, 18-23.
138. Anelli, P.; Montanari, F.; Quici, S. A General Synthetic Method for the Oxidation of Primary Alcohols to Aldehydes: (S)-(+)-2-Methylbutanal. *Organic Synthesis*, **1990**, *69*, 212-215.

139. Angelin, M.; Hermansson, M.; Dong, H.; Ramstrom, O. Direct, Mild, and Selective Synthesis of Unprotected Dialdo-Glycosides. *Eur. J. Org. Chem.* **2006**, 4323-4326.
140. Ciriminna, R.; Pagliaro, M. Industrial Oxidations with Organocatalyst TEMPO and its Derivatives. *Org. Process Res. Dev.* **2010**, *14*, 245-251.
141. Semmelhack, M.; Schmid, C.; Cortes, D.; Chou, C. Oxidation of Alcohols to Aldehydes with Oxygen and Cupric Ion, Mediated by Nitrosonium Ion. *J. Am. Chem. Soc.* **1984**, *106*, 3374-3376.
142. *Carotenoids, Volume 2: Synthesis*. Edited by G. Britton, S. Liaen-Jensen and H. Pfander. Birkhauser, 1996. Basel, Switzerland. Chapter 3: Carotenoid Synthesis. Part I: Polyene Synthons. Robert K. Muller. Page 117-118.
143. Buddrus, J. Dehydrohalogenierung von Phosphoniumhalogeniden durch Epoxide. *Chem. Ber.* **1974**, *107*, 2050-2061.
144. Ishikawa, Y. The Synthesis of β -Ionylideneacetaldehyde. *Bull. Chem. Soc. Jpn.* **1964**, *37*, 207-209.
145. Khachik, F.; Chang, A.; Gana, A.; Mazzola, E. Partial Synthesis of (3*R*,6'*R*)- α -Cryptoxanthin and (3*R*)- β -Cryptoxanthin from (3*R*,3'*R*,6'*R*)-Lutein. *J. Nat. Prod.* **2007**, *70*, 220-226.
146. Haugan, J.; Liaanen-Jensen, S. Total Synthesis of Acetylenic Carotenoids. 2. Synthesis of (*all-E*)-(3*R*,3'*R*)-Diatoxanthin and (*all-E*)-(3*R*)-7,8-Didehydrocryptoxanthin. *Acta Chemica Scandinavica* **1994**, *48*, 899-904.
147. Rugg, R.; Schwieter, U.; Ryser, G.; Schudel, P. Syntheses in the Carotenoid Series. XVII. γ -Carotene, *dl*- α - and β -Carotene from Dehydro- β -apo-12'-Carotenal. *Helv. Chim. Acta* **1961**, *44*, 985 -993.
148. Leal, W.; Kuwahara, Y.; Suzuki, T.; Nakano, Y.; Nakao, H. Identification and Synthesis of 2,3-Epoxyneral, a Novel Monoterpene from the Acarid Mite *Tyrophagus Perniciosus* (Acarina, Acaridae). *J. Agric. Biol. Chem.* **1989**, *53*, 295-298.